UNIVERSITY OF SOUTHAMPTON

FACULTY OF MEDICINE

Cancer Sciences Unit

‘SIP1/ZEB2 induced epithelial to mesenchymal transition promotes metastasis and chemoresistance in colorectal cancer’

by

Rahul Sreekumar

DM/PhD

DEC 2017

Supervisors:

Dr.Emre Sayan

Prof. Alexander H. Mirnezami

ABSTRACT

Colorectal cancer (CRC) is the second commonest cause of cancer-associated mortality in Europe, and a key public health issue. Cancer metastasis is the principle cause of death and occurs in up to 30% at presentation, and subsequently develops in 50% after curative surgery. The majority of patients with metastases are incurable, and can expect a median survival of only up to 2 years, even with the latest chemotherapeutic and biological agents. Additionally, not all patients respond and side effects are frequent and at times life threatening. These findings highlight the pressing need for identification of new markers of metastatic capability and chemotherapy response, to improve precision with which therapy can be tailor to patients. Although development of primary CRC has served as a paradigm for understanding multistage carcinogenesis, the mechanisms influencing metastasis and chemoresistance are still poorly understood.

Epithelial-Mesenchymal Transition (EMT) is an embryologically conserved genetic program by which cancer cells down regulate epithelial junctions, express mesenchymal markers, and manifest a migratory phenotype. While the significance of EMT during development and embryogenesis is well established, an emerging role is its involvement in metastasis and chemo/radio resistance in cancer. EMT is activated by TGFβ, FGF, EGF, WNT and Notch signalling pathways, which converge to activate transcription factors that subsequently repress the expression of critical epithelial genes. Key transcription factors in this process include members of the SNAIL, Twist, and ZEB families, which promote cellular phenotypic switch. In addition to enhanced migration, metastatic cells also acquire apoptosis resistance to chemo/radio therapy through currently poorly understood mechanism. Despite growing evidence that EMT promotes apoptosis resistance to DNA damaging agents, ZEB family of transcription factors have been sparsely studied in gastrointestinal malignancies and the molecular mechanism mediating apoptosis resistance poorly understood.

Based on these observations the following hypothesis was formulated:

- SMAD interacting protein (SIP1/ZEB2) induced EMT promotes metastasis and apoptosis resistance in colorectal cancer (CRC).

The primary objectives of the study are: -

1. Assess if SIP1/ZEB2 induces EMT in CRC.
2. Investigate whether expression of SIP1/ZEB2 could serve as a biomarker to detect patients at high risk or recurrence after surgical resection in CRC.
3. Study the molecular mechanisms that promote SIP1/ZEB2 induced apoptosis resistance to chemotherapeutic and radiotherapeutic treatment regimens.
4. Validate in-vitro findings in a murine model

SIP1/ZEB2 expression resulted in the acquisition of all the cardinal features of EMT, namely E-cadherin down regulation, increased metastatic capacity and apoptosis resistance to chemotherapeutic agents commonly using in clinical practice. SIP/ZEB2 expression in primary CRC, exhibited a statistically significant association with increased risk of distant recurrence in two independent patient cohorts. Addition of SIP1/ZEB2 expression status to the TNM staging system improved precision in the ability to identify patients at high risk of disease recurrence after curative surgery. Further studied also highlighted an important association between SIP1/ZEB2 expression and chemoresistance to cytotoxic drugs used to in the FOLFOX regimen. A qPCR array, with a focus on DNA damage response highlighted SIP1/ZEB2 induced EMT associated with increased expression of multiple components of the nucleotide excision repair (NER) pathway, in particular excision repair cross complementation group 1 (ERCC1).

ERCC1 hetero-dimerises with excision repair cross complementation group 4, which functions as an exonuclease during repair of DNA crosslinks generated by platinum based chemotherapeutic agents such as oxaliplatin. Stable over expression of ERCC1; lead to attenuate DNA damage, apoptosis resistance and enhanced viability. Whilst siRNA mediated knockdown (KD) sensitise cells to oxaliplatin treatment. Assessment of DNA repair kinetics, as a mechanism of repair kinetics revealed higher expression levels of

ERCC1 associated with faster kinetics of DNA cross-link clearance. The influence of ERCC1 over expression *in vivo* was demonstrated by impaired tumour regression in ERCC1 over-expressing cells in an orthotopic murine model of primary CRC.

ZEB proteins have also been implicated with the enhanced ability to repair DNA DSB's and consequently promote resistance to ionising radiation. For many decades, models of DNA DSB repair have highlighted the critical influence of the histone architecture in accessing damaged DNA and subsequently undertaking DNA repair. Heterochromatin rich DNA domains are known to be prone to accruing mutations, due to attenuated DNA repair. Recent studies have suggested EMT leads to epigenetic reprograming, which results in genome wide loss of heterochromatin rich domains. SIP1/ZEB2 expression in DLD-SIP1 cells enhanced apoptosis resistance secondary to faster repair of DNA DSB's. ChIP-Seq analysis of SIP1/ZEB2 expressing mesenchymal cells highlighted genome wide loss of heterochromatin mark H3K27me3. The mechanism responsible for this epigenetic change was found to be direct transcriptional repression of the methyltransferase EZH2, by SIP1/ZEB2. Inhibition of EZH2 by small molecule inhibitor GSK126 in uninduced DLD-SIP1 cells enhanced apoptosis resistance and viability in response to IR. The above results suggest the epigenetic architecture of mesenchymal cancer can influence DNA repair kinetics and consequently resistance to IR. The above body of work clearly demonstrates SIP1/ZEB2 plays a central role in promoting metastasis and treatment resistance in CRC. Further in vitro studies and clinical trials to dissect the impact of SIP1/ZEB2 expression in CRC will facilitate clinical translation in future years.

Table of Contents

List of Tables

List of Figures

DECLARATION OF AUTHORSHIP

I, ...[please print name]

Declare that this thesis and the work presented in it are my own and have been generated by me as the result of my own original research.

[title of thesis] .....

.....

I confirm that:

1. This work was done wholly or mainly while in candidature for a research degree at this University;
2. Where any part of this thesis has previously been submitted for a degree or any other qualification at this University or any other institution, this has been clearly stated;
3. Where I have consulted the published work of others, this is always clearly attributed;
4. Where I have quoted from the work of others, the source is always given. With the exception of such quotations, this thesis is entirely my own work;
5. I have acknowledged all main sources of help;
6. Where the thesis is based on work done by myself jointly with others, I have made clear exactly what was done by others and what I have contributed myself;
7. [Delete as appropriate] None of this work has been published before submission [or] Parts of this work have been published as: [please list references below]:

Signed: .....

Date:

Acknowledgement

I would like to take this opportunity to extend my sincere gratitude to my supervisor's Dr. Emre Sayan, Professor Alexander Mirnezami and Professor John Primrose. Without their continued encouragement and guidance I may have never attempted this daunting task.

Dr. Hajir Alsahati, thank you for your guidance and help in the lab, this work was certainly more enjoyable to undertake due to your support and input.

This work has been supported by the generous contribution of the Medical Research Council (MRC).

I am most grateful to Professor Brendan Price for hosting me at Dana Faber Cancer institute, Harvard medical school, which made it possible to investigate cellular mechanisms that drive resistance to ionising radiation in colorectal cancer.

I would like to extend my gratitude to my family and my wife for their unfailing love and support through all the highs and lows.

This study has given me an insight into cancer biology, which I could have never achieved without undertaking this challenging but highly rewarding endeavour. I believe I am now far better equipped to pursue my career aspirations of becoming a clinician scientist, undertaking translational research in future years.

This work is dedicated to my aunt Chandrakala Venkatswamy who lost her life to cancer at the age of 30.

Definitions and Abbreviation

ABBREVIATION	DEFINITION
5-FU	5-Fluorouracil
ABCG2	ATP binding cassette subfamily G member 2
ALDH1	Aldehyde dehydrogenase 1
AJCC	American Joint Committee on Cancer
AKT	Serine threonine kinase
Alt-EJ	Alternative End-joining
APC	Adenomatous polyposis coli
ATCC	American Type Culture Collections
ATP	Adenosine triphosphate
ATM	Ataxia-Telangiectasia-mutated
ATR	Ataxia-Telangiectasia-related
BER	Base excision repair
bHLH	Basic/helix-loop-helix
BM	Basement membrane
BMP	Bone morphogenetic protein
BSA	Bovine serum albumin
BVs	Blood vessels
CAFs	Cancer associated fibroblasts
CBP	CREB binding protein
CDC42	Cell division cycle 42
CDH1	E-cadherin gene/promoter
CEA	Carcinoemboryonic antigen
CHD	Chromatin helicase DNA binding
Chk1	Checkpoint kinase 1
Chk2	Checkpoint kinase 2

ChIP	Chromatin immuno-precipitation
CIN	Chromosomal instability
CK	Cytokeratin
c-MET	Hepatocyte growth factor receptor
CRC	Colorectal cancers
CSC	Cancer stem cell
CtBP	C terminal binding protein
DLD-I	DLD-SIP1 induced
DLD-UI	DLD-SIP1 un-induced
DNMT	DNA methyl transferases
DMEM	Dulbecco's Modified Eagle's Medium
DMSO	Dimethyl sulphoxide
DOT1L	DOT1 like methyltransferase
DR	Direct repair
ECM	Extracellular matrix
ECs	Endothelial cells
EDTA	Ethylene-diamine-tetra acetic acid
EGF	Epidermal growth factor
EGF-TKI	Epidermal growth factor tyrosine kinase inhibitor
EGFR	Epidermal growth factor receptor
EMT	Epithelial mesenchymal transition
ERCC1	Excision repair cross complementation group1
ERCC4	Excision repair cross complementation group4
ERK	Extracellular signal–regulated kinase
ESRP	Epithelial spicing regulatory protein
EZH1	Enhancer of Zeste homolog 1
EZH2	Enhancer of Zeste Homolog 2
FAP	Familial adenomatous polyposis

FBS	Foetal bovine serum
FF	*Firefly*
FOX	Fork-head box
FRA1	FOS related AP1
FGF	Fibroblast growth factor
FSC	Forward scatter
FSP1	Fibroblast specific protein 1
G9a	Euchromoatic lysine methyl transferase
GAGs	Glycosaminoglycans
GFP	Green fluorescent protein
GFs	Growth factors
GRHL2	Grainy head like transcription factor 2
GSK3β	Glycogen synthase kinase 3 beta
GTPase	Guanosine Triphosphate
H	Histone
H & E	Haematoxylin and eosin
HCC	Hepatocellular carcinoma
HDAC	Histone deacetylase
HGF	Hepatocyte growth factor
HIF-1	Hypoxia inducible factors 1
HNPCC	Hereditary Non-Polyposis Colorectal Cancer
HR	Homologous recombination
HRP	Horseradish peroxidase
ID	Inhibitor of DNA binding
IGF	Insulin like growth factor
IL-6	Interleukin 6
IHC	Immunohistochemistry
IP	Immuno-precipitation

ISWI	Imitation SWI
K	Lysine
K-RAS	Kirstein rat sarcoma
Ks	Cytokeratins
LB	Luria Bertani
LSD	Lysine demethylase 1A
M	Mesenchymal
MET	Mesenchymal-epithelial transition
EM	Metastable
MAP-K	Mitogen activated protein kinase
MDR	Multiple drug resistance
miRNA	Micro RNA
MMPs	Matrix metallo-proteinases
MMR	Mismatch repair genes
MSCs	Mesenchymal stem cells
MLH1	MutL homolog
MRN	Mre50-RAD50-NBS
MSH2	MutS homolog
mTORC1	Mammalian Target of Rapamycin Complex
mTORC2	Mammalian Target of Rapamycin Complex 2
NER	Nucleotide excision repair
NF- κB	Nuclear Factor –κB
NHEJ	Non homologous end joining
NuRD	Nucleosome remodelling deacetylase
PBS	Phosphate Buffer Saline
PCR	Polymerase chain reaction
PCNA	Proliferating cell nuclear antigen
PDAC	Pancreatic ductal adenocarcinoma

PDGF	Platelet-derived growth factor
PDGFR	Platelet-derived growth factor receptor
PDK1	Phosphoinositide-dependent kinase 1
PI3K	Phosphatidylinositol-3-Kinase
PIC	Protease Inhibitor Cocktail
PK	Protein kinase
PLB	Passive Lysis Buffer
PMSF	Phenylmethylsulfonyl fluoride
PMTs	Photomultiplier tubes
POL	Polymerase
PRRX1	Pair related homeobox 1
PRC1	Polycomb repressor complex 1
PRC2	Polycomb repressor complex 2
PRMT1	Protein arginine methyl transferase 1
PTEN	Phosphatase and tensin homolog
RACK	Receptor for activated C kinase
RBFOX1	RNA Binding protein Fox-1 homolog 1
RN	Renilla
RHO	Rhodopsin
ROS	Reactive oxygen species
RT	Room temperature
RTKs	Receptor tyrosine kinases
RT-PCR	Reverse transcriptase PCR
SHC	SRC homology domain containing
SGH	Southampton general hospital
SGS	Stop & Glow ® Substrate
Shc	Src homology 2 domain–containing transforming protein

SIP1	Smad interacting protein 1
SIRT1	Sirtuin 1
SMAD	Mother against DPP homolog
SNAI	Snail family transcriptional repressor
SOS1	Son of sevenless homolog 1
SRSF2	Serine and arginine rich splicing factor 2
SSB	Single strand break
SSC	Side scatter
Streptavidin-RPE	Streptavidin conjugated to R-Phycoerythrin
SUV39H1	Supressor of varegation 3-9 homolog 1
SWI/SNF	Switch sucrose non-fermentable
TAE	Tris acetate EDTA buffer
TBS-T	Tris buffered saline with Tween
TE	Tris EDTA
TFs	Transcription factors
TFIIH	Transcription factor 2 H
TGS	Tris/glycine/SDS buffer
TGF-β	Transforming growth factor β
TGF-βRI	TGF-β receptor type I
TGF-βRII	TGF-β receptor type II
TIP60	Lysine acetyl transferase 5
TNF-α	Tumour necrosis factor alpha
TNM	Tumour, Node, Metastasis staging system
TNM7	7th edition TNM
TP53	Tumour protein-53
UV	Ultraviolet
WB	Western blot

XP	Xeroderma pigmentosum
XRCC1	X-ray repair cross complementing 1
ZEB1	Zinc finger E-box binding homeobox 1
ZEB2	Zinc finger E-box binding homeobox 2
ZO-1	Zonula occludens protein 1
ZO-3	Zonula occludens protein 3
α-SMA	Alpha-smooth muscle actin

Chapter 1: Introduction

1.1 Colorectal Cancer

Colorectal cancer is a major public health issue and the second highest cause of cancer related death in Europe (1). Metastasis is the principle cause of mortality and can affect up to 50% of patients after surgical resection with curative intent (2) (3). The vast majority of patients that experience recurrence remain incurable with median survival not exceeding 12-16 months after treatment with the most advanced therapeutic strategies (4). Understanding molecular mechanism driving malignant transformation in CRC has resulted in the emergence of targeted therapies in recent years, however clinical trials have proved disappointing, improving oncological outcomes by only a few months (5) (6). There are currently no biomarkers in routine clinical use that can prognosticate disease trajectory or predict response to chemotherapeutic agents. The use of KRAS mutation in codon 12 or 13 as a marker of resistance to monoclonal antibodies (Cetuximab and Panitumumab) against epidermal growth factor (EGF) receptor provides proof of principle that improved molecular characterisation can result in the development of novel strategies to personalise cancer care and improve patient outcome in future years (7).

1.1.1 The pathogenesis of colorectal cancer

The pathogenesis of CRC can be divided into those occurring from sporadic or hereditary mutations. It is estimated that 20% of CRC's are familial, with 5 – 10 % resulting from known hereditary genetic syndrome (8). Broadly; hereditary CRC's are divided into non-polyposis and polyposis syndromes. Genetic analysis of patients with hereditary syndromes has shed great insight into pathways governing progression from adenoma to invasive carcinoma in patients with sporadic CRC, as identical genes have been found to be deregulated by acquired mutations or epigenetic silencing (9) . Although there are a multitude of hereditary syndromes, the most common and well characterised are HNPCC (Lynch syndrome) and familial adenomatous polyposis (FAP).

1.1.2 Familial adenomatous polyposis

Familial adenomatous polyposis (FAP) is an autosomal dominant inherited syndrome and accounts for 1% of all CRC's. FAP is characterised by the development of 100's of adenomatous colonic polyps, with resulting incidence of CRC approaching 100% by the age of 50 years (10). FAP results as a consequence of a germ line mutation of the adenomatous polyposis coli (*APC*) gene. The APC gene encodes a large multifunctional scaffolding protein that acts as a tumour suppressor by down regulating the activity of β - Catenin induced Wnt signalling(8). Aberrant activation of the Wnt signalling pathway, up regulates genes involved in cell proliferation apoptosis and differentiation, eventually resulting in malignant transformation. It is important to highlight, a single mutation in the APC gene is inadequate for malignant transformation. However, the initial mutation significantly increases the risk of accruing further genetic aberrations (KRAS, P53, TGFβR) that are required for the transition from benign adenoma to an invasive carcinoma as proposed in Vogelstein's hypothesis (11). Somatic mutations and deletions of APC are also found in most sporadic cancers, highlighting its critical role as a gatekeeper in the pathogenesis of CRC.

1.1.3 Hereditary non-polyposis colorectal cancer (HNPCC)

Hereditary non-polyposis colorectal cancer or Lynch syndrome is the most common hereditary CRC syndrome accounting for 2-3% of all CRC's. It follows an autosomal dominant inheritance pattern and renders affected patients susceptible to multiple types of cancer including CRC. The tumours are often right sided, poorly differentiated, express high degree of microsatellite instability and Crohns like lymphoid aggregates (12). Despite these high-risk histological features, HNPCC related CRC demonstrates less nodal and distant metastatic spread when compared with sporadic CRC (12). HNPCC or Lynch syndrome occurs secondary to germ line mutations in a group of genes responsible for repair of base mismatches in DNA (most common – MLH1, MSH2, MSH6 and PMS2)(8). Like HNPCC, mismatch repair genes are often epigenetically silenced in sporadic tumours conferring an identical microsatellite instability observed in patients with

HNPCC. This genomic instability results in sequential loss of function of genes regulating hallmark processes of carcinogenesis, ultimately manifesting as invasive CRC (9).

1.1.4 Regulators of Sporadic colorectal cancer

The identification of genes involved in the evolution of CRC, in patients with germ line mutations lead to the recognition, sporadic tumours also demonstrated loss of function of identical genes through deletions, somatic mutations, or epigenetic silencing (10). For example, aberrant DNA methylation results in loss of expression of *MLH1*, a critical component of the DNA mismatch repair machinery. Somatic mutation or deletions of the APC gene occurs in most sporadic CRC's, which in-turn leads to inappropriate Wnt signalling, a driver of malignant transformation (10). The inactivation of p53 pathway by mutation of *TP53* gene results in apoptosis resistance and coincides with the transition from adenoma to invasive carcinoma (13). Oncogenic mutations of the RAS, BRAF signalling pathways, results in aberrant activation of the mitogen activated protein kinase (MAPK) pathway (10). Comprehensive analysis of human CRC by whole genome sequencing has identified on average a stage IV tumour has 15 candidate cancer genes and 61 mutated passenger genes (low frequency mutation events), highlighting the enormous genetic heterogeneity of the disease (14). Further knowledge of critical genes, pathways and dissecting their interplay in driving malignant progression may provide novel targets for cancer therapeutics in the future.

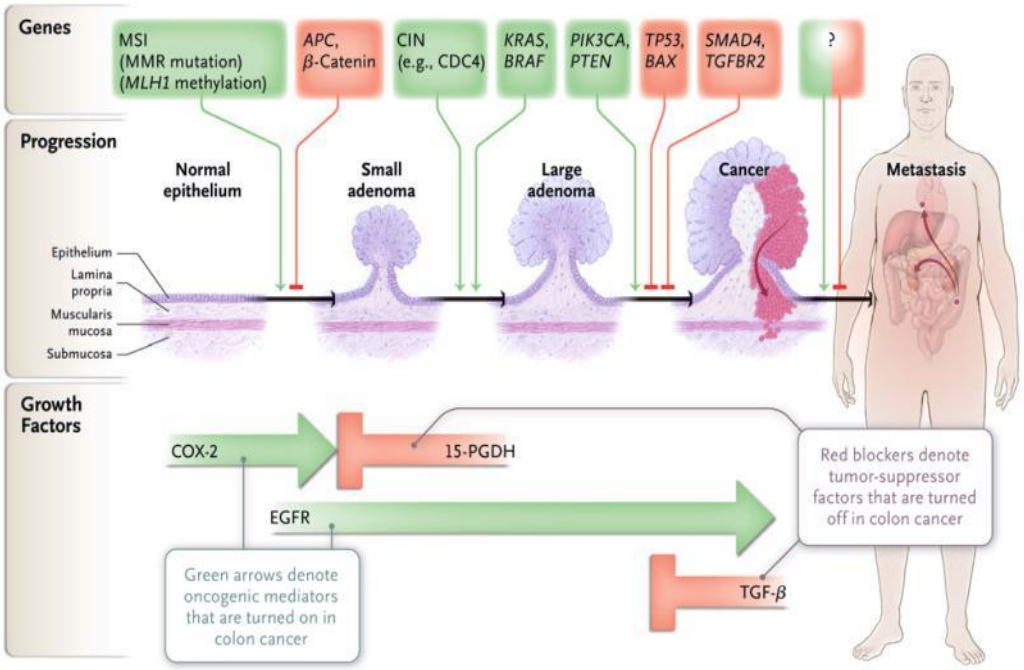

Figure 1: Schematic representation of the adenoma carcinoma sequence Genes and growth factors that drive the progression from adenoma to invasive carcinoma. The top panels presents genes that are mutated or epigenetically silenced during malignant progression. Mutations or epigenetic silencing of the MMR (*MLH1, MSH2*) pathway is associated with microsatellite instability and downstream mutations in key genes such as BAX and TGFβR2 that promote malignant transformation. Key growth factors pathways that are altered during colon neoplasia are shown in the bottom of the diagram. From Markowitz SD et al (10)

1.1.5 Colorectal cancer staging

The Dukes staging system was initially used to classify CRC progression. Dukes A was defined as tumour infiltrating bowel wall. Dukes B specifies infiltration beyond the colonic wall, Duke C indicates presence of nodal metastasis and Duke D refers to tumour infiltration with associated distant metastasis (15). This system has since been completely replaced by the tumour, node metastasis (TNM) staging system of the American joint Committee on Cancer (AJCC). The TNM staging system has been revised multiple types and is currently in its 7th edition (16). The UK continues to use the 5th edition to classify CRC progression (17). TNM classification is further grouped into four stages, to better inform prognosis and guide clinical decision-making. An outline of TNM classification and staging is provided in Figure 2 (18).

Dukes	TNM stage	
-	TX	Primary tumour cannot be assessed
-	T0	No evidence of primary tumour
-	Tis	Carcinoma in situ: intraepithelial or invasion of laminaamna propria
A	T1	Tumour invades submucosa
A	T2	Tumour invades muscularis propria
B	T3	Tumour invades through the muscularis propria into pericolic tissues
B	T4a	Tumour penetrates to the surface of the visceral peritoneum
B	T4b	Tumour directly invades or is adherent to other organs or structures
-	NX	Regional lymph nodes cannot be assessed
B	N0	No regional lymph node metastasis
C	N1a	Metastasis in one regional lymph node
C	N1b	Metastasis in 2--3 regional lymph nodes
C	N1c	Tumour deposit(s) in the subserosa, mesentery or nonperitonealized pericolic or perirectal tissues without regional nodal metastasis
C	N2a	Metastasis in 4-6 regional lymph nodes
C	N2b	Metastasis in seven or more regional lymph nodes
C	M0	No distant metastasis
D	M1a	Metastasis confined to one organ or site (e.g. liver, lung, ovary, nonregional lymph node)
D	M1b	Metastasis in more than one organ/site or the peritoneum

Figure 2: AJCC TNM staging system. Outline of the TNM 5th edition staging system for CRC (18).

1.1.6 Colorectal Cancer Management

The management of colorectal cancer involves multiple treatment modalities and involves complex multidisciplinary planning with treatment approaches based on cancer stage, patients characteristics, symptoms, and tumour characteristics. Disease recurrence is the primary cause of mortality and patients are risk stratified by staging (30% stage II and 50% stage III) cancer progression at the time of presentation (19). Treatment options include surgery, radiotherapy, systemic chemotherapy and interventional radiology based techniques. Surgical resection alone is curative for patients with early stage (I and II) disease. For patients with stage II disease with high-risk features (pT4, Extramural

vascular invasion) or stage III (nodal involvement) disease, adjuvant chemotherapy is recommended (20). Anti-metabolites and DNA damaging agents such as 5-flurouracil (5FU) and oxaliplatin or irinotecan used as combination therapy continues to represent the main treatment options (21). In more recent years, monoclonal antibodies against EGFR (Cetuximab) and VEGFR (Regorafenib) have been added to chemotherapeutic regimes to improve outcomes. However, their efficacy in the adjuvant setting has remained controversial. If the patient experiences disease recurrence; surgical resection of metastasis from the liver or lung may be offered to carefully selected groups, with survival ranging between 25 to 50% at 2 years. Unfortunately, up to 75% of these patients experience recurrence within 18 months (22). If surgical resection is not an option, chemo-radiotherapy is the only available treatment modality and oncological outcomes in these patients continue to remain poor. Diagnostic approaches to better risk stratify disease trajectory and predict drug response to therapeutic agents are urgently required to improve outcomes in patients with CRC.

1.1.7 Neo-adjuvant and Adjuvant Chemo-radiotherapy for CRC

Section 1.1.6 provides an overview of the management of CRC. In this section, I will discuss in more detail the clinical evidence for administering chemo-radio therapeutic treatment modalities and discuss the need for greater precision in prognosticating risk and selecting drugs from which patients might derive maximal benefit. In 2004, the MOSAIC trial (Multicentre international study of oxaliplatin / 5-Flurouracil/ Leucovorin in the adjuvant treatment of colon cancer) reported addition of oxaliplatin to 5-FU / Leucovorin (FOLFOX) resulted in improvements in oncological outcome in the adjuvant setting, making it the standard of care for patients considered to be at high risk for disease recurrence after surgery (20). The improvement in progression free survival achieved by administering FOLFOX therapy in the adjuvant setting is undeniable. However, the MOSAIC trial data also highlights that up to 25% of patients derive no benefit in terms of survival outcome from FOLFOX therapy, but endure the significant side effects associated with systemic chemotherapy, due to the current inability to identify patients with tumours

that are resistant to FOLFOX therapy (23). Alternative adjuvant regimens, including FOLFIRI and targeted therapies such as Cetuxmiab or Bevacizumab have also failed to improve outcome in the adjuvant setting (24-26). This clearly highlights the need for advances in adjuvant treatment options to achieve greater precision and improve outcome in patients with CRC.

Historically, the primary management of rectal carcinoma was surgical resection, however up to 25% of patients experienced local recurrence, before the total mesorectal excision (TME) plane was described (27). Although, local failure rates have since considerably reduced, a significant proportion of patients continued to experience recurrent disease. This prompted clinical trial of adjuvant and neo-adjuvant chemo/radio therapeutic strategies to improve oncological outcomes. Multiple studies have investigated the impact of pelvic radiation in rectal cancer and reported a significant reduction in local recurrence (28). Whilst studies that examined a role for adjuvant chemotherapy have reported reduced incidence of distant recurrence (29). In more recent times, clinical trails have strived to decipher the most optimal sequence for application of adjuvant and neo-adjuvant treatment modalities and tried to more precisely categorise patients that will acquire maximal benefit from the administered treatment.

Two trials, namely the European organisation for research and treatment of cancer (EORTC) (30) and the Federation Francophone de Cancerologie (FFCD) (31) investigated the impact of neo-adjuvant chemo-RT over radiotherapy (RT) alone in patients with T3/T4 resectable rectal cancer. The trials concluded combined therapy reduced 3-year local failure rates, but no significant difference in 5-year overall survival or 3 year progression free survival was noted. However, due to the impact of combined therapy in reducing local recurrence, neo-adjuvant chemo-RT has become the standard of care for patients with rectal cancer. Although studies have since investigated the impact of pre-operative short course vs. long course radiotherapy, the benefit in reducing local failure rates cannot be disputed. A significant proportion of patients however continue to experience recurrence, for whom treatment options are limited. Emerging data in recent years

suggests, all cancers do not respond homogenously to therapy and biomarkers to detect resistant tumours may aid in the application of radio-sensitisers for patients with radio resistant rectal cancer in future years (32).

1.1.8 Prognosticating and predicting outcome in patients with CRC

Over the years there has been growing acknowledgement of the molecular heterogeneity of CRC and its contribution to stage independent variability in disease trajectory and treatment response (33). It has been shown for example that, molecularly defined sub-populations of patients with stage III disease have survival estimates comparable to that of certain patients with low risk stage II disease (34). The need for biomarkers, particularly to risk stratify patients with early stage disease is urgently required to improve oncological outcomes. Unfortunately, validated predictive markers to quantify recurrence risk or predict response to adjuvant chemotherapeutic treatment strategies are currently not available.

Some of the best-described prognostic markers of poor outcome are pathological features of a tumour. The most robust histopathalogical indicator of poor prognosis in stage II and III colon cancer is T4 disease. Lympho-vascular and perineural invasion have also been highlighted as high-risk features. Some retrospective studies have suggested patients with node negative / Perineural invasion positive tumours can have oncological outcomes inferior to patients with node positive disease (35). In contrast, tumour grade has been shown to be inconsistently associated with poor outcome in patients with stage II disease. The reason for this observed inconsistency is the association between poor differentiation and microsatellite instability (MSI). In this subset of patients, poor differentiation status does not negatively impact prognosis. Therefore it can be extrapolated, that the aggressiveness of poorly differentiated tumours is restricted to microsatellite stable tumours. This example clearly highlights the significant influence the genetic make up of a tumour can have on behaviour and treatment response. This example provides proof of principle that greater insight into the biological contribution of gene mutations or protein expression to tumour behaviour can significantly improve

precision in prognosticating disease trajectory or predicting response to adjuvant chemo-radiotherapeutic modalities.

1.1.9 CRC gene expression signatures

As discussed, defective mismatch repair status has become a validated prognostic factor in patients with CRC. This effect is particularly pronounced in stage II patients where MSI is associated with improved oncological outcome. It is important to highlight however that, once nodal involvement is established defective mismatch repair has limited impact on disease trajectory (36). Studies investigating the potential role of MSI as a predictive biomarker in colon cancer have reported mixed results. Selective sensitivity of tumours with MSI to irinotecan and bevacizumab was initially reported by preclinical and clinical trials (37). However, retrospective analysis of clinical trial data in the adjuvant setting has reported a limited contribution as a predictive biomarker (38).

The *RAF* gene family include BRAF a serine threonine kinase involved in the RAS-RAF-ERK signalling pathway which influences cell growth, invasion and metastasis. BRAF mutations are highly variable with rates ranging from 5% in microsatellite stable tumours to 50% in the setting of MSI. Up to a 6 fold increase in recurrence risk and mortality has been reported in left sided, micro-satellite stable tumours with BRAF mutations. Whilst in the setting of right-sided tumours with MSI, BRAF mutations do not significantly impact disease trajectory. As a predictive biomarker, BRAF mutation is associated with poor response to anti-EFGR therapies with pooled analysis of clinical trial data suggesting reduced disease free and overall survival when compared to wild type tumours regardless of treatment group (39).

An extensive number of studies have confirmed that KRAS exon 2 (codons12 or13) mutations predict resistance to anti-EGFR monoclonal antibodies. However, approximately 65% of patients with wild type KRAS status have also been shown to be resistant to therapy, due to factors that are currently unclear (40). A potential contributing factor to this observation may be secondary to BRAF mutation status not being considered routinely. When treated with Cetuximab in conjunction with conventional

chemotherapy, KRAS mutations were found to confer reduced response rate when compared to WT in the metastatic CRC setting. However in the adjuvant setting, addition of cetuxmiab to FOLFOX or FOLFIRI therapy did not confer any significant benefit in oncological outcome (41). Genetic analysis of the CALGB/SWOG 80405 clinical trial confirmed, KRAS WT patients randomised to conventional chemotherapy plus cetuxmiab or bevacizumab demonstrate an overall improvement in median survival however no differences were observed between treatment arms with the addition of targeted therapies (40). These results suggest, in selected RAS- wild type populations' targeted therapies enhance clinical endpoints in metastatic colorectal cancer (mCRC).

The Phosphoinositide 3-kinase is a heterodimeric lipid kinase with regulatory and catalytic roles in cell growth, proliferation, survival and apoptosis due to activation of the mTOR/AKT-PTEN pathway. *PI3KA* encodes the catalytic subunit of p110a, which is rendered constitutively active by mutations in 10-20% of CRC's (40). Of the *PI3KA mutations* observed, exon 9 and 20 are responsible for >80% of the mutations found in CRC. Currently the predictive influence of *PI3KA* mutations as a biomarker for resistance to targeted therapies remains unclear. Initial studies evaluating the response of patients with *PI3KA* mutations to targeted therapies have reported inferior clinical end points when compared to WT tumours. However, reported results have not been consistent, with resistance to treatment being observed only in *PI3KA* exon 20 mutations, but not exon 9. The underlying mechanism for this resistance mechanism is currently unclear considering both mutations result in constitutive activation of the PI3K pathway. Greater understanding of the signalling cascade will aid in the development of this mutation into a predictive biomarker in future years.

Due to the growing acknowledgement of the genetic heterogeneity of CRC and the limitations presented by risk stratifying patients using histopathalogcial features, independent scientific groups (CRC subtyping consortium) pooled data sets to investigate the presence or absence of core gene signature subtypes in CRC (33). Despite the heterogeneity of datasets, all groups highlighted the negative impact of mesenchymal

gene signatures for CRC patients. Patients with tumours belonging to the mesenchymal tumour subtype were repeatedly found to have reduced survival and increased risk of distant recurrence in all subgrouping algorithms (38). Differences in clinical outcomes observed by subtyping for specific gene signatures confirm that the biological processes implicated in the mesenchymal subtype are clinically relevant. Mesenchymal gene signatures in cancer are associated with the embryologically conserved process of epithelial to mesenchymal transition (EMT). *In-vitro* studies, pre-clinical models and human tissues analysis have all suggested that EMT is associated with increased risk of disease recurrence and poor response to conventional chemotherapeutic agents currently used in the clinical setting (42, 43). Therefore one can hypothesise, targeting EMT related processes or recognising EMT in tissue specimens obtained from patients with early stage CRC could be used to identify patients at high risk of recurrence and thus modify clinical management to improve cancer outcomes in future years. In the next section I will overview the process of cancer cell metastasis and discuss evidence highlighting the contribution of EMT to cancer spread and chemotherapy resistance.

1.1.10 Cancer metastasis

Cancer metastasis is a highly complex, multi stage process during which certain cells acquire the ability to break free from sister cells, invade the extra-cellular matrix (ECM) and basement membrane (BM), intravasate into the systemic circulation, evade the immune system, extravasate into distant organs and proliferate to form metastatic foci as shown in figure 3 (44, 45). The traditional 'late dissemination model' suggests, acquisition of metastatic capacity occurs at a late stage after the accrual of multiple mutations during tumorigenesis(46). The more contemporary 'early dissemination model' suggests tumorigenesis and metastatic capacity represents divergent cellular events and consequently does not have to occur as a late event during the progression of a malignant tumour (46, 47).

CRC is an epithelial adenocarcinoma that was thought to metastasise by 'collective invasion' of clusters of epithelial cells (48). In recent years, aberrant expression of embryonic transcription factors that induce epithelial to mesenchymal transition (EMT) have been identified as playing a key role in promoting metastasis (49, 50). EMT facilitates the down regulation of epithelial junctions, promoting the dissemination of single mesenchymal cells into the circulation. Understanding the cellular mechanism driving metastasis is particularly relevant in CRC as the vast majority of cancer deaths are not associated with the primary tumour, but to metastatic spread (22). Up to 30% of patients with stage II disease and 50% of patients with stage III disease experience recurrence within 5 years (22). Long-term survival outcomes in these patients continue to be poor even with the latest therapeutic modalities. Better dissection of cellular mechanism driving metastasis and development of biomarkers, that can prognosticate recurrence risk, are urgently required to tackle this complex disease process.

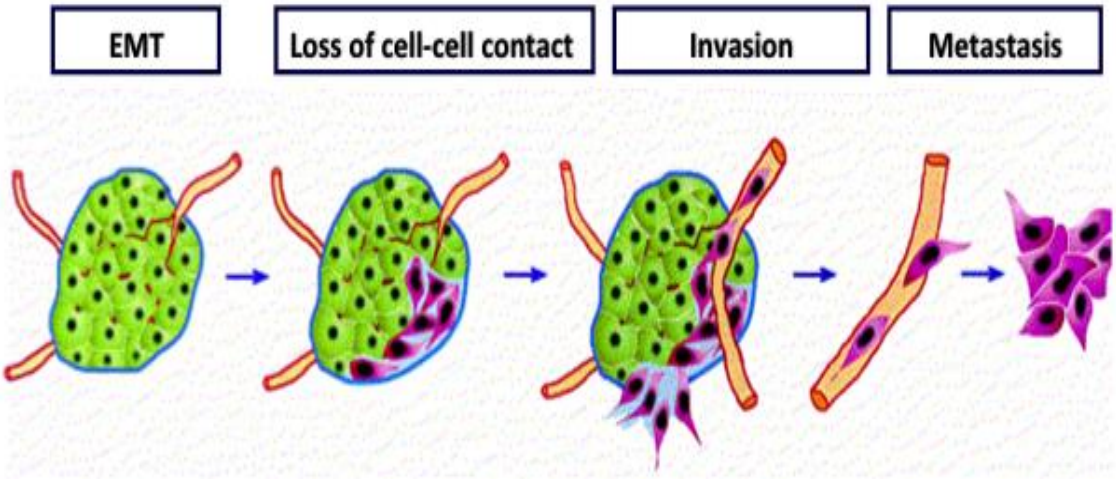

Figure 3: Schematic representation of the metastasis cascade. This figure provides a schematic representation of the multiple stages of metastasis. Cancer cells disseminate from the primary tumor into the circulation by down regulating adhesion molecules and dissociating from sister cells. Disseminated tumor cells are found very early during tumorigenesis and may consist of single cells or clusters. In the circulation, mesenchymal cancer cells exhibit capacity to evade the immune system and seed in distant organs. Mesenchymal cancer cells subsequently proliferate to establish detectable macro-metastatic foci. Adapted from Cavallaro et al (51).

1.2 Epithelial to mesenchymal Transition (EMT)

EMT is a conserved genetic programme that promotes events such as neural crest formation and gastrulation during embryogenesis (52). Emerging evidence suggests this conserved genetic programme that promotes cell migration during embryogenesis may also play a critical role in promoting metastasis and chemo resistance in cancer (44, 53). EMT has been classified into three different subtypes, developmental (Type 1), fibrosis / wound healing (Type 2) and cancer (Type 3) (44). The term “epithelial to mesenchymal transformation” was initially coined by Hay et al following her observations from studies in developmental biology (54). The term ‘transformation’ was later changed to ‘transition’ to reflect the plasticity and reversibility of this cellular event.

EMT was initially considered a binary (epithelial or mesenchymal) event, marked by the acquisition of cardinal features such as E-cadherin down regulation, acquisition of a mesenchymal phenotype, expression of stem cell markers, increased metastatic capacity and apoptosis resistance through poorly understood mechanisms (55). More recently however, cells are thought not to oscillate between a full epithelial or mesenchymal phenotype. Instead, cells in which EMT has been triggered are thought to transition through a range of intermediary phases, described as a partial EMT (53). The identification of intermediary states in circulating cancer cells has further confirmed the *in-vivo* relevance of the partial EMT hypothesis previously only observed in 2D cell culture models (56).

The model proposes, within a solid tumour a subpopulation of cells undergo EMT, this results in a change of expression in adhesion molecules, resulting in dissociation from neighbouring cells and adoption of a metastatic phenotype. EMT is associated with increased capacity to intravasate into the blood stream, escaping detection by immune cells and extravasation into distant organs. Once in distant organs, the reverse process of mesenchymal to epithelial transition or ‘MET’ is triggered to form metastatic foci (56). EMT is executed in response to pleiotropic signalling factors that can promote the expression of EMT inducing transcription factors (TF), (SIP, ZEB, TWIST, SNAIL) thought to be master regulators of EMT (57). In this section, I will use the four pillars of EMT,

namely change in expression of adhesion molecules, increased metastatic capacity, stemness and chemo resistance as reference points to discuss EMT in detail.

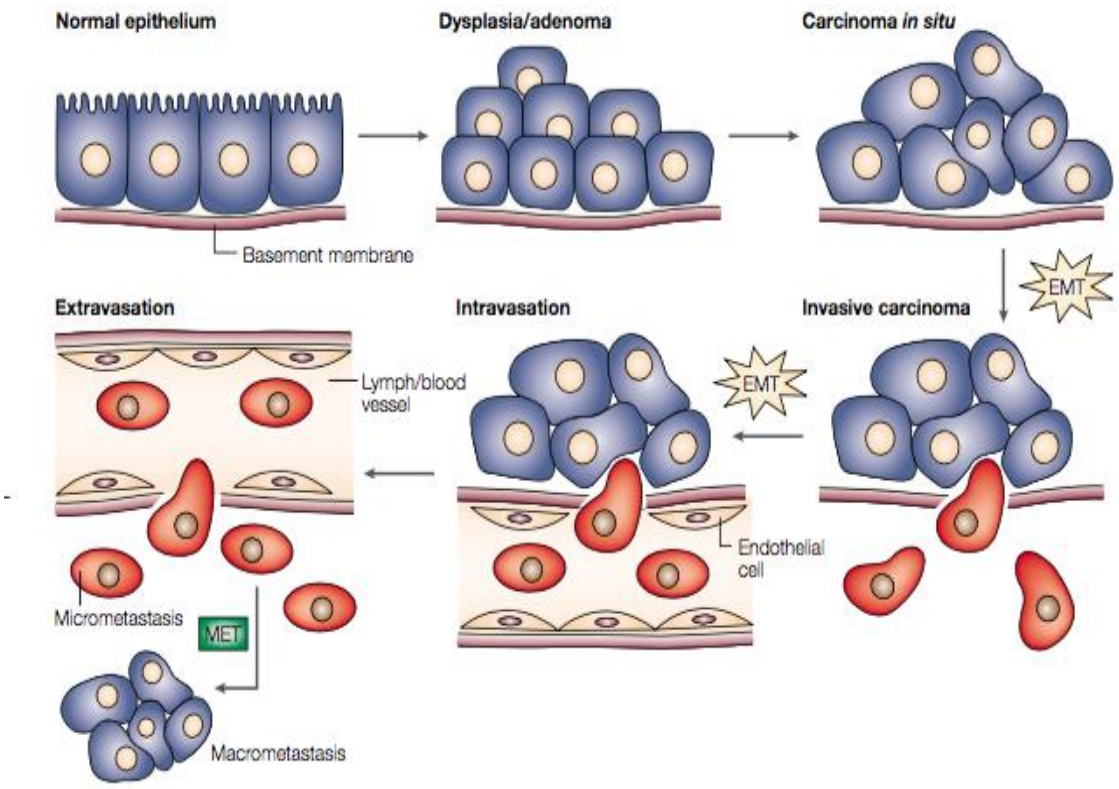

Figure 4: Schematic expression of the role epithelial to mesenchymal transition (EMT) in cancer metastasis. Epithelial cells lined by a basement membrane can transform into an adenoma through aberrant local proliferation. Further accumulation of genetic mutations results in malignant transformation. A sub-population of cells within a solid tumour undergo EMT, which promotes fragmentation of the basement membrane. Mesenchymal cancer cells poses cytoskeletal adaptations that facilitate metastasis and intravasation into the systemic circulation. At secondary sites solitary carcinoma cells can either remain senescent or proliferate to form macro-metastasis by undergoing the reverse process of mesenchymal to epithelial transition (MET). Thierry et al (58).

1.3 EMT cytoskeleton and cell adhesion markers

Epithelial tissues specialise in forming an effective barrier against pathogens and secrete or absorb macromolecules. To perform these functions effectively, epithelial cells have to form specialised association through the assembly of adhesion junctions that stabilises the integrity of the tissue (44). Epithelial cells contain several major classes of functionally diverse cell-cell junctions, namely adherens junctions, desmosomes, gap junctions and tight junctions (59). Of the sub-classes, junctional complexes, adherens and tight junctions

have been demonstrated to be most central in maintaining epithelial morphology and behaviour (59). One of the first adhesion complexes to form when epithelial cells interact is an adherens junction, initiated by interaction of opposing cadherin domains. Cadherins are trans-membrane proteins linking two adjacent cells to the intracellular actin cytoskeleton using an anchoring protein complex, that includes p120 catenin, β-catenin and α-catenin (60). The classical cadherin's are E-, R, N- and P- cadherin (59). A hallmark of EMT is the down regulation of E-cadherin and up regulation of N-cadherin in fully transformed mesenchymal cells (53). Although structurally similar, N-cadherin mediates a weak and transient association with sister cells and is strongly associated with migratory behaviour (59). Yamada and co-workers demonstrated N-cadherin knock down in mesenchymal cells inhibited migratory behaviour in a 3D matrix (61). Kotb et al found that knock in interference of E-cadherin with N-cadherin predisposed to malignant transformation in a murine model (62).

E-cadherin has long been of interest to cancer biologists, as its absence has been associated with increased metastatic potential. Oka et al and others reported up to 85% of cancer metastases from multiple primary tumour sites lacked E-cadherin (59). It is postulated, down-regulation of E-cadherin results in dissociation of β-catenin from the cytoplasmic cadherin complex, which in turn translocation to the nucleus and activates the Wnt pathway promoting EMT (63). However, β-catenin KD in shE-cadherin induced EMT phenotype demonstrated only a partial reversal of EMT. Further, transduction of a constitutively active mutant β-catenin was insufficient to induce mesenchymal transformation, implying β-catenin is necessary but not sufficient to induce EMT (59) . Recent studies have now demonstrated, EMT inducing transcription factors (TF) including SNAIL, Slug and SIP1/ZEB2 directly binds to the promoter of the *CDH1* gene thus repressing transcription (64). These transcription factors that have been found to be up regulated in many adenocarcinomas and expression associated with poor oncological outcomes (65, 66). E-cadherin down-regulation has also been reported to up regulate Twist expression possibly through increased RAS signalling, however the exact mechanism requires further mechanistic dissection(67).

Tight junctions form the most apical junctional complex in epithelial cells and play several essential structural roles. Most critically they form a seal between cells that selectively regulate exchange of ions, macromolecules and immune cells between the apical, luminal and baso-lateral compartments. Secondly, they form a diffusion barrier in the plasma membrane that results in separate apical and baso-lateral domains. Thirdly, tight junctions link adhesion molecules to an intracellular scaffold, thus anchoring cytoskeletal elements and signalling molecules that regulate cell proliferation and differentiation (59). Claudins are the most diverse component of tight junction. Twenty-four family members have been identified to date. They poses 4 trans-membrane segments and a cytoplasmic PDZ domain which interacts with zonula-occludens family (ZO1, ZO2, ZO3) of proteins (59).

The initial observation that EMT inducing TF's supress claudins, lead to the expectation of familial uniformity in behaviour (68). However, evolving evidence has demonstrated a more varied and inconsistent expression profile in mesenchymal cancer cells. Dhawan and colleagues reported increased expression of nuclear claudin-1 in metastatic colon cancer cells but not in the primary tumour or normal colonic mucosa (69). Further, ectopic expression of claudin-1 in SW480 cells promoted EMT whilst its KD in SW620 (metastatic cell) promoted MET and reduced liver metastasis in murine xenografts (69). On the other hand, results from other primary cancers including breast and lung adenocarcinoma have been inconsistent, suggesting claudin-1 may have different tissue and tumour specific roles (59). Other claudins that have been studied include claudin-6 and 7, where reduced expression has been shown to promote increased migration, invasion and anoikis resistance (70, 71). To the contrary, increase expression of claudin-2,3,4 and 5 have been shown to promote invasion and increased metastatic capacity in breast cancer cells (59).

Occludins like other cell adhesion molecules are down regulated during EMT. Occludins in general play a tumour suppressive role and epigenetic silencing results in increased tumour metastasis (70), whilst ectopic expression sensitises cells to apoptosis and inhibits migration (72). Regulatory molecules (ZO1, 2 and ZONAB) also play a role in epithelial differentiation and EMT. ZO 1 and 2 link the cytoplasmic tails of adhesion proteins to signalling molecules. Georgiadis and co-workers found that ZO-1 KD or ZONAB overexpression results in increased proliferation and EMT like changes in retinal pigmented epithelium (59). Integrin's facilitate the adhesions of cells to the extracellular matrix. The interaction between integrin's and the ECM can trigger activation of intracellular signalling pathways. αVβ6 is an integrin that is up regulated in CRC cells that have undergone EMT, when compared to normal colonic epithelium, however the biological consequence of this event in CRC remains unclear (73). Vimentin is a type III intermediate filament that forms a major constituent of the cytoskeleton in mesenchymal cells such as normal fibroblasts, endothelial cells and neuronal precursors (74, 75). Vimentin provides resistance against mechanical stress and maintains cellular integrity. EMT inducing transcription factors have been associated with increased expression of vimentin and acquisition of a spindle like phenotype in many cancers (58). Increased expression of vimentin is now considered a hallmark of EMT and its expression is associated with invasion and poor oncological outcomes in patients (76-78).

Alterations to the expression profile of proteins associated with cell motility have also been reported after EMT. α-SMA is an actin variant often expressed in vascular smooth muscle cells and myo-epithelial cells. It contributes to transduction of mechanical forces and used as a marker of myo-fibroblasts (79). Over expression of α-SMA has been associated with EMT, motility and cancer metastasis (80). β-catenin is an integral part of cadherin junctions and serves as a structural and signalling protein (81). E-cadherin down regulation results in dissociation from the cadherin complex and translocation to the nucleus. Increased abundance β-catenin in the cytoplasm results in Wnt signalling activation and induction of EMT pathways (82). APC mutations result in reduced β-catenin degradation and was proposed as a critical event in the transition of adenoma to invasive

carcinoma by Vogelstein. E-cadherin down regulations and increased β-catenin expression in the nucleus has been used as marker of EMT in various studies (63).

Cytokeratins are intermediate filament proteins that interact with components of adherens junctions to provide integrity and mechanical stability for cells (83). Cytokeratins are coded for by 54 genes, which are classified into acidic (type I CK 9-40) and neutral (type II, CK 1-8 and 71-86) subtypes. These proteins hetero-dimerise to form functional complexes composed of one acidic and one neutral CK. The expression profile of CK's is often used as biomarkers of cancer differentiation or disease states (84). For example CK 7/20 has been associated with CRC progression (85). CK19 expression is associated with primary biliary cirrhosis (86). Recently, CK 8/18 loss has been associated with increased metastatic capacity (87). These cells also exhibit features of EMT such as increased metastatic capacity and apoptosis resistance (88). Actin, a highly abundant microfilament has been demonstrated to be modulated by EMT pathways. Actin plays a critical role in cell motility and polarity. Recent studies have demonstrated expression of actin bundling protein fascin is regulated by EMT inducing TF SLUG, promoting migration and metastasis in pancreatic cancer (89).

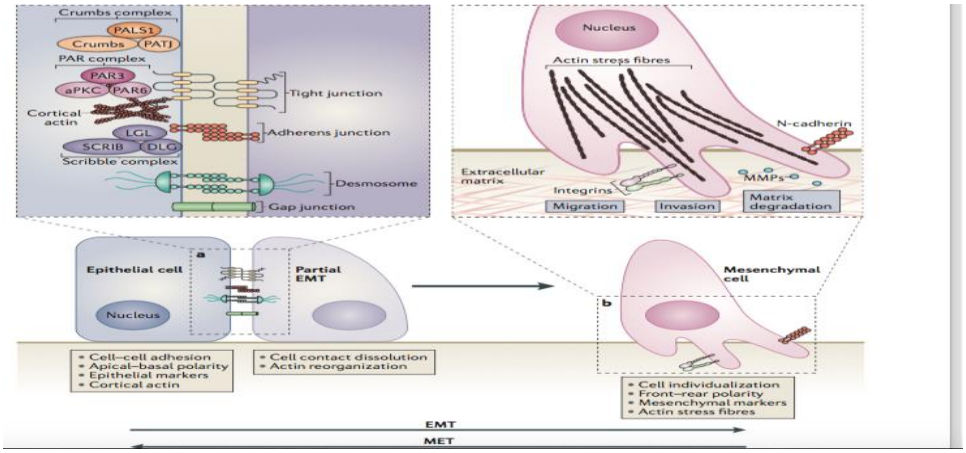

Figure 5: Cell adhesion and cytoskeletal changes that occur during EMT. a) The initiating step of EMT is the dissolution of epithelial cell-cell adhesion molecules, which include tight junctions, adherens junctions, gap junctions and desmosomes. EMT also involves dissolution of the Crumbs and Scribble polarity complexes, leading to a switch from apical-basal polarity to front-back polarity. The repression of epithelial genes is concomitantly associated with expression of mesenchymal ones. B) Next the cell undergoes cytoskeletal reorganisation and acquires increased metastatic capacity, which phenotypically manifests through the formation of lamellipodia, invadopodia and filopodia. Mesenchymal cells also express matrix metallo-proteases resulting in fragmentation of the basement membrane. These changes promote dissemination of single cell and formation of secondary metastasis (57).

1.4 EMT and Cancer metastasis

As discussed previously in section 1.1.10, metastasis is a complex multistep process. Firstly, epithelial cancer cells become motile and degrade the surrounding extracellular matrix (ECM) to invade the surrounding parenchyma. These cells subsequently intravasate across the endothelial lamina of blood or lymphatic vessels and enter the systemic circulation. Within the circulation, cancer cells evade the immune system and extravasate across the capillary endothelium to the parenchyma of distant organs. In the new stromal environment, small subsets of cells establish micro-metastasis that subsequently transform into secondary tumour deposits that become life threatening to patients. In this section, I will discuss the contributory role of EMT pathways in each stage of the metastatic cascade to provide an outline of the available evidence that links cancer metastasis and mesenchymal transformation. The notion that EMT pathways play a critical role in promoting metastasis comes from the observation that early stage adenocarcinomas continue to express epithelial biomarkers (E-cadherin, Cytokeratins) whilst advanced carcinomas display mesenchymal traits (90). However, the more contemporary 'early dissemination model' suggests invasion and metastasis pathways are divergent in nature and the ability to form secondary deposits is primarily influenced by the intrinsic genetic make-up and tumour microenvironment of cells that have undergone malignant transformation.

In support of the 'early dissemination model', studies have reported Twist1 (EMT-TF) mRNA expression in atypical duct hyperplasia, a very early stage of breast cancer development in the MMTV-Neu mouse model (91). Inter-crossing RIP-Tag2, a mouse pancreatic cancer model with transgenic mice that maintain E-cadherin expression in pancreatic cancer cells, arrested tumour progression at the adenoma stage, whereas dominant negative E-cadherin expression resulted in early metastasis (92). Finally, genetic deletion of E-Cadherin in a p53 null model resulted in lobular ductal carcinoma, a subtype of breast cancer that presents as individual migrating tumour cells. The above evidence strongly suggests, activation of EMT pathways facilitates down regulation of cell-cell epithelial adhesions and promotes metastasis irrespective of tumour invasion (93).

Once malignant cells down regulate epithelial adhesion molecules and undergo mesenchymal transformation, invasion of the surrounding parenchyma requires the ability to degrade the underlying basement membrane and ECM. EMT facilitates this process by up regulating expression of matrix degradation enzymes and proteases. SNAIL expression in breast cancer cells leads to up regulation of matrix metallo-proteases (MMP) and breakdown of the basement membrane, whilst inhibition leads to decreased MMP9 expression, tumour growth and metastasis (94). More recent evidence has shown EMT pathways also promote the formation of invadopodia, which are actin based structures that recruit proteases to cell-matrix contact points to degrade the ECM and facilitate invasion (95). The above data suggests EMT pathways not only play key roles in down regulating epithelial cell dissociation but also provide the ability to breakdown the ECM and initiate the metastatic cascade.

Invading cancer cells need to be able to intravasate into the systemic circulation, by trans-endothelial migration and survive anoikis for successful dissemination. Using a trans endothelial migration assay Drake et al reported ZEB1 (EMT-TF) expression in prostate cancer cells (PC-3) enhanced migration through the endothelial barrier (96). Using a modified chick chorioallontronic membrane (CAM) assay, Ota et al reported SNAIL expressing breast cancer (MCF-7) cells exhibited enhanced capacity to intravasate into the host vasculature by activation of membrane bound MT1-MMP (94). Up on entering the systemic circulation, the migrating cancer cells need to be able to evade the immune system, survive anoikis and extravasate. Evidence that activation of EMT pathways, promotes successful dissemination into the systemic circulation was reported by Rhim et al, who reported detection of SIP1/ZEB2 expressing CTC's during premalignant stages of pancreatic cancer progression (97). Similar findings were reported in squamous cell carcinoma, where Twist1 expression resulted in a significant increase in the number of malignant cells in the systemic circulation. The association between mesenchymal tumour markers and circulating tumour cells (CTC's) has also been demonstrated in many clinical trails (98). CTC's from breast cancer patients revealed high levels of mesenchymal markers and low levels of epithelial markers. CTC's from

hepatocellular carcinoma patients that experienced metastasis expressed 20 times more Snail transcripts when compared with patients with no metastasis (99). The above data confirms EMT pathways not only promote dissociation from the primary tumour, but also play a critical role in promoting extravasation and survival in the systemic circulation.

The final stages of cancer metastasis involve extravasation and formation of secondary deposits in distant organs. A number of studies have associated mesenchymal cancer cells with increased capacity to extravasate the systemic circulation and form secondary deposits. However, most of these studies have relied up on injecting large cell numbers into the tail vein of mice and assessing tumour formatting in the lungs. This findings need to be interpreted with caution as tail vein injections can result in the rapid arrival of a large number of cells in the lung micro-vasculature, thus promoting intra-vessel growth rather than true extravasation. Recently, Stoletov et al using a zebra fish model demonstrated EMT marker expression in breast cancer cells promotes extravasation and successful formation of micro-metastasis (100). After successful extravasation, mesenchymal cancer cells have to undergo the reverse process of mesenchymal to epithelial transition or 'MET' to form macro-metastasis. The process of MET is critical to successfully establish macro-metastasis as EMT leads to senescence and inhibition of cell proliferation by depleting cyclin dependent kinases (101). Experimental evidence for MET was strongly demonstrated by Tsai et al, using a Twist1 inducible skin cancer model, that demonstrated the loss of EMT inducing signals at the distant site was essential for cell proliferation and macro-metastasis formation (99). Similarly, Ocana et al reported loss of novel EMT inducer Prrx1 is required for successful distant metastasis formation of lung metastasis in a murine breast cancer model (102).

Experimental and clinical evidence supporting a critical role for EMT in cancer metastasis is overwhelming. EMT inducing TF's are often expressed at the invasive front of tumours and associated with increased metastatic capacity and poor oncological outcomes (65, 66, 103). The role of EMT in cancer metastasis is however far from fully understood (53). The notion that aberrant activation of EMT pathways is essential for all

carcinomas to metastasise needs to be qualified and frequently disputed by clinical pathologists (104). A substantial part of this reluctance comes from contradicting results observed in studies reporting oncological outcomes in patients expressing EMT-TF's. Methodological variation in scoring, TF studied, tumour type investigated and laboratory technique applied may have however contributed to these inconsistencies. The development of a standard scoring system by Tan et al may help standardise reporting in the future and help translate mesenchymal traits into biomarkers (105). EMT inducing TF's face a further technical challenge; mesenchymal biomarkers are often expressed by tumours associated stromal tissue, making it difficult to differentiate carcinoma cells from their surrounding stroma. Studies in breast and ovarian cancer have also highlighted the existence of cells expressing both epithelial and mesenchymal features (79, 106). Therefore binary scoring systems, which do not consider cells of an intermediate phenotype, may have underestimated the contribution of EMT to metastasis thus resulting in contradicting reporting of results.

Mechanistic studies investigating the contribution of EMT to metastasis in mouse models, have demonstrated Twist1 activation although important for invasion and formation of CTC's is not essential for metastatic colonisation (107, 108). These findings are, consistent with the plastic nature of EMT and the requirement to undergo MET for colonisation. Zheng et al demonstrated loss of SNAIL or Twist does not block systemic dissemination in pancreatic ductal adenocarcinoma (PDAC) (107). The study however does not address the issue of co-operation between different EMT-TF and consequently it is plausible absence of a single TF may not be sufficient to block EMT pathways. To the contrary, enrichment of mesenchymal markers has been reported in CTC's (106, 109, 110) and intravital microscopy has demonstrated both EMT and MET *in vivo (111)*. An elegant study by Krebs et al using the same murine model (KPC) of pancreatic cancer, driven by Pdx1-cre mediated activation of mutant *Kras* and *p53,* reported ZEB1 to be a key TF for the formation of precursor lesions, invasion and notably metastasis. Depletion of ZEB1 supressed phenotypic/metabolic plasticity, stemness and colonisation capacity resulting in reduced metastasis(112). These studies provide compelling evidence for a

role for EMT in the metastasis cascade. The question of whether EMT is essential for metastasis is yet to be fully answered, more studies in different primary tumours is required before a critical role for EMT in metastasis can be ruled out.

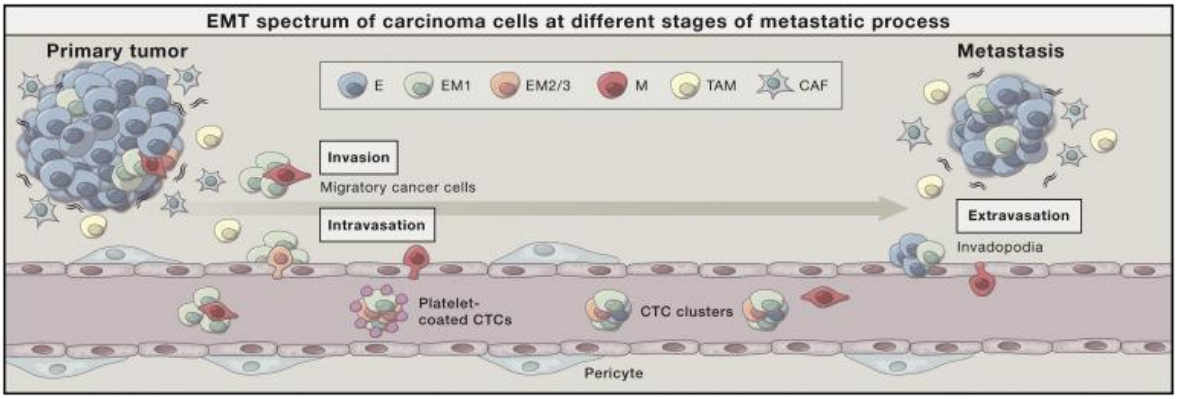

Figure 6: This schema highlights the spectrum of transition states during EMT. Cells that have undergone EMT dissociate from sister cells and acquire increased capacity to metastasis. Mesenchymal cells degrade the ECM and intravasate across the endothelial lamina. Within the systemic circulation, mesenchymal cells poses increase ability to survive anoikis and evade the immune system. Mesenchymal differentiation in the circulation is maintained by secretion of TGFβ by adherent platelets. Extravasation occurs at distant sites where cells undergo the reverse process of MET and proliferate to form secondary deposits. Adapted from Nieto 2015 (53).

1.5 EMT induces resistance to chemotherapy and radiotherapy

Sommers et al was the first to describe the link between EMT and chemo resistance in 1992. The study observed that MCF7 cells with mesenchymal traits were resistant to treatment with Adriamycin and Vinblastine (113). A seminal study by Mani et al reported induction of an EMT in mammary epithelial cells results in acquisition of stem cell markers promotes mammosphere formation and enhances tumour-initiating capacity (110). A subsequent drug screen of 16000 agents performed by Gupta and colleagues highlighted breast cancer cells that had undergone an EMT exhibited apoptosis resistance to 97% of conventional chemotherapeutic agents used in the study. Since then it has been increasingly recognised, that EMT is accompanied by chemoresistance in pancreatic, breast, colon and prostrate cancer (66, 113-116). Subsequent studies have reported, oxaliplatin resistant CRC cells exhibit a mesenchymal morphology and display features suggestive of an EMT (117). SNAIL expression in CRC cells promotes apoptosis resistance to 5-FU and ionising radiation (IR) (118), whilst over expression of mir200c a negative regulator of EMT restored sensitivity (119). Recently, Fischer et al developed a

mesenchymal lineage tracing system and demonstrated EMT significantly contributes to formation of recurrent lung metastasis after treatment with cyclophosphamide. In this study, metastasis that occurred in control mice primarily exhibited cells of an epithelial lineage, whilst the treated animals exhibited a significantly greater population of mesenchymal cells. The authors postulated the observed resistance is secondary to acquisition of EMT associated properties such as; apoptosis resistance, reduced proliferation and increased expression of chemoresistance related genes. The critical contribution of EMT TF's towards promoting chemoresistance was proven by abrogating the acquired apoptosis resistance by over-expressing mir-200 (108). Zheng and co-workers also performed an elegant experiment to demonstrate the importance of EMT-TF's in inducing chemoresistance in pancreatic ductal adenocarcinoma (PDAC). Using a genetically engineered SNAIL deficient and KRAS/P53 mutant mouse model, the researchers showed enhanced apoptosis and reduced tumour burden in SNAIL deficient mouse when compared to controls (KTC), after treatment with gemcitabine (107). Transcriptions factors and pathways promoting EMT have also been associated with chemotherapy resistance. Expression of EMT-TF SNAIL, TWIST and ZEB associates with poor response to chemotherapy in many cancers (66, 107, 116, 120-122). Treatment of cancer cells with an antibody against EMT associated cytokine TGFβ sensitises cancer cells to alkylating agents (123). Overexpression of Wnt/β-catenin signalling pathway promotes mesenchymal transition and resistance to trastuzumab in HER2 overexpressing breast cancer cells (124).

Several chemotherapy resistance mechanisms have been identified as contributing towards apoptosis resistance in mesenchymal tumour cells. An important mechanism promoting drug resistance in mesenchymal cancer cells is excessive drug efflux by multiple cell membrane transport proteins termed ATP binding cassettes (ABC) (125). Multiple drug transporters MDR1, MDR1 associated protein and breast cancer resistance protein (ABCG2) are know to be involved in promoting drug resistance to Doxorubicin in mesenchymal breast cancer cell lines (126). Saxena et al highlighted the presence of E-box binding elements in the promoter region of these genes, and reported increased

expression after induction of EMT (127). TWIST expression promotes resistance to oxaliplatin by up regulating expression of multidrug resistance protein MDR1 in colorectal cancer (128). Slug an EMT inducing TF is believed to promote resistance to epidermal growth factor tyrosine kinase inhibitor (EGF-TKI) by modulating genes regulating apoptosis signalling (129).

ZEB1 promotes apoptosis resistance to ionising radiation by enhancing DNA double strand break repair. ATM mediated phosphorylation of ZEB1 after exposure to ionising radiation (IR), is though to stabilise the TF. A subsequent interaction between ZEB1 and deubiquitinase USP7 improves its ability to stabilise CHK1, thus promoting cell cycle arrest and DNA repair (120). Silencing ZEB1 expression in cancer cells have also been demonstrated to increase radio sensitivity *in vitro* and *in vivo (130).* The above studies provide strong evidence for the role of EMT inducing TF in promoting chemo-radioresistance in cancer. Although some mechanisms driving resistance have been identified, it is clear that EMT induced chemoresistance occurs secondary to multiple resistance mechanisms that require urgent investigation to improve cancer outcomes.

1.6 Partial EMT and plasticity

The traditional binary model of EMT, defined mesenchymal transition by the loss of epithelial and gain of mesenchymal biomarkers. It was suggested, the switch in biomarker expression occurred in isolation and never simultaneously (53). Traditionally, epithelial cells were defined by the expression of adhesion proteins such as E-Cadherin, cytokeratin's and occludins (ZO1, 2 and 3) (53, 81), whilst the expression of N-cadherin, Vimentin and certain integrins (αVβ6) were thought to depict a mesenchymal phenotype (73, 77, 82). The definition of EMT has now however been broadened to include the existence of hybrid cells expressing both epithelial and mesenchymal markers simultaneously (53). Cells bearing this hybrid phenotype are referred to as 'metastable' reflecting the flexibility of further progression towards a full mesenchymal state or reversal to an epithelial phenotype (49, 53).

Evidence of transitional EMT states comes from studies reporting co-expression of epithelial and mesenchymal markers in the same cell. The expression of mesenchymal markers is not however an absolute necessity to define a 'metastable' phenotype. Even when a cell is defined as 'mesenchymal' by the expression of a certain biomarkers, much heterogeneity in terms of mesenchymal characteristics exists (49). An analysis of 43 ovarian cancer cell lines, thought to represent an intermediate phenotype by the co-expression of cytokeratin's and vimentin, up regulated N-cadherin in only 50% of cases (131). It can thus be perceived the two populations of cells belong to differing stages of mesenchymal transition and are likely to behave distinctly in terms of metastasis and colonisation (132, 133). During renal fibrosis, renal epithelial cells undergo a partial EMT and remain in this intermediary state indefinitely, highlighting in some instance that a partial EMT may represent a final state of differentiation (134). In summary, intermediate states probably reflect the balance between EMT inducing transcription factors and their suppressive regulators (miRNA). When trying to decipher the differentiation (epithelial vs. mesenchymal) status of a cell other characteristics of EMT such as apoptosis resistance, cell cycle attenuation and epigenetic changes should also be given careful consideration, before differentiation status can be determined.

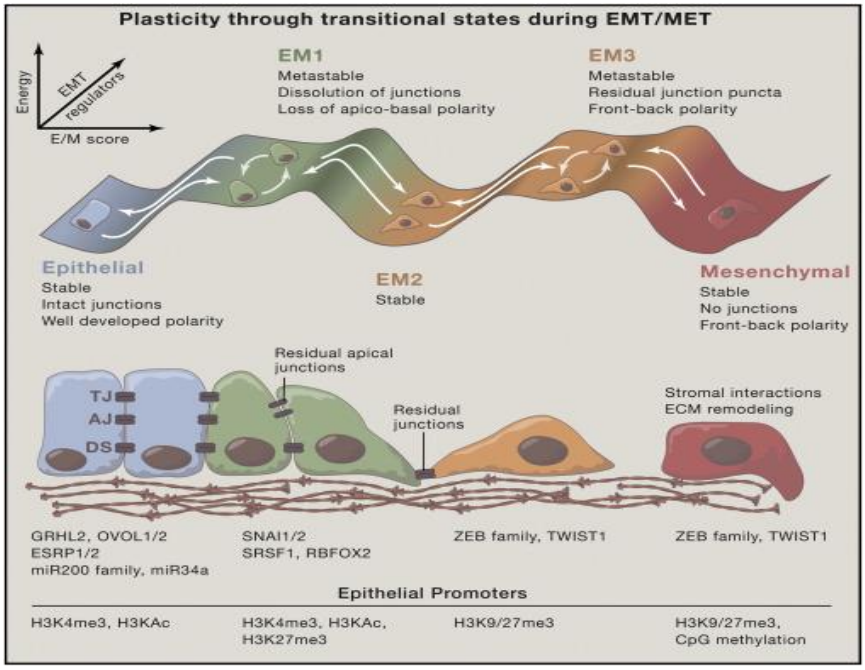

Figure 7:Epithelail to mesenchymal transition involves transition through an intermediate plastic state. Growing evidence suggests EMT is a continuum represented by epithelial, intermediate and mesenchymal states. These changes are regulated by transcription factors that modify gene expression by promoting epigenetic modifications at epithelial and mesenchymal genes. The transitions are associated with changes in cell adhesion molecules, loss of apical basal polarity and gain of front-back polarity. These changes can occur in a plastic manner both in forward and reverse direction. It is not as yet clear if there is a point of no return with regards to returning to an epithelial state after EMT (53).

1.7 EMT and Cancer stem cells

It was first proposed in the mid 1800's, that cancers are composed of a stem cell and differentiated cell population. Over a hundred years later cancer stem cells from acute myeloid leukaemia were isolated (CD34+/CD38-) and shown to be able to form derivative leukaemia after transplantation into NOD/SCID mice in limiting dilutions (135). These cells exhibit the ability to seed new tumours with the same heterogeneity as the tumour from which it was initially derived (136). Similar approaches were subsequently used to derive and isolate stem cells from a range of solid cancers including colon, pancreas, prostate, melanoma and lung (135). Over the years many stem cell markers including $CD44^{high}/CD24^{low}$ surface expression profile, high intracellular aldehyde dehydrogenase (ALDH1), CD133+, C-met and Nestin expression have been used as markers of stem cell status, but none have proven to be universal to all malignancies (137). The first evidence to associate the surprise link between EMT and stem cell status was provided by Mani and co-workers (110). After EMT, human mammary epithelial cells exhibited a

mesenchymal phenotype, $CD44^{high}/CD24^{low}$ surface expression profile, increased ability to form mammosphere and improved tumour initiating capacity in immune compromised mice (110). The ability of EMT-TF's to promote stem cell properties was further proven expressing ZEB1 in pancreatic cancer. Wellner et al reported ZEB1-TF in pancreatic cancer promotes tumorigenicity by repressing stemness inhibiting miRNA's (138). However a generic mechanism underlying acquisition of stem cell traits after EMT is as yet poorly understood. SNAIL; an EMT inducing TF, shifts cell division from asymmetric (one stem cell, one differentiated cell) to symmetric cell (2 stem cells) division implying a role for EMT in increasing the stem cell pool (139). Further, Wnt signalling promotes an EMT and acquisition of stem cell features by stabilisation of EMT inducing TF's SNAIL1 and expression of Slug and Twist (135). These results demonstrates the phenotype shared between stem cells and EMT derived tumour initiating cells are driven at least in part by the same molecular mechanisms.

Cancer associated fibroblasts (CAF's) are though to play a key role in promoting EMT and stemness properties (53). TGFβ induces programs in stromal cells that correlate with poor prognosis in colorectal cancer patients. The mechanism driving poor oncological outcomes has been linked to cancer associated fibroblasts (CAF's), that increase the frequency of cells with tumour initiating capacity (140) . CAF's with features indicative of myofibroblasts have been shown to promote the appearance of stemness features in HCC (141). These studies suggest the tumour microenvironment may also play a key role in regulating EMT and stemness properties in cancer. Despite strong evidence linking stemness and EMT, recent studies have postulated EMT and stemness may represent two independent and parallel events (53). PRRX1 a potent EMT inducer, when down regulated in breast cancer cell line BT-549 is linked with MET and increased proliferation, but also with gain of stemness traits such as $CD44^{high}$ expression and mammosphere formations (102). Parallels can also be seen between the induction of stemness properties and acquisition of pluripotency during fibroblast reprogramming. The latter requires MET, compatible with the fact, embryonic stem cells are epithelial and consequently do not innately activate EMT pathways (142). Further mechanistic studies

investigating the interactions between pathways promoting stemness and EMT are required to dissect the interdependence or independence of these cellular properties.

1.8 Regulation of EMT pathways

Several key signalling pathways including transforming growth factor β (TGF-β), Wnt, Notch and Hedgehog are involved in inducing EMT (44). These signalling pathways, promote the expression of EMT inducing TF's such as SNAL1, SNAL2, TWIST1, TWIST2, ZEB1 and SIP1/ZEB2 (57). Activation of EMT inducing TF's by paracrine signalling results in a complex series of cellular changes leading to down regulation of epithelial and up regulation of mesenchymal genes (143). EMT is tightly regulated at multiple levels by integrating epigenetic, transcriptional, translational, protein degradation and subcellular localisation strategies(53).

MiRNA's are important regulators of EMT (144), for example transcription factors of the ZEB family form a double negative feedback loop with the miR-200 family, enabling a bi-stable switch between an epithelial and mesenchymal state (145). A similar regulatory interaction has also been described between mir-34 and Snail1 (146). miR-34 binds to the highly conserved 3' UTR of SNAIL1 mRNA thus promoting its transcriptional repression. However, the effect of a miRNA–TF interaction loop may not be equivocal in repressive potency (53). For example miRNA's of the miR-200 family, miR200a/b/c, miR-429 and miR-141 target ZEB1 transcription, but to varying degrees of strength (53). Further dissection of regulatory interaction between EMT-TF's and miRNA's may provide novel diagnostic and therapeutic opportunities in future years.

Alternative splicing is another mechanism utilised to regulate EMT (53). Expression of epithelial specific regulatory protein 1 and 2 (ESRP1 and ESRP2) influences the maintenance of epithelial features by promoting the production epithelial mRNA isoforms (147). Whilst splicing factors such as Quaking, RBFOX2 and SRSF2 promote expression of mesenchymal mRNA isoforms and thus induce mesenchymal differentiation (148-150). Epigenetic modification of chromatin is a critical regulator of gene expression in EMT (64). For example, SNAIL regulates E-cadherin repression by recruiting chromatin modifiers

that convert the promoter region of E-cadherin from euchromatin (H3K4me3) to heterochromatin (H3K9me3) (151). SNAIL also influences epigenetic regulation by recruiting histone modifiers such as de-acetylases, lysine specific de-methylase and components of the polycomb repressive complex (PRC) to genes that determine epithelial or mesenchymal differentiation status (151-154). Whilst EMT inducing TF can promote recruitment of epigenetic regulators to modify gene expression, EMT-TF's themselves are regulated by histone modifiers. For example ZEB1 expression is affected by epigenetic changes induced by methyltransferase PRDM14 (155, 156). Therefore, histone modifiers play a key role in controlling expression of EMT inducing TF's and repression of epithelial genes to promote mesenchymal transformation during EMT.

At the protein level, posttranslational modification of EMT-TF's plays a regulatory role in determining differentiation status. Phosphorylation of SNAI1 and TWIST1 by GSK3β or MAP kinases regulate their degradation(157, 158). Phosphorylation of EMT-TF's has also been demonstrated to affect subcellular localisation adding a further layer of complexity (53). It is evident regulatory mechanisms driving EMT are complex and achieving a complete understanding seems a daunting task. However, improved knowledge of regulatory mechanisms governing EMT may provide the key insight required for therapeutic application in the clinical setting.

1.9 Major EMT transcription factors interaction and regulation

Gene expression changes during epithelial to mesenchymal switch is regulated by transcription factors, considered master regulators of EMT (57). EMT-TF including SNAIL, TWIST and Zinc finger E-box binding transcription factors (ZEB) are activated early in EMT, and reported to have central roles in both embryonic development, fibrosis and cancer progression (57). These transcription factors have distinct expression profiles and their contribution to gene regulation depends on the tissue type involved and the signalling pathways initiated (57). Together, the EMT TF's poses the capacity to repress epithelial genes and promote expression of mesenchymal genes simultaneously (57).

1.9.1 SNAIL transcription factors

SNAIL proteins 1 and 2 have been reported to activate EMT programmes during development fibrosis and cancer (159). TGFβ, Wnt family proteins, Notch and growth factors that act through RTK's to activate SNAIL expression depending on the physiological context (57, 160). SNAIL1 can induce expression or promote repression of genes by binding E-box elements through their carboxy terminal zinc finger domains (154, 160). Epigenetic mechanisms mediating E-cadherin repression have been investigated in detail (64). Binding of SNAIL1 to E-boxes in the E-cadherin promoter recruits chromatin modifiers PRC2 complex which contains the methyltransferase enhancer of zeste homolog 2 (EZH2), G9a of suppressor of variegation 3-9 homologue 1 (SUV39H1), histone de-acetylase 1,2 and 3 and lysine specific de-methylase 1 (LSD1) to the proximal promoter (151, 152, 154, 161, 162). These components modify chromatin marks on histone H3 at sites K9, K27 and K4, catalysing methylation or acetylation of lysine residues. Studies have suggested these modifiers leave both repressive (H3K9 Methylation) and activation (H3K4 methylation, H3K9 acetylation) marks creating a poised state promoting plasticity in gene expression required for EMT and subsequent MET(163).

Post translational modification controlled by Glycogen synthase kinase 3β (GSK3β) also plays a pivotal role in controlling SNAIL induced EMT. Phosphorylation of SNAIL1 at Ser97 and 101 facilitates nuclear export whilst phosphorylation at Ser 108, 112, 116 and 120 promotes ubiquitin-mediated degradation (57). EMT inducing signalling pathways (Wnt, PI3-AKT) inhibits Snail1 phosphorylation by GSK3β thus increasing Snail1 stability. Conversely, small C terminal domain phosphatase (SCP1) antagonises phosphorylation by GSK3β thus promoting retention in the nucleus, where it represses gene expression (164). SNAIL1 also co-operates with ETS1 to activate expression of matrix metalloproteases (MMP's), which facilitate cell migration (165), whilst its interaction with SMAD proteins induce E-cadherin repression after treatment with TGF-β (166).

1.9.2 bHLH transcription factor

Homodimeric and heterodimeric basic helix-loop-helix (bHLH) transcription factors also functions as master regulators of EMT (167). Among these transcription factors TWIST1, TWIST2, E12, E47 and inhibitor of differentiation (ID) play key roles (167). Like the SNAIL family of TF's, Twist expression down regulates epithelial genes and promotes expression of mesenchymal genes (57). Like the SNAIL family, these transcription factors also assemble chromatin modifying complexes to regulate gene expression (64). For example, TWIST1 recruits SET8 to the E-cadherin promoter and monomethylates H3K20 a mark associated with repression of E-cadherin (168). In head and neck tumours TWIST1, promotes the expression of B lymphoma Mo-MLV insertion region 1 homologue (BMI1), a component of the PRC1 complex, TWIST1 subsequently cooperates with BMI1 to promote formation of heterochromatin at the E-cadherin promoter (169). Transcription factor expression can in itself be regulated by a variety of signals. An ischaemic environment can promote expression of hypoxia inducible factor 1α (HIF1*α*), a TF that promotes TWIST1 expression (170). Mechanical stress has also been demonstrated to promote TWIST1 expression in a β-Catenin dependent manner (171). ID genes bind bHLH TF's inhibiting their interaction with DNA. TGFβ signalling performs a counter regulatory role by suppressing expression of ID proteins promoting EMT (172). Whilst post-translational phosphorylation by MAP-Kinase at Ser68 inhibits ubiquitination and degradation of TWIST, promoting EMT (157).

1.9.3 ZEB transcription factors

The two vertebrate transcription factors ZEB1 and SIP1/ZEB2 regulate EMT by inducing expression of genes promoting mesenchymal differentiation (160, 173). Like other EMT inducing TF's, ZEB protein expression is induced by TGFβ, Wnt and growth factors that activate RAS-MAP kinase signalling (160, 173). Recent studies have also suggested, EMT-TF's can trans-activate expression of each other; for example, ZEB1 expression is up regulated by the combined influence of SNAIL and Twist1 at the promoter region of the *ZEB1* gene (174).

ZEB1 mediated gene repression usually involves recruitment of C-terminal binding protein (CTBP) co-repressor, however a CTBP independent mechanism involving recruitment of BRG1, a chromatin remodelling protein to the E-cadherin promoter has also been reported (175). ZEB1 also interact with transcriptional co-activators p300/CBP associated factor (PCAF), which facilitates switch from transcriptional repressor to activator (176). Like other EMT inducing transcription factors, ZEB proteins bind to E-box elements in the promoter region of genes, thus modulating transcription (57). ZEB1 expression is tightly regulated by members of the miR-200 family of miRNA's, which represses the translation of ZEB mRNA (177). A double negative feedback loop of ZEB repressing miR-200 expression and miR-200 inhibiting ZEB protein translation is an important regulatory mechanism governing ZEB mediated EMT(178). Apart from regulation by miRNA's, ZEB protein's cytoplasmic localisation is influenced by PRC2 mediated sumoylation, which prevents association with CTBP and attenuates EMT(179)

1.9.4 Novel transcription factors

Apart from the above well-known TF families, novel EMT inducers have recently been identified (57). Fork head box (FOX) TF's defined by a DNA binding fork head domain, have recently been identified as an EMT inducer (180). GATA family of TF's characterised by a DNA binding dual zinc finger module controls the differentiation of a diverse cell lineages (181). SRY box (SOX) transcription factors synergise with SNAIL TF's to promote EMT (182). A diverse array of transcription factors regulate EMT and MET pathways; greater insight into the interaction between TF's and their regulators will help differentiate master regulators from tissue specific mediators of EMT and help identify their unique influence in health and disease.

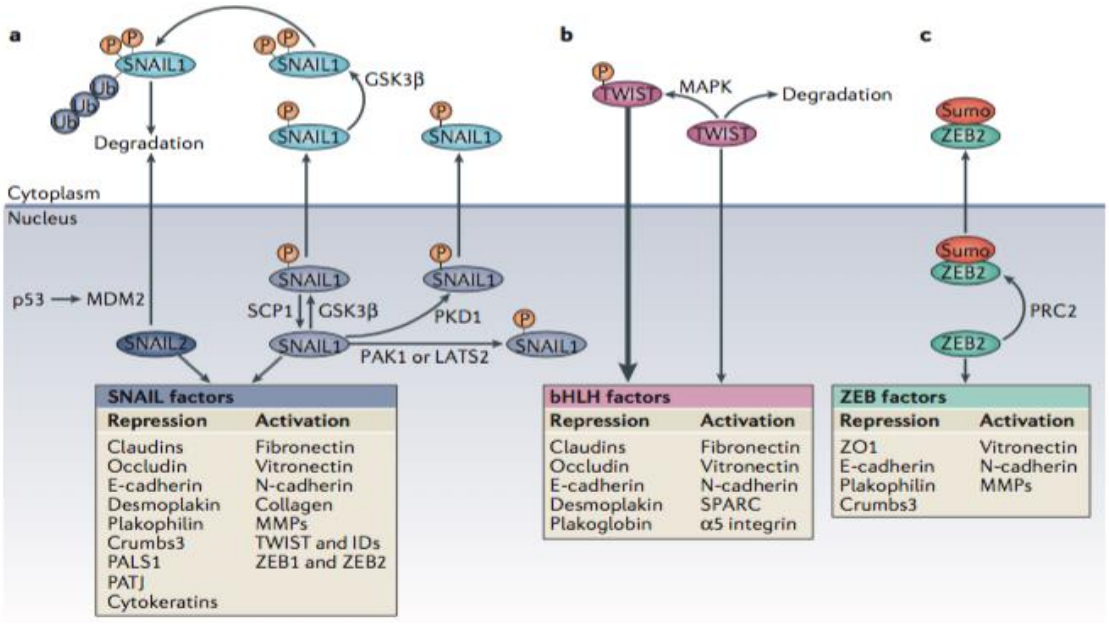

Figure 8: Regulation of EMT by Transcription factors. Epithelial to mesenchymal transition is regulated by SNAIL, zinc finger E-box binding (ZEB) and basic helix-loop-helix family of transcription factors that repress epithelial genes and promote expression of mesenchymal genes. Post-translational modification can have a dramatic influence on TF localization within the cell and consequently differentiation. A) Glycogen-synthase-kinase-3β (GSK3β) can phosphorylate Snail1 at two different sites, phosphorylation at the first site facilitates nuclear transport, whilst the second phosphorylation site promotes ubiquitilation and degradation by E3 ligases. Other kinases that modulate SNAIL localization are protein kinase D1 (PKD1), large tumour suppressor 2 (LATS2) and p21activate kinase (PAK1). PAKD1 mediated phosphorylation promotes nuclear transport, whilst the latter two protein kinases promotes nuclear retention and increased activity. B) Twist is phosphorylated by the MAP kinase p-38, JUN N-terminal kinase and Erk. Phosphorylation inhibits degradation and promotes EMT. C)SIP1/ZEB2 gets sumoylated by the PRC2 complex which reduces its activity as a transcription factor. E-cadherin – epithelial cadherin, ID, inhibitor of differentiation, MMP, Matrix metalloproteases, N-Cadherin, Neural cadherin, PALS1, protein associated with Lin 71, SPARC, secreted protein acidic and rich in cysteine, ZO1, Zonula occludens (67) .

1.10 Signalling pathways and EMT

The TGFβ family of receptors comprises of three TGFβ's, two activins, many bone morphogenic proteins (BMP) and ligands that act through binary combination of trans membrane dual specificity kinase receptors (57). TGFβ is recognised as a critical signalling cascade promoting EMT during development, wound healing and cancer progression. For example, TGFβ1 and 2 is required for the formation of the endocardial cushion during embryogenesis (183). TGFβ1 expression promotes progression of pulmonary and hepatic fibrosis (184, 185). Whilst expression in cancer is linked to EMT, increased metastatic capacity and chemoresistance in many malignancies (186-188).

TGFβ signalling occurs via SMAD dependent or SMAD independent mechanisms. Binding of TGFβ family of proteins to the tetrameric cell surface receptor complex, enables type II TGFβ family receptors to phosphorylate and activate type-1 trans membrane kinases that phosphorylates the C-termini of SMAD's (189). TGFβ receptor-1 (TβR1) and TGFβ receptor-2 (TβR2) activate SMAD phosphorylation leading to the formation of trimeric SMAD complexes that can translocate to the nucleus and act as a transcriptional activator or repressors. SMAD activation is negatively regulated by inhibitory SMAD's (SMAD 6,7), which compete with SMAD 2 AND 3 to bind to type 1 receptors (190, 191). The importance of TGFβ signalling in mediating EMT has been demonstrated by expression of dominant negative receptors, pharmacological inhibition and manipulation of SMAD protein expression (192-194). TGFβ signalling has also been shown to induce ZEB1 expression, which in turn interacts with SMAD 3-4 to up regulate mesenchymal genes (176).

TGFβ also induces signalling through RHO like GTPases, MAP kinase pathway and PI3K via a SMAD independent mechanism (194-196). Activation of RHO, RAC and CDC42 drives cytoskeletal reorganisation required for metastasis (197). Pharmacological inhibition or knock down of RHO and RACK prevents EMT in response to TGFβ treatment (198, 199). In epithelial cells undergoing EMT, TGFβ activates AKT via PI3K, which in turn activates mammalian TOR complex 1 (mTORC1) and 2 (mTORC2) (193, 196). mTORC1 is required for protein synthesis, increase in cell size, invasion and motility, whilst mTORC2 is required for transition to a mesenchymal phenotype (196). Pharmacological inhibition of PI3K pathway prevents TGFβ induced EMT highlighting its significance in the process (200). Inhibition of AKT decreases SNAIL1 expression and mTORC2 inhibition impedes metastatic behaviour highlighting the importance of this signalling pathway in promoting EMT (193). TGFβ receptor also possesses dual kinase activity and is able to weakly phosphorylate Tyr residues and thus activate the MAP kinase pathway via phosphorylation of the adapter protein SRC homology 2 domain containing transforming protein 1 (SHC1) (201). Although the contribution of this pathway to EMT is less clearly understood, pharmacological inhibition of ERK represses TGFβ

induced EMT (202). Previous studies have also reported ERK signalling promotes E-cadherin down regulation and N-Cadherin expression, hallmark features of EMT (203, 204).

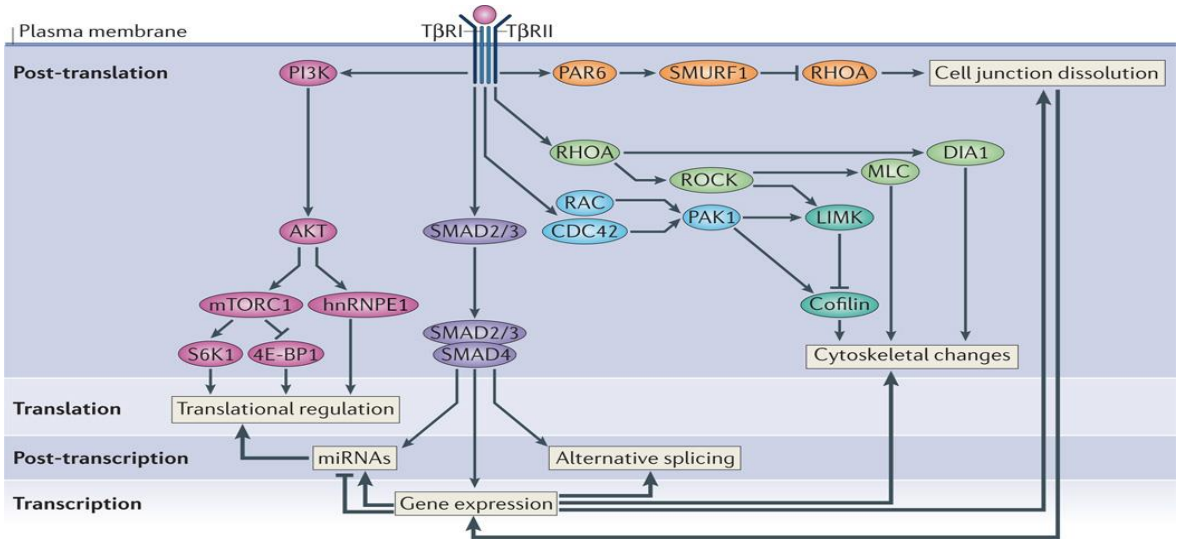

Figure 9: Transforming growth factor-β (TGFβ) induces EMT by acting through SMAD-mediated and non-SMAD mediated signaling pathways induce EMT. Interaction of TGFβ with the tetrameric (TβR1 and TβR2) results in activation of SMAD 2/3, which then combines with SMAD4, translocates to the nucleus to modulate gene expression. TGFβ signaling can also modulate gene expression by regulating miRNA expression profile and splicing regulatory proteins (e.g. ESRP1). The non-SMAD dependent signaling occurs secondary to activation of PI3K-AKT-mTORC1 signaling cascade, which increases translation, cell size and de-represses mRNA expression of certain genes by heterogeneous ribonucleoprotein E1. TGFβ signaling also leads to dissolution of cell adhesion complexes and cytoskeletal rearrangement by activation of RHO-GTPases. Polarity complexes also alter to favor a mesenchymal phenotype (57).

1.10.1 Receptor tyrosine kinase mediated EMT

Several growth factors that act via receptor tyrosine kinases (RTK's) have been reported shown to induce EMT (57). Interaction between a growth factor ligand and associated receptor results in auto-phosphorylation of tyrosine residues in the intracellular domain. This auto-phosphorylation event leads to activation of signalling pathways (PI3-AKT / ERK-MAP kinase (57) that up regulate the expression of EMT inducing TF's. For example, constitutive activation of the RAS-RAF pathway, results in aberrant ERK signalling and expression of SNAIL1, an EMT inducing TF (205). Fibroblast growth factor and insulin like growth factor signalling, induces EMT by up regulating expression of SLUG and ZEB1 (206, 207). Hepatocyte growth factors interact with c-MET, resulting in expression of SNAIL1 (206, 208). Epidermal growth factor (EGF) signalling induces EMT by up

regulating expression of SNAIL and Twist (209, 210), which enhances motility and invasiveness (211, 212).

1.10.2 Other extracellular regulators of EMT

Another example of an extracellular regulator of EMT is Wnt ligand interaction with Frizzled receptors. The ligand receptor interaction results in inhibition of GSK3β mediated degradation of EMT inducing TF's β-Catenin and SNAIL (213). Hedgehog signalling via patch receptors up regulates EMT-TF factor through increased expression of glioma family of transcription factor Gli1 (214). Notch receptor activation by jagged or Delta like ligand promotes expression of SNAIL1 (215). Other micro environmental factors such as hypoxia, promote HIF1α expression and inflammatory cytokines, IL-6 and transcription factors such as NF-κB have also been shown to induce EMT(170, 216, 217). An overview of the extracellular signalling pathways mediating EMT is provided in figure 10.

It is now accepted that signalling pathways induce EMT during development and cancer progression. Recent studies have added a further layer of complexity by suggesting crosstalk between signalling pathways can repress or promote EMT (57). TGFβ signalling destabilises adherens junctions thus promoting β-catenin translocation to the nucleus leading to activation of Wnt signalling (57). Synergy between TGFβ signalling and RTK activation by FGF or EGF has also been demonstrated in cancer (218). Constitutive RAS activation resulting in ERK phosphorylation facilitates TGFβ induced EMT (219). To the contrary, RTK activation may also deter EMT. HGF signalling inhibits TGFβ induced EMT by promoting skil related novel protein N (SnoN) a transcriptional co-repressor of SMAD's (220). In the cytoplasm, GSK3β phosphorylation by AKT promotes its degradation indirectly by promoting translocation of SNAIL to the nucleus (158). It is however important to highlight that cancer cells often posses mutations that may render cell lines susceptible to activation by certain extra cellular signals whilst rendering them unreactive to others. Therefore, the above observations may not be universally applicable to all cancer cell lines. Further dissection of the complex interaction

between signalling pathways will provide greater insight for translational efforts in the future.

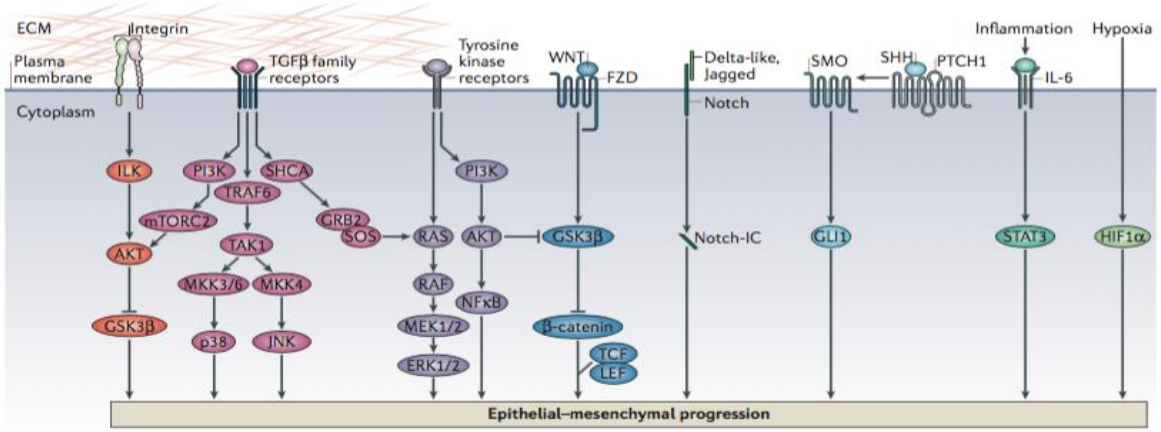

Figure 10: Overview of signaling pathways that induce EMT. The above schema provides an overview of the different signaling pathway that can promote EMT. TGFβ mediated signaling was discussed in detail previously. However briefly, TGFβ induced EMT can occur via a SMAD dependent or SMAD independent mechanism. TGFβ can activate signaling via PI3-AKT, ERK MAPK, P38 MAPK and JNK pathways. RAS-RAF-MEK-ERK signaling is mediated via the SRC homology 2 domain containing transforming A (SHCA), whilst P38 and JNK activation results from association of TRAF6 with the TGFβR1. Several growth factors activate receptor tyrosine kinases to induce EMT. The RAS-RAF-MEK-ERK pathway activation by growth factors leads to expression of EMT inducing TF's that promote EMT. Wnt, Notch and Hedgehog activation can also induce EMT. Wnt signaling stabilizes β-Catenin by inhibiting GSK3β, thus promoting transition of mesenchymal genes. Hedgehog and NOTCH signaling activates expression of SNAIL TF's leading to EMT. A hypoxic tumour microenvironment and inflammation can also induce EMT HIF1α and STAT3 induced SNAIL expression (57)

1.11 Epigenetic regulation of EMT

In eukaryotic cells, DNA is wrapped around histone octamers to form the nucleosome, the basic repeating subunits of chromatin (64). Histone modification, remodelling, variants and DNA methylation can have major impact on gene expression and consequently cell behaviour and differentiation (221, 222). A growing body of studies suggest EMT programmes result in a plethora of epigenetic changes that play a key role in promoting mesenchymal characteristics such as increased metastatic capacity and apoptosis resistance (53, 223-225). ATP dependent chromatin remodelling is a well-known mechanism that permits compaction and de-compaction of chromatin, thus influencing gene expression (64). Four major chromatin re-modellers that have been characterised are, SWI/SNF, CHD, ISWI and INO80 (226, 227). MTA3, a subunit of the NuRD complex (CHD family) directly inhibits transcription of EMT inducing transcription factor SNAIL1 in

breast cancer (228). BRG1 the catalytic subunit of the SWI/SNF complex is commonly mutated in cancer, whilst recent studies have also demonstrated its recruitment to the E-cadherin promoter facilitating transcriptional repression (175). BAF60C, another subunit of the SWI/SNF family has been shown to activate Wnt signalling thus promoting EMT and tumour progression (229).

DNA methylation is a covalent modification that occurs at the 5'-position of the cytosine ring (5mC) within CpG dinucleotide repeats and is associated with transcriptionally repressed chromatin (230). Three active DNA methyltransferases (DNMT's) have been identified as undertaking 80% of the enzymatic activity in mammalian cells (230). Disruption of DNA methylation has long been recognised in cancer, although genome scale methylation changes are yet to been reported in detail after EMT (224). Multiple studies have investigated DNA methylation at the E-cadherin and miR-200 regulatory regions and (231-233) reported EMT-TF's SNAIL1 and ZEB recruit DNMT's to repress gene expression via a SMAD dependent manner (234, 235).

The histone core is composed of one H3-H4 tetramer and two H2A-H2B dimers. The N-terminal tail of histone H3 is flexible and lysine rich, permitting biochemical modification that alter histone interactions and transcription (64). Four well-documented histone modifications are methylation, ubiquitination, phosphorylation and acetylation. Given that transcriptional reprogramming occurs during EMT, histone modification provides a platform to regulate alterations in gene expression (230). Histone acetylation is a modification found in abundance in euchromatin and creates open chromatin conformation promoting transcription. Histone acetylation is performed by several families of histone acetyl-transferases including p300/CBP, TIP60 and hMOF (236). In WNT signalling induced EMT, β-catenin promotes gene expression by recruiting P300-CBP to the transcription activation complex on target gene promoters (237, 238). In breast cancer cells, acetylation of H4K16 by acetyl-transferase hMOF promotes expression of tumour suppressor genes associated with EMT such as E-cadherin (239). In addition to E-boxes, the E-cadherin promoter also harbours hepatocyte nuclear factor 3 (HNF3) binding sites.

HNF3 is expressed in epithelial cells and co-operates with p300/CBP at the CDH1 promoter to facilitate gene expression and antagonise EMT (240). In cells, lysine acetylation is counteracted by de-acetylation, which is enzymatically performed by histone deacetylases (HDAC's). SNAIL and ZEB family of TF's recruits HDAC's to the E-cadherin promoter thus inhibiting transcription (154, 241). SNAIL family of TF's also bind to E-box elements in the BRACA2 gene promoter and silence gene expression by recruiting the HDAC1 containing CTBP complex (242). This data suggests acetylation of lysine residues plays a critical role in mediating gene expression during EMT.

Another prominent regulatory epigenetic modification is methylation of lysine and arginine residues primarily on histone H3 (64). The balance between methylation and de-methylation is controlled by activity of DNA methyltransferases and demethylases. Unlike acetylation, methylation can promote gene expression or repression based on the lysine residue that is modified. In general, a well-recognised permissive mark is H3K4me3, which decorates euchromatin, whilst H3K36 and H3K79 methylation associates with transcribed genes (230). H3K27 and H3K9 methylation are repressive in nature and used as makers of heterochromatin. Widespread histone methylation changes at the gene and genomic level has been reported during EMT (224, 225). Expression of DOTL1 a H3K79 histone methyltransferase associated with disease recurrence in breast cancer (243). DOTL1 forms complexes with c-Myc and p300 at the promoter region of SNAIL and ZEB family of TF's to promote EMT and metastasis (244). Furthermore, asymmetric arginine methylation by protein arginine methyltransferase PRMT1 promotes ZEB1 expression and EMT in breast cancer cells (245). In a TGF-β and SNAIL induced model of EMT, mesenchymal transformation was accompanied by genome scale increases in H3K4me3 and H3K36me3, whilst this gain in permissive marks was accompanied by loss heterochromatin marks H3K9me3 and H3K27me3(224).

Histone methylation is counter balanced by demethylation by histone demethylases. LSD1, a demethylase is overexpressed in breast and colorectal cancer (246) and its inhibition promotes expression of epithelial genes such as E-cadherin and ZO-1 (247-

249). SNAIL recruits LSD1/CoREST complex to demethylate H3K4 thus repressing E-cadherin expression(249). LSD1 exists in the ZEB1 containing CTBP1 Co-repressor complex thus highlighting its role in ZEB induced EMT(250). Whilst the above data suggests LSD1 promotes EMT, evidence to the contrary has also been reported. LSD1 posses the ability to remove repressive K9 methylation marks suggesting its role might vary in accordance with other regulatory subunits of histone modifying complex (251). For example LSD1 is a subunit of the NurD complex which supresses TGF-β1 induced EMT (252).

Histone H3K9 and K27 methylation are repressive marks and decorate heterochromatin (230). K9 methyltransferase activity is primarily undertaken by G9a, SETDB1, SUV39H1 and GLP(64). Whilst K27 methylation is co-ordinated almost singularly by EZH2, which is part of the poly-comb repressive complex (PRC2)(230). A link between repressive (K9,K27) marks and EMT was reported by studies demonstrating SNAIL1 recruits G9a and SUV31H1 to the E-cadherin promoter to repress gene expression (162, 234). Reduced expression of SETDB1 antagonises mesenchymal transition in breast cancer cells, suggesting K9 methylation promotes EMT. However, other studies have suggested SETDB1 indirectly up regulates STAT3 expression and induces Twist and C-Myc to promote EMT(253).

EZH2 or its close homolog EZH1 containing PRC2 complex is known to play a fundamental role in embryonic development and cancer stem cell formation (254). Recent studies in pancreatic and colorectal cancer have demonstrated, SNAIL1 an EMT inducing TF directly interacts with EZH2 promoter thus repressing E-cadherin expression (151). Aggressive breast, bladder and prostate cancer cells have also been reported to over-express EZH2 (255). Thus, it could be postulated EZH2 mediated repression of adherens junctions promotes the increased metastatic potential observed in these cells. However the exact mechanistic details remains un-dissected (255).

Other proposed models of EZH2 induced EMT include; tri-methylation of H3K27 by EZH2 promotes the recruitment of PRC1 complex to the histone modification (256). The

PRC1 complex contains the BMI1 subunit, which is deregulated in many cancers and poses the ability to induce EMT by stabilising expression of SNAIL (257-259). An alternative mechanism that has been reported is, TWIST1 expression enhances BMI1 protein expression, which consequently results in EMT in a TWIST and BMI dependent manner (169). Although many correlative studies have reported an increase in EZH2 expression in adenocarcinomas, the opposite has also been reported in several instances (225, 260, 261). Further mechanistic detail of epigenetic regulation of EMT in physiology and cancer is urgently required, before the precise function of EZH2 in cancer can be accurately deciphered.

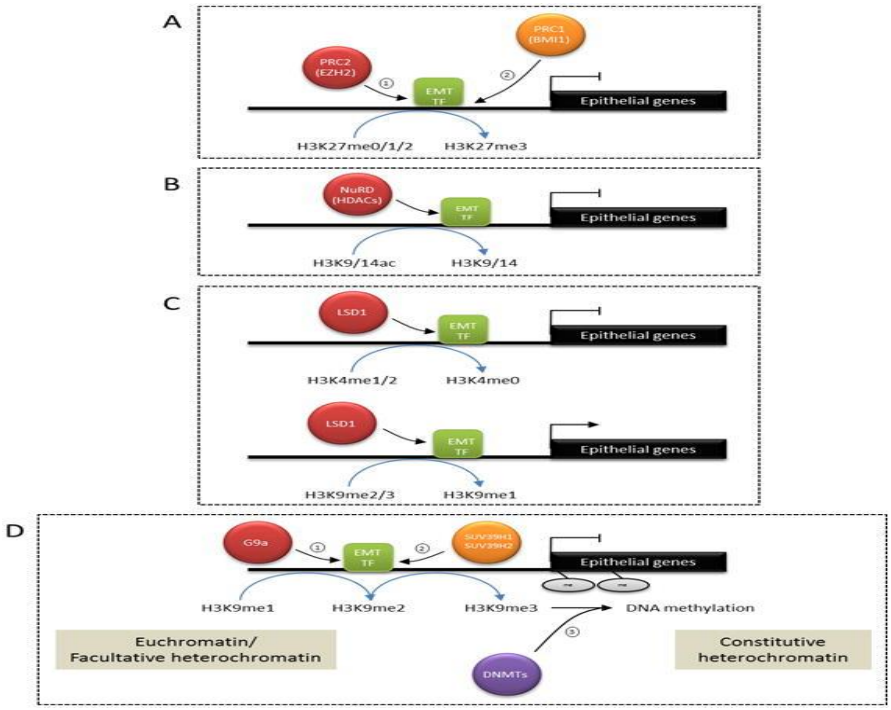

Figure 11: Epigenetic regulation of gene expression by EMT inducing transcription factors. The primary mechanism by which EMT inducing TF's silence of epithelial genes is by promoting epigenetic histone modification. **a)** SNAIL binding to the promoter of the CDH1 gene promotes repressive histones marks (H3K27me3) by recruiting the PRC2 complex, (**b**). EMT-TFs associate with the NuRD complex, which contains HDACs, which catalyse the removal of acetyl groups from lysine residues of histones thus repressing gene expression. (**c**) SNAIL mediated recruitment of LSD1 can have opposing outcomes, depending on the constituents of the complex. LSD1 can promote removal of euchromatin marks or heterochromatic marks thus promoting or repressing gene expression (**d**) SNAIL mediates silencing of epithelial genes by recruiting G9a and SUV39H1, which results in the tri-methylation of H3K9. The H3K9me3 mark promotes recruitment of DNMTs, which in turn leads to CpG methylation blocking transcription (64).

1.12 EMT associated proteins as Biomarkers in CRC

EMT has long been recognised as a cellular event promoting metastasis. Aberrant expression of transcription factors associated with EMT have been reported in many adenocarcinomas including CRC (104). β-Catenin, an EMT inducing TF and activator of WNT signalling is deregulated during CRC progression and EMT (262, 263). However, studies correlating β-catenin expression with oncological outcomes reported no differences in oncological outcomes (264, 265). Numerous studies have investigated the potential role of E-cadherin as a biomarker of recurrence risk in CRC. Of over 20 studies that have been conducted, three studies have reported worse oncological outcomes in E-cadherin negative tumours (266-268). The validity of these results are however plagued by inconsistencies in reporting standards.

EMT inducing TF's are considered master regulators of EMT have been studied as prognostic biomarkers in primary CRC. Shiori et al reported, 37% of CRC specimens analysed in the study expressed SLUG and univariate analysis associating SLUG expression with patient outcomes revealed worse oncological outcomes in patients scored SLUG positive. Multivariable analysis highlighted SLUG as an independent prognostic marker of disease free and overall survival in primary CRC(268). SNAIL1 another EMT inducing TF has also been studied in primary CRC. Of three studies conducted, two reported worse outcomes in patients scored SNAIL positive (43, 262, 269). Only one study to date has assessed Twist1 expression in CRC. The study investigated survival outcomes in patients with primary CRC and concluded Twist positivity associated with poor overall and disease free survival (270). ZEB TF's have also been studied in primary CRC, Kahlert and colleagues reported SIP1/ZEB2 expression at the invasive front of colorectal adenocarcinoma and reported cytoplasmic SIP1/ZEB2 expression at the invasive front associated with poor oncological outcomes. Multivariable analysis highlighted SIP1/ZEB2 as an independent prognostic marker of both disease free and cancer specific survival (65). 30% tumour positivity was reported in a study that evaluated ZEB1 expression in CRC. Nuclear ZEB1 expression associated with early recurrence and reduced survival. Multivariate analysis was however not undertaken (271). The evidence

pertaining to use of EMT biomarkers is however currently sparse and limited by the heterogeneity in reporting standards and study design.

Apart from the work that has been carried out investigating the potential role of EMT inducing TF's using IHC, a consortium of leading scientist within the colorectal field have recently highlighted the importance of identifying a mesenchymal tumours based on transcriptional subtyping(33). Six independent studies classified a large cohort of CRC specimens and in every case a mesenchymal tumour profile was associated with worse survival outcomes and attenuated response to chemotherapy(42, 272-276). Although this collaborative effort has produced promising results, it is not without its own limitations. Recent studies have reported transcription-based patient classifiers are biased by the stromal derived cellular content, which predominates particularly if the tumour was sampled at the invasive front(277). To abrogate this sampling bias Isella and colleagues developed the CRC intrinsic subtypes (CRIS) classifier derived by analysing a large cohort of patient derived Xenografts (Pdx) CRC, since in these tumours the human stromal component is substituted by the mouse counterparts(278). Analysis of a number transcription based classifiers that defined the mesenchymal subtype, using different gene signatures demonstrated that the CRIS sub-classification was immune to the bias induced by sampling from different regions of the same tumour (277). A significant limitation of all these studies however is that, none have clearly addressed the question of the relative contribution of each sub-classification to the currently clinically used TNM staging system. Further, transcription-based analysis of the tumour subgroups requires the specialised application of sequencing techniques and subsequent complex bioinformatics analysis which may be subverted if the same tumour subtypes may be clinically identified by a simple immuno-histochemical analysis for a single or panel of mesenchymal tumour markers. Greater standardisation of study designs, gene signatures, scoring systems and reporting standards may help unlock the potential of a EMT phenotype as predictive or prognostic biomarkers that is routinely applied in the clinical setting in future years.

1.13 EMT and cancer therapeutics

Since its fruition as a concept, EMT has been identified as a major mediator of metastasis and chemo resistance in cancer. Consequently, drugs reversing EMT have been proposed as a therapeutic option to inhibit recurrence and abrogate drug resistance (53). TGF-β inhibitors are the most intensively investigated anti-EMT compounds and recent Phase I studies have trialled their use in both hepatocellular carcinoma and glioblastoma (279, 280). Unfortunately, the results were inconclusive, warranting further investigation in the future (279). Src inhibitors have also been trialled in recent years, however outcome of clinical trails after its use as a mono-therapy or in combination have been disappointing (53). PF-00562271 a focal adhesion kinase inhibitor is being tested in a phase 1 dose escalation trial against solid tumours with promising results. However, the combination of drugs required to inhibit EMT whilst minimising side effects requires careful consideration (281, 282). Drug developments platforms are currently hindered by the absence of tumour representative models that encompass all aspects of the tumour microenvironment such as fibroblasts and the immune infiltrate. Studies using microfluidic co-culture platforms and organoid models may improve predictive capacity of drugs in the clinical setting (53). A further layer of complexity has been added to reversing EMT in cancer, due to the existence of intermediate transition states. Better understanding of transition states and optimal cell phenotype for drug sensitisation is required before effective clinical translation is likely to be achieved.

There is now overwhelming evidence, that EMT induces resistance to chemotherapeutic agents such as oxaliplatin, 5-flurouracil, doxorubicin and ionising radiation (44, 66, 107). Even studies that suggest a limited contribution of EMT to metastasis have report a significant contribution to chemo resistance (107). Therapeutic strategies therefore may find success by targeting pathways that are critical in maintaining mesenchymal phenotype. For example EGFR mutant non-small cell lung cancer cells become Axl receptor dependent after switching to a mesenchymal phenotype. Therefore it can be envisaged EGFR mutant cells may be targeted by inhibitors or antibodies against the Axl receptor (283, 284). Gupta and colleagues identified salinomycin as an agent with

specific toxicity against mesenchymal cells (115). However, clinical trails are yet to report improvement in oncological outcomes from its administration to patients. There have also been pipelines that target specific components of growth factors signalling pathways such as HGFR, insulin like growth factor 1, EGFR and PDGFR. Whilst these treatments could be considered anti-EMT drugs, the pipelines were not designed with specificity to target cancer cells that have undergone mesenchymal transformation (53).

The recognition of the critical influence of epigenetic modification and miRNA's in maintaining mesenchymal differentiation has lead to the development of new targets for therapeutic intervention (64, 230). For example DNA methylating agent 5-AzaC activates expression of miR-200 reversing EMT in ZEB expressing cells (285, 286). Further, histone de-acetylate sirtuin (SIRT1) promote the expression of E-Cadherin and miR-200. These agents are now being studied in trials assessing their efficacy in myelodisplastic syndrome and leukaemia(287). Histone deacetylase inhibitors have also been trialled and show promise in haematological malignancies, but have exhibited limited efficacy in solid tumours. Conflicting evidence has emerged with regards to safety of HDAC inhibitors in recent years. HDAC inhibitors (HDAC1 & 2) inhibit EMT in a TGF-β dependent manner in hepatocytes and head and neck tumours. However, more recent studies have suggested HDAC inhibitors can induce EMT in prostate and nasopharyngeal cancer cells. Hence the utility and application of these inhibitors remain unclear and require careful consideration (64).

1.14 Apoptosis

The principle aim of administering chemotherapeutic drugs to patients with cancer is to induce 'programmed cell death' or apoptosis. Signalling for apoptosis occurs through multiple independent pathways that are initiated by triggering events within (Intrinsic) or outside (Extrinsic) the cell (288). Both signalling pathways converge on common machinery to induce cell death by activating cysteine proteases (Caspases) that cleave proteins at aspartate residues (289). Morphological and molecular changes that ensue can be detected using a variety of laboratory techniques to detect apoptotic cells.

Morphological hallmarks of apoptosis include chromatin condensation, cytoplasmic shrinkage and plasma membrane blebbing; whilst phosphotidylserine externalisation, mitochondrial depolarisation and inter-nucleosomal DNA cleavage are used as molecular hallmarks (290).

The intrinsic pathway is tightly regulated by the Bcl-2 family of pro (Bax, Bad, Bim) and anti-apoptotic (Bcl-2, Bcl-w, Bcl-X_L) proteins (288). Pro-apoptotic BH3-only members of the Bcl-2 family respond to death signals by trans-locating to the outer membrane of the mitochondria and inactivating anti-apoptotic Bcl-2 proteins. The resulting oligomerisation of Bak and Bax leads to permiabilisation of the outer membrane of the mitochondria and release of pro-apoptotic factors that activate caspases (291). Proteins that are released from the inter-membrane space (IMS) include Cytochrome C, apoptosis inducing factor (AIF), endonuclease-G, Smac/Diablo and Omi/HtrA2. Cytochrome C release into the cytosol leads to the oligomerisation of Apaf-1 and formation of the apoptosome (cytochrome C/Apaf1/Caspase-9) (291). Apoptosis inducing factors (AIF) and endonuclease-G, translocate to the nucleus from the IMS and cleave DNA. Smac/Diablo and Omi/HtrA2 activate caspases by neutralising the inhibitory effects of IAP's (inhibitors of apoptosis proteins) (291).

The extrinsic pathway is initiated by activation of death receptors (DR's) that belong to the tumour necrosis factor (TNFα) superfamily (289). The TNFα superfamily consist of >20 proteins that regulate a broad range of biological agents including survival, differentiation and immune regulation. Members of the TNFα share similarities in structure, including a cysteine rich extracellular domain and an 80 amino acid intracellular death domain (DD) that plays a crucial role in transmitting extracellular death signals to the intracellular apoptosis pathways (288). The best described death receptors are, CD95, TNF receptor 1 (TNFR1), TNF related apoptosis inducing ligand receptor 1 (TRAIL1) and TRAIL2. The corresponding ligands for death receptors are, CD95 ligand (CD95L), TNFα, lymphotoxin-α and TRAIL (288).

Activation of DR's by ligand/receptor interaction leads to trimerisation and clustering of the intracellular death domains. The clustering of DR's leads to homophilic interactions between the death domains and adaptor molecules such as FAS associated death domain (FADD). FADD in turn recruits caspase 8 to the activated DR, to form the death inducing signalling complex (DISC). Oligomerisation of caspase 8 results in self-cleavage of the pro-caspase and activation of downstream caspase 3 (291). In some instances the amount of caspase recruited to the DISC complex is insufficient to initiate activation of down stream caspases and a mitochondrial amplification loop is required. A similar pattern of events has been reported on interaction of TRAIL with its cognate death receptors (TRAIL1 and TRAIL2) (288).

Cancer cells have evolved numerous strategies to resist initiation of apoptosis via the intrinsic or extrinsic pathway. For example cancer cells down regulate cell surface expression DR's making them resistant to extrinsic apoptosis signalling (292). Deficient Transport of TRAIL receptors from the endoplasmic reticulum to the cell surface has been reported as a mechanism driving resistance in CRC. Decoy CD95 receptors that competitively bind the CD95L to inhibit transmission of apoptosis signalling has also been observed in breast and colon cancer (291). Other mechanism including epigenetic silencing of DR expression, improved potency in negative regulation by phospho-protein enriched in diabetes (PEA-15) or FLIP has also been reported as resistance mechanisms against apoptosis (290). Resistance to apoptosis by disruption of the intrinsic pathway is also well recognised in cancer. For example overexpression of Bcl-2 due to translocation of the Bcl-2 oncogene into the immunoglobulin heavy chain gene locus is associated with 85% of human follicular lymphoma. Loss of pro-apoptotic BH3-only members through deletions accelerates B-cell lymphogenesis and mantle cell lymphoma progression. Besides Bcl-2 proteins, absence or decreased activity of the Apaf-1 oligomer was found in ovarian cancer and melanoma (292). *p53* the most common genetic mutation on human cancer plays a central role in activation of intrinsic apoptosis pathways, partly by up-regulating expression of BH3-only proteins Noxa, Puma and Bax. It has also been reported *p53* can bind to Bcl-2 and $BclX_L$ at the mitochondria thereby promoting

mitochondrial destabilisation (288). The above evidence clearly demonstrates that apoptosis pathway play a critical role in regulating tumorigenesis, cell survival and treatment resistance, making it a key biological event to consider in cancer diagnostics and therapy.

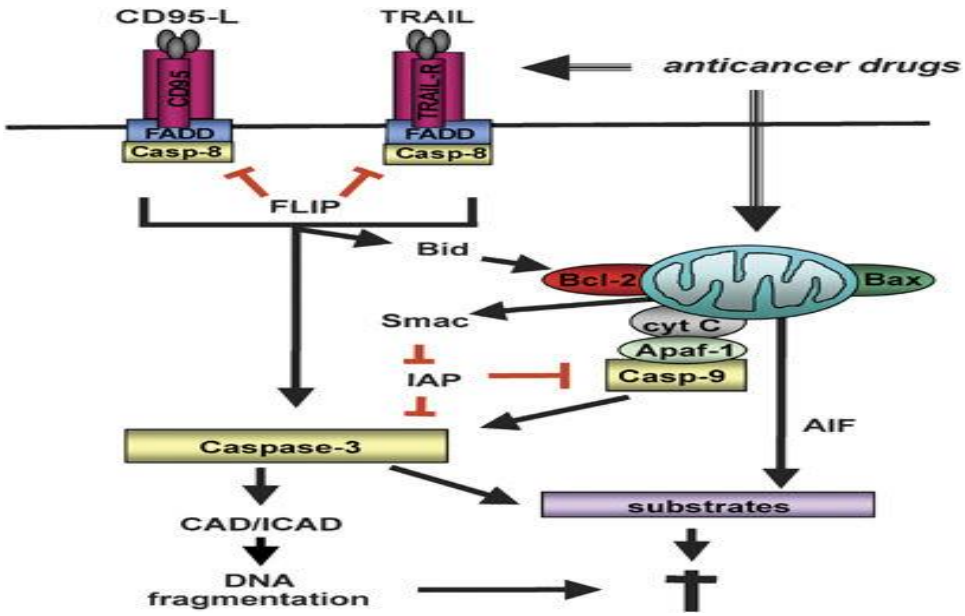

Figure 12: Intrinsic and extrinsic apoptosis signaling pathway. The apoptosis pathway can be activated via death receptor ligation or mitochondria depolarisation. Ligand / receptor interaction between TNFα family of death receptors (CD95/TRAILR1/TRAILR2) and the cognate ligand (CD95L/TRAIL) results in receptor trimerisation and assembly of the Fas associated death domain (FADD) and caspase-8. Activation of caspase-8 results in downstream activation of effector caspases-3 and cell apoptosis. Mitochondrial depolarization by the assembly of pro-apoptotic Bcl-2 proteins Bak and Bax results in of release pro-apoptotic factors form the inter-membrane space (IMS). Cytochrome C release into the cytosol results in activation of caspase-3 through aggregation of the apoptosome. Endonuclease –g and Apoptosis inducing factor-1 translocate to the nucleus and undertake inter-nucleosome DNA cleavage. Smac /Diablo and Omi/HtrA2 promoter apoptosis by counteracting the inhibitory effects of inhibitory apoptosis proteins (IAP's). Apoptosis pathways are negatively regulated by FLIP, which competes with caspase-8 to inhibit activation after ligand/receptor interaction at death receptors (291).

1.15 DNA Damage

Preservation of genomic integrity is essential for faithful transmission of the genome to the progeny. However, environmental factors and chemical make up of DNA do not guarantee the life long preservation of the genome. Genomic injury undermines all basic biological processes and its successful repair is critical for normal cellular function. DNA lesions arise from three primary sources: environmental agents such as ultraviolet light, ionising radiation, and numerous genotoxic chemicals; reactive oxygen species generated as a by-product of respiration and lipid peroxidation; and spontaneous hydrolysis of

nucleotide residues resulting in abasic sites and deamination of C, A and G (293). From a therapeutic perspective, a wide variety of chemotherapeutic agents induce DNA damage with the aim of driving neoplastic cells towards apoptosis. However, DNA repair of genomic insults and the resulting damage response have long been recognised as resistance mechanisms to treatment (290). In the following sections, I will provide an overview of common DNA lesions, associated damage response and the repair machinery that works to preserve genomic integrity and avoid cell death.

Table 1: DNA lesions and corresponding repair pathway.

DNA lesions	Cause	Repair machinery
Abasic site / Uracil (hypo)Xanthine	Spontaneous hydrolysis/ Spontaneous deamination	Base excision repair
Thymine glycol / 8-oxo-DG	Reactive oxygen species (ROS) / respiration	Base excision repair
Mismatches / Small insertions and deletions	Replication error / replication slippage	Mismatch repair
Cyclobutane pyramidine dimers (CPD) / 6-4 Pyramidine pyramidone photoproducts (6-4 PP)	Ultraviolet rays from Sunlight	Nucleotide excision repair
Intrastrand crosslinks / Interstrand cross links	Chemotherapy (Platinum drugs)	Nucleotide excision repair / Double strand break repair / Fanconie anaemia pathway
Single strand / Double strand	Ionising Irradiation /ROS	Double strand break repair

1.16 DNA damage response

Due to the vital importance of maintaining genomic integrity, DNA damage is recognised and repaired or apoptosis pathways activated when repair is not feasible. The DNA damage response (DDR) machinery can be viewed as a classical signal transduction cascade in which damage is detected by a 'sensor' (DNA damage binding proteins), which then triggers the activation of 'transducers' (protein kinase cascade) that amplify and diversify the signal by targeting a series of 'effectors' (292). In this section, I will discuss cellular DNA damage response using DNA double strand breaks (DSB) as an example. The mammalian DDR machinery regulates two key responses, namely the rapid activation of cell cycle check-points and recruitment of DNA repair proteins onto the chromatin (290).

The MRN (mre11-rad50-nbs1) complex is the first to get recruited to DSB's where it functions to recruit and activate ataxia telangiectasia mutated (ATM) protein kinase. Activated ATM phosphorylates 100's of proteins including proteins involved in apoptosis, check-point activation (e.g. p53 and chk2) and DNA repair proteins such as BRACA1 and 53BP1 (292) .

A key target of ATM is the phosphorylation of the c-terminal of the histone variant H2AX. Phosphorylation leads to the formation of γH2AX, which creates a binding site for BRCT domain of the mdc1 protein(294). Positioning of mdc1 at the double strand break creates a docking site for additional DSB repair proteins, including the MRN-ATM complex. The docking of ATM propagates H2AX phosphorylation that extends for 100's of kilo-bases from the site of DSB (295). The mdc1 protein also facilitates docking of ubiquitin ligases RNF8 and RNF168, which ubiquitinates chromatin and promotes loading of BRACA1 and 53BP1 (296). In a similar fashion to the spread of γH2AX, chromatin ubiquitination also spreads for 100's of bases from the DSB site (297). If the DSB's forms as a consequence of replication collapse, the resulting single strand DNA overhang binds to the RPA protein which in turn leads to activation of ATM related (ATR) proteins kinase(290). Activation of ATM and ATR leads to phosphorylation of checkpoint kinases chk2 and chk1 respectively. Phosphorylation of checkpoint kinase results in depletion of cyclin-dependent kinases and cell cycle arrest, providing time for repair and reinstatement of genomic integrity (298). Another important protein, DNA dependent protein kinase (DNA PK) and regulatory heterodimer Ku70/80 are also activated in response to DNA DSB breaks and play a key role in non homologous end joining and repair of DSB's (298). Four major determinants of the DNA repair pathway choice include the nature of the DNA lesion and the stage of cell cycle during which the lesion is encountered. In the next section, I will discuss the five main DNA repair pathways that get activated as a result of DNA damage response in mammalian cells.

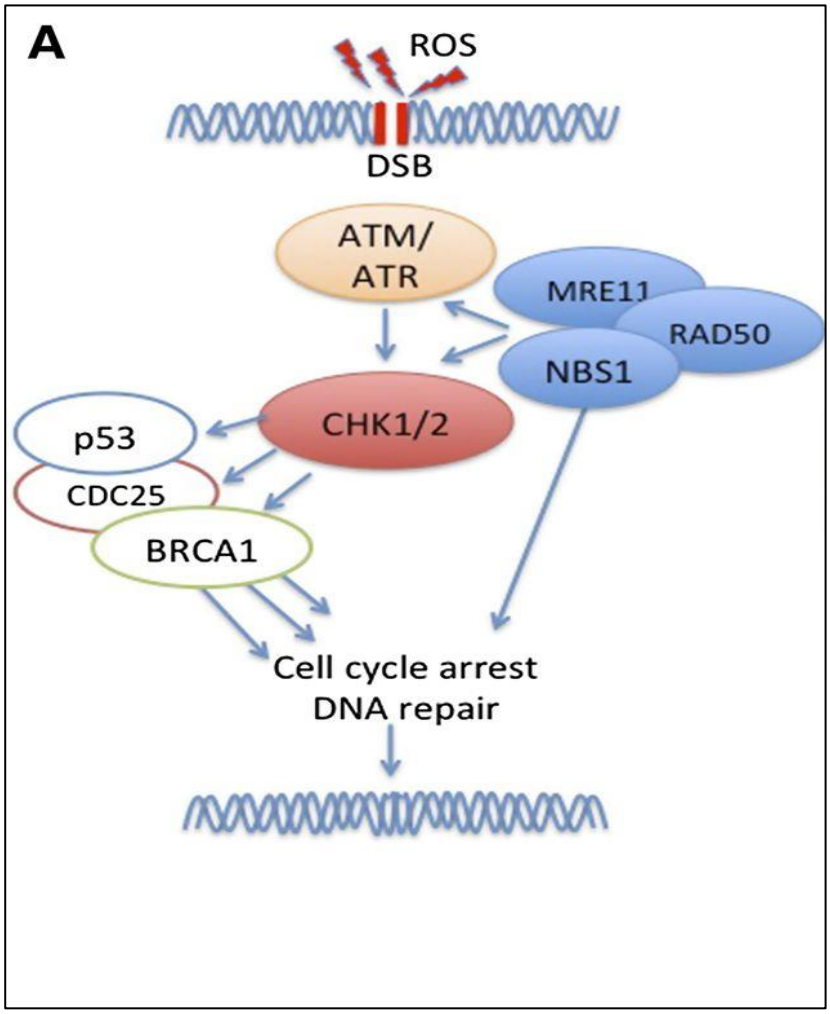

Figure13: DNA damage response to DSB's. DSB results in recruitment of MRN (mre11-rad50-nbs1) to the site of repair. Docking of the MRN complex to the DSB leads to activation ATM activation and phosphorylation of H2AX at serine 139 (γH2AX). Single stranded DNA attracts RPA, which in turn activates ATR. Activation of these master protein kinases, leads to amplification and diversification of the damage signal. 2 key signal traducing protein kinases are CHK1 and CHK2, which play critical role in regulating cycle progression, DNA repair and apoptosis (299).

1.17 DNA damage repair

All life forms have the ability to respond to alterations in genomic DNA that occurs spontaneously or caused by environmental agents (300) . The options presented are to repair the damaged DNA or to tolerate the damage in ways that reduces their lethal effects (301). DNA damaging agents such as oxaliplatin and 5-FU continue to present the main stay of treatment for patients with colorectal cancer (3). These agents induce genotoxic stress and consequently it could be postulated improved repair mechanism would promote resistance. In this section, I will briefly discuss cellular DNA repair mechanism and their potential contribution to treatment resistance in neoplastic cells.

DNA damage repair pathways can be divided into 5 main types: -

1. Direct repair
2. Base excision repair
3. Nucleotide excision repair
4. Mismatch repair
5. Double strand break repair

1.17.1 Direct repair

During direct repair the abnormal chemical bonds between bases or nucleotides and an abnormal substituents are broken. For example, exposure of DNA to UV irradiation results in the formation of pyrimidine dimers. An enzyme termed DNA photolyase binds to DNA and catalyses the removal of the adduct using a flavin co-factor without disturbing the ribose backbone (302, 303). Photolyase also binds to cisplatin induced DNA damage with high affinity (304). It holds the capacity to improve efficacy of excision repair through currently unknown mechanism. Another example is the suicide enzyme methyl guanine methyl transferase (MGMT). This enzyme directly removes, methyl groups from guanine bases to maintain DNA integrity (305, 306). There are similar suicide enzymes that are capable of removing methyl groups from cytosine and adenine nucleotide bases.

1.17.2 Base excision repair (BER)

Bases with small chemical alterations that do not disrupt DNA double helix are substrates for base excision repair. These damages or group of lesions are targeted by a group of DNA specific glycosylases that recognise and remove the base from the sugar phosphate backbone e.g. OGG1 (8-oxoguanine glycosylase), UDG (uracil DNA glycosylase) and AAG (3-alkyladenine DNA glycosylase). The resulting abasic site is excised by apurinic/apyrimidinic (AP) endonucleases and the resulting gap filled and ligated by BER specific DNA polymerase β and XRCC1/DNA ligase III complex. Long patch BER results from DNA single strand breaks (SSBR) that requires repair of 2-13 base pairs at a stretch. SSBR results in recruitment of poly-ADP ribose polymerase to the break site. This leads

to end processing of DNA by endonucleases such as aprataxin. The resulting gap in filled by DNA polymerases and ligated by XRCC1/ligase III complex (307).

1.17.3 Mismatch repair (MMR)

The DNA Mismatch repair pathway plays a key role in stabilising the genome and the protein components of this system are highly conserved in both pro and eukaryotic cells. Mismatch of nucleotides occurs secondary to two primary mechanisms: Error made by DNA polymerase or mismatches that occur during replication. In mammals the importance of mismatch repair genes in cancer progression was recognised by patients with HNPCC. These patients lack the ability to undertake DNA mismatch repair and consequently accrue mutations at a much higher rate, when compared to the normal population. MMR pathways involves four distinct steps: 1) recognition of the mismatched nucleotides, 2) Recruitment of additional MMR factors, 3) search for signals that identify the newly synthesised strand its excision and 4) re-synthesis of the excised tract. In humans, damage recognition is undertaken by two heterodimers hMutSβ (MSH2-MSH3) and hMutSα (MSH2-MSH6) that poses varying affinities towards mismatch errors. The MLH1-/PMS2 complex interacts with the MSH proteins and replication factors facilitating excision by the enzyme Exonuclease-1. Re-synthesis of the excised strand in performed DNA polymerase δ and the nick sealed by DNA ligases I (301).

1.17.4 Nucleotide excision repair (NER)

Nucleotide excision repair plays a critical role in mediating DNA damage response. In contrast to limited substrate specificity of most DNA glycosylases, NER operates on a large spectrum of base damage produced by mutagenic and carcinogenic agents. Unlike more simple forms of excision repair, which is performed by a few enzymes, NER requires the presence of 25 polypeptides for its successful completion. The importance of NER in humans is highlighted by genetically inherited disorders Xeroderma pigmentosum (XP) and Cockayne syndrome (CS) that occur secondary to inherited mutations in excision repair proteins. The disease is autosomal recessive, with symptoms falling into 2 categories: photodermatosis and neurological dysfunction. Nearly 90% of patients with XP

develop skin malignancies in their early teenage years due to extreme sensitivity to UV irradiation from sunlight. Mutations in any one of seven classical XP complementation groups (XPA-XPG) have been identified as the cause of these symptoms form clinical studies investigating genetic heterogeneity in these patients (293, 307).

In vitro studies have demonstrated sixteen polypeptides grouped into six fractions are sufficient to reconstitute NER. The repair process can be divide into three distinct stages: 1) DNA damage recognition, 2) dual incision / repair synthesis and 3) ligation. Although not proven, damage recognition is considered the rate-limiting step in the reaction as a wide range of adducts are recognised by a limited number of genes. Dual incision of the adduct requires the formation of a pre-incision complex. The initial recognition step involves binding of XPA-RPA complex to DNA. XPA and replication protein A (RPA) are complexes with high affinity to DNA, which is increase by their interaction with each other. XPA-RPA recruits the TFIIH complex to the lesion, resulting in unwinding of DNA. This allows intimate DNA protein interactions and makes the damaged strand accessible to XPC-HHR23B complex which interacts with TFIIH and XPA. Once the pre-incision complex is constructed, incision at the 3' end is made by recruitment of XPG, whilst XPF-ERCC1 complex makes the 5' incision. The 3' incision is made 3-5 nucleotides from the lesion whilst the 5' incision is made 20-24 nucleotides from the lesion. The post-incision complex is dissociated by RFC molecular matchmaker which loads the PCNA trimeric circle and facilitates DNA synthesis by Pol ε and δ. The repaired patch is subsequently ligated by DNA ligase (300, 307-309).

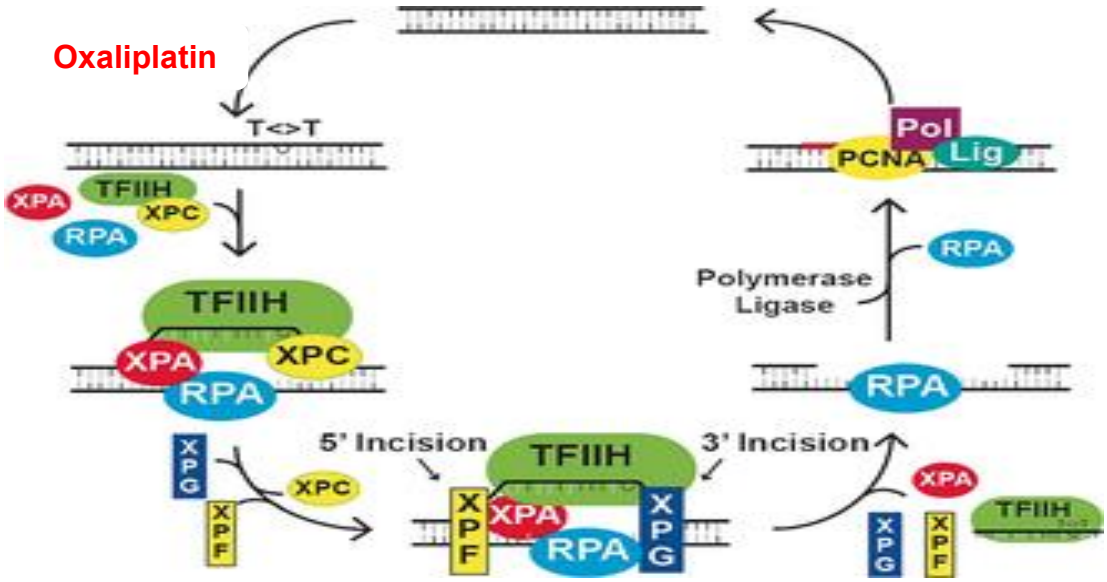

Figure 14: **Stages in DNA repair by nucleotide excision repair pathway.** The damage induced by platinum based chemotherapeutic agents is recognized by cooperative interactions of RPA, XPA, and XPC followed by recruitment of TFIIH. The helicase activity of TFIIH provides the major specificity by kinetic proofreading and results in formation of a tight complex. Subsequently XPG and XPF nucleases are recruited to make the 3′ and 5′ incisions. The excised "19-30-mer" is released in a tight complex with TFIIH. The excision gap is filled in by DNA polymerases and ligated to produce a 30 nt long repair patch. Adapted from Sancar (310).

1.17.5 Double-strand break repair

The DNA repair mechanisms discussed previously in this section have relied on injury to a single strand. The activated repair mechanism excises the adduct and uses the complementary strand to repair the patch. However, insults can result in a break on both strand of the DNA. The resulting DNA double strand breaks (DSB) are cytotoxic lesions that threaten genomic integrity and cell viability. Many chemotherapeutic agents such as oxaliplatin, doxorubicin and ionising irradiation (IR) induce DSB thus promoting cell death in both normal and neoplastic cells (311). There are two major mechanism governing DSB repair in eukaryotic cells, namely homologous recombination (HR) and non-homologous end joining (NHEJ) (311). A key determinant of repair mechanism choice is phase of cell cycle. HR requires a sister chromatid and consequently occurs at S and G2 phases. Whilst NHEJ predominates at M and G1 stages of cell cycle (312). During NHEJ, two broken ends of DNA are ligated independent of homology and consequently the mechanism is intrinsically error prone. By contrast, HR uses a homologous sequence from a sister chromatids and thus error free (311).

NHEJ is a complex process that involves many proteins, however 6 proteins have currently been identified as required for direct catalysis of DSB repair (313). Three are components of the DNA dependent protein kinase (DNA-PK), which include Ku70/Ku80 and DNA-PKc, which is the catalytic subunit. Ku proteins bind to DNA after end processing at DSB's and bringing the broken DNA together. The binding of Ku proteins to the double strand break results in targeting of DNA-PKC's to the DSB, leading to its activation. Other important catalytic proteins are Artemis, which is an exonuclease that is phosphorylated and activated by DNA-PKC's. The final two components are DNA ligase IV and XRCC4, which functions as a complex to ligate the DNA ends. The above process is highly conserved from yeast to human (313, 314).

A large number of proteins are known to be involved in catalysing HR after at double strand break. The first step in HR is DNA end binding by RAD52 or other mammalian homologues, which compete with the Ku proteins to channel the DSB towards HR. ATM, ATR or DNA-PK activation results in histone H2A.X phosphorylation that facilitates binding of the conserved MRN complex to DNA. The MRN complex promotes end resection resulting in the creation of single stranded DNA end flanking the DSB. This single strand is bound by proteins including RPA, RAD54 and RAD51, which finds a homologous template and promote strand invasion. These strands are extended by a polymerase and sealed to appropriate parental strand by a DNA ligase. This process results in the formation of Holliday junctions, which are resolved by DNA cleavage and ligation. In mammalian cells proteins such as BRCA1, BRCA 2 and Fanconi anaemia genes are also known play a central role in this process (313, 315).

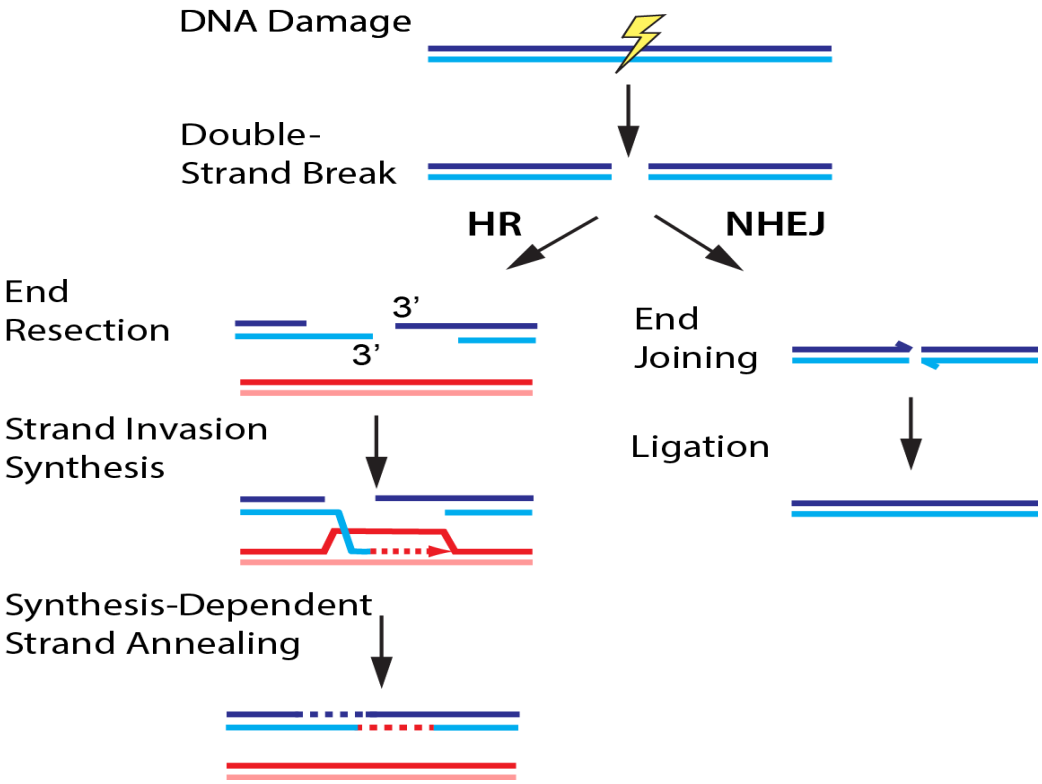

Figure 15: **Stages in double strand break repair by non-homologous end joining and homologous recombination.** (A–D) The repair of DNA DSBs relies primarily upon two major mechanisms, the error prone non-homologous end joining (NHEJ) or the error free homologous recombination (HR). NHEJ is activated by binding of Ku proteins (Ku70-Ku80 complex) to damaged DNA at double strand breaks (DSB's). The Ku proteins attract the DNA dependent protein kinase catalytic subunit (DNAPKc's) and activate its kinase activity. DNAPKc's activate important endonucleases Artermis, which performs end processing and finally the repaired DNA ends are ligated by ligase IV-XRCC4 complex. The end processing of damaged DNA by endonucleases results in loss of genetic information making the repair process intrinsically error prone. Homologous recombination (HR) is an error free homology directed repair mechanism. The initials steps of HR involve end resection, regulated by the MRN complex to generate single stranded DNA tails followed by pairing and exchange of strands mediated by RAD51. BRC1/2 interact with RAD51 to regulate its function. The 3' single-stranded end of the damaged DNA invades the homologous chromosome to form a displacement loop (D loop). These strands are extended by a polymerase and sealed to appropriate parental strand by a DNA ligase (313).

1.18 DNA repair and chromatin

When considering DNA repair it is vital to consider the protein core (Histones) around which DNA is wrapped. Despite growing acknowledgement of the influence of chromatin on DNA damage recognition and repair, a detail mechanistic overview is still lacking. The Access-Repair-Restore model currently provides a construct around which chromatin and DNA repair pathways may be studied (226). This model assumes that histone modifications are required for access of damaged DNA and subsequent restoration of chromatin integrity is critical once DNA repair is complete to avoid aberrant

gene expression. For example histone H3/H4 chaperone CAF1 and anti-silencing function 1 (ASF1) have been identified as proteins that restore chromatin structure after nucleotide excision repair (316). The most dramatic histone modification that occurs in response to DSB's is the phosphorylation of H2AX at ser-139 to form γH2AX. Flanking of DSB's by the spread of γH2AX for several mega-bases provides a docking site for several DNA repair and DNA damage signalling molecules (226). The importance of γH2AX in maintenance of genomic integrity has been demonstrated by the sensitivity of H2AX null mice to IR. However, these mice were only partially deficient in repair and continued to be able to activate checkpoint kinases (290).

The influence of higher order chromatin structures on DNA repair is an area of research where scientists continue to have limited insight. The influence of tightly compacted heterochromatin (H3K9me3, H3K27me3) or transcriptionally active euchromatin (H3K4me3) on DNA repair kinetics remains an area of active research. Evidence that heterochromatin delays repair kinetics comes from yeast models where absence of an acetyltransferase Gcn5, which promotes open chromatin conformation delayed repair kinetics at specific loci where Gcn5 was known to remove heterochromatin marks (317). Studies in mammalian cells have reported the requirement for release of heterochromatin factors KAP associated protein (KAP1) for efficient DSB repair. With regards to EMT, there is growing acknowledgement that mesenchymal transition requires genome scale reorganisation of the chromatin structures (318). Evidence for this suggestion has recently been provided by studies suggesting loss of heterochromatin and gain of euchromatin marks after Twist1 and TGFβ induced EMT (224, 225). The impact of these genome scale changes on DDS, chromatin stricture and repair are as yet poorly understood and requires urgent investigation.

1.19 Faster repair, greater tolerance or both

A contributing role for EMT in inducing chemoresistance is beyond doubt (53, 107). However, the mechanism mediating treatment resistance is only partially understood. EMT has been closely affiliated with the acquisition of stem cell features(110). It is now emerging stem cells deal with DNA damage in a more efficient manner when compared to differentiated cell populations (319, 320). For example embryonic stem cells express higher levels of BER genes such as OGG1, thus repairing DNA adducts created by ROS more efficiently (319). SNAIL an EMT inducing transcription factor up regulates expression of ERCC1 in head and neck cancer, promoting resistance to platinum based chemotherapeutic agents (321). Studies in neural stem cells have demonstrated, NER is attenuated upon differentiation of precursors cells, suggesting higher repair capacity in de-differentiated stem cells (322, 323). Pluripotent stem cells also express high levels of MMR genes and repair DNA damage more efficiently when compared differentiated cells (319). Expression levels of genes involved in NHEJ and HR are also increased in some stem cell populations thus exhibiting increased capacity for double strand break repair (319). These findings highlight the notion that stem cells in general exhibit a higher efficiency in DNA damage repair. Although the link between EMT and stemness has long been recognised, it is as yet unclear if pluripotent stem cells and cancer cells expressing EMT markers share the same mechanisms promoting DNA damage resistance. Further, mechanistic detail pertaining to pathways promoting EMT and the precise contribution of different EMT-TF's towards promoting chemo resistance warrants further investigation.

1.20 Summary, Hypothesis and Objectives

Colorectal cancer (CRC) is the second commonest cause of cancer death in Europe, and a key public health issues. Metastases are the principle cause of death and occur in up to 30% at presentation, and subsequently develop in 50% after potentially curative surgery from occult micro-metastases. The majority of patients with metastases are incurable, and can expect a median survival of only up to 2 years, even with the latest chemotherapeutic and biological agents. Additionally, not all patients respond, and side effects are frequent, cumulative, and at times life threatening. These limitations in therapeutic avenues that are available for patients with metastatic disease, highlights the pressing need for the identification of new biomarkers to predict metastatic (and micrometastatic) capability, to tailor aggressive therapy to higher risk cases. Although development of primary CRC has served as a paradigm for understanding multistage carcinogenesis, the mechanisms mediating metastasis and chemoresistance are still poorly understood.

Epithelial-Mesenchymal Transition (EMT**)** is an embryologically conserved genetic program by which epithelial cells down regulate cell-cell adhesions complexes, express mesenchymal markers, and manifest a migratory phenotype. While the significance of EMT during development and embryogenesis is well established, an emerging role is its involvement in metastasis and chemoresistance. EMT is activated by TGFβ, FGF, EGF, WNT and Notch signaling pathways, which converge to activate transcription factors that subsequently repress the expression of critical epithelial genes. Key transcription factors in this process include members of the SNAIL, Twist, and ZEB families, which promote cellular phenotypic switch. In addition to enhanced migration, metastatic cells also acquire apoptosis resistance, through as yet poorly understood mechanisms. Among EMT inducing transcription factors, SIP1/ZEB2 is the least studied in general, and specifically in CRC, due to the absence of specific and sensitive antibodies. Dr Sayan's group recently overcame this hurdle by raising antibodies against different epitopes of SIP1/ZEB2 and validating its specificity.

Although the contribution of EMT to metastasis is disputed, there is overwhelming consensus that EMT induces chemoresistance. A previous drug screen performed by our group demonstrated significant apoptosis resistance after treatment with DNA damaging agents in SIP1/ZEB2 expressing mesenchymal cells. Although not well understood, mechanisms contributing to chemoresistance after EMT could include increased drug efflux, efficient DNA repair or tolerance to DNA damage. Emerging evidence now suggest components of the DNA repair machinery are over expressed by mesenchymal cells expressing SNAIL1 in head and neck tumours. Sayan and colleagues reported SIP1/ZEB2 expressing carcinoma cells are resistant to platinum based chemotherapeutic agents due to reduced activation of DNA damage recognition signalling. This data suggests improved DNA damage may at least in part contribute to chemoresistance observed after EMT. However little is known about mechanisms promoting metastasis and chemoresistance in SIP1/ZEB2 expressing cells in CRC. Consequently I hypothesised:

- **SMAD interacting protein (SIP1)/ Zinc finger E-box binding homeo-box 2 (ZEB2) induced EMT promotes metastasis and apoptosis resistance to DNA damaging agents in colorectal cancer (CRC).**

AIM: The aim of this study is to determine the biological contribution of SIP1/ZEB2 to metastasis and chemo/radio resistance pathways in CRC.

OBJECTIVES:

1. Assess if SIP1/ZEB2 induces EMT in CRC.
2. Investigate if SIP1/ZEB2 induced EMT promotes metastasis and chemo/radio resistance.
3. Study the molecular mechanism mediating SIP1/ZEB2 induced apoptosis resistance.
4. Validate in-vitro findings in a murine model

RESEARCH PLAN:

Objective 1: I will use DLD-SIP1 a doxycycline inducible cell line developed and validated by Berx and colleagues (324) to demonstrate SIP1/ZEB2 induces EMT *in vitro*. Changes to the expression profile of epithelial and mesenchymal cytoskeletal and cell adhesion

proteins considered hallmarks of EMT will be assessed by IF and WB. The proliferation, motility and cell cycle kinetics of SIP1/ZEB2 expressing cells will also be assessed. Careful validation of these hallmark characteristics of EMT is critical, as alteration to these characteristics after induction of EMT can modify response to chemotherapeutic agents and thus bias functional experiments. I will assess, if SIP1/ZEB2 induces chemoresistance to drugs routinely used in the clinical setting (Oxaliplatin, 5FU and Doxorubicin) by WB for PARP cleavage. Further, I will also investigate if SIP1/ZEB2 promotes apoptosis resistance by improved drug efflux using the intrinsic fluorescence properties of doxorubicin.

Objective 2: I will investigate if SIP1/ZEB2 expression in primary CRC cells promotes metastasis and chemoresistance *in vivo*. To achieve this aim I will construct a retrospective database of patients that underwent primary resection for CRC between 2004-2013. I will subsequently undertake IHC analysis on these samples and correlate SIP1/ZEB2 expression with long-term oncological outcomes.

Objective 3: Undertake a micro-array with a focus on DNA damage repair to identify candidate genes promoting chemo resistance after EMT. I will validate my findings and undertake functional assays to investigate mechanism promoting chemo resistance after SIP1/ZEB2 expression.

Objective 4: I will investigate if SIP1/ZEB2 expression results in resistance to ionising radiation and investigate whether the acquired resistance to apoptosis is secondary to faster repair of double strand breaks created by exposure ionising radiation or tolerance to the DNA damage inflicted. I will also undertake ChIP-Seq analysis to determine whether genome scale epigenetic changes can influence DNA repair kinetics and apoptosis resistance.

Objective 5: Develop an orthotopic CRC model in immune compromised mice to investigate if SIP1/ZEB2 expression promotes metastasis and chemo resistance *in vivo.*

Chapter 2: Materials and Methods

2.1 Tissue Culture

2.1.1 General principles

Tissue culture was undertaken in a laminar flow hood and cells grown in a incubator with a humidified environment, temperature of 37° C with 5-10 % CO_2. Reagents were stored at recommended temperatures as per manufacturers guidelines. Stock solutions of buffers were prepared and stored at room temperature.

2.1.2 Cell Culture

The cell lines used were regularly tested for mycoplasma. No positive test results were found during the period of this research work in the cell lines used. All cell culture was undertaken in a Dulbecco's Modified Eagle Medium (DMEM) (Sigma) supplemented with 10% foetal calf serum (FCS), 2mM L-Glutamine and 1% of 100X Penicillin / Streptomycin.

2.1.3 Cell lines

DLD-SIP1 (DLD-WT stably transfected with tetracycline inducible SIP1/ZEB2) a SIP1/ZEB2 inducible EMT model of CRC was used to conduct experiments to study the impact of SIP1/ZEB2 at mediating metastasis and chemoresistance(324). A further eleven CRC cell lines were purchased from American type culture collection. DLD-SIP1 was kindly provided by Prof. Eugene Tulchinsky. All cell lines used are listed in the Appendix section in Table 23.

2.1.4 Cell propagation

Cell propagation was undertaken in a T75 flask in DMEM. Cells were trypsinised in 1x Trypsin EDTA (Sigma), re-suspended in DMEM at the appropriate concentration and seeded in wells or dishes for experimentation. Cell growth was monitored using an inverted microscope and confluence was not allowed to exceed 80% during propagation. Cells were collected by spinning down at 1500 rpm and washed in 1 x Phosphate Buffer Saline pH 7.0 (PBS), pelleted and frozen at -20C°.

2.1.5 SIP1/ZEB2 induction in DLD-SIP1 cells

DLD-SIP1 cells were cultured in the presence of Doxycycline (2mg/ml stock solution) (Sigma) dissolved in DMEM at a concentration of 1/250). Cells were allowed to propagate for 48 hours and then re-split and cultured for a further 72 hrs. Cellular phenotypic switch to a mesenchymal morphology was observed using an inverted light microscope.

2.1.6 Defrosting cells

Cells were transferred from a liquid nitrogen tank (-196°C) onto dry ice to avoid exposure to sudden temperature changes. Rapid thawing was undertaken by immersing the frozen cell vial into a 37° C water bath for 2 minutes. Cells were then re-suspended in 10mls of warm DMEM and centrifuged at 1500 RPM for 5 min to pellet the re-suspended cells. This was done to ensure any residual DMSO was removed from culture medium. Cells were then re-suspended in 1ml of warm DMEM and seeded in a T75 flask. (Corning® Incorporated) containing 10mls of culture media. Defrosted cells were allowed to recover from the effects of cryo-preservation for at least one passage before use in experiments.

2.1.7 Freezing cells

Freeze media (73% complete DMEM, 20 % FCS and 7 % dimethyl sulphoxide (DMSO; Sigma) was prepared in advanced and kept on ice. Cells were cultured in a T75 flask, trypsinised and re-suspended in freeze media. A haemocytometer was used to manually count cell numbers. A volume containing 2 million cells was aliquoted into cryo-vials (Grenier Bio-one Ltd) and placed in an -80 °C freezer (NALGENE® Mr. Frosty). Cells were then moved into a liquid nitrogen tank after 24hrs for long-term storage.

2.1.8 Cell Counting

Cell counting was undertaken manually using a haemocytometer. Cells within 25 squares were counted after placing 20 μl of the final dilution into the chamber. A light microscope was (10x lens) used to count cell numbers. The final cell count was calculated using the formula (Number of cells in the 25 squares x dilution factor $^{\Psi}$ x 10/μl).

2.2 Protein expression

2.2.1 Cell lysis, SDS-PAGE and Western blotting

Western Blotting is a technique that can be used to identify single proteins from cell lysates using molecular weight and antibody specificity. The technique involves SDS – page electrophoresis, transferring proteins onto a nitrocellulose membrane and incubating the membrane in antibodies and detecting bands by chemiluminescense. The Protocol below briefly outlines the technique used to achieve my results. The recipes for all buffers used in this protocol are shown in Table 19 in the Appendix.

Cells were collected in eppendorf tubes washed in PBS, centrifuged and kept frozen in a -20 °C freezer. Cells were lysed in a sonicator at 1.5 mWatts output for 30 seconds in 2X laemli buffer. Protein quantitation of lysates was undertaken using BCA protein assay reagent and a spectrophotometric plate reader (Bio-rad). A standard curve was generated using known concentrations of bovine serum albumin (BSA) and sample concentrations calculated using a formula generated from the standard curve. SDS – PAGE gels were prepared in accordance with Dr Sayan laboratory protocol. Details of relative quantities of acrylamide water, SDS, APS and buffers for gel construction are provided in Table 1.

Volumes relating to equal quantities of protein concentration were loaded after addition of 5x loading dye. A protein marker (Precision Plus Protein™ 10–250 KD, Bio-Rad) was used to detect bands at the appropriate molecular weight. Gels were run at 180 V for 65 min using 1 x Tris/glycine/SDS buffer (TGS; Geneflow; Main stock 10 x and subsequently transferred onto nitrocellulose membrane (Whatman Protran, GE healthcare) using wet transfer technique.

After transfer the membrane was blocked in 3% non-fat dry milk dissolved in TBS + 0.1% tween (TBS-T). The membranes were subsequently incubated in primary antibodies dissolved in 2.5% BSA for 1 hours at room temperature. Three 10 minute washes were undertaken using 0.1% TBS-T. The membrane was then incubated at room temperature in horseradish peroxide conjugated secondary antibody (Cell signalling) diluted in 2.5% BSA. A further three washes was undertaken in 0.1% TBS-T and immune-blots visualised using Supersignal ® West Dura chemiluminescent detection kit (Thermo Scientific, Rockford, USA). The enzymatic reaction and band intensity were detected using X-ray film and developer machine.

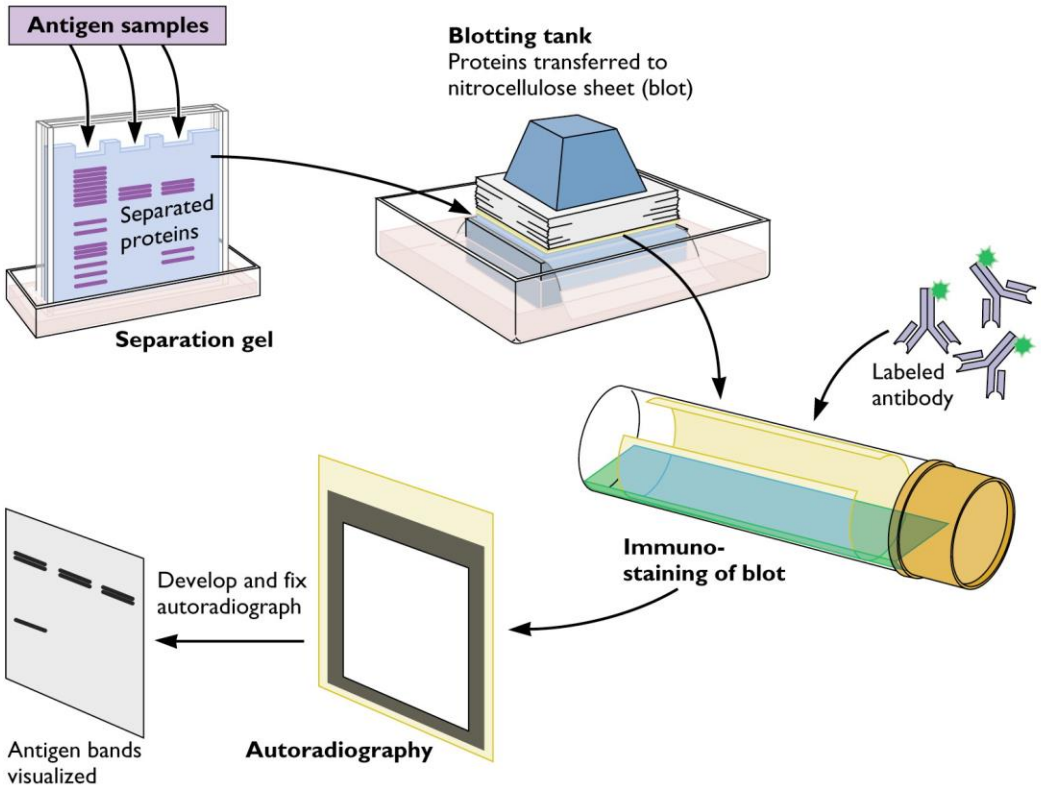

Figure 16: Work flow diagram demonstrating steps involved in western blotting. Briefly, volumes relating to equal quantities of protein were loaded into the columns of an SDS page gel. The proteins from the lysate are subsequently transferred onto a nitrocellulose membrane. Antibodies are used detect the protein of interest that is isolated into the membrane. The primary antibody is detected using HRP conjugated secondary antibody and autoradiography.

2.3 Flowcytometry

Flow cytometry is a technique used to analyse the characteristics of single cells in a liquid stream under the action of pressure. The device uses lasers pre-set to specific wavelengths to analyse cells as they pass through in a liquid stream. Passage of single cells past the laser results in light scattering that is detected by the device. Forward scatter (FSC) determines the size of the cell whilst the side scatter (SSC) granularity. These outputs are converted to voltage pulses that are proportional to particle size and granularity. In addition antibodies conjugated to flurophores or dyes bound to cells can also be detected. Flurophores and dyes absorb energy from lasers set at specific wavelengths and emit photons of light that are captured. The photons of light are converted into electrical impulses by a photomultiplier tube to attain a numerical output. The intensity of the colour is subsequently visualised as a histogram by computer software.

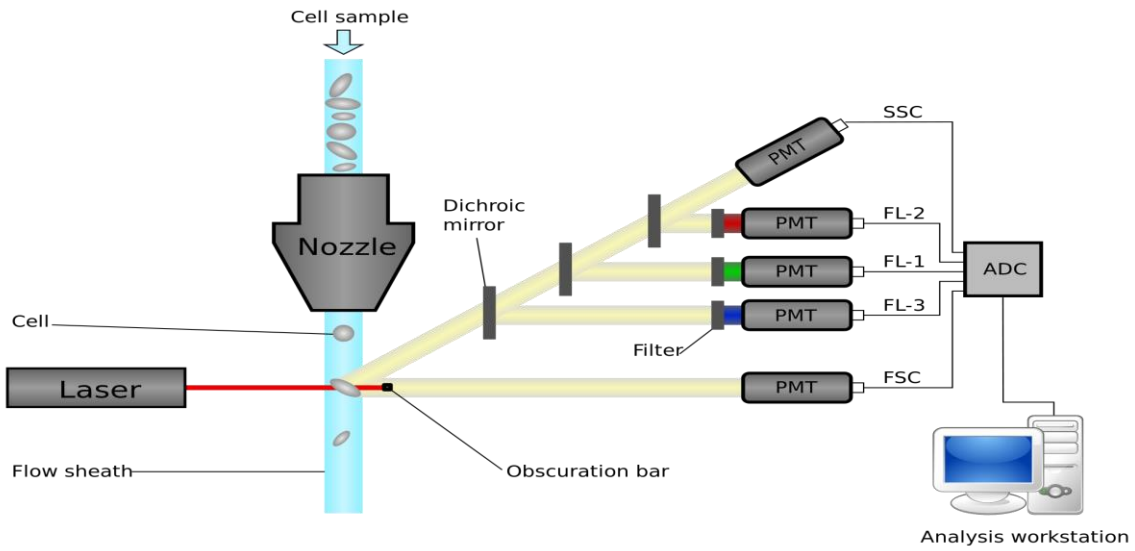

Figure 17: **Diagrammatic expression of the principles of Flowcytometry**. Flowcytometry is a laboratory technique that can detect physical (size, granularity) and biochemical (antibodies, dyes) properties of a single cell in suspension. The cell sample is passed through a pressurised fluidics system to assess each cell individually. During passage, cells interact with inbuilt lasers set to specific wavelengths, (535, 555 and 585) resulting in disruption of the beam. This results in light scattering and fluorescence signals, which will ultimately manifest as a stream of electrons, generated by a photomultiplier tube (PMT). The electrical signal generated by the passage of a cell past the laser beam is studied for physical and biochemical characteristics through specialized computer software.

2.3.1 Flowcytometry - Doxorubicin uptake assay

DLD-SIP1 un-induced and induced cells in culture were treated with 0.5µg/µl and 2.0µg/µl of doxorubicin for 2 hours, washed with PBS and allowed to recover for a further 1 hour. Cells were then trypsinised and collected in an eppendorf tube by centrifugation at 1250rpm for 3 min, washed in PBS and analysed in a Becton Dickinson FACScalibur machine. Due to Doxorubicin's intrinsic florescence property, cellular drug absorbance peaks were used as a read out for drug uptake in DLD-SIP1 cells. FL3 channel was used in the analysis of Doxorubicin uptake. Briefly, particles registering at an appropriate eukaryotic cell size (E-01) were gated using Forward Scatter (FCS) and Side Scatter (SSC). The gated cells were then analysed in FL3 channel (set to logarithmic scale) for the presence or absence of Doxorubicin. The results were visualised using a doxorubicin uptake histogram. Untreated cells were used as controls and compared to un-induced and induced DLD-SIP1 cells.

2.3.2 Flowcytometry - Annexin V / PI Apoptosis assay

Apoptosis is defined as programmed cell death and required for normal physiology and development. It is differentiated from other forms of cell death by morphological and cellular characteristics such as fragmentation of nuclear chromatin, cytoplasmic shrinkage, cell membrane blebbing and phosphatidylserine (PS) externalisation. The human anticoagulant Annexin V is a Ca2+ dependent phospholipid that has high affinity for PS. Consequently Annexin V labelled with a flurophore or biotin can identify apoptotic cells by binding to PS externalised on the cell membrane of apoptotic cells and captured by flowcytometry.

To conduct my experiment I cultured cells in DMEM and trypsinised as described previously. Treated and untreated controls were washed twice in 1X PBS. Cells were subsequently re-suspended in 500 µl of FITC Conjugated annexin V diluted 1:100 in binding buffer (HEPES buffer: 10mM HEPES/ NaOH, (pH 7.4), 150 mM NaCL, 5mM KCL, 5mM $MgCl_2$ and 1.8mM CaCl). Samples were incubated in the dark on ice for 30 minutes. 100µl of 50µg/ml of PI was added was added and incubated for a further 10 minutes. All

samples were analysed by flowcytometry using FL1 (for Annexin V-FITC) and FL3 (for PI) channels. Briefly, cell size particles were identified in the FCS/SSC dot plot and gated to analyse fluorescence emissions from FL1 and FL3 channel, in a new dot plot and split into 4 quarters. The increase in FL1 (upper left quadrant) is registered as early apoptosis, the increase of FL3 (upper right quadrant) is considered as necrosis. When FL1 and FL3 signals are both increased, this is considered as late apoptosis. The cells with no obvious increase in FL1and FL3 (bottom left quadrant) are considered live cells.

2.4 Immunofluorescence

Immunofluorescence (IF) is a technique used to detect target proteins in cells using antibodies conjugated to a fluorophore. Immunofluorescence is termed indirect if a secondary fluorophore conjugated antibody is used, whilst direct IF uses fluorophore conjugated to the primary antibody. A fluorescence or confocal microscope may be used to visualise the protein of interest. During my PhD I performed indirect immunofluorescence to obtain my results. Un-induced and induced cells were cultured in 6cm dishes containing 19mm glass cover slips (VWR international). Induction of DLD-SIP1/ZEB2 cells was undertaken as previously described. Prior to use in cell culture, all cover slips were immersed in absolute ethanol and air-dried to ensure sterility. Once cells had attached to the cover slips, they were removed, placed in a 6 well plate and fixed by incubating for 20 min in Ice cold 4% Paraformaldehyde in 1X PBS. Once fixed, the cells were washed in 3X PBS-T (1%) and permeabilised using 0.5% Triton-X (5min incubation) followed by 3 washes in PBS-T.

3% bovine serum albumin (BSA) in PBS-T (1%) was used as a blocking reagent to minimise non-specific antibody binding. Primary antibodies were diluted to an appropriate concentration in 3% BSA in PBS-T (1-10 µg / ml) and cells treated in a cold room under gentle agitation for 2 Hrs. Primary antibody exposure was followed by 3 X washes in PBS-T and incubation with the appropriate secondary antibody diluted to a concentration of 1:100 in 3% BSA for 1 hr. Counterstaining was achieved using DAPI

used at a dilution of (1:10000) in PBS-T (1%). The cover slips were subsequently mounted onto super frost slides on 50% glycerol and fixed into position using nail varnish

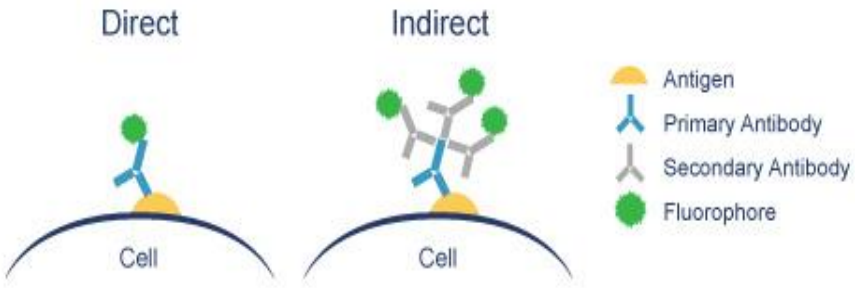

Figure 18: Schema demonstrating principles of direct and indirect IF. In direct IF the primary antibody is conjugated with a fluorophore enabling detection using a confocal or fluorescence microscope. Indirect IF is dependent on a secondary antibody conjugated with a fluorophore to detect the antigen of interest.

2.5 Immunohistochemistry (IHC) and Survival analysis

IHC is a process by which protein expression in fixed tissue or cells is detected using antibodies. Briefly, the process involves samples fixation and wax embedding; tissue sectioning, antigen retrieval, immuno-staining using primary antibody and HRP conjugated secondary antibody and counterstaining with Mayer's Haematoxylin and Eosin. The tissue sections are subsequently visualised by light microscopy.

2.5.1 Patients and samples

All patients were prospectively recruited as part of an on going UK National Institute of Health Research Clinical Research Network study (UK CRN ID 6067) investigating the molecular pathology of CRC and designed to identify novel biomarkers. Other results and further details from this on-going study have been previously described (325-328). All patients provided written informed consent, and the regional research ethics committee approved the study. Following recruitment and surgery, tissue samples were deposited in a UK Human Tissue Act approved tumour bank. Pathological verification of diagnosis and staging was used in accordance with the Association of Coloproctology of Great Britain

and Ireland guidelines (329). Consecutive paraffin embedded tissue specimens were retrieved for the present study. Exclusion criteria included evidence of a hereditary tumour, R1/R2 surgical resection, presence of multiple tumours, tumours with histologically identified extensive necrosis, and tumours with synchronous metastases at presentation. The database was queried for information relating to patient demographics, pre-operative risk, imaging, surgery, pathological features, post-op management and oncological outcomes and used for statistical analyses.

2.5.2 Immunohistochemistry

All IHC was conducted at the histochemistry research unit at University hospital Southampton using an automated immuno-staining device (Autostainer XL, Leica). Stained sections were assessed for the presence of nuclear SIP1ZEB2 expression in neoplastic and normal tissue. Two independent blinded pathologists scored the sections as SIP1/ZEB2 positive or negative using previously established scoring criteria. Where a disparity in scores was noted, slides were re-reviewed to reach a consensus. SIP1ZEB2 expression was correlated to oncological outcomes to evaluate its role as a prognostic or predictive biomarker. All results have been reported in line with reporting standards for biomarker development proposed by REMARK guidelines.

2.5.3 Statistical Analysis

IBM SPSS statistic software (version 22) was used to undertake survival analysis and associate clinical and pathological features with SIP1/ZEB2 expression. Pathologists blinded to patient outcome performed all biomarker scoring. Primary study endpoints of OS and DFS were defined as time from date of primary resection to date of death or recurrence. Patient outcomes are represented as Kaplan-Meier survival curves and differences in survival outcomes calculated using log rank test. Multi-variable analysis using Cox proportional hazard model was used to investigate the prognostic value of SIP1/ZEB2 in a model encompassing conventional pathological risk factors and hazard ratio tables used to compare differences. Association of SIP1/ZEB2 with clinical and pathological parameters was undertaken using a Chi-squared or Fishers exact test as

appropriate. Power calculation was performed using nQuery statistical software. The reported *p*- values are two sided and statistical significance was set to 0.05 for all tests in the study. Hazard ratios are presented with 95% CI.

2.5.4 Nomogram generation

A binary logistic regression model composed of conventional pathological risk factors with or without addition of the SIP1/ZEB2 score was utilised to construct nomograms in the training cohort. The validity of the model was investigated by applying the model to the validation cohort. The capacity to predict risk of distant recurrence within 3 years of surgical resection was calculated before and after the addition of SIP1/ZEB2 to TNM staging criterion, differentiation and EMVI. The predictive capacity and contribution of adding SIP1/ZEB2 to the nomograms is reported as a concordance index (C-index) and incremental area under the curve (iAUC) respectively in accordance with AJCC guidelines (330).

The C-index estimates the probability of concordance between the predicted and observed outcomes in rank order and equivalent to the area under the receiver operating characteristic (ROC) curve. The C-index represents the ability of the model to discriminate between patients that developed distant recurrence and those that did not. The iAUC represents the improvement in the C-index as a result of addition of SIP1/ZEB2 expression score to the nomogram. With an equal interest in sensitivity and specificity, the optimum thresholds were selected to generate two risk scores with and without SIP1/ZEB2 expression status. Patients scoring equal to or above the threshold were classified as high risk and below the threshold low risk. Kaplan-Meier plots were then generated to assess the clinical utility of the risk score. Calibration plots were generated using R 3.4.1 and rms package to assess the relationship between observed outcome and predicted probabilities. An identical methodology was followed during subset analysis of patients with node negative disease. Risk factors used in the stage I-II model included: Age; ASA; presence of bowel obstruction; presence of bowel perforation; T-stage; differentiation; EMVI; perineural invasion; and lymphatic invasion; with or without

SIP1/ZEB2 score. The aim of constructing these nomograms was to investigate if addition of SIP1/ZEB2, a mesenchymal cancer cell marker, increases the ability to identify patients at higher risk of early recurrence when used in conjunction with conventional pathological or clinical risk factors in current usage.

2.6 Chromatin immunoprecipitation (ChIP)

Chromatin immune-precipitation (ChIP) is a technique used to study protein DNA interactions. The CHIP experiments were done using the Active Motif's CHIP-IT high sensitivity kit. The process involves the following steps: -

- Cell fixation
- Sonication
- Input preparation and shearing optimisation
- Immunoprecipitation
- Cross-linking reversal
- PCR or QPCR

2.6.1 Cell fixation and Homogenisation

Two 10cm dishes were used to culture DLD-SIP1 cells. SIP1/ZEB2 induction by treatment with tetracycline was undertaken as previously described. Cells were cultured to ensure two 80% confluent 10cm dishes were used for each immunoprecipitation reaction. Each plate was fixed with 1 ml of freshly prepared Cell fixation solution (For 2.5 ml: add 180 µl fixation buffer+1.57 ml dH_2O+ 750 µl 37% formaldehyde solution containing 10% methyl alcohol) and agitated gently at room temperature for 15 min. The fixation reaction was stopped by addition of stop solution (550µl). A rubber policeman was used to collect cells into pre-chilled canonical 15ml falcon tubes. Cells were collected by centrifugation at 1250 x g at 4ºC for 3 min. The collected cells were washed 3X in PBS and re-suspended in 15mls of chromatin prep buffer supplemented with 15µl of protease inhibitory cocktail and 15µl of 100 mM Phenylmethylsulfonyl fluoride (PMSF) and incubated for 10min. After incubation induced and un-induced cells were transferred to a

dounce homogeniser (Type A), homogenised for 30 strokes and centrifuged at 1250 rpm for 3 min at 4ºC to lyse cells but keep nucleus intact. Following the centrifugation, the supernatants were discarded and the pellets were re-suspended in 1 ml ChIP buffer supplemented with 15 µl PIC and 15 µl 100 mM PMSF, mixed gently by pipetting up and down and incubated on ice for 10 min before proceeding to chromatin sonication.

2.6.2 Chromatin sonication

Prior to undertaking the experiment, optimal shearing conditions to achieve 250 – 1000 bp fragments of DNA for DLD-SIP1 cells were determined (Figure 19). This was achieved by fixing and homogenising cells as described in section 2.6.1. Subsequently a sonication device was used to shear DNA obtained from two 10 cm dishes that were 80% confluent with cells. Cells were sheared at 1.5Hz for 30 sec and allowed to rest for 30 seconds on ice. During the optimisation stage, samples were exposed to 4, 5 ,6 or 7 cycles of sonication and centrifuged at 18000 x g at 4ºC for 10 min to remove cellular debris. The optimisation stage demonstrated 5 cycles of sonication was required for DLD-SIP1 cells. 50µl of each sheared chromatin sample was aliquoted to generate input and the rest stored at -80°C for later use.

2.6.3 Input generation and sonication optimisation

To generate input, 175µl of TE buffer (10 mM Tris-HCl, 1 mM disodium EDTA, pH 8.0) and 1 µl of RNase A was added and incubated at 37°C for 30 min. Protein degradation was achieved by adding 2µl of Proteinase K and incubating in a thermocycler at 55°C and then temperature increased up to 80°C for 2 hours to deactivate the enzyme. Subsequently, 83µl of precipitation buffer, 2µl of carrier DNA (Supplied with the kit) and 750µl of absolute ethanol was added to the reaction, vortexed and incubated at -80°C overnight. The next day, the samples were centrifuged at maximum speed for 15 min at 4 °C to precipitate DNA, the supernatant removed and pellets washed with 500 µl of 70% ethanol. The eppendorf tubes were re centrifuged at maximum speed, supernatant removed and tubes allowed to air dry for 30min to 1 hour. Once all the ethanol had evaporated, the DNA was re-suspended in DNA purification elution buffer (25µl) and

incubated at RT for 30 min. This suspension was used as input for all further analysis. The quantity of DNA isolated was measured using a Nanodrop. The shearing efficacy of the sonication process was validated by loading 2 µg of DNA with 6x loading dye and undertaking agarose gel electrophoresis (1%) **(Figure 19)**. Optimal sonication conditions would be represented by a smooth DNA smear between 200 and 1200bp, without evidence of laddering. This appearance was found to be present after 5 cycles of sonication.

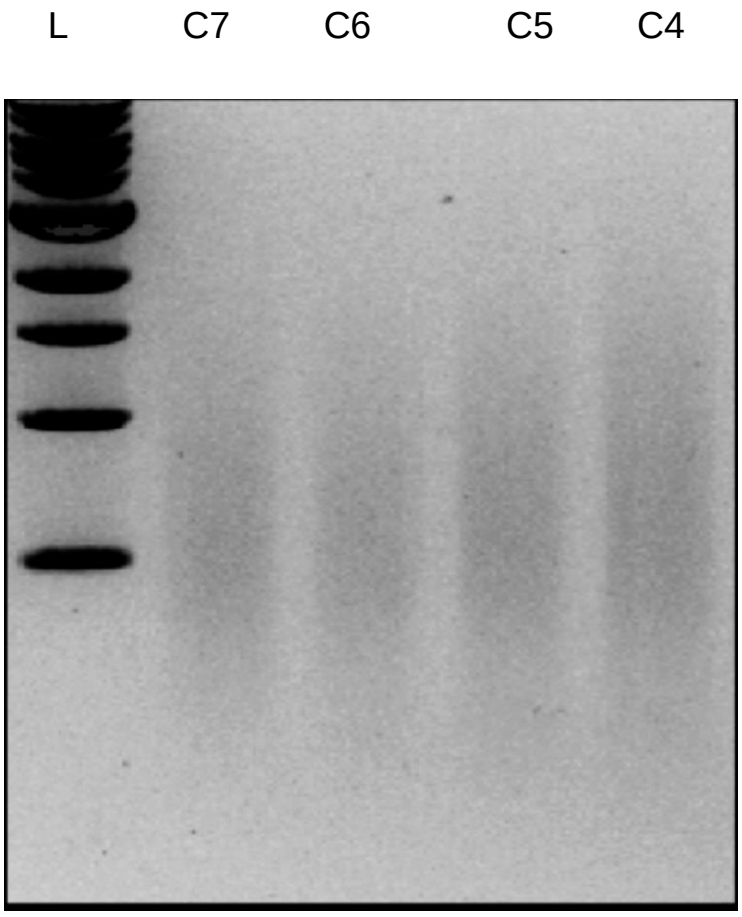

Figure 19: DNA sonication optimization for chromatic immunoprecipitation (ChIP). Figure demonstrates the appearance of sheared DNA after optimization with multiples sonication cycles (L –DNA ladder, C-cycle).

2.6.4 Immuno-precipitation

The sonicated chromatin was removed from the -80 °C freezer and thawed on ice. The thawed chromatin was centrifuged at maximum speed at 4°C for 2 min and the supernatant used to set up the IP step of the experiment. To enhance the efficacy of the

IP step 2 µg of mouse bridging antibody was used, the reaction was set up by adding the following components:

- 20 µg Sheared chromatin
- Top up to 200 µl ChIP buffer
- 1 µl Protease Inhibitor Cocktail (PIC)
- 4 µg Antibody*
- 5 µl Blocker mix Total Volume 240 µl

Table 2: List of antibodies used during the ChIP experiment

ChIP antibody	Concentration used	Purpose	Supplier
Human anti-mouse IgG (Stock conc.0.2 µg/µl)	4 µg	Negative control	Active Motif. ChIP-IT® Control kit catalogue no. 53010
Bridging antibody anti-mouse (stock conc. 1.0 µg/µl)	2 µg	To improve the binding of protein G beads to mouse IgG primary antibodies.	Active Motif. ChIP-IT® Control kit catalogue no. 53010
RNA Pol II human anti-mouse monoclonal (Stock conc. 0.2 µg/µl)	2 µg + 2 µg anti-mouse Bridging antibody	Positive control	Active Motif. ChIP-IT® Control kit catalogue no. 53010
Human anti-mouse monoclonal c-MYC (Stock conc.)	2 µg + 2 µg anti-mouse bridging antibody	SIP1/ZEB2 targeted antibody (tagged domain)	Sigma

Once the reactions were set up they were securely placed on an end-to-end rotor overnight at 4°C. 30µl of protein G agarose beads were subsequently added and the reactions placed on an end to rotor for a further 4 hours at 4°C. After the incubation period, filtration columns provided in the kit were placed in a 1ml pipette tip box. 600µl of ChIP buffer was added to the reaction, vortexed and allowed to pass through the filtration column by gravity. A further five washes were undertaken using 900 µl of wash buffer provided in the kit. To extract chromatin pulled down from the IP reaction the filtrations columns were placed in a new eppendorf tube and 100 µl of pre-warmed elution buffer (provided in the kit was) used. At this stage the eluted chromatin was placed on ice to proceed to reversal of crosslinking and DNA purification steps.

2.6.5 Cross-linking reversal and DNA purification

The eluted reactions were transferred to 250µl PCR tubes and 2 µl of Proteinase K was added to the reaction. The tubes were placed in a thermocycler for 55 °C for 30 min and 80 °C for 2 hours. After protein digestion 500µl of DNA purification buffer (provided in kit) was added to the tubes and vortexed. DNA filtration columns provided in the kit were used to extract the DNA by centrifugation. The process involves passage of the reaction through the filtration column, five washes with DNA purification wash buffer with 70% ethanol and DNA extraction using DNA purification elution buffer (100µl). The volume of elution buffer is reduced to 25 µl if a more concentrated sample is required e.g. (ChIP – seq). Eluted DNA can be stored at -20°C or used immediately for downstream applications such as PCR, QPCR or ChIP-Seq analysis.

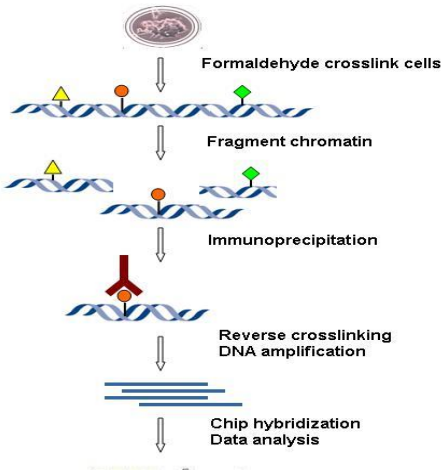

Figure 20: Schematic representation of stages involved in ChIP. Chromatin immunoprecipitation (ChIP) involves the following major stages. Cells are sonicated to release chromatin from the nucleus and sheared into a homogenous sample. Anti-bodies are used to immuno-precipitate the antigen of interest. Once this stage is complete the cross-links between antigen and antibody is reversed. The eluted DNA can subsequently be applied in a multitude of techniques including PCR, QPCR and Chip-Seq.

2.7 ChIP-Seq

ChIP was performed on DLD-SIP1 cells before and after mesenchymal transition for well-recognised euchromatin (H3K9me3, H3K27me3) and heterochromatin (H3K9me3, H3K27me3) methylation marks. The aim of the experiment was to understand genome wide changes in methylation marks induced by expression of EMT inducing TF's. The extracted DNA that was acquired after reversal of crosslinking was quantified using a

nano-drop and sent for sequence at the Dana Faber cancer institute (DFCI) bio-informatics facility. All bioinformatics data analysis was performed by Dr Ricardo De-Matos of DFCI radiation oncology department.

2.8 Exposing cells to ionising radiation (IR)

Cells were treated with ionising radiation (IR) using the Gamma cell 40 Exactor, low dose rate research irradiator (Best® Theratronics) at Dana Faber Cancer institute. The source of the IR emitted by the irradiator is Caesium-137 and modulating exposure time modified dose of radiation. DLD-SIP1 cells were exposed to IR before and after induction of EMT to study the impact of mesenchymal transition on DNA repair and treatment response.

2.9 Total RNA extraction

TRIzol® was used to extract RNA from DLD-SIP1 cells. It is a monophasic solution, which contains phenol and guanidine isothiocyanate, which facilitate the isolation of nucleic acids (DNA and/or RNA) and proteins. Homogenisation with the reagent disrupts cellular organelles and facilitates separation of macromolecules in liquid phases. The homogenised sample, when centrifuged separates into three monophasic layers; of which the clear upper layer contains the extracted RNA. The RNA is precipitated from the aqueous layer and re-suspended in water to be used in downstream application e.g. RT-PCR, dot blot etc. DLD-SIP1 cells were induced with doxycycline as described previously. Frozen/fresh cell pellets (up to 10^7 cells) were defrosted on ice and suspended in 1 ml TRIzol to facilitate cell lysis. 200µl chloroform was added to each sample and centrifuged at 10000x g for 15 min. The upper aqueous layer containing RNA was collected and precipitated by adding 0.5 ml of 100% isopropanol. The precipitated RNA was washed with 1 ml of 75% ethanol, and centrifuged to isolate the RNA. The extracted RNA pellets were air-dried for 10 min at room temperature (RT). The RNA pellets were re-suspended in 50-100µl RNase-free water by vortexing and incubating at 55-60°C for 10 min. The total RNA yield was measured using a NanoDrop 1000 Spectrophotometer (Thermo Scientific). The extracted RNA was used immediately to synthesise cDNA or frozen at -80°C.

2.10 cDNA synthesis

RevertAid™ M-MuLV Reverse Transcriptase (RT) Kit (MBI, Fermentas) was used in this project. The RevertAid™ M-MuLV RT is active at 42-50°C. The reaction also involves addition of RiboLock™ RNase inhibitor, which protects RNA from degradation. Oligo (dT) primer that selectively anneal to the 3´end of poly(A) RNA was used to ensure synthesis of extracted mRNA. Random hexamer primers that bind to RNA templates at a more random but frequent fashion may be used if total RNA extraction was intended. As my experiments focused on expression analysis, Oligo (dT) primers were used for cDNA synthesis. The synthesised cDNA was used as a template for primers in RT-PCR experiments. The cDNA synthesis reactions were performed in sterile, nuclease-free, PCR tubes as follows:

- 2.5 µg extracted total RNA (Template)
- 1 µl Oligo (dT) primer (stock conc. 0.5 µg/µl)
- Top the volume up to 12 µl with dH_2O

The PCR machine was set up with the following temperatures (70°C for 5 min, 37°C for 3 min, 42°C for 45 min, 70°C for 5 min, 4°C forever). Upon reaching the last minute of the 37°C, the programme was paused and 8µl Master Mix (MMX) was added to each reaction. The MMX contains the following reagents:

- 4 µl of 5X Reaction Buffer (250 mM Tris-HCl (pH 8.3), 250 mM KCl, 20 mM $MgCl_2$, 50mM DTT)
- 2 µl 10 mM dNTP Mix
- 1 µl RiboLock™ RNase inhibitor (stock conc. 20 U/µl)
- 1 µl RevertAid™ M-MuLV Reverse Transcriptase (stock conc. 20 U/µl)
- 1 µl dH_2O

The final cDNA product was either used immediately for reverse transcriptase PCR (RT-PCR) or stored at -20°C.

2.11 QPCR Micro array

After synthesis of cDNA from un-induced and induced DLD-SIP1 and A431-SIP1 cells a DNA damage micro-array with a focus on DNA damage response was undertaken. A RT^2 Profiler™ PCR Array with a focus on DNA damage signalling was purchased from Qiagen to analyse gene expression changes after SIP1/ZEB2 induction. The micro array PCR plate contains pre designed primer pairs and a master mix consisting of SYBR green for quantifications and analysis. The procedure involves mixing the pre-prepared master mix with appropriate cDNA quantity and aliquoting equal volumes to the wells containing the primers. The thermocycler was set up to predefined temperatures for 40 cycles. The data was analysed as described below.

2.12 Quantitative PCR (QPCR) data analysis

Quantitative PCR was undertaken using exactly the same principles as PCR, however Fast start Universal syber green master (Rox) was used instead for My Taq Red™ Mix. All reaction was set up in triplicate and expression levels normalised to GAPDH as controls. Quantitation was done using the ΔΔCt method and presented as bar graphs generated on Prism version 4.06 (Graph software Inc., USA). Data was presented as fold change in gene expression after SIP1/ZEB2 induction for each gene. Statistical significance was calculated using a paired student t-test.

2.13 Semi-Quantitative Polymerase chain reaction (PCR)

Polymerase chain reaction (PCR) is a technique used to amplify segments of DNA by several orders of magnitude by thermal cycling. PCR was performed using MyTaq™ Red Mix (BIOLINE). This product contains all necessary reagents required for a reaction (1.5 mM $MgCl_2$, 200µM dNTP mix, Taq polymerase and DNA loading dye). Each reaction was set up by addition of the following components.

- 10 µl 2 x MyTaq™ Red Mix
- 6 µl dH20 water
- 1 µl forward primer (stock conc.10 pmol/µl)
- 1 µl reverse primer (stock conc.10 pmol/µl)
- 2 µl of cDNA

The thermocycler was set up to cycle through the following temperatures after optimisation:

1. 95 °C for 5 min (Denaturation)
2. 95°C for 30 sec (Denaturation)
3. 57-60°C for 30 sec (Annealing) (Stages 2-4 repeat 20-40 Cycles)
4. 72 °C for 30 sec (Extension)
5. 72 °C for 95 min (Extension)
6. 4°C for ∞ (Stabilise product)

The exact temperatures used during thermal cycles varied depending on the primer and product size. In general <30 sec extension is required for products less than 1 Kb and >30 sec is required for products >1kb. 1.5 % agarose gel prepared in 1 x Tris-acetate EDTA buffer (1 x TAE) and ethidium bromide was used to visualise the PCR product. 20µl of each PCR reaction was loaded with 3µl of DNA ladder (NORGEN) into the gel. The gel was run in 1X TAE buffer at 140V for 40-60 min. A UVP transilluminator (3UV™transilluminator; Thermo Scientific) was used to visualise the amplified product.

2.14 Generating Stably transfected cell lines

Stable transfection enables the overexpression of a gene of interest into eukaryotic cells for longer period of time when compared to transient transfection where maximal gene expression is observed for only 24-96 hours. Clonal selection of cells overexpressing the gene is achieved by the use of eukaryotic antibiotic resistance genes that are co-transfected with the gene of interest (e.g: neomycin, blasticidin, and zeocin). The

antibiotics resistance gene is found in plasmid containing the gene of interest. The protocol to stably transfect a eukaryotic cell line consists of the following steps: -

1. Plasmid construction
2. Generation of antibiotic kill curve, to identify the concentration that kills non-transfected cells
3. Transfection of plasmid with genes of interest
4. Selection and expansion of transfected polyclonal colonies
5. Validation of Gene expression
6. Expansion of single clones stably over-expressing the gene of interest

2.14.1 Plasmid construction

The ERCC1 plasmid was kindly provided by Prof. Aziz Sancar. A schematic representation of the plasmid construct is provided below.

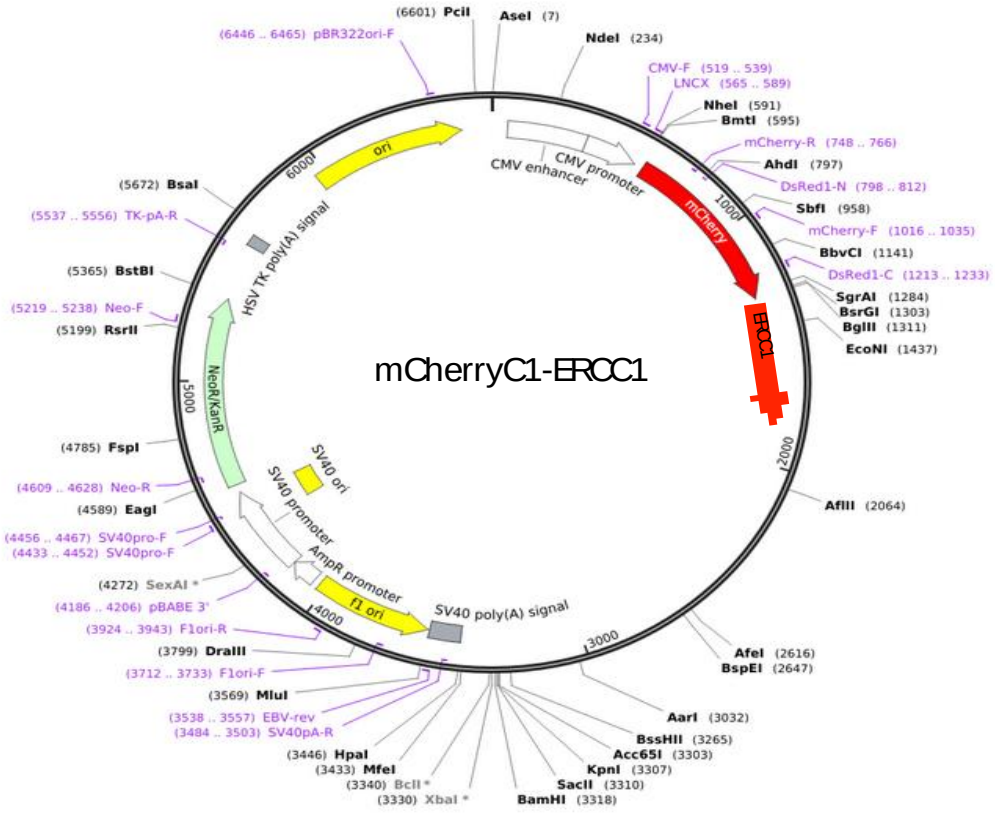

Figure 21: Scheme representing the mCherryC1-ERCC1 plasmid.

2.14.2 Neomycin kill curve

0.5 x 10^4 DLD-1 cells were seeded into two 12 well plates. Increasing concentrations of neomycin (100-500 µg/ml) was added to culture media in duplicate and cell toxicity followed using a light microscope for 7 days. Cells cultured without the presence of neomycin were used as controls. Optimal concentration (200 mg/ml) for selection of cells was chosen by inspecting cells for signs of toxicity for a maximum of 7 days.

2.14.3 Transfection

Cells were seeded at 60% confluency in a 10cm dishes and allowed to attach. 5µg of the plasmid construct (mcherry-ERCC1) containing ERCC1 and control empty Mcherry vector was transfected into the cells using Lipofectamine 3000 reagent as described in section 2.13. After 48 hours 200 µg/ml of neomycin was added to the culture media. Cells were left in culture for 7 days. DLD-1 cells that were un-transfected were selected out due to absence of antibiotic resistance gene to neomycin found in the plasmid.

2.14.4 Selection and expansion of monoclonal colonies

Cells were cultured in the presence of antibiotics for a total of 2 weeks, during which media change (DMEM containing 200 µg/ml of neomycin) was undertaken twice a week. Through visual inspection polyclonal colonies containing transfected cells were picked diluted and seeded in a 96 well plate at a density of 0.8 cells/well. The wells containing 1 cell were monitored and maintained in the presence of antibiotics until confluency. The cells were then expanded into 6 well and 24 well plates as they reached confluency.

2.14.5 Examination of ERCC1 expression

Validation of ERCC1 overexpression was confirmed by undertaking western blots on the clones selected after transfection. The WB procedure was undertaken as described previously in section 2.2.

2.14.6 Expansion and freezing of single clones with high ERCC1

After analysing ERCC1 expression by western blotting, DLD cells with ERCC1 expression were expanded in T75 flasks with low dose antibiotic (50µg/ml) until they reached 80% confluency. Cells were then trypsinised and frozen down in freeze media, placed in a Mr frosty to an -80 freezer. Cells were they transferred to liquid nitrogen for long-term storage.

2.15 Transfection

Transfection is the process by which nucleic acids are introduced into the eukaryotic host cell for stable or transient integration into the host genome. Commonly used methods of transfection include Calcium phosphate transfection, electroporation and lipid mediated transfection. During my thesis I used the lipid mediated transfection method (Lipofectamine 3000). The principle of this technique relies on the positive surface charge of liposomes that bind negatively charge nucleic acids (Phosphate back bone). These complexes (Lipid/nucleic acids), fuse to the cell wall by direct interaction with the negatively charged cell membrane and endocytosis. Once the nucleic acids are transferred to the cytoplasm they are either expressed temporarily or integrate with the genome for stable expression. This technique is simple fast non-toxic and suitable for many types of cells including adherent, suspension, and insect cells.

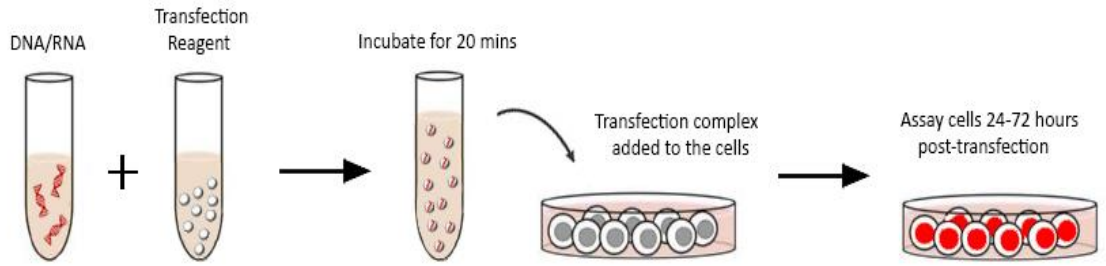

Figure 22: Stages involved in lipofectamine transfection protocol. Lipid transfection involves incubating the plasmid of interest with the lipid reagent to enable the formation of micelles that contain the DNA/RNA of interest. After incubation the mixture is added to cells enabling transfection across the lipid bilayer. Transfection efficiency may be assessed using a fluorescence microscope if the vector contains a fluorescence protein.

2.15.1 Lipofectamine® 2000/3000 Protocol

Lipofectamine® 2000/3000 (Thermo Scientific; Catalogue no. L3000001) was used as the reagent of choice for transfection. The lipofectamine 3000 kit contains 2 lipid reagents, namely p3000 and lipofectamine 3000. Transfection procedure involves diluting lipofectamine in Opti-MEM®, vortex and keep aside at room temperature. The plasmid of interest or a control plasmid (e.g. pGFP) is diluted in Opti-MEM® / P3000 reagent of appropriate volume. The mixtures are added to each other and allowed to incubate at room temperature for 5 min. After the incubation, the lipid/DNA mixture is added to cells in culture. Care must be taken to add the reagent drop by drop and gentle agitation aids a uniform transfection. The transfected cells were incubated for 6 hours and optimum removed and replaced with DMEM. If a pGFP control plasmid is used, transfection efficiency can be assessed by fluorescence microscopy, 24-48 hours after transfection. Up or downstream effects of the transfected nucleic acids can be assessed using an appropriate assay (e.g. WB). The only difference with the protocol whilst using lipofectamine 3000 is the use of p300 reagent to dilute the DNA before incubation with the lipid component of the transfection reagent. siRNA was transfected using lipofectamine 2000 reagent, whilst all other DNA constructs were transfected using lipofectamine 3000.

2.16 RNAi Interference

RNAi interference (RNAi) involves the use of small interfering RNA (siRNA) transfected into cells to disrupt the expression of specific gene with complementary sequences. siRNA are double stranded sequence of RNA that are 20-25 nucleotides long. Sequences are constructed to complement the gene of interest and consequently disrupt transcription. DLD-1 cells lines were transfected with siRNA targeting ERCC1 using lipofectamine 2000 reagents. 1 x 10^5 Cells were seeded in a six well plate and allowed to adhere over night. Three siRNA constructs targeting ERCC1 and 1 control non-targeting siRNA were transfected into the cells. 48 hours post transfection cells were treated with oxaliplatin of varying concentration for 24 hours and cells collected and stored in a -20

freezer. The impact of ERCC1 knockdown on apoptosis resistance to chemotherapy were assessing by western blotting.

2.17 Cloning and Recombination

DNA cloning is defined as the production of identical copies of a DNA sequence using genetic engineering techniques. Cloning has a wide array of applications including analysis of function, effect of mutation or protein synthesis in large quantities. The process involves the following steps: -

1. DNA amplification
2. DNA extraction
3. DNA ligation
4. Transformation
5. Purification

2.17.1 DNA amplification

Cloning was undertaken as part of an experiment to analyse whether SIP1/ZEB2 binds directly to E-boxes in the *ERCC1* promoter. To achieve this goal, special primers with restriction enzyme sites were designed to incorporate segments of the ERCC1 promoter that contained E-box clusters. In total 3 primer sets were used (Appendix Table 8) and human genomic DNA obtained from Prof John Stafford's group was used to setup a PCR reaction using KOD polymerase (Novagen®). Gel electrophoresis (1.5% agarose gel) was undertaken to visualise the product and the DNA extracted using QIAquick Gel Extraction kit using a micro-centrifuge (Qiagen, Catalogue no. 28704)

2.17.2 Gel extraction

The amplified DNA product visualised under UV light was cut from the gel using a scalpel. The gel was weighed and 300µl of buffer (QG) was added for each 100mg slice. The gel was dissolved in the buffer by incubation at 50 °C for 30 min. To increase the yield of DNA, 100µl of isopropanol was added to every 100 mg of gel. The samples were then passed through a QIAquick spin column by centrifugation at max speed for 1 min. The

flow through was discarded and the samples washed with buffer PE to remove impurities. The DNA in the column was extracted by pipetting 50µl of de-ionised water into the column. To obtain high elution efficiency, the pH of the water should be between pH 7-8.5. The collected DNA was used immediately or stored at -20°C to avoid degradation.

2.17.3 DNA ligation into the vector

The extracted ERCC1 promoter was ligated into the PGL3 basic vector (Figure 20). The 3 segments of the ERCC1 promoter was labelled A, B and C. A 10 µl reaction was set up using the following reagents : -

- 5µl of 2x Ligation buffer (Takara, Clontech)
- 50ng of PGL3 and
- 200ng of ERCC1 promoter segment A,B or C.

The reaction was incubated for 15 min and heat shock transformed into E-coli.

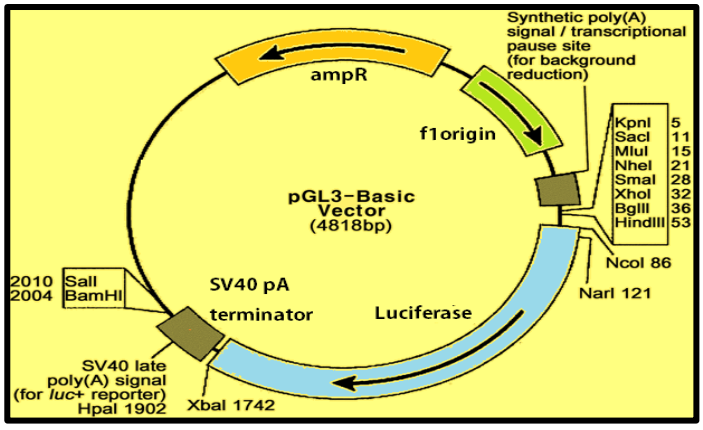

Figure 23: pGL3 vector used to clone ERCC1 promoter.

2.17.4 Plasmid transformation

JM109 E-coli cells were used to transform the ligated PGL3-ERCC1 (A,B and C) plasmids. The plasmid / E-coli mixture was mixed gently and incubated on ice for 30 min. The cells were then exposed to a 42°C water bath for 45 sec and then placed back immediately on ice for a further 2 minutes. The entire content is added to 400 µl of SOC medium. The tubes are then incubated at 37 °C under constant agitation (200 rpm) for 1

hour. The tube was then centrifuged and the pellet dissolved in 50 µl of Luria Bertani (LB; 10 g/L Tryptone, 5 g/L Yeast extract and 10 g/L NaCl) and spread onto LB-Agar (LB+20g/L agar) containing 100µg/ml ampicillin. The plate was incubated overnight at 37°C and five colonies picked. The presence of the plasmid was checked by performing PCR with pre-designed target primers for all three segments of the promoter.

2.17.5 Plasmid DNA purification

Plasmid DNA purification was performed using the Qiagen miniprep kit. The transformed e-coli containing the PGL3-ERCC1 promoter (A,B and C) was cultured overnight in 5mls of LB media containing 100 µg/ ml of ampicillin at 37°C under constant agitation overnight. 1.5mls of the media was then harvested and a bacterial isolated by centrifugation. The bacterial pellet was re-suspended in 250 µl of buffer P1 in the presence of RNAase A and lyse blue reagent to ensure complete suspension of the pellet and elimination of RNA. 250µl of buffer P2 is then added to the mixture and a colour change to blue indicates complete cell lysis. Buffer N3 (350 µl) is then added to the suspension and this should turn the mixture colour less. This indicates the SDS has effectively precipitated and the lysate is neutralised and adjusted to high salt binding conditions. The tube was then centrifuged to isolate the plasmid DNA from the remaining cellular components, which is found in the supernatant. The aqueous supernatant was applied to a QIAprep spin column and centrifuged at 10,000 x g for 1 min. The column was then washed with buffer PB to remove high endonuclease activity found in JM109 cells. Further washes with buffer PE was undertaken to remove impurities and DNA in the column extracted in a fresh tube eluted with 50 µl of deionised water. The DNA product was validated by sending the sample for sequencing.

2.18 Promoter reporter assay

The Cloning step described previously was undertaken to ascertain if SIP1/ZEB2 directly binds to the ERCC1 promoter and induces gene expression. PGL-3 plasmid contains the luciferase gene isolated from the *firefly* "*Photinus pyralis*". This enzyme oxidises D-luciferin in the presence of ATP, 02 and Mg2+ resulting in the emission of

bioluminescence. Another luciferase enzyme renilla is co-transfected into the cells as means of normalising transfection efficiency. *Renilla reniformis*, oxidises the substrate coelenterazine also resulting in the emission of bioluminescence. The ratio of renilla: firefly enzyme activity is used as an indirect measure of promoter activity in the presence of SIP1/ZEB2

The dual-Luciferase® reporter assay system (Promega; catalogue no: E1910) was used to measure *ERCC1* promoter activity in un-induced and induced DLD-SIP1 cells. After the ERCC1 promoters segments (A and B) were cloned into the vector. DLD-SIP1 cells were transfected using lipofectamine 3000 reagent as described previously. ~20,000 cells were seeded per well in a 96 well plate. DLD-SIP1 cells were induced and seeded as described previously in section 2.1.5. Un-induced and induced cells were transfected with the PGL-3- ERCC1 promoter (A and B) using lipofectamine 3000 as described previously in section 2.13.3. Cells were allowed to recover for 24 hours. Before starting the protocol, all luciferase reagents supplied in the kit (5 x Passive Lysis Buffer (PLB), Luciferase Assay Substrate (LAS) and 1X Stop & Glo® Substrate (SGS)) were prepared as recommended. Cells were lysed by the application of PLB for 15 min at room temperature. After lysis LSA and SGS was applied in turn and bioluminescence measured using a luminometer (Thermo Scientific). The ratio of Firefly: Renilla luciferase activities was analysed using Microsoft Excel.

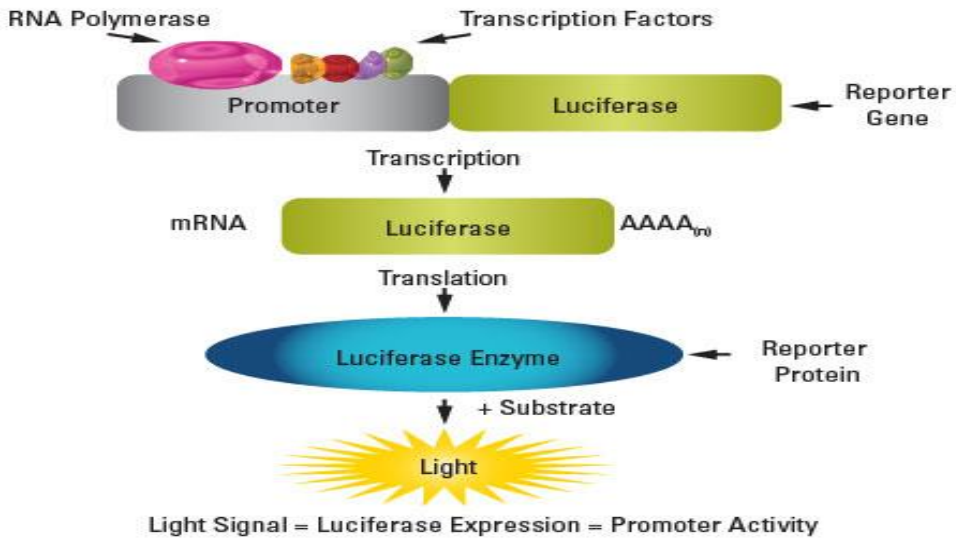

Figure 24: Principles of bioluminescence generation by promoter reporter assay. Luciferase assay was undertaken to decipher if SIP1/ZEB2 an EMT inducing transcription factor binds directly to the promoter segment of the ERCC1 gene. To achieve this aim 3 segments of the ERCC1 promoter were cloned into the PGL3 vector and transfected into DLD-SIP1 cells. Tetracycline treatment of DLD-SIP1 cells leads to SIP1/ZEB2 expression. If SIP1/ZEB2 promotes transcription of ERCC1, induction of EMT will lead to expression of the luciferase enzyme instead, which can be detected as a bioluminescence signal when the enzyme is exposed to the relevant substrate.

2.19 Proliferation assay

Proliferation assays were undertaken using Cell Titre-Glow® assay (CTG) (Promega). The assay relies on the mono-oxygenation of beetle luciferin by ultraglow-luciferase enzyme in the presence of ATP, oxygen and Magnesium. As ATP levels are indicative of metabolically active cells, the intensity of the bioluminescence signal is used as indirect marker of cell number (Figure 21). The assay was undertaken by inducing DLD-SIP1 cells as described previously. 5000 un-induced and induced cells were seeded per well in triplicate in a 96 well plate. Cells were allowed to adhere overnight and induced cells were cultured in the presence of doxycycline. CTG reagent was prepared as per manufacturers instruction and 100µl of the reagent pipetted into each well using a multiple channel every 24 hrs. The reagent was mixed with the medium by pipetting to promote cell lysis and allowed to incubate at RT for 15 min. The luminescence signal was read using an illuminometer (Thermo fisher). Mean signal intensity and standard deviation was calculated on excel and graphs generated using GraphPad prism.

2.20 Colony formation assays

The viability of DLD-SIP1 cells after exposure to ionising radiation was assessed using a colony formation assay. Approximately 5000 cells were seeded onto a 6cm dish and incubated overnight at 37°C. Un-induced and induced DLD-SIP1 cells were exposed to ionising radiation at varying doses and allowed to recover for 10 days. At the end of 10 days cells were fixed using paraformaldehyde and stained using crystal violet. The number of colonies formed, was manually counted and graphically present as viability curves generated using GraphPad prism software.

2.21 Viability assay

Viability assay was undertaken using the Cell Titre-Glow® (Promega). DLD-SIP1 cells were induced as described previously. 50000 cells were seeded in triplicate in a 96 well plate and allowed to adhere to the plate overnight. The cells were then treated with a variety of chemotherapeutic agents at varying concentrations for 48 hrs. Optimisation of drug concentration was undertaken to ensure a accurate drug response curve could be generated. After 48 hours, 100 µl of CTG reagent was pipetted using a multichannel and incubated at RT for 15 min. The plate was read on a luminometer (Thermo-fisher). Sham treated (DMSO) cells were used as controls to measure cell viability of un-induced and induced cells. Drug response curves and IC50 was measured using Graph pad.

2.22 Slot blot

Platinum based chemotherapeutic agents such as cisplatin and oxaliplatin induces DNA damage primarily by creating GG and TT inter and intra-strand adducts. These DNA adducts can hamper a multitude of cellular processes leading to activation of apoptotic pathways. Nucleotide excision repair (NER) is the DNA repair pathway primarily responsible for removal of DNA adducts created by exposure to platinum based chemotherapeutic agents. Slot Blot is a technique that can be use for quantitative detection of NER activity using DNA damage specific antibodies such as anti-cisplatin DNA adduct antibody (clone ICR4, Millipore). The process involves, DNA extraction, vacuum transfer of DNA to a nitrocellulose membrane using a micro-filtration apparatus (Bio-DOT SF microfiltration apparatus, Bio-Rad), immune blotting, DNA staining and development using chemiluminescence.

2.22.1 Cell treatment

Cells were cultured in DMEM as described previously. Varying concentrations of oxaliplatin was added to the media and cells exposed to the chemotherapeutic agent. After 2 hours the media was removed, cells washed in 1X PBS, fresh DMEM added and cells allowed to recover. Cells were trypsinised, collected and stored at -20 °C before analysis using a slot blot assay.

2.22.2 DNA extraction

Gene Elute Mammalian DNA purification kit (Sigma Aldrich) was used to extract DNA from cultured cells. A chatropic salt containing buffer is used for lysis of macromolecules. The DNA is separated from the lysate by centrifugation in a spin column (Provided in Kit). A filtration column is used top remove cell debris. After washings with wash buffer (provided in kit) DNA is eluted into a fresh eppendorf using DNA elution buffer. The quantity of DNA extracted is measured (λ) using a nanodrop.

2.22.3 Vacuum transfer

After DNA extraction, appropriate volume of DNA was diluted in 6X SSC (NaCL 3M, 300mM Sodium citrate) (pH 7) to load 1µg in each slot. DNA was denatured by placing on a 100°C hot plate for 10 min. Two filter papers and one nitrocellulose membrane pre-soaked in 6x SSC was placed in the vacuum manifold as demonstrated in figure x. After locking the manifold tight, the nozzle was attached to a vacuum line. Volume equivalent to 1µg of DNA was loaded into each slot and the vacuum turned on gently and left until the sample is no longer visible. The nitrocellulose membrane was removed from the manifold and placed in an 80°C oven for 2 hours until dry.

2.22.4 Immuno-blotting

After transfer the membrane was blocked in 3'% BSA dissolved in 0.1% TBS-T. The nitrocellulose membrane was subsequently incubated in primary antibody dissolved in BSA for 8 hours at room temperature. Three 10 minute washes were undertaken using 0.1% TBS-T. The membrane was then incubated at room temperature in horseradish peroxide conjugated secondary antibody diluted in BSA. A further three washes was undertaken in 0.1% TBS-T and immune-blots visualised using Supersignal ® West Dura chemiluminescence detection kit (Thermo Scientific, Rockford, USA). The enzymatic reaction and the band intensity were then detected by X-ray film and developer machine. The equal loading of DNA was ensured by staining the nitrocellulose membrane with propidiumiodide (PI) and visualising the bands using an UVP transilluminator (3UV™

Transilluminator; Thermo Scientific). Band intensity was later quantified using image J during data analysis.

2.23 *In-vivo* murine models

Animal experiments were undertaken to investigate the impact of ERCC1 overexpression in promoting resistance to oxaliplatin. Two stable clones of DLD-ERCC1, clone 11 (ERCC1-red fluorescence protein, in-cis) and clone 5 (red fluorescence protein only) were used for the animal experiments. All animal experiments were done on SCID mice in the BRF facility at Southampton general hospital. ~2 $x10^6$ cells per animal of each clone was trypsinised, washed and suspended in matrigel. Orthotopic injections were undertaken on a sterile laminar flow hood. Animals were anaesthetised using increasing concentration of isoflurane. After induction of anaesthesia, a small nozzle was used to maintain depth of anaesthesia. Animals were prepped using iodine and a small midline incision made for access. The caecum was isolated and an orthotopic injection performed taking care not to enter the lumen. The incision was closed in layers and animals recovered in a heated chamber. Animals were treated with an analgesic and antibiotic to reduce pain and risk of infection. The mice that underwent orthotopic injections were housed separately and monitored twice a day for any signs of distress. In total 20 animals underwent orthotopic injections. After 4 weeks of recovery, the treatment arm was given IP injection of oxaliplatin (10mg/g) whilst the control animals were administered PBS once a week for a further 5 weeks. At the end of 11 weeks animals were culled in a CO_2 chamber and their organs (Caecum, lungs, liver, spleen) retrieved. An IVIS Lumina imaging system was used to detect the presence of primary tumours or metastasis by fluorescence emission from mCherry transfected cells. After analysis, the organs were paraffin fixed, cut into sections and H/E stained. Sections representative of the whole organ were carefully analysed for the presence of primary tumour and metastasis.

2.24 Bioinformatics analysis

External validation of survival outcomes was investigated using the open access portal progeneV2. mRNA expression profile from the database GSE28814 (PMID for citation 21251323) was queried for an association between, high ZEB2/CDH1 ratio and reduced time to metastasis. Prognostic importance is demonstrated by generating Kaplan-Meier survival curves and statistical significance calculated by log rank test. Bioinformatics analysis for ChIP-Seq data was performed by Dr. Ricardo De-Mateos of Dana-Farber cancer institute.

2.25 Motility and migration assay

Cell migration after SIP1/ZEB2 induced EMT was assessed using Transwell membrane inserts (8 micron pore size, BD Biosciences) in 24 well tissue culture plates. DLD-SIP1 cells were induced as previously described and seeded at a density of $2X10^5$ cells/well. Two hours after seeding the top layer of the chamber was filled with serum free media to establish a chemo-attractant gradient. 24 hours after, inserts were taken out fixed in acetone/methanol (50/50) and the bottom and top parts stained with DAPI and Eoisin respectively. Following the staining, cells at the top were removed using a cotton wipe, imaged in the UV channel (to detect DAPI staining) and counted using imageJ. The experiments were performed in triplicate and results presented as a mean and standard deviation. Cell motility was assessed by tracking cells in culture using open access TrackMate software. Uninduced and induced DLD-SIP1 cells were seeded at 50% confluency in a 6 well plate and allowed to adhere overnight. The cells were subsequently transferred to a time lapse microscope facility (Olympus microscope and Hamamatsu camera system) where they were kept in CO2 enriched and humidified environmental chamber. Representative pictures were obtained every 10 minutes in epi-light for 72 hours. The acquired images were stacked and put together (5 frames/second) in “avi” format to be analysed as movies. The acquired images were presented in original (greyscale) format. Open access TrackMate software was used to quantify single cell motility and presented as pixels/frame before and after EMT.

RESULTS

Chapter 3: SIP1/ZEB2 induces EMT in CRC cells

Epithelial to mesenchymal transition (EMT) is a conserved genetic programme that promotes cell migration during embryogenesis. Emerging evidence suggests this cellular programme may also play a key role in mediating metastasis and chemoresistance in cancer. The cardinal features of EMT include, E-cadherin down regulation, acquisition of a more mesenchymal phenotype, attenuation of cellular proliferation and development of resistance to chemotherapeutic agents. Although the role of EMT in promoting metastasis is clear, the contribution of SIP1/ZEB2 in the setting of CRC is sparsely studied. I used DLD-SIP1, a stable inducible model to investigate the impact of SIP1/ZEB2 in promoting metastasis and chemoresistance in colorectal cancer (CRC).

3.1 SIP1/ZEB2 expression induces EMT in CRC

A cardinal feature of EMT is the down regulation of E-Cadherin from the cell surface and acquisition of a more spindle like or mesenchymal phenotype. To investigate whether SIP1/ZEB2 TF induces EMT in CRC cells, DLD-SIP1 a tetracycline inducible model of EMT, was studied by RT-PCR, WB and IF. Monitoring cellular phenotype by light microscopy revealed induced (DOX +VE) cells adopt a spindle like or mesenchymal phenotype. Mesenchymal transition also resulted in the inability to form cell-cell adhesion complexes and consequently epithelial islands (**Figure 25A**). WB and RT-PCR on un-induced and induced DLD-SIP1 cells; demonstrated exposure to tetracycline in cell culture, resulted in mRNA and protein expression of SIP1/ZEB2 with associated down-regulation of E-cadherin (**Figure 25B**). These findings were further validated by IF, whereby nuclear SIP1/ZEB2 expression (Green) resulted in E-cadherin down regulation from the cell surface (Red) and mesenchymal transformation (**Figure 25C**). These results confirm SIP1/ZEB2 expression promotes EMT in DLD-SIP1 CRC cells, as previously described by Vandewalle and colleagues (324). To ensure the observed results are not cell line specific, CRC cell lines in the CCLE database were probed for associations between SIP1/ZEB2 TF's and epithelial or mesenchymal genes. SIP1/ZEB2 TF expressing cell lines associated with low levels of epithelial markers (E-cadherin (*CDH1*),

PKP3 and mir200B) and high expression levels of mesenchymal markers such as Vimentin (VIM), ZEB1 and SNAIL2. These findings suggest SIP1/ZEB2 expression in CRC cells leads to activation of EMT programmes and mesenchymal transformation.

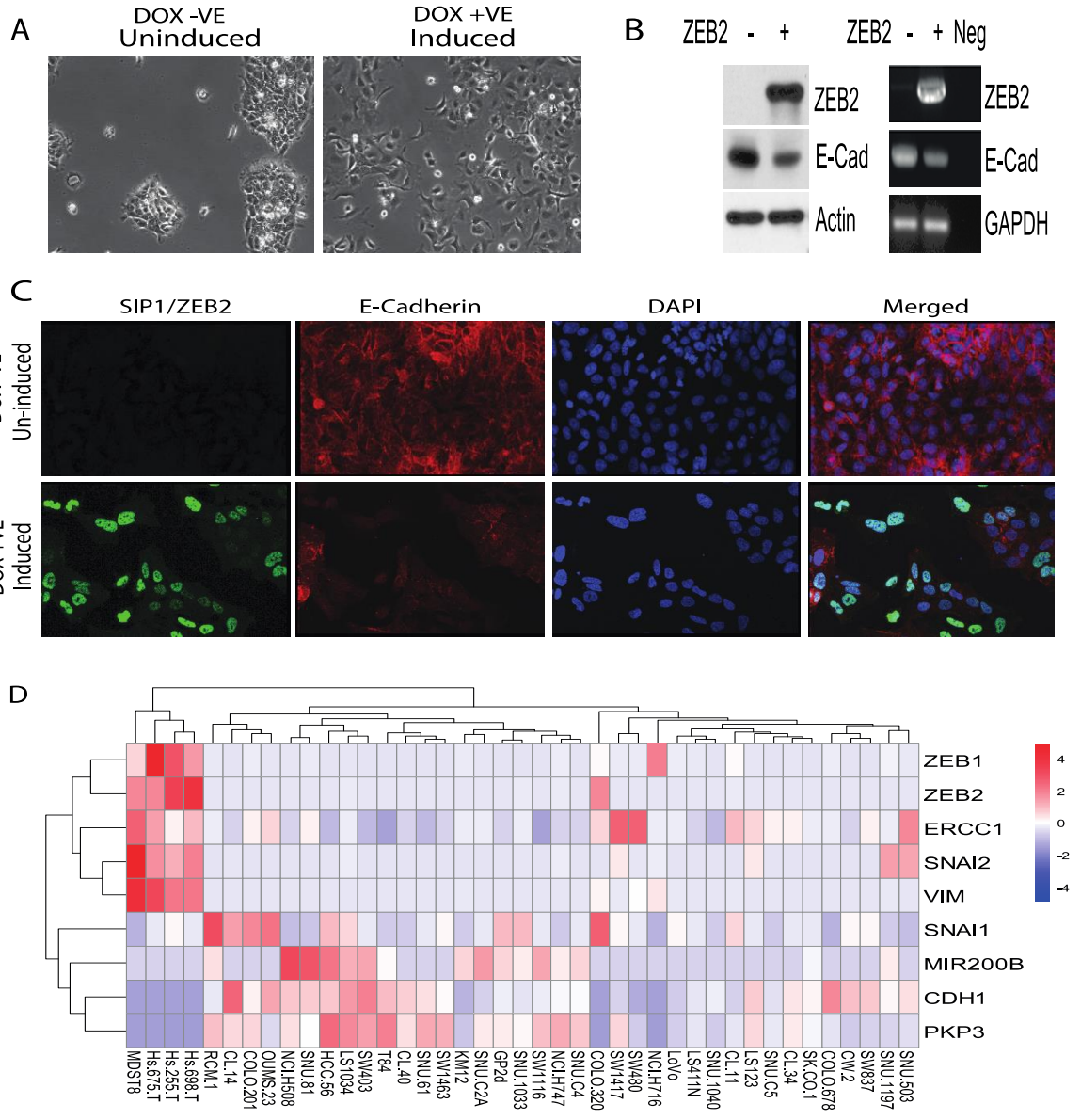

Figure 25: SIP1/ZEB2 expression promotes expression of mesenchymal cells, E-Cadherin down-regulation and expression of a mesenchymal phenotype in CRC. The above experiments were undertaken to investigate whether SIP1/ZEB2 TF expression in DLD-SIP1 results in EMT. (A) DLD-SIP1 cells were treated with doxycycline to induce SIP1/ZEB2 expression and cell morphology studied by light microscopy. After 5 days of induction the doxycycline treated cells (DOX +VE) lost the ability to form epithelial islands and expressed a more mesenchymal phenotype. (B) WB and RT-PCR of DLD-SIP1 cells before and after induction of EMT resulted in protein and mRNA expression of SIP1/ZEB2 and associated down regulation of E-cadherin. Actin and GAPDH were used as equal loading controls (C) IF further validated these findings by demonstrating, induction of EMT results in nuclear SIP1/ZEB2 expression and down regulation of E-cadherin from the cell surface. (D) Analysis of genes in the CCLE gene-atlas revealed a notable association between SIP1/ZEB2 TF expression with low levels of epithelial markers (mir200b, *CDH1*) and high levels of mesenchymal markers (VIM).

3.2 SIP1/ZEB2 expression promotes chemoresistance

A cardinal feature of EMT is the acquisition of apoptosis resistance to commonly used cytotoxic chemotherapeutic agents (66, 115). Mechanisms that mediate this feature however remain elusive. Poly (ADP ribose) polymerase (PARP) is an enzyme that signals DNA damage to cellular DNA repair machinery, thus promoting cell survival. Apoptosis, results in caspase mediated PARP cleavage, resulting in loss of function and activation of programmed cell death (291). Another early hallmark of apoptosis is externalisation of Phosphotidylserine (PT), a phospholipid detected by human anti-coagulant Annexin V, conjugated with a flurophore. Annexin V is often used in conjunction with PI in the Annexin V/ PI assay to discriminate apoptosis from necrosis.

To examine the impact of SIP1/ZEB2 on chemoresistance; un-induced (ZEB2 –VE) and induced (ZEB2 +VE) cells were exposed to oxaliplatin, 5-flurouracil and doxorubicin. Apoptosis was quantified by detecting PARP cleavage by WB and phosphotidylserine (PT) externalisation by flowcytometry. Cleaved PARP band intensity was reduced in SIP1/ZEB2 expressing cells at all doses tested, regardless of chemotherapeutic agent used **(Figure 26A)**. Untreated cells were used as negative controls and actin as a marker of equal loading. Annexin V/PI assay was also used to quantify the apoptotic cell population after treatment with the cytotoxic agents mentioned above. Cells were gated to ensure, quadrant A **(Figure 26B)** of the dot plot contained non-apoptotic cells, quadrant B/C contained apoptotic populations determined by high annexin V-FITC and PI signal and quadrant D necrotic cells in which cell membrane architecture is destroyed. The results further validated the findings of the WB experiment and highlighted a significant increase in apoptosis resistance of SIP1/ZEB2 expressing (DOX +VE) mesenchymal cells. A 20-40% reduction in the apoptotic cell population was observed in SIP1/ZEB2 expressing mesenchymal cells after exposure to identical doses of the same chemotherapeutic agent as the uninduced epithelial counterpart. Untreated uninduced and induced cells were again used as negative controls during the experiment.

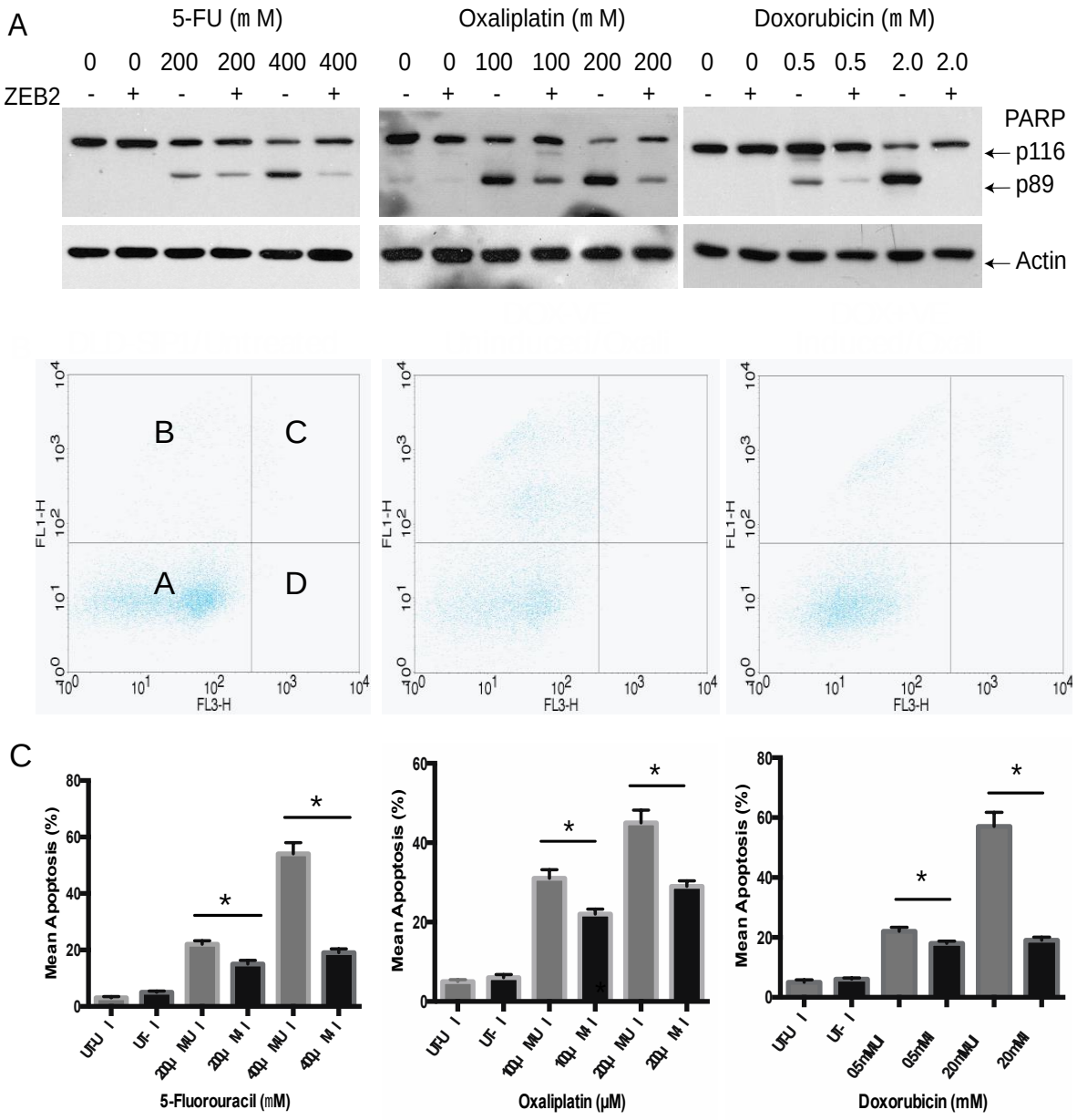

Figure 26: SIP1/ZEB2 expression promotes apoptosis resistance to chemotherapeutic agents. (A) Uninduced (SIP1/ZEB2 –VE) and induced (SIP1/ZEB2 +VE) DLD-SIP1 cells were treated with increasing concentrations of 5-FU, Doxorubicin and Oxaliplatin. Apoptosis in response to drug treatment was detected by PARP cleavage. WB highlighted a dramatic reduction is cleaved PARP (p89) band intensity after ZEB2 induced EMT to all chemotherapeutic agents and across all doses tested. (B) Represents example dot plots acquired by flowcytometry during the Annexin V/ PI assay. Quadrant B/C contains cells cell populations that emit a high Annexin V/PI signal indicating activation of apoptosis pathways. The middle (DOX -VE) and the right (DOX+VE) dot plots provide examples of results obtained from DLD-SIP1 cells treated wit 200µM of oxaliplatin before and after SIP1/ZEB2 expression. It is evident that SIP1/ZEB2 expression results in a smaller increase of the apoptotic cell population indicating acquisition of chemoresistance with SIP1/ZEB2 expression. (C) Histograms representing mean apoptosis (%) as a response to drug treatment before and after SIP1/ZEB2 expression, detected by the Annexin V / PI assay. Uninduced (UI) cells were consistently more sensitive to apoptosis induced by all three chemotherapeutic agents, when compared to the induced (I) counterparts. Statistical differences in mean apoptosis between UI/I cells were calculated using a student *t*-test and the * symbol indicates a *p*-value <0.05.

3.3 SIP1/ZEB2 expression enhances migration and motility

The association between EMT and increased motility has been recognised since its initial description by Hay et al. Previous studies have observed an association between increased metastatic capacity and SIP1//ZEB2 expression in bladder and CRC cell lines (65, 66). To investigate whether SIP1/ZEB2 expression in DLD-SIP1 CRC cells increases metastatic capability, a transwell migration assay and a cell motility assay was undertaken. The motility assay, performed by tracking single cells, using TrackMate software highlighted an eight-fold increase in cell motility after SIP1/ZEB2 expression when compared to their uninduced counterparts **(Figure 27A-B)**. The transwell migration assay revealed a 3-fold increase in the number of cells that had migrated across the pores of the Boyden chamber **(Figure 27C)** after induction of EMT in DLD-SIP1 cells. These results exhibit consistency with previous studies that have observed increased motility and migration capacity in SIP1/ZEB2 expressing mesenchymal cells (65, 66).

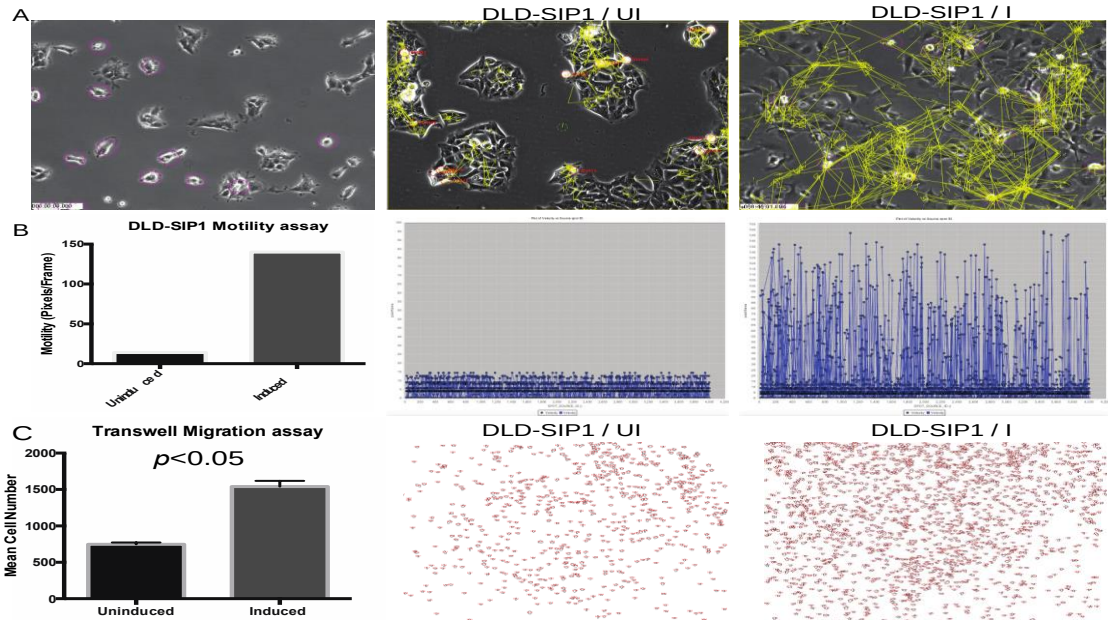

Figure 27: **SIP1/ZEB2 migration promotes increased motility and migration.** (A) TrackMate software was used to quantify single cell motility from time-lapse microscopy images of DLD-SIP1 cells before and after EMT. The first image provides an example of single cell selection (Pink Circles) by TrackMate software. The middle and the right panels exhibit tracks (yellow lines) established by cell motility. (B) An eight- fold increase in cell motility was observed after SIP1/ZEB2 expression. The middle and right panels are dot plots of cell motility in all cells tracked by the software as pixels/frame. (C) The transwell migration assay highlighted a 3-fold increase in cells that had migrated across the pores of the polycarbonate membrane of the Boyden chamber. Migrated cells were quantified by staining with DAPI and quantifying cell numbers using imageJ. Examples images of the automated cell counting process are provided. Statically significance was calculated using student t-test. UI-induced, I –induced.

3.4 SIP1/ZEB2 expression increases cells in G1 phase of the cell-cycle and reduces proliferation kinetics

Cell proliferation is well known to influence sensitivity of cancer cell lines to DNA damaging chemotherapeutic agents. Cancer cells that proliferate at a faster rate are more sensitive to DNA damage when compared to quiescent cells (331) . Transcription factors that promote EMT have been shown to induce cell cycle arrest in certain cell lines (101). Consequently, I investigated the proliferation kinetics of DLD-SIP1 cells before and after induction of EMT by SIP1/ZEB2. The assay was performed using the Cell Titre-Glow® assay (CTG) (Promega) as described previously. The results demonstrated no statistically significant difference in proliferation kinetics between induced and uninduced cells **(Figure 28A)**. It is important to note, that previous experiments performed to assess chemoresistance properties to commonly used cytotoxic agents, were analysed after a 36hr exposure to the drugs. Consequently, the significant differences in apoptosis resistance that were observed cannot be attributed to changes in proliferation kinetics.

Previous studies have also reported SIP1/ZEB2 expression results in a G1 cell cycle arrest, a cardinal feature of EMT that could explain the attenuation in proliferation kinetics observed after day 3 of the proliferation assay. Consequently, I examined the cell cycle profile of DLD-SIP cells before and after expression of SIP1/ZEB2. The experiment was performed by staining uninduced and induced cells with propidium iodide (PI) and detecting cells belonging to different phases of the cell cycle using flowcytometry. DLD-SIP1/ZEB2 cells that had been induced for 4 days showed an increase in G1 and decreased S phase cells suggesting a slowdown of cell cycle, however the differences did not reach statistical significance **(Figure 28B)**. These results demonstrate SIP1/ZEB2 expression results in acquisition of all the cardinal features, which include E-cadherin down regulation, acquisition of a more metastatic phenotype, G1 cell cycle arrest and chemoresistance to cytotoxic agents through currently poorly understood mechanisms.

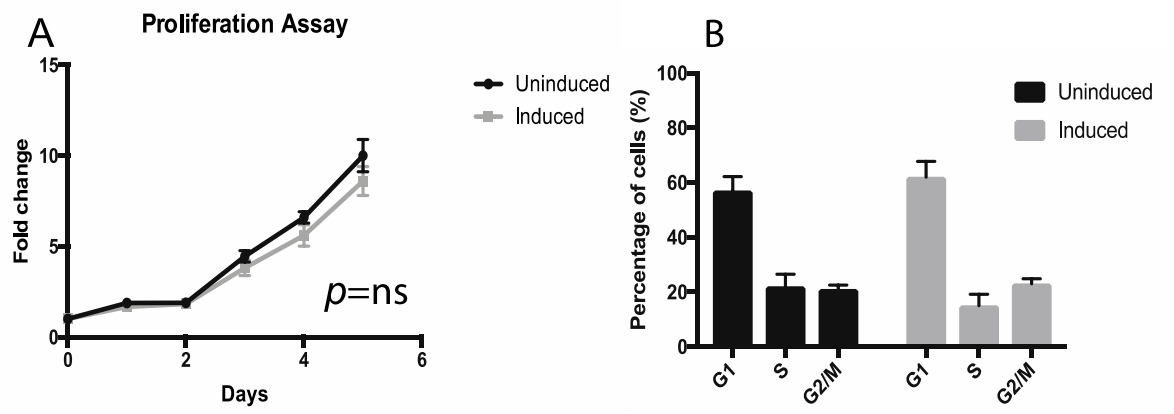

Figure 28: SIP1/ZEB2 expression in DLD-SIP1 cells does not attenuate cell proliferation. (A) To investigate the influence of SIP1/ZEB2 on proliferation, DLD-SIP1 cells were plated in the wells of a 96 well plate and induced for 5 days (D1-D5). Cell numbers were calculated using Cell Titre-Glow® assay (CTG) (Promega). The assay relies on the mono-oxygenation of beetle luciferin by ultra-glow-luciferase enzyme in the presence of ATP, oxygen and Magnesium. As ATP levels are indicative of metabolically active cells, the intensity of the bioluminescence signal is used as indirect signal of cell number. **(B)** DLD-SIP1 cells were induced for 4 days and their cell cycle profile was assessed using PI staining. SIP1/ZEB2 expressing cells showed an increase in G1 and decrease in S phase cells suggesting a slowdown of the cell cycle. Statistical analysis was performed using the student t-test and significance set at $p<0.05$, however the differences did not reach statistical significance.

3.5 Drug uptake is comparable between uninduced and induced cells

A resistance mechanism that neoplastic cells use to abrogate the effect of chemotherapeutic agents is drug efflux or reduced drug uptake. Up regulation of drug efflux proteins by direct transcription activation by TF's that induce EMT have been previously reported (127). To investigate whether variations in drug uptake, or increased drug efflux contributes apoptosis resistance previously observed in SIP1/ZEB2 expressing CRC cells the intrinsic fluorescence property of doxorubicin was utilised. Uninduced and induced cells were treated with two increasing concentrations of doxorubicin for 1hr, washed and allowed to recover for 4 hrs. Induced cells had previously exhibited apoptosis resistance, detected by reduced PARP cleavage and PT externalisation, at these concentrations of doxorubicin when compared to uninduced counterparts **(Figure 26)**. Drug uptake was measured as intracellular fluorescence intensity detected by flowcytometry. Comparison of the fluorescence intensity histograms of uninduced and induced cells revealed an identical shape and signal intensity, suggesting no differences in drug uptake or efflux after SIP1/ZEB2 induced EMT **(Figure 29)**. These results

suggest, the mechanism promoting apoptosis resistance in DLD-SIP1 cells is not secondary to intrinsic variations in intracellular doxorubicin concentration.

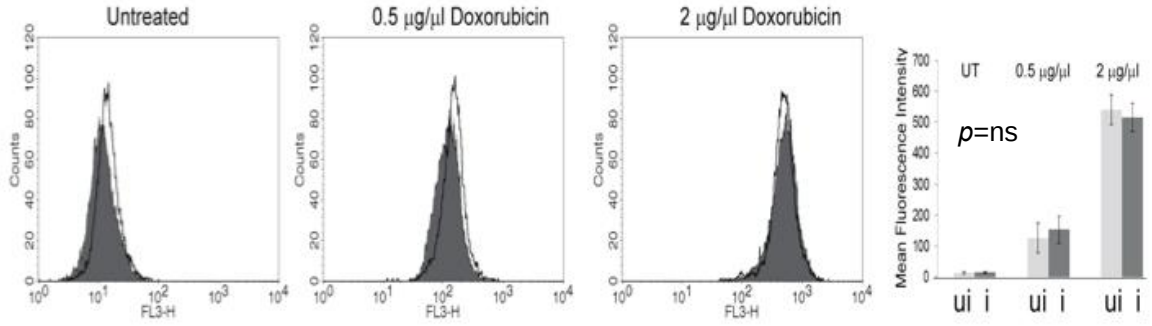

Figure 29: SIP1/ZEB2 expression does not alter Doxorubicin uptake or efflux. DLD-SIP1 cells were treated with 2 increasing concentrations of doxorubicin. The concentrations used in the assay previously highlighted a disparity in apoptosis resistance between uninduced (UI) and induced (I) DLD-SIP1 cells. After treatment for 1hr DLD-SIP1 cells were washed and allowed to recover for 4 hours. Intracellular fluorescence intensity was measured by flowcytometry. The fluorescence intensity histograms, highlighted an increased in intracellular fluorescence signal, however the signal intensity detected from UI and I cells were almost identical at both concentrations, suggesting SIP1/ZEB2 expression does not alter drug uptake or efflux of doxorubicin, and consequently cannot be the mechanism promoting resistance to apoptosis.

3.6 Results summary and discussion

The above work was undertaken to delineate in detail the properties of DLD-SIP1 cells as a model to investigate mechanism mediating chemo/radio resistance in CRC. Induction of SIP1/ZEB2 expression after treatment with doxycycline resulted in E-cadherin down regulation, increased metastatic capacity, attenuated proliferation kinetics, cell cycle (G1) arrest and chemoresistance. Despite displaying apoptosis resistance to doxorubicin, assessment of intracellular drug uptake remained identical between uninduced and induced cells. SIP1/ZEB2 expressing DLD-SIP1 cells displayed apoptosis resistance to treatment with oxaliplatin and 5-FU; the primary components of the first-line FOLFOX adjuvant chemotherapy regimen administered to patients deemed to be at high risk of disease recurrence after surgery for CRC. These findings provide compelling evidence that SIP1/ZEB2 expression alone is sufficient to promote chemoresistance and thus promote disease recurrence in patients with CRC.

The first aim of this study was to establish whether SIP1/ZEB2 expression in CRC leads to EMT and acquisition of associated features. A cardinal feature of EMT is the down regulation of epithelial cell adhesion proteins such as E-cadherin and expression of

mesenchymal genes. Western blotting, IF and data mining of the CCLE database demonstrated, SIP1/ZEB2 expression in CRC cell lines results in E-cadherin down regulation and expression of mesenchymal marker such as Vimentin. Traditionally EMT was defined as a binary event, whereby cells were classified as either epithelial or mesenchymal. Growing evidence now suggests EMT involves transition to multiple intermediary states during which cells can express both epithelial and mesenchymal markers simultaneously. To ensure consistency in induction, DLD-SIP1 cells were consistently induced by treatment with doxycycline and for an identical period of time. Detailed analysis of SIP1/ZEB2 induced repression of epithelial genes after induction of EMT was demonstrated and published by Vanderweele and colleagues using the DLD-SIP1/ZEB2 cells line in 2005 (324).

The second aim of the above experiments was to investigate whether SIP1/ZEB2 induced EMT promoted chemoresistance and metastasis. To ensure experiments were not biased by differences in proliferation and cell cycle kinetics, I undertook a proliferation assay and flowcytometry to delineate in detail any differences between induced and uninduced cells. Mejlvang and colleagues had previously demonstrated SIP1/ZEB2 induced EMT promoted cell cycle arrest at stage G1 of the cell cycle by direct repression of cyclin-D1, in A431 epidermoid cancer cells (101). However, in DLD-SIP1 cells, expressed very small differences in proliferation and cell cycle kinetics after EMT. This discrepancy is most likely secondary to DLD-SIP1 cells being APC and AXIN mutant. Webster and colleagues demonstrated AXIN mutation in DLD1 cells inhibits GSK3 mediated phosphorylation and accumulation of cytoplasmic and nuclear β-catenin. Constant activation of the canonical Wnt/β-catenin pathways may be postulated to off set the repressive effects of SIP1/ZEB2 on cell cycle kinetics (332). This feature however makes DLDS-SIP1 cells an ideal model to study chemoresistance properties, as the results will not be biased by differences in proliferation kinetics and cell cycle profiles between epithelial and mesenchymal cohorts.

A cardinal feature of EMT is the acquisition of chemoresistance. Seminal studies by Zheng and Fischer demonstrated EMT is dispensable for metastasis but promotes chemoresistance using a murine model (107, 108). However, little mechanistic detail is understood with regards to cellular programs promoting resistance. To investigate if SIP1/ZEB2 induced EMT promotes chemoresistance to DNA damaging agents routinely used in clinical care, WB analysis of PARP cleavage and phospotidylserine externalisation detected by flowcytometry was used to assess apoptosis after exposure to Oxaliplatin, 5-FU and Doxorubicin. The results demonstrated SIP1/ZEB2 expression alone was adequate to promote apoptosis resistance to all three chemotherapeutic agents. These findings are supported by multiple other studies that have reported apoptosis resistance after EMT induction in multiple cancer cell lines (66, 107, 115, 127, 333).

EMT is associated with chemoresistance and a mechanism by which cancer cells can become resistant to chemotherapeutic agents is by increased efflux. Mesenchymal breast cancer cells have been shown to over express multi-drug resistant ABC transporters thus acquiring chemoresistance. Promoter regions of ABC transporter genes, have also been found to contain several EMT-TF binding sites, which suggests the mechanism driving gene expression is through direct transcriptional activation (127). To investigate whether SIP1/ZEB2 induced chemoresistance was mediated by increased expression of cell membrane transport proteins that promote drug efflux; DLD-SIP1 cells were treated with increasing concentrations of doxorubicin. Single cell drug uptake was quantified by flowcytometry measuring fluorescence intensity emitted by intracellular doxorubicin concentration. The results demonstrated an identical pattern of drug uptake when uninduced and induced cells were compared, ruling out drug uptake or efflux as a potential resistance mechanism of apoptosis resistance in DLD-SIP1 CRC cells.

Chapter 4: Nuclear SIP1/ZEB2 expression associates with poor oncological outcomes and predicts recurrence.

As previously highlighted, colorectal cancer (CRC) is a key public health issue, representing the commonest gastrointestinal malignancy in western civilisations and the second most common cause of cancer-associated mortality in Europe (1). Surgery remains the mainstay of curative intent treatment for predicted non-metastatic CRC, however metachronous systemic and to a lesser extent local recurrence of disease from occult micro-metastatic spread is common, and remains the principal cause of mortality in CRC. (2). One method to reduce the risk of recurrence is with the application of modern combination adjuvant chemotherapy (AC) regimens. Nevertheless decision making on the application of AC is challenging and inexact, and toxic side effects can be frequent, cumulative, and at times life threatening. As a result, many patients without occult micro-metastases may be over treated, and are exposed to the detrimental effects of chemotherapy. Similarly, up to 35% with initially predicted early stage disease do not receive AC and yet subsequently develop systemic recurrence and are therefore undertreated. These observations underscore our imprecise methods for staging and selection for AC, and highlight the critical need for better markers to identify occult disease spread(334).

For decades, the TNM staging system, based on depth of tumour invasion through the bowel wall and lymph node or distant organ spread has been used to stratify patient risk and to predict the need for AC (36). However, in more recent years there has been growing acknowledgement of the limitations of the TNM system and of tumour heterogeneity and its contribution to stage independent variability in disease trajectory and treatment response (33). For example in node negative disease incremental benefit from adjuvant chemotherapy for the average patient remains at less than 5% at 5 years (335). Identifying patients at high risk of recurrence therefore remains imprecise as current clinical decision-making relies primarily on histological features. Despite the drive to improve precision in defining criteria to identify patients at high risk of recurrence, there are currently no biomarkers in routine clinical use to guide clinical management.

Refinement of the TNM classification system by the addition of validated biomarkers of micro-metastatic spread would therefore greatly improve identification of patients at high risk of recurrence and guide further individualisation of treatment.

In CRC, numerous *in vitro* and preclinical studies have demonstrated that EMT leads to increased metastatic capacity and apoptosis resistance to commonly used chemotherapeutic agents (66, 110, 115). An association between expression of mesenchymal markers and poor oncological outcomes in patients has also been reported in multiple other solid organ malignancies (65, 66, 268, 336). More recently, several high quality independent studies have conducted molecular profiling of CRC, and while they have differed in the number of molecular subtypes noted, they have all agreed that tumours displaying a mesenchymal profile have a very poor outcome and are characteristic of very aggressive tumours with poor response to chemotherapy (42, 272, 273, 275). Despite these compelling observations, the presence of a mesenchymal tumour phenotype is not routinely considered when stratifying recurrence risk or choosing adjuvant chemotherapeutic compounds to treat patients with CRC. The aim of the following work is to assess the utility of SIP1/ZEB2 as a marker of micro-metastatic spread in CRC and precisely analyse the added value of its expression status in predicting disease recurrence after curative surgery.

4.1 Patient demographics and clinic-pathological correlation

Basic patient demographics and association of SIP1/ZEB2 with clinical and pathological parameters for the training cohort are provided in **Table 3 and 4** below. Of the 126 patients in the training set, 11 (8.7%) were aged <60 and 115 (91.3) aged >60. 61 (48.4%) patients were male and 65 (51.6%) female. 89 (70.6%) of the primary tumours were located in the colon, whilst 33 (26.2%) tumours were rectal carcinomas. 77 (61.2%) patients were classified as stage 1 or 2 disease, whilst 38.8% (48) had lymph node metastasis. SIP1/ZEB2 expression was observed in 52 (41.3%) of the analysed samples. Clinical and pathological association by Chi-squared analysis revealed a statistically important association between SIP1/ZEB2 and lymph node metastasis *($p<0.02$)* and

consequently advanced stage (*p<0.06*). No statistical association was observed between SIP1/ZEB2 expression and differentiation. In the validation cohort (n=210), 25 (12.4%) were aged <60. 111 (52.9%) patients were male, 159 (75.7%) tumours were colonic and 51 (24.3%) rectal. Assessment of SIP1/ZEB2 immuno-expression, revealed 104 (49.5%) tumours to be SIP1/ZEB2 positive and 106 (50.5%) SIP1/ZEB2 negative. Clinical and pathological association by Chi-squared test mirrored the associations observed in the training cohort and demonstrated a statistically significant association with stage III disease (*p=0.03*) and node positivity (*p<0.06*). Positive samples from both cohorts expressed nuclear SIP1/ZEB2 expression at the invasive front and the centre of the tumour. Positivity varied from 10% to ubiquitous expression. Nuclear SIP1/ZEB2 expression was not always associated with a mesenchymal phenotype. Morphologically epithelial islands strongly expressed SIP1/ZEB2, suggesting induction of chemoresistance may be independent of E-cadherin down regulation. Discrepancy in scoring was noted in less than 10% of tumour samples; in these instances, the specimens were re-analysed and a consensus reached.

Table 3: Patient demographics of the training and validation cohorts.

	Training cohort		Validation cohort	
	n	%	n	%
Age (Yrs)				
<60	11	8.7	25	11.9
>60	115	91.3	185	88.1
Missing	0	0	0	0
Sex				
Male	61	48.4	111	52.9
Female	65	51.6	99	47.1
Missing	0	0	0	0
ASA grade				
1	9	7.1	21	10.0
2	56	44.4	95	45.2
3	34	27.0	82	39.0
4	5	4.0	7	3.3
Missing	22	17.4	5	2.4
Site of tumours				
Right	49	38.9	96	45.7
Left	40	31.7	63	30.0
Rectum	33	26.2	51	24.3
Missing	4	3.2	0	0.0
Differentiation				
Well	2	1.6	25	11.9
Moderate-well	47	37.3	4	1.9
Moderate	54	42.9	103	49.0
Moderate-poor	8	6.3	72	34.3
Poor	14	11.1	4	1.9
Missing	1	0.8	2	1.0
Stage				
Stage 1	22	17.5	32	15.2
Stage 2	55	43.7	111	52.9
Stage 3	48	38.1	67	31.9
Stage 4	0	0	0	0
Missing	1	0.8	0	0
T-stage				
T1	10	7.9	6	2.9
T2	16	12.7	42	20
T3	30	23.8	108	51.4
T4	69	54.8	54	25.7
Missing	1	0.8	0	0
N-Positivity				
N0	78	61.9	144	68.2
N1	48	38.1	67	31.8
Missing	0	0	0	0
Adjuvant Chemotherapy				
Yes	82	65.0	85	40.5
No	42	33.3	125	59.5
Missing	2	1.6	0	0
ZEB2 Positive				
Yes	52	41.3	104	49.5
No	74	51.7	106	50.5

Table 4: Association between clinico-pathalogical features and SIP1/ZEB2 expression. *p*-values were calculated using Chi-Squared or Fischer's exact test as appropriate.

	Training Cohort			Validation cohort		
Characteristics	**ZEB2+VE**	**ZEB2 –VE**	***p-value***	**ZEB2+VE**	**ZEB2-VE**	***p-value***
Age						
<60	3	8	*p = 0.52*	15	11	*p = 0.52*
>60	49	66		89	95	
Sex						
M	20	41	*p = 0.06*	51	60	*p = 0.27*
F	32	33		53	46	
T-stage						
T1	3	7		4	2	
T2	5	11		14	28	
T3	12	18	*p = 0.62*	56	52	*p = 0.16*
T4	32	37		30	24	
Nodal Positivity						
NO	30	48	*P=0.06*	61	75	*p* < 0.05
N1/N2	22	26		43	31	
Stage						
1	6	16		11	21	
2	20	35	*p = 0.06*	52	59	*p* < 0.05
3	26	22		41	26	
4	0	0		0	0	
Differentiation						
Well	1	1		2	4	
Mod-well	18	29		49	54	
Moderate	23	31	*p = 0.95*	34	38	*p = 0.19*
Mod-poor	3	5		4	0	
Poor	7	7		15	10	

4.2 Nuclear SIP1/ZEB2 expression prognosticates risk of early recurrence and reduced survival.

IHC was initially performed on the training cohort of 126 consecutive CRC specimens for SIP1/ZEB2 expression and positivity recorded using a previously published scoring system (66). No ubiquitous expression of nuclear SIP1/ZEB2 was detected in normal colonic epithelium **(Figure30A/B)**. Mesenchymal cells such as fibroblasts or lymphocytes in the tissue naturally express SIP1/ZEB2 and served as a positive control. Two independent pathologists blinded to the groups and outcomes scored 41.3% (52) of the 126 specimens as SIP1/ZEB2 positive **(Figure 30 C-H)**. Survival analyses by log rank highlighted increased recurrence rates (DFS) **(Figure 31B)** and reduced survival (OS) **(Figure 31A)** in SIP1/ZEB2 expressing patients. Mean OS of SIP1/ZEB2 expressing patients was 43.8 months compared to 60.4 months for SIP1/ZEB2 negative patients (log rank, p = 0.02). Mean DFS, in SIP1/ZEB2 positive patients was 48.0 months compared to 60.5 months in SIP1/ZEB2 negative patients (log rank, p =0.001). Multi variable analysis by Cox regression highlighted SIP1/ZEB2 as an independent prognostic marker of both OS (HR 1.7, 95% CI 1.1 - 2.8, p<0.04) and DFS (HR =1.82, 95% CI 1.4 – 3.7, p=0.01) **(Table 5 and 6)**. SIP1/ZEB2 positive patients had a 1.7 fold increased risk of mortality (OS) and two fold increase in recurrence risk within 5 years of surgical resection, when compared to SIP1/ZEB2 negative patients.

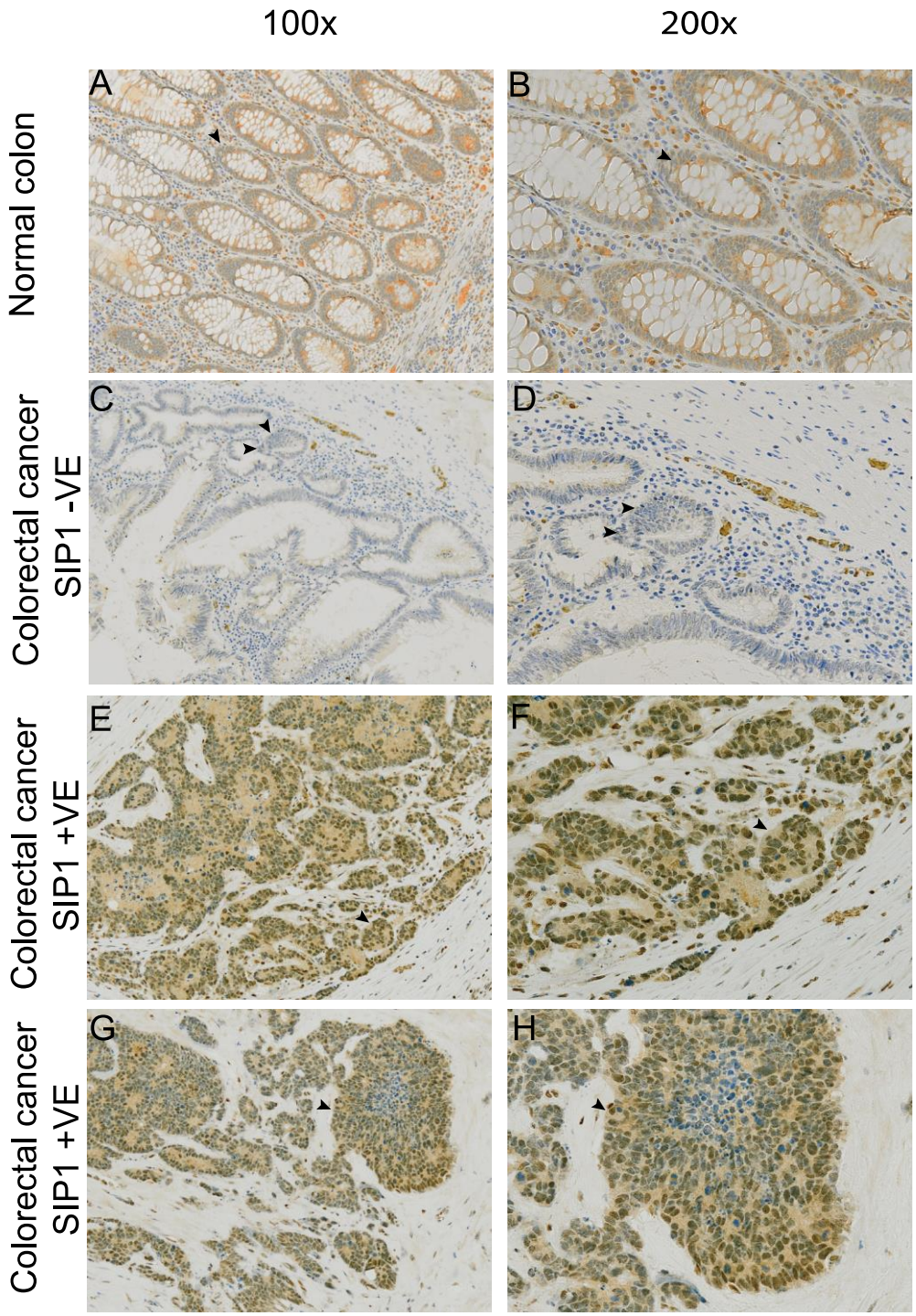

Figure 30: SIP1/ZEB2 expression in normal colonic epithelium and CRC.(**A/B**) shows normal colonic epithelium with absence of SIP1/ZEB2 nuclear staining. **(C/D)** is an example of a CRC specimen that stained negative for SIP1/ZEB2. The arrows highlight the absence of staining in the nucleus. The nuclear staining of certain fibroblasts and immune cells serve as internal positive controls **(E-H)** CRC specimens expressing nuclear SIP/ZEB2 at the invasive front and the center of a tumour. The blue (Haematoxylin) staining of cells in the middle of the cluster neoplastic cells in section G/H provides evidence for the specificity of the antibody.

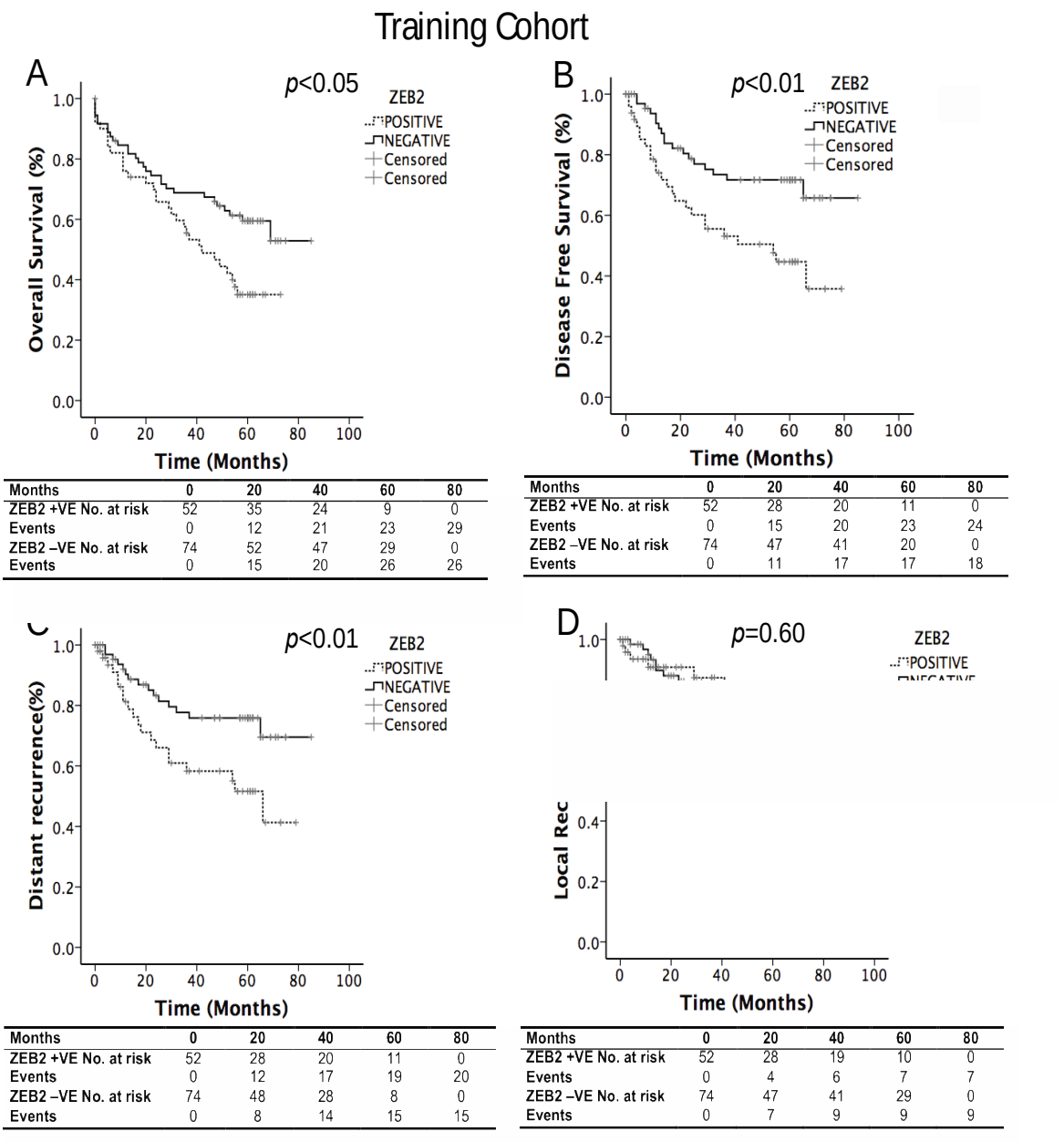

Months	0	20	40	60	80
ZEB2 +VE No. at risk	52	35	24	9	0
Events	0	12	21	23	29
ZEB2 –VE No. at risk	74	52	47	29	0
Events	0	15	20	26	26

Months	0	20	40	60	80
ZEB2 +VE No. at risk	52	28	20	11	0
Events	0	15	20	23	24
ZEB2 –VE No. at risk	74	47	41	20	0
Events	0	11	17	17	18

Months	0	20	40	60	80
ZEB2 +VE No. at risk	52	28	20	11	0
Events	0	12	17	19	20
ZEB2 –VE No. at risk	74	48	28	8	0
Events	0	8	14	15	15

Months	0	20	40	60	80
ZEB2 +VE No. at risk	52	28	19	10	0
Events	0	4	6	7	7
ZEB2 –VE No. at risk	74	47	41	29	0
Events	0	7	9	9	9

Figure 31:**Association between SIP/ZEB2 expression and oncological outcomes in the training cohort. (A/B)** Kaplan-Meier (KM) survival curves demonstrating differences in overall survival (OS) and Disease free survival (DFS) when patients were stratified as SIP1/ZEB2 negative **(Green)** or positive **(Blue)**. Tables below indicate numbers at risk at each time point and *p*-values were calculated using log rank test. **(C/D)** KM curves were generated by differentiating a DFS event as either distant or local recurrence, SIP1/ZEB2 expression associated with increased risk of distant but not local recurrence.

Table 5: Multi-variable Cox-regression analysis of OS in the training cohort, presented as hazard ratio (HR) with a 95% confidence interval (CI).

Characteristic	HR	95% CI	*p* - value
Age (<60 vs. >60)	2.3	0.6 - 9.2	0.24
T-stage (Overall)			<0.01
T stage (T1/2 vs. T4)	2.1	0.9 – 4.5	0.06
T stage (T3 vs. T4)	1.1	0.3 – 2.0	
N-stage (N0 vs. N1/2)	1.4	0.4 - 1.7	0.32
Differentiation			<0.01
Differentiation (Well vs. Poor)	3.4	1.7 – 6.8	<0.01
Differentiation (Mod vs. Poor)	1.0	0.6 – 1.9	0.89
ZEB2 Status (pos vs. neg)	1.7	1.1 - 2.8	<0.05

Table 6: Multi-variable Cox-regression analysis of DFS (DR) in the training cohort, presented as hazard ratio (HR) with a 95% confidence interval (CI).

Characteristic	HR	95% CI	*p* - value
Age (<60 vs. >60)	1.00	0.2 – 4.4	1.00
T-stage (Overall)			<0.05
T stage (T1/2 vs. T4)	4.30	1.3 – 14.6	<0.05
T stage (T3 vs. T4)	0.95	0.2 – 4.8	0.96
N-stage (N0 vs. N1/2)	1.20	0.6 – 2.3	0.70
Differentiation			0.52
Differentiation (Well vs. Poor)	1.55	0.4 – 1.9	0.36
Differentiation (Mod vs. Poor)	0.91	0.6 – 4.0	0.81
ZEB2 Status (pos vs. neg)	1.82	1.4 – 3.7	<0.05

4.3 Nuclear SIP1/ZEB2 expression prognosticates risk of early recurrence and reduced survival in a validation cohort.

Based on the results obtained from the test cohort, a power calculation was undertaken. We identified a cohort size of 180 patients and 46 events as a requirement to achieve 80% power using a two-sided test, at a significance of 5%, assuming a hazard ratio of 2.0. The validation cohort consisted of 211 consecutive patients that underwent a surgical resection for primary colorectal adenocarcinoma between 2008-2013. Patients with metastatic disease at the time of diagnosis (n=26) were excluded from the analysis. An identical scoring criterion was implemented to identify SIP1/ZEB2 positive patients. 49.5% of the tumours were scored SIP/ZEB2 positive whilst 50.5 % SIP1/ZEB2 negative. Survival analysis by log rank test maintained consistency with results from the pilot cohort.

A 6.9 month reduction in mean OS (log rank, *p*<0.01) **(Figure 32A)** and 13 month reduction (log rank, *p*<0.001) **(Figure 32B)** in mean DFS was observed in SIP1/ZEB2 positive patients when compared to SIP1/ZEB2 negative. Multivariable analysis by Cox regression again highlighted SIP1/ZEB2 as an independent prognostic marker of OS (HR =1.4, 95% CI 1.2 – 2.1, *p*=0.05) and DFS (HR =3.2, 95% CI 1.6 – 6.6, *p*<0.01) **(Table 7-8)**. pN stage and SIP1/ZEB2 positivity were identified as independent prognostic markers of OS. pT stage, pN stage and differentiation were identified as independent prognostic markers of DFS.

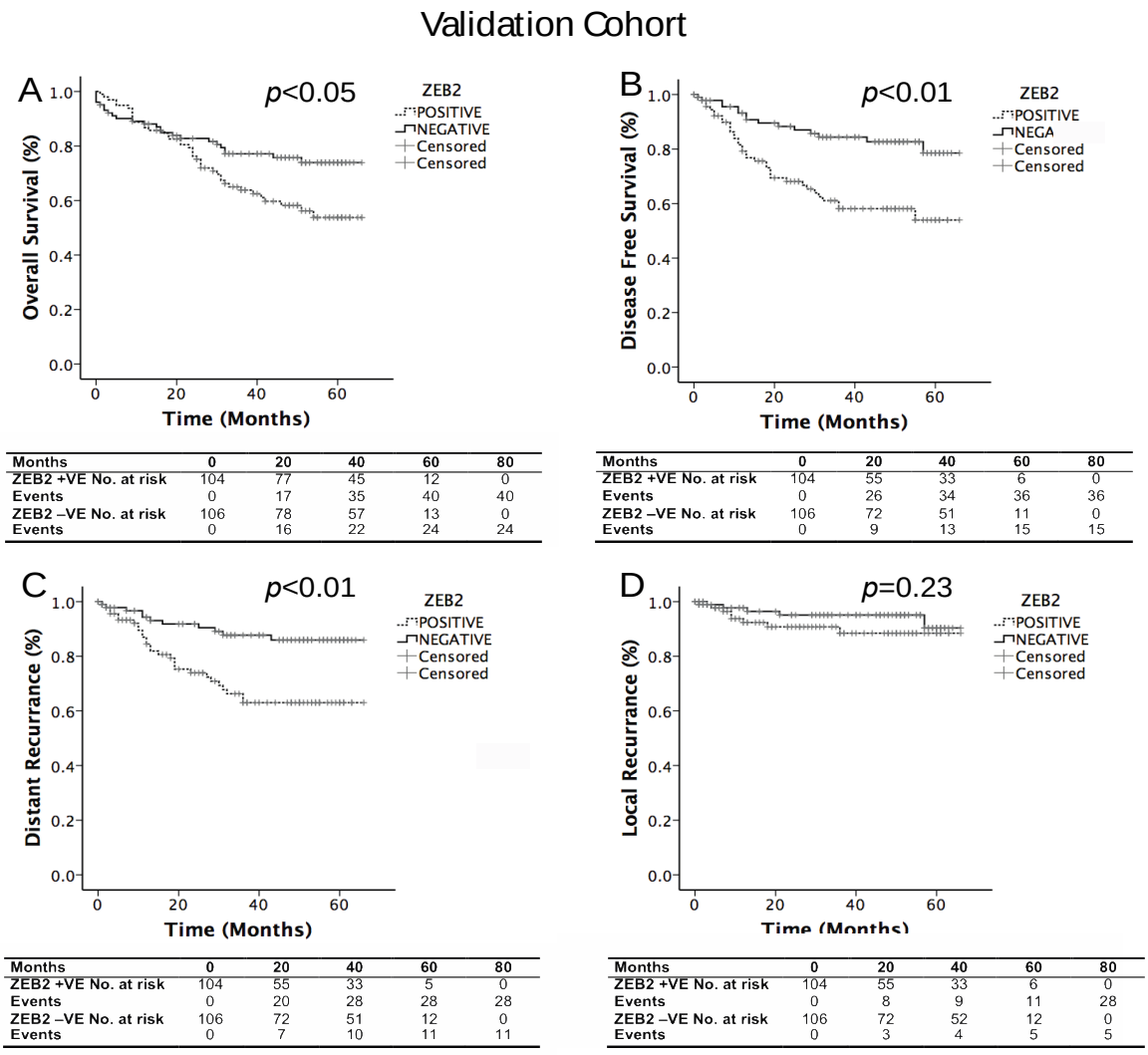

Figure 32: **Association between SIP/ZEB2 expression and oncological outcomes in the validation cohort (A/B)** Kaplan-Meier (KM) survival curves demonstrating differences in overall survival (OS) and Disease free survival (DFS) when patients were stratified as SIP1/ZEB2 negative **(Green)** or positive **(Blue)**. Tables below indicate numbers at risk at each time point and *p*-values were calculated using log rank test. **(C/D)** KM curves were generated by differentiating a DFS event as either distant or local recurrence, SIP1/ZEB2 expression associated with increased risk of distant but not local recurrence.

Table 7: Multi-variable Cox-regression analysis of OS in the training cohort, presented as hazard ratio (HR) with a 95% confidence interval (CI).

Characteristic	HR	95% CI	*p* - value
Age (<60 vs. >60)	1.4	0.6 - 3.4	0.45
T-stage (Overall)			<0.05
T stage (T1/2 vs. T4)	2.8	1.2- 6.3	<0.05
T stage (T3 vs. T4)	1.5	0.7 - 3.1	0.32
N-stage (N0 vs. N1/2)	1.8	1.1 - 2.9	<0.05
Differentiation (Overall)			0.86
Differentiation (Well vs. Poor)	1.2	0.6 - 2.5	0.64
Differentiation (Mod vs. Poor)	1.1	0.5 - 2.4	0.89
ZEB2 Status (pos vs. neg)	1.4	1.2 - 2.1	<0.05

Table 8: Multi-variable Cox-regression analysis of DFS (DR) in the validation cohort, presented as hazard ratio (HR) with a 95% confidence interval (CI).

Characteristic	HR	95% CI	*p* - value
Age (<60 vs. >60)	1.2	0.5 - 3.7	0.72
T-stage (Overall)			<0.01
T stage (T1/2 vs. T4)	4.3	1.5 - 12.4	<0.01
T stage (T3 vs. T4)	1.3	0.5 - 3.5	0.65
N-stage (N0 vs. N1/2)	3.1	1.6 - 6.6	<0.01
Differentiation (Overall)			<0.01
Differentiation (Well vs. Poor)	4.3	2.3 -13.2	<0.01
Differentiation (Mod vs. Poor)	3.3	0.8 - 5.4	0.07
ZEB2 Status (pos vs. neg)	3.2	1.6 - 6.6	<0.01

4.4 Nuclear SIP1/ZEB2 expression prognosticates risk of early recurrence and reduced survival in a validation cohort.

Several *in vitro* and *in vivo* studies have reported that the process of EMT results in an enhanced capacity to metastasise to distant organs(65, 103, 268). Hence, we differentiated distant (DR) from loco-regional recurrence (LR) and investigated the association of SIP1/ZEB2 in these contexts. Distant recurrence was defined as any disease recurrence outside the colon or rectum. Local recurrence was defined as disease recurrence, progression, or development at the anatomical site of resection or in adjacent anatomical mesenteric lymph nodes. For rectal cancer the definitions put forward by the Beyond TME collaborative was utilised (337) .

Survival analysis in both training and validation cohorts revealed that SIP1/ZEB2 positivity selectively prognosticates for distant but not local recurrence, exhibiting consistency with the enhanced motility and migration features observed in *in vitro* EMT models. The mean time to DR was significantly shorter in SIP1/ZEB2 positive patients in both cohorts. An 18-month reduction (49.6 vs. 67.6, log rank, p<0.01) in time to DR was noted in the training cohort **(Figure 31C)** and an 11.4-month reduction (48.0 vs. 59.4, log rank, p<0.01) in the validation cohort **(Figure 32C)**. At 5 years, a 2 to 3 fold increased incidence of distant recurrence was observed in both training and validation cohorts. In contrast, no statistically significant differences in risk of LR were observed in the training (log rank, p = 0.61; **Figure 31D**) or validation cohorts **(Figure 32D)** (log rank, p = 0.23). Multivariable analysis by Cox proportional hazards model identified SIP1/ZEB2 as an independent prognostic marker of DR in both training (HR =1.82, 95% CI 1.4 – 3.7, p<0.05) and validation cohort (HR =3.28, 95% CI 1.7 – 6.1, p<0.01) **(Table 6 and 8)**.

4.5 External validation confirms association between SIP1/ZEB2 expression and reduced disease free survival.

To externally validate the above results of survival outcomes were investigated using the open access portal progeneV2. mRNA expression profile from the database GSE28814 (PMID for citation 21251323) was queried for an association between, high SIP1(ZEB2)/CDH1 ratio and time to metastasis. As observed in the test and validation cohort, high SIP(ZEB2)/CDH1 mRNA ratio, which is suggestive of SIP1/ZEB2 expressing mesenchymal phenotype, resulted in a statistically significant reduction in time to metastasis (Log rank, p=0.01). Patients classified as expressing high SIP1(ZEB2)/CDH1 ratio were at a significantly greater risk of experiencing metastasis when compared to patients with a SIP1(ZEB2)/CDH1 low expression ratio (Hazard ratio 2.1, 95%CI 1.2-3.8) **(Figure 33)**.

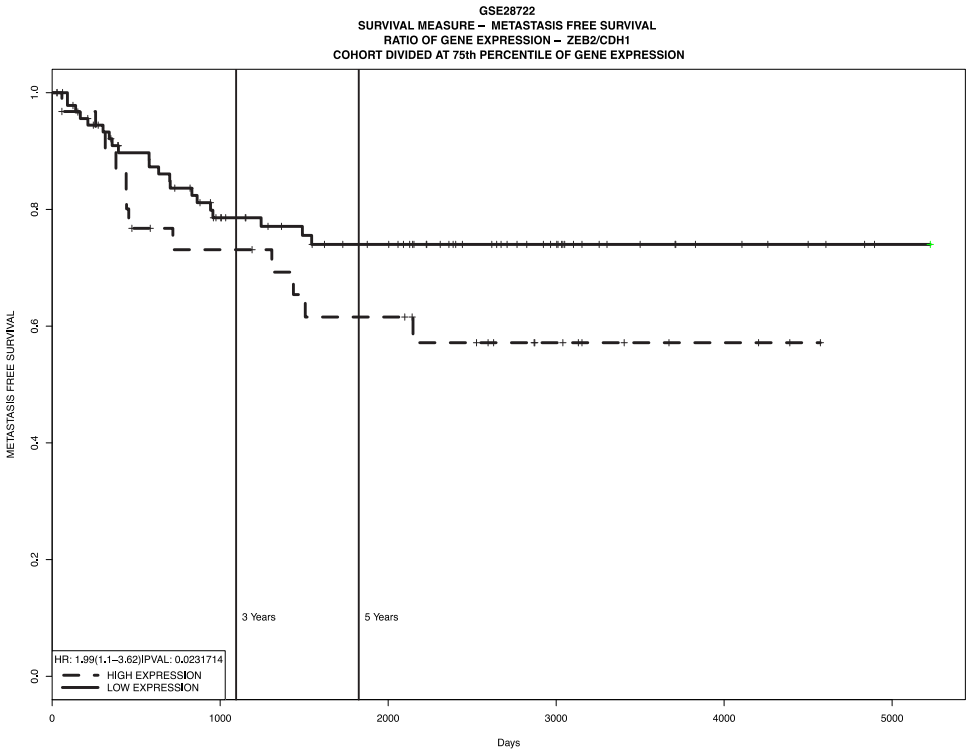

Figure 33: Association between SIP1(ZEB2)/CDH1 expression and disease recurrence. mRNA expression profile from the database GSE28814 (PMID for citation 21251323) was queried for an association between, high SIP1(ZEB2)/CDH1 ratio and reduced time to metastasis. Univariate analysis highlighted a statistically significant association, (Log Rank p<0.01) between High SIP1(ZEB2)/CDH1 ratio. All analysis was performed using the open access platform proggeneV2.

4.6 SIP1/ZEB2 expression identifies patients at a high risk of disease recurrence in stage II disease

The benefit of administering adjuvant chemotherapy in stage III CRC is well-recognised (23). Selecting patients with node negative disease that will derive maximal benefit from adjuvant chemotherapy using conventional clinical and pathological risk factors remains suboptimal, and the accurate identification of patients with occult micro-metastatic disease remains a significant clinical challenge (335, 338). Our previous observations demonstrate that SIP1/ZEB2 expression in CRC associates with earlier recurrence and reduced overall survival. Consequently we undertook subset survival analysis to investigate whether SIP1/ZEB2 expression in node negative (stage I or II) CRC could aid in identifying patients at higher risk of recurrence. In total 222 patients with node negative tumours from both training and validation cohorts were cumulatively analysed to ensure a sufficient number of cases were available. Patient demographics and clinico-pathological associations between SIP1/ZEB2 and conventional risk factors are outlined in **Tables 9**

and 10. 93 (41.9%) of the specimens were scored as SIP1/ZEB2 positive. A statistically significant association was observed between SIP1/ZEB2 expression and poor differentiation status (*p=0.01*). Survival analysis by log rank test revealed SIP1/ZEB2 expression associates with a statistically significant reduction in OS and DFS. Patients with SIP1/ZEB2 positive, but node negative tumours experienced a 19.4-month reduction in time to recurrence *(*log rank*, p<0.05*) and 23.8-month decrease in overall survival (log rank*, p*<0.008**) (Figure 33A-B)**. SIP1/ZEB2 expression again associated with early recurrence with specificity to distant (log rank*, p*=0.04) but not local recurrence (log rank, *p*=0.15) **(Figure 33 C-D)**. An 18.2-month reduction in time to distant recurrence from date of surgery was observed in patients scored SIP1/ZEB2 positive, when compared to negative. Multivariable analysis by Cox regression, which incorporated known clinical and pathological risk factors of stage I and II disease identified SIP1/ZEB2 expression as an independent prognostic marker of recurrence (HR =1.9, 95% CI 1.2 – 3.2, *p*=0.009) and overall survival (HR =1.9, 95% CI 1.6 – 6.6, *p*=0.001) **(Table 11 and 12)**. At 5 years SIP1/ZEB2 expressing patients were almost twice as likely to have experienced disease recurrence or succumb to their disease when compared to SIP1/ZEB2 negative patients.

Table 9: Patients demographics of stage I & II disease

	n	%
Age (Yrs)		
<60	23	10.4
>60	199	89.6
Missing	0	0
Sex		
Male	116	53.3
Female	106	47.7
Missing	0	0
ASA grade		
1	17	7.6
2	87	39.1
3	94	42.3
4	7	3.1
Missing	17	7.7
Site of tumours		
Right	87	39.2
Left	69	31.0
Rectum	62	27.9
Missing	4	1.8
Differentiation		
Well	6	2.7
Moderate-well	107	48.2
Moderate	81	36.5
Moderate-poor	5	2.3
Poor	23	10.4
T-stage		
T1	12	5.4
T2	47	21.2
T3	99	44.6
T4	64	28.8
Nodes Sampled		
<12	95	42.8
>12	125	56.3
Missing	1	0.9
Perineural/ Lympatic/EMVI		
POSTIVE	44	19.8
NETATIVE	173	77.9
Missing	5	2.3
Adjuvant Chemotherapy		
Yes	54	24.8
No	167	74.8
Missing	1	0.4
SIP1 Positive		
Yes	93	41.9
No	129	58.1

Table 10: Clinico-Pathalogical association and SIP1/ZEB2 expression in stage I &II disease

Characteristics	ZEB2 +VE	ZEB2 –VE	*p-value*
Age			
<60	10	13	*p = 0.87*
>60	83	116	
Sex			
M	45	71	*p = 0.32*
F	48	58	
T-stage			
T1	3	9	
T2	17	30	*p = 0.50*
T3	44	55	
T4	29	35	
Nodes Sampled			
<12	37	58	*p* = 0.45
>12	55	70	
Lymphatic / Perineural /EMVI			
Yes	22	22	*p = 0.23*
No	71	102	
Differentiation			
Well	19	9	*p < 0.01*
Mooderate	29	52	
Poor	45	68	

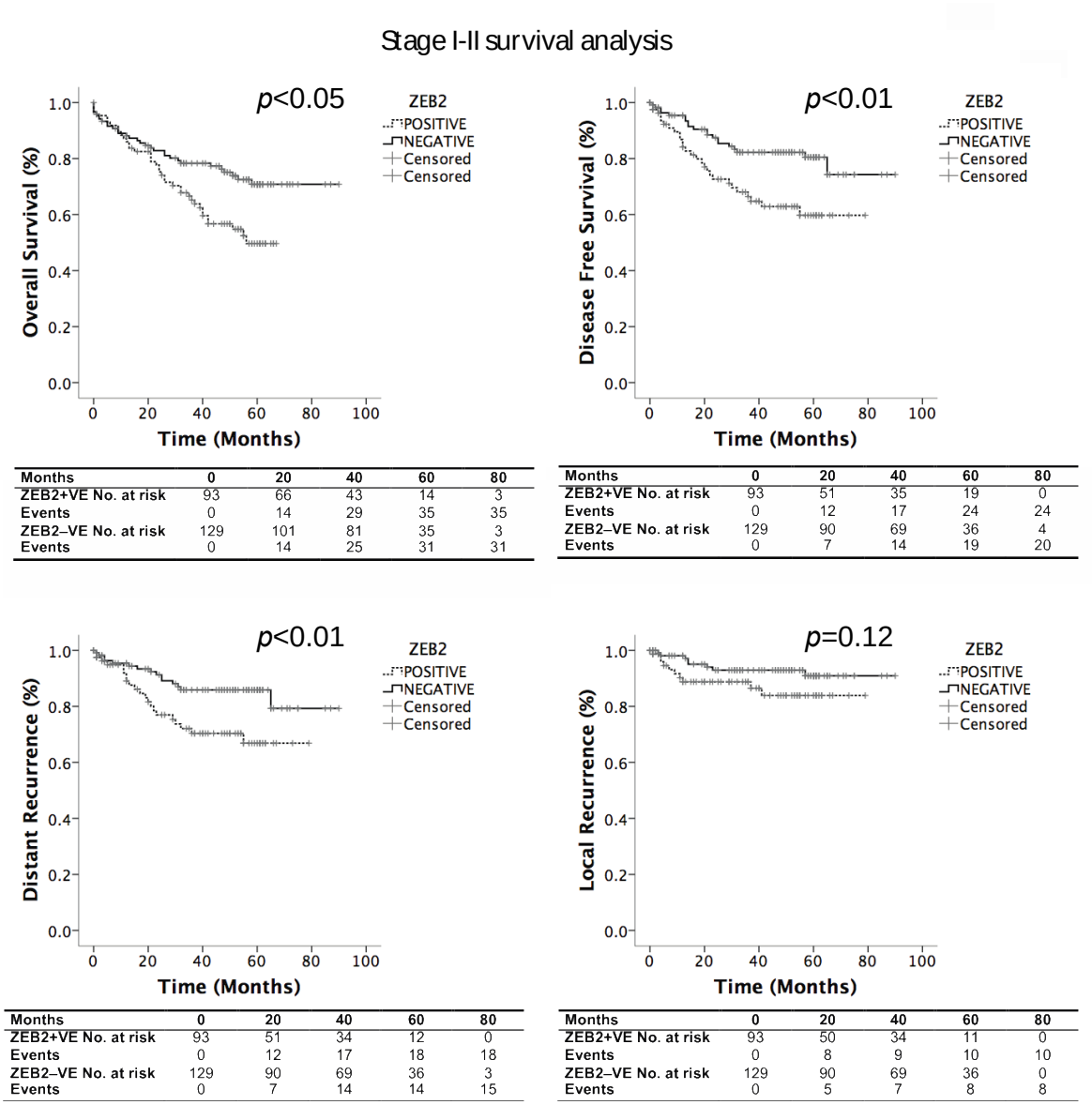

Months	0	20	40	60	80
ZEB2+VE No. at risk	93	66	43	14	3
Events	0	14	29	35	35
ZEB2–VE No. at risk	129	101	81	35	3
Events	0	14	25	31	31

Months	0	20	40	60	80
ZEB2+VE No. at risk	93	51	35	19	0
Events	0	12	17	24	24
ZEB2–VE No. at risk	129	90	69	36	4
Events	0	7	14	19	20

Months	0	20	40	60	80
ZEB2+VE No. at risk	93	51	34	12	0
Events	0	12	17	18	18
ZEB2–VE No. at risk	129	90	69	36	3
Events	0	7	14	14	15

Months	0	20	40	60	80
ZEB2+VE No. at risk	93	50	34	11	0
Events	0	8	9	10	10
ZEB2–VE No. at risk	129	90	69	36	0
Events	0	5	7	8	8

Figure 34: Association between SIP/ZEB2 expression and oncological outcomes in node negative disease.(A/B) Kaplan-Meier (KM) survival curves demonstrating differences in overall survival (OS) and Disease free survival (DFS) when patients were stratified as SIP1/ZEB2 negative **(Green)** or positive **(Blue)** in subset analysis of patients with node negative disease. Tables below indicate numbers at risk at each time point and *p*-values were calculated using log rank test. **(C/D)** KM curves were generated by differentiating a DFS event as either distant or local recurrence, SIP1/ZEB2 expression associated with increased risk of distant but not local recurrence.

Table 11: Multi-variable Cox-regression analysis of overall survival in patients with node negative disease, presented as hazard ratio (HR) with a 95% confidence interval (CI).

Characteristic	HR	95% CI	*p* - value
Age (<60 vs. >60)	1.82	0.5 – 6.1	0.33
T-stage (Overall)			<0.01
T stage (T3 vs. T4)	1.24	0.5 – 2.1	0.84
T stage (T1/2 vs. T4)	4.12	1.2 – 4.5	<0.01
Nodes sampled (<12 vs >12)	1.52	0.9 – 2.5	0.09
EMVI (Pos vs. Neg)	2.10	1.1 – 2.4	<0.05
Differentiation			0.28
Differentiation (Well vs. Poor)	0.82	0.3 – 1.9	0.64
Differentiation (Mod vs. Poor)	1.27	0.5 – 2.4	0.54
Chemotherapy (Yes vs. No)	2.57	1.3 – 5.0	<0.01
ZEB2 Status (pos vs. neg)	1.91	1.2 – 3.2	<0.01

Table 12: Multi-variable Cox-regression analysis of disease free survival (DFS) in patients with node negative disease, presented as hazard ratio (HR) with a 95% confidence interval (CI).

Characteristic	HR	95% CI	*p* - value
Age (<60 vs. >60)	1.06	0.5 – 6.1	0.33
T-stage (Overall)			<0.01
T stage (T3 vs. T4)	1.00	0.5 – 2.1	0.13
T stage (T1/2 vs. T4)	4.00	1.2– 4.5	<0.01
Nodes sampled (<12 vs. >12)	1.19	0.9 – 2.5	0.09
EMVI (Pos vs. Neg)	2.82	0.9 – 2.4	0.03
Differentiation			<0.01
Differentiation (Well vs. Poor)	7.64	1.5 – 7.8	<0.01
Differentiation (Mod vs. Poor)	2.83	0.5 – 4.8	0.22
Chemotherapy (Yes vs. No)	1.20	0.5 – 2.8	0.69
ZEB2 Status (pos vs. neg)	1.91	1.6 – 6.6	<0.01

4.7 SIP1/ZEB2 expression improves capacity to predict early recurrence.

The above data demonstrates a significant association between SIP1/ZEB2 expression and increased incidence of DR, independent of stage. To investigate if addition of SIP1/ZEB2 expression status to conventional histological risk factors improves predictive capacity to identify patients at higher risk of experiencing early DR (<3yrs) after curative surgery; nomograms **(Figure 35F)** with or without SIP1/ZEB2 expression score were developed as described previously. The nomograms were developed in the training cohort and applied to the validation cohort to assess external validity. In the training cohort, the C-index to predict DR within 3 years of surgery using conventional histological risk factors was 0.73 (95% CI: 0.62-0.84) and improved to 0.77 (95% CI: 0.66-0.87, iAUC = 0.04) with

the addition of SIP1/ZEB2 expression score. Application of the nomograms to the validation cohort (n=185) highlighted an identical trend with C-indexes improving from 0.82 (95% CI: 0.75-0.87) to 0.87 (95% CI: 0.80-94, iAUC-0.05) **(Figure 35A/B)**. Kaplan-Meier survival plots generated by applying the risk score to the validation cohort revealed greater separation and improvements in both sensitivity and specificity **(Figure 35C/D)**. Calibration plots demonstrated good concordance between expected and observed outcome (data not shown). Taken together, these observations suggest that SIP1/ZEB2 expression, if used in conjunction with conventional histological staging, improves the ability to identify patients at increased risk of experiencing distant recurrence after surgical resection.

4.8 SIP1/ZEB2 expression improves ability to predict recurrence in patients with stage I & II disease.

The inability to stratify patient risk more precisely in node-negative CRC impedes clinicians' ability to identify patients that will derive maximum benefit from adjuvant chemotherapy. To investigate whether SIP1/ZEB2 expression aids detection of patients at increased risk of recurrence in lymph node negative CRC, a multivariable logistic regression model containing conventional pathological and clinical risk factors was constructed, to identify independent variables. Clinical and pathological variables considered and subsequently incorporated into the multivariable model are listed in Table 8. In node negative disease the C-index for the prediction of distant recurrence and overall survival at 36 months were 0.83 (95% CI:0. 70 - 0.95) and 0.84 (95% CI: 0.78 - 0.90). The C-index improved from 0.80 to 0.83 with the addition of SIP1/ZEB2 to predict DR within 3 years **(Figure 35E)**, demonstrating that the addition of SIP1/ZEB2 expression to conventional risk factors in node-negative CRC increases the ability to identify patients at increased risk of disease recurrence.

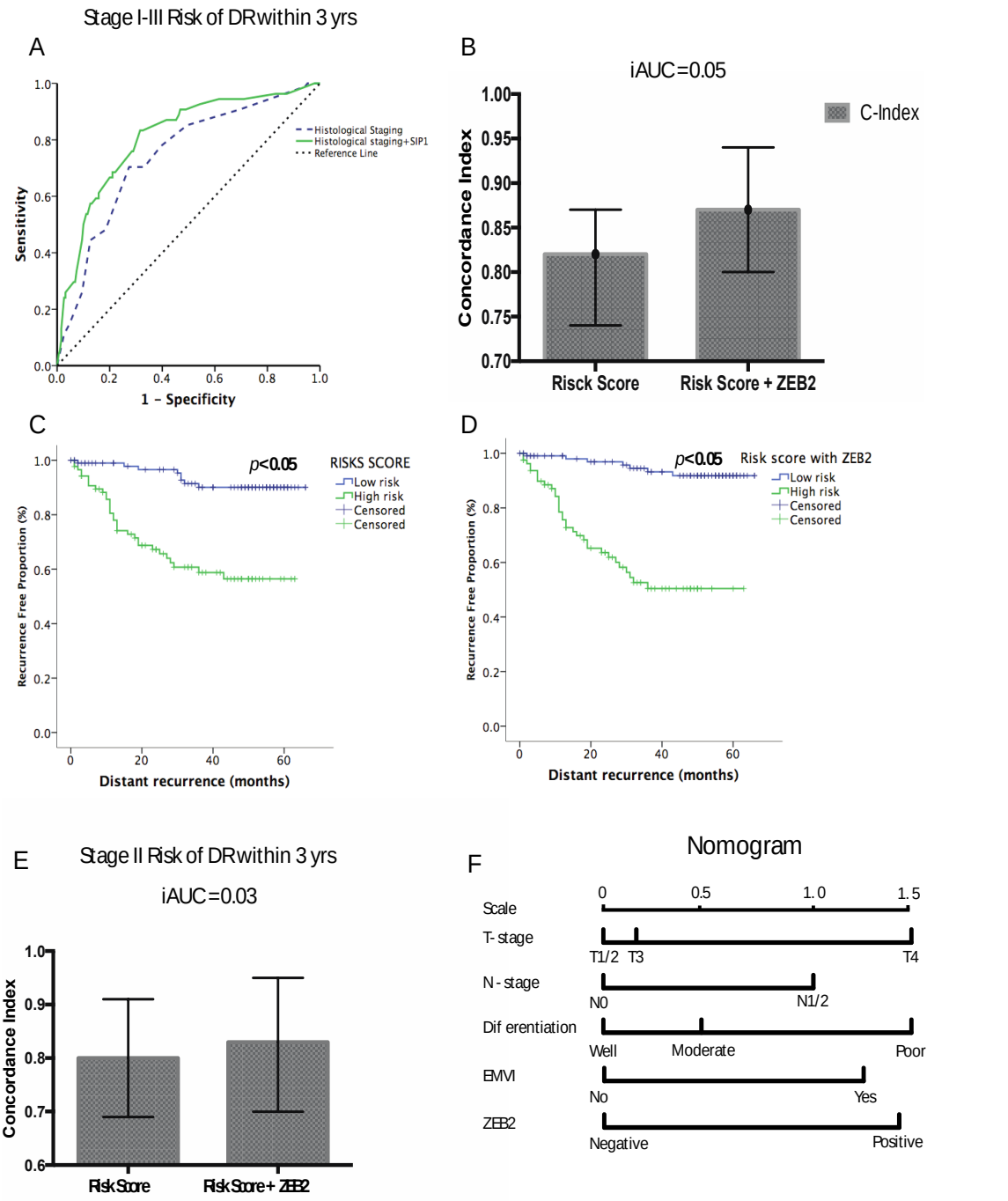

Figure 35: Addition of SIP1/ZEB2 to TNM staging system imporves ablity to idenity patients at high risk of early disease recurrence. (A/B) ROCcurves was generated with and withoud addition of SIP1/ZEB2 to TNM staginig system to demonstrate the imporvement in incremenatl area under the curve (iAUC). Green ROC curve is after the additon of SIP1/ZEB2 whilst the dotted blue line is the TNM staging crieteion only. Panel B highlights the imporvement in iAUC secondary to additon of SIP1/ZEB2 as a histogram. Confidence intervals (95% CI) are represented as error bars. (C/D) KM curves show an imporvement in stratification when SIP1/ZEB2 is addeded to the nomogram. Patients were stratified as either high risk or low based on scores that give equal weigting for sensitivity and specificty, Score of >1.2 was scored a high risk patient. (E) Histogram representing imporvement in incremenatl area under the curve (iAUC) in the subset of patients with node negative disease. (F) Visual representation of the histogram which was used to construct risk scores the predict risk of ditant recuurence in patients with CRC after surgery.

4.9 Results summary and discussion

Currently CRC is treated as a genetically homogenous disease. Despite the drive towards precision medicine, only KRAS mutational status has been approved as a negative predictive factor in patients treated with Cetuximab (339, 340). There are currently no molecular biomarkers in routine clinical use to stratify risk of recurrence after surgical resection of the primary tumour. In this study, we demonstrate that SIP1/ZEB2, an EMT inducing transcription factor expressed in mesenchymal cancer cells, predicts an increased risk of distant recurrence and reduced OS after curative surgery. Subset analysis of patients with node negative disease highlighted SIP1/ZEB2 as a biomarker with the ability to predict recurrence independent of stage. Addition of SIP1/ZEB2 to nomograms encompassing conventional pathological risk factors improved the predictive capacity to identify patients at high risk of recurrence. These results if validated in a prospective clinical trial will accelerate clinical application of SIP1/ZEB2 as a biomarker, to identify patients at high risk of recurrence.

EMT is thought to be a critical event in cancer metastasis (44, 52). The association between EMT, down regulation of epithelial adhesion molecules (57), modulation of the extracellular matrix to promote invasion (341) and cytoskeletal alterations that increase motility (57) have been reported in *in vitro* models. Consequently, it can be postulated that biomarkers detecting features of an EMT phenotype in the primary tumour may aid in identifying patients at high risk of recurrence due to increased probability of these patients harbouring occult micro-metastases that are undetectable by current imaging modalities. E-cadherin down regulation is a cardinal feature of EMT and has been extensively investigated as a biomarker (266-268). However, studies proposing the use of E-cadherin have reported conflicting results (43). Factors contributing towards these inconsistencies include, variations in methodology, biomarker scoring, data analysis and reporting standards (104).

A further layer of complexity has been introduced by the concept of cellular plasticity (49). It recent years it has been proposed cancer cells can transition into an intermediary phenotype during which they may simultaneously express both epithelial and mesenchymal features (53). An analysis of 43 ovarian cancer cells revealed co-expression of Vimentin and N-cadherin only occurred in 50% of cases (129). Thus defining mesenchymal phenotype solely based on expression or repression of a single adhesion molecules, may bias scoring systems and make identification of fully de-differentiated mesenchymal cancer cells challenging. Gaining a global consensus on adhesion molecule expression profile of cancer cells belonging to an intermediary transition states, using *in vitro* models and further tissue specimen analysis is required before application in the clinical setting is feasible.

Transcription factors that belong to the Twist, SNAIL and Zinc finger enhancer binding (ZEB) families are known to induce EMT (145). Of the above transcription factors ZEB proteins and their potential role as a biomarker has been sparsely studied in the setting of CRC. Further, there have been no studies that have validated their findings on an independent patient cohort, making transition to a clinical trial challenging. Kahlert et al previously reported cytoplasmic expression of SIP1/ZEB2 at the invasive front of primary CRC's prognosticated for poor cancer specific survival (65). However, nuclear expression of SIP1/ZEB2, the ability to differentiate local from distant recurrence, applicability in node negative disease and predictive capacity to identify patients at high risk of distant recurrence was not considered. Our scoring system emphasised the importance of nuclear positivity, as SIP1/ZEB2 proteins modulate gene expression through epigenetic regulation in the nucleus (324). Thus, nuclear expression may more accurately denote activation of EMT pathways and improve identification of mesenchymal CRC cells.

A large-scale consortium of leading scientist within the colorectal field have recently highlighted the importance of identifying tumours expressing a mesenchymal phenotype (33). Cumulative analysis of six independent cohorts by genomic subtyping studies reported that patients with tumours expressing a mesenchymal gene profile were

repeatedly found to have a worse prognosis and increased risk of distant recurrence (42, 272, 273, 275, 276, 342). These findings are consistent with oncological outcomes observed in patients expressing SIP1/ZEB2 in our cohort. A major advantage to using SIP1/ZEB2 to identify mesenchymal cancer cells is its non-dependence on specialised genetic testing. IHC is routinely performed in all clinical pathology laboratories and therefore readily translated into routine clinical practice, without the need for specialist and expensive molecular profiling platforms. Further, most gene expression platforms quantify mRNA expression and transcriptional changes. *In vitro* studies have however proven beyond doubt that EMT is highly regulated by microRNA's; consequently mRNA expression does not automatically result in protein expression and activation of EMT pathways therefore cannot be assumed based on transcriptional changes only (67). A further limitation of polymerase chain reaction (PCR) based assays relates to tumour sampling. EMT often occurs in a subset of cancer cells within a solid tumour (51). Therefore, quantifying the gene expression profile by sampling a small area of the tumour may fail to be representative of the true genetic heterogeneity of the sample. This limitation can be significantly reduced by analysis of multiple section of a single tumour by IHC.

A recognised feature of EMT is the acquisition of chemoresistance to compounds routinely used in clinical practice (66, 107). Gupta and co-workers reported breast cancer cells that had undergone EMT acquired apoptosis resistance to most conventional chemotherapeutic agents used in a drug screen (115). Patients with tumours that express a gene profile signature suggesting activation of EMT pathways acquired limited benefit from conventional chemotherapeutic strategies and expressed selective sensitivity to certain targeted agents (42). Therefore, detection of a mesenchymal gene expression profile or SIP1/ZEB2 expression not only prognosticates recurrence risk, but may also predict response to chemotherapeutic agents routinely used in the adjuvant setting. Although agents with specific toxicity to mesenchymal CRC cells are yet to be validated in prospective clinical trials, its is likely that biomarkers such as SIP1/ZEB2 may guide

identification of high risk patients and subsequently aid in selecting compounds from which patients will derive maximum benefit in future years.

In this study, we demonstrate using a training and validation cohort that nuclear SIP1/ZEB2 expression in CRC prognosticates for a high risk of relapse with specificity to distant recurrence after curative surgery. Subgroup analysis of patients with node negative disease identified SIP1/ZEB2 as an independent prognostic marker of early recurrence and reduced survival. Addition of SIP1/ZEB2 expression status to nomograms composed of conventional pathological risk factors improved the ability to identify patients at higher risk of recurrence. Recent large-scale gene profile analysis, have proven beyond doubt the importance of identifying tumours that belong to the mesenchymal subtype, due to their consistent association with distant recurrence and resistance to conventional chemotherapeutic agents (33). Detection of SIP1/ZEB2 expression by IHC simplifies the process of detecting these mesenchymal tumours and could aid in development of an easily translatable IHC assay to identify mesenchymal CRC cells. In future years, simplifying CRC subtyping akin to the four-biomarker panel (ER, PR, HER2 and Ki67) used to classify breast cancer could aid improvements in risk stratification and guide administration of treatment strategies from which patients will derive maximal benefit(343, 344)

Chapter 5: SIP1/ZEB2 induced EMT and drives chemoresistance activating nucleotide excision repair in colorectal cancer.

Disease progression and recurrence are the principle causes of death in colorectal cancer and occurs in up to 30% at presentation and subsequently develop in 50% after curative surgery (2, 3). The majority of patients with recurrent disease are incurable and experience a median survival of less than 3 years, even with the latest chemotherapy and targeted biological agents (345). Surgical resection combined with DNA damaging agents such as 5-flurouracil (5-FU), irinotecan and oxaliplatin based chemotherapeutic strategies (FOLFOX or FOLFIRI), with or without addition of biological agents remains the standard of care in patients with high-risk stage II and advanced disease. Majority of patients, however, fail to respond to treatment, and can suffer toxic side effects without therapeutic benefit (346). Despite the drive towards personalised care in recent years the only biomarker in standard clinical use is KRAS mutation status, which predicts response to EGFR inhibitors such as Cetuximab (274). Nevertheless, this example provides proof-of-principle that a mechanistic understanding of CRC biology can be translated to improved patient outcomes in the clinical setting and highlights the pressing requirement for the identification of new markers predictive of therapy response.

The association between EMT, poor oncological outcomes and treatment resistance has been highlighted in many solid tumours (347). Earlier studies described a link between drug resistance and EMT by incubating epithelial carcinoma cells with DNA damaging agents for extended periods and reporting the mesenchymal morphology of the selected (chemo-resistant) CRC cells (117). In line with these *in vitro* observations, molecular stratification of CRC patients revealed patients displaying a mesenchymal gene expression pattern respond poorly to adjuvant chemotherapy, experience earlier recurrence and reduced survival (33) (42). Despite these compelling observations, the cellular mechanisms driving EMT induced chemoresistance are poorly understood. Increased drug efflux, improved DNA repair, rewiring of cellular signalling, attenuated

DNA damage response and pro-apoptotic signalling have thus far been suggested as contributing factors (53, 66, 127, 347).

The ZEB family of transcription factors comprises of two genes, *ZEB1* and SIP1/ZEB2, which have thus far been sparsely studied in CRC and in the context of chemotherapy response. Here we report, nuclear SIP1/ZEB2 immuno-expression as a marker of poor response to adjuvant FOLFOX chemotherapy. In Chapter 3 I demonstrated, CRC cells expressing SIP1/ZEB2 undergo EMT and became resistant to oxaliplatin and 5-FU; compounds administered in the FOLFOX regime to treat CRC patients. In this chapter I demonstrate, critical components of the nucleotide excision repair (NER) pathway, such as ERCC1, are induced upon SIP1/ZEB2 expression. High ERCC1 abundance in CRC cells enhanced kinetics of oxaliplatin induced DNA crosslink clearance, thus promoting DNA repair and resistance to apoptosis both *in vitro* and *in vivo.* Taken together, these findings identify the mechanism of SIP1/ZEB2 induced chemoresistance, and suggest nuclear SIP1/ZEB2 may have clinical utility in predicting recurrence and response to oxaliplatin- based chemotherapy regimes in CRC.

5.1 Nuclear SIP1/ZEB2 expression associates with poor response to FOLFOX chemotherapy

Dr Sayan group previously published SIP1/ZEB2 overexpression induces resistance to DNA damage induced apoptosis (66). To investigate if this *in vitro* feature translates to poor survival in CRC patients, IHC for SIP1/ZEB2 and survival analysis were performed on a pilot cohort of 34 consecutive patients who received the FOLFOX chemotherapy regimen after surgical resection of primary CRC between 2005 and 2006. SIP1/ZEB2 scoring was performed using previously established criteria (66, 348). Nuclear SIP1/ZEB2 was not detectable in normal colonic epithelium whereas more than 70% (24/34) of the CRC specimens registered SIP1/ZEB2 positive **(Figure 36A)**. Survival analysis demonstrated a reduction in mean Overall Survival (OS) of 15.6 months and Disease Free Survival (DFS) of 19.5 months if SIP1/ZEB2 is expressed. However, these differences did not reach statistical significance **(Figure 36B).** Based on this data, a power calculation

was undertaken to exclude the possibility of a type 2 error. We identified a minimum cohort size of 86 patients and 24 events as a requirement to achieve 80% power using a two-sided test, at a significance of 5%, and assuming a hazard ration of 3.0. Consequently, a validation cohort consisting of 99 further consecutive patients matching the previous inclusion/exclusion criteria (Appendix : Table 21)were identified and analysed. A 15.9-month reduction in mean OS (log rank, *p* <0.002) and 19.5 month reduction in mean DFS (log rank, *p* <0.002) was observed in patients with SIP1/ZEB2 positive tumours when compared to SIP1/ZEB2 negative **(Figure 36C)**. These results, for the first time, strongly demonstrate SIP1/ZEB2 positive patients that received FOLFOX adjuvant chemotherapy experienced a poor response, indicated by reduced survival and increased recurrence rates. Association of clinico-pathalogical variables with SIP1/ZEB2 and patient demographics are listed in tables 10 and 11 in compliance with REMARK biomarker reporting guidelines (349). Multivariable Cox-regression analysis highlighted SIP1/ZEB2 as an independent prognostic marker of OS (HR 3.13, 95% CI 1.59 -6.16, *p*=0.001) and DFS (HR 3.12, 95% CI 1.53 -6.65, *p*=0.002 **Tables15, 16**).

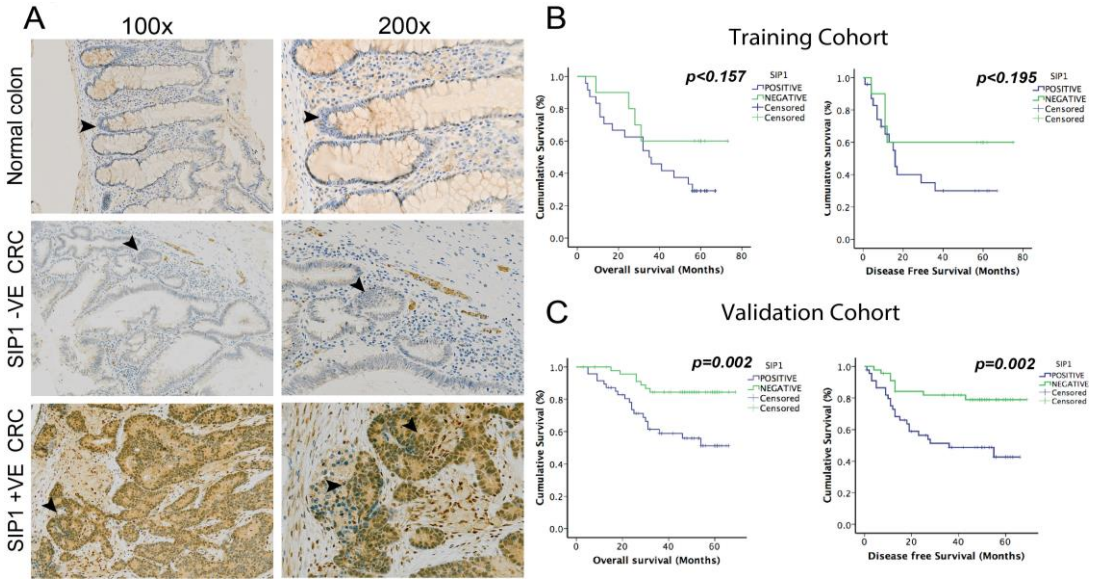

Figure 36: **SIP1/ZEB2 expression in normal colon and CRC. (A)** Normal colon, SIP1/ZEB2 negative (-VE) CRC and positive (+VE) CRC staining. Normal colonic cells and SIP-VE CRC registered no positive staining other than occasional stromal cells, whereas strong nuclear staining was observed in SIP+VE tumours as marked by arrows. Kaplan-Meier curves displaying overall survival (OS) and disease free survival (DFS) in accordance with nuclear SIP1/ZEB2 expression (Blue = SIP1/ZEB2 +VE, Green = SIP1/ZEB2 -VE) of patients in the pilot study **(B)** and validation cohort **(C)**. Nuclear SIP1/ZEB2 expression associated with reduced OS and DFS in the validation cohort (log rank, *p*<0.002).

Table 13: Clinical and pathological parameters of patients in the pilot and validation study.

	Pilot study		Validation study	
	n	**%**	**n**	**%**
Age (Yrs)				
<60	2	5.8	24	24.3
>60	32	94.6	75	75.8
Sex				
Male	16	47.0	53.5	53.5
Female	18	53.0	46.5	46.5
Site of tumours				
Right	15	44.1	34	34.3
Left	15	44.1	34	34.3
Rectum	4	22.8	30	30.3
Missing	0	0	1	1
Differentiation				
Well	0	0.0	3	3.0
Moderate-well	14	41.2	54	54.5
Moderate	11	32.4	27	27.2
Moderate-poor	2	5.9	4	4.0
Poor	7	20.6	10	10.1
Missing	0	0	1	1
Stage				
Stage 1	0	0	0	0
Stage 2	11	41.7	44	44.2
Stage 3	23	58.3	54	54.5
Stage 4	0	0	0	0
Missing	0	0	1	1
T-stage				
T1	0	0	0	0
T2	0	2.8	10	10.1
T3	14	41.2	50	50.5
T4	20	58.8	38	38.3
Missing	0	0	1	0
N-Positivity				
N0	11	41.7	44	44.5
N1	23	58.3	55	55.5
Missing	0	0	0	0
SIP1 Positive				
Yes	24	53.8	49	49.5
No	10	47.2	50	50.5

Table 14: Clinical and pathological parameters of patients in the pilot and validation study and their association with nuclear SIP1 expression. *p*-values were derived by using Chi squared or fishers exact test as appropriate.

	Pilot study			Validation cohort		
Characteristics	**SIP1+VE**	**SIP1-VE**	***p-value***	**SIP1+VE**	**SIP1-VE**	***p-value***
Age						
<60	1	1	***p=0.51***	14	10	***p=0.60***
>60	23	9		36	39	
Sex						
M	10	6	***p=0.46***	24	29	***p=0.40***
F	14	4		25	21	
pT-stage						
T1	0	0	***p=0.15***	0	0	***p=0.30***
T2	0	0		5	5	
T3	8	6		27	23	
T4	16	4		18	21	
pN status						
N0	8	3	***p=0.85***	19	25	***p=0.30***
N1/N2	16	7		30	25	
AJCC Stage						
1	0	0	***p=0.17***	0	0	***p=0.25***
2	8	3		18	26	
3	16	7		31	23	
4	0	0		0	0	
Differentiation						
Well	0	0	***p=0.64***	2	1	***p=0.84***
Mod-well	10	4		26	28	
Moderate	9	2		13	14	
Mod-poor	1	1		3	1	
Poor	4	3		5	5	

Table 15: Multivariate analysis (Cox proportional hazard regression model) of prognostic parameters for overall survival in colorectal cancer patients that received adjuvant FOLFOX therapy.

Characteristic	HR	95% CI	*p* - value
Age (<60 vs. >60)	1.2	0.48 – 3.24	0.66
T-stage (Overall)			0.01
T stage (T1/2 vs. T4)	7.01	1.60 – 30.89	0.01
T stage (T3 vs. T4)	3.10	0.69 – 13.67	0.15
N-stage (N0 vs. N1/2)	2.10	1.60 – 6.17	0.03
Differentiation			0.18
Differentiation (Well vs. Poor)	1.29	0.58 – 2.85	0.537
Differentiation (Mod vs. Poor)	1.04	0.23 – 1.63	0.33
SIP1 Status (pos vs. neg)	3.13	1.59 - 6.16	0.001

Table 16: Multivariate analysis (Cox proportional hazard regression model) of prognostic parameters for disease free survival (DFS) in colorectal cancer patients that received adjuvant FOLFOX therapy.

Characteristic	HR	95% CI	*p* - value
Age (<60 vs. >60)	1.91	0.738 – 4.98	0.19
T-stage (Overall)			0.006
T stage (T1/2 vs. T4)	7.03	1.53 – 32.25	0.01
T stage (T3 vs. T4)	2.29	0.50- 10.50	0.29
N-stage (N0 vs. N1/2)	2.04	1.02 – 4.12	0.05
Differentiation			0.19
Differentiation (Well vs. Poor)	0.97	0.430 -2.16	0.92
Differentiation (Mod vs. Poor)	0.46	0.17 – 1.23	0.12
SIP1 Status (pos vs. neg)	3.12	1.53 – 6.65	0.002

5.2 SIP1/ZEB2 expression is maintained in a sub-population of cells in CRC liver metastasis.

The above data suggest SIP1/ZEB2 expression in primary CRC increases risk of recurrence after treatment with FOLFOX therapy. This may be due to SIP1/ZEB2 promoting chemoresistance in occult micro-metastases as previously shown using *in vitro* models (66). Canonical models of metastasis have proposed a requirement to down regulate EMT inducing transcription factors (EMT-TF's), such as SIP1/ZEB2, and revert back to epithelial morphology (mesenchymal to epithelial transition, MET) for successful distant colonisation (44). It is also well known that the plastic/stem-cell nature of metastatic cells at the distant site can define chemotherapy response and prognosis

(reviewed in (350). However, SIP1/ZEB2 protein expression in CRC metastases remains unexplored; therefore it is not clear if SIP1/ZEB2 may directly promote chemoresistance in distant metastatic foci. To investigate if SIP1/ZEB2 expression persists in distant metastasis, we investigated 30-paired samples from patients that underwent a surgical resection for primary CRC and synchronous/metachronous liver metastasis. Clinical and pathological variables of this cohort are presented in **Table 17**. Nuclear SIP1/ZEB2 was observed in 87% (26/30) of the primary CRC tumors and 83% (25/30) of the paired liver metastases. More than 96% (25/26) of SIP1/ZEB2 positive primary tumors also stained positive for SIP1/ZEB2 in their corresponding liver metastases. No SIP1/ZEB2 negative primary tumor exhibited SIP1/ZEB2 in the recurrence. This data suggests SIP1/ZEB2 expression can persist at the metastatic foci. The intrinsic chemoresistance properties of SIP1/ZEB2 expressing mesenchymal cancer cells may result in the reduced survival observed in patients administered adjuvant FOLFOX therapy.

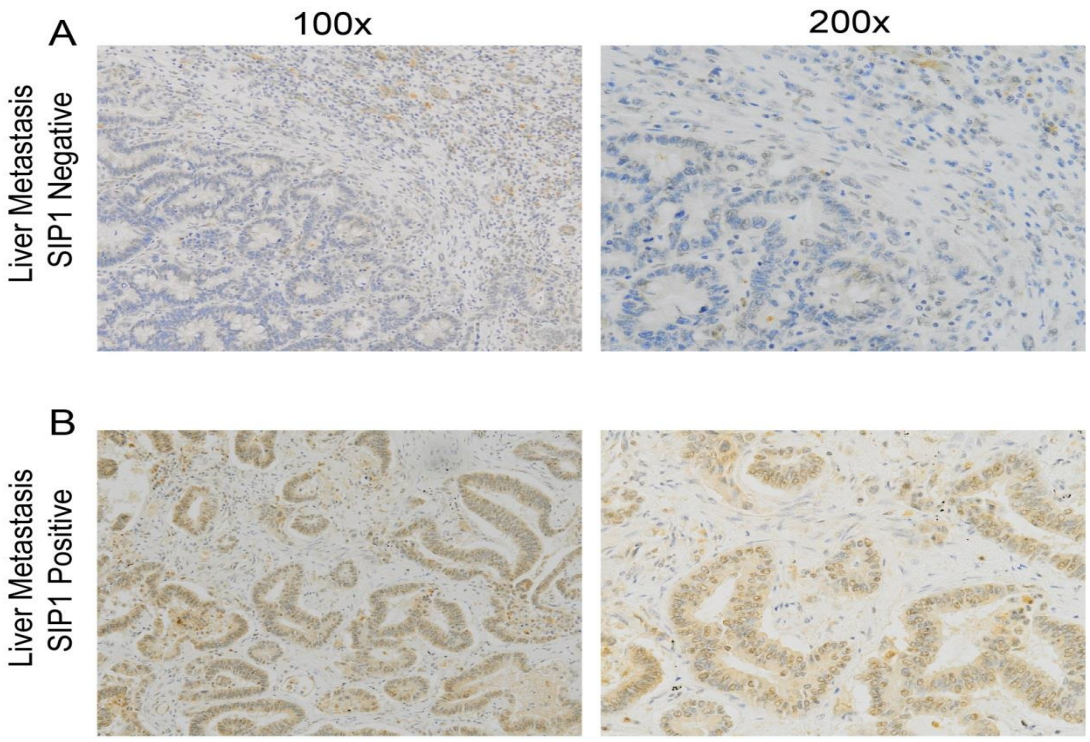

Figure 37: SIP1/ZEB2 expression in CRC liver metastasis. SIP1/ZEB2 expression in CRC-liver metastasis. SIP1/ZEB2 expression is analyzed in a cohort of CRC 30 patients with synchronous/metachronous metastasis as paired with their primary tumour. Both negative (A) and positive nuclear SIP1/ZEB2 (B) have been observed.

Table 17:Clinical and pathological parameters of patients with primary colorectal cancer and matched colorectal liver metastasis.

	n	%
Age (Yrs)		
<60	8	26.7
>60	22	73.3
Site of tumour		
Colon	14	46.7
Rectum	16	53.3
pT stage		
1	0	0
2	3	10
3	21	70
4	6	20
pN-Positivity		
N0	12	40
N1/2	18	60
Metastasis at presentation		
MO	12	40
M1	18	60
Stage		
Stage 1	0	0
Stage 2	4	13.3
Stage 3	8	26.7
Stage 4	18	60
Synchronous vs. metachronous		
Synchronous	12	40
Metachronous	18	60
Differentiation		
Well	0	0
Moderate-well	9	30
Moderate	18	60
Moderate-poor	0	0
Poor	1	3.3
Missing	2	6.7
Neo Adjuvant Chemotherapy		
Yes	11	63.3
No	19	36.6
SIP1 Positive primary		
Yes	26	86.6
No	4	13.4
SIP1 positive Liver metastasis		
Yes	25	83.3
No	5	16.7

5.3 SIP1/ZEB2 induced EMT up-regulates expression of multiple components of Nucleotide Excision Repair pathway.

A striking feature of the above data is the association of SIP1/ZEB2 with chemotherapy resistance, disease recurrence and reduced survival. EMT has been associated with chemoresistance in previous studies, however the mechanism remains unclear. We previously reported that SIP1/ZEB2-induced EMT attenuates DNA damage response upstream of ATM/ATR activation (66). A potential explanation of this observation could be improved DNA repair capacity in SIP1/ZEB2-expressing carcinoma cells. A qPCR array, with a focus on DNA damage response, performed on two SIP1/ZEB2 inducible cell line models (A431-SIP1 and DLD-SIP1), highlighted increased expression of multiple components of the nucleotide excision repair (NER) pathway **(Figure 38)**. NER is responsible for removal of DNA adducts generated by UV mimetic (e.g. mitomycin C) or platinum-based chemotherapeutic agents (351). Efficient removal of oxaliplatin induced DNA crosslinks via NER, therefore, may represent a survival strategy that could be adopted by mesenchymal CRC cells to combat DNA damage induced cell death (321). Among the up-regulated genes, Excision Repair Cross Complementation group 1 (ERCC1) demonstrated a 2.5 fold increase after SIP1/ZEB2 induced EMT both in RNA and protein level **(Figure 39A)**.

ERCC1 forms a heterodimer with XPF (ERCC4) and acts as part of the 5'-endonuclease complex during nucleotide excision and double strand break (DSB) repair (352). Deficiency of any component of the NER machinery renders cells sensitive to DNA crosslinking agents, however ERCC1 heterozygosity/loss produces the most prominent DNA repair deficient phenotype (351). ERCC1 expression has been investigated in several clinical trials as a predictive biomarker of platinum resistance with conflicting results (353). Consequently, we probed whether full length ERCC1 (ERCC1-202, 891 nucleotides) overexpression is associated with EMT status of CRC. We found strikingly higher ERCC1 levels in CRC cell lines expressing low/no E-Cadherin **(Figure 39B)**. This observation was extended to the CCLE cohort of Geneatlas database where 41 CRC cell lines are present (354). *ERCC1* expression was highest when epithelial genes such as

CDH1, *mIR200b* or *PKP3* were low or mesenchymal genes such as *SIP1/ZEB2, SNAIL2(SLUG)* or *vimentin* were high **(Figure 39C)**. These observations suggest ERCC1 overexpression and enhanced NER capacity may be the underlying mechanism of oxaliplatin resistance of metastatic CRC cells.

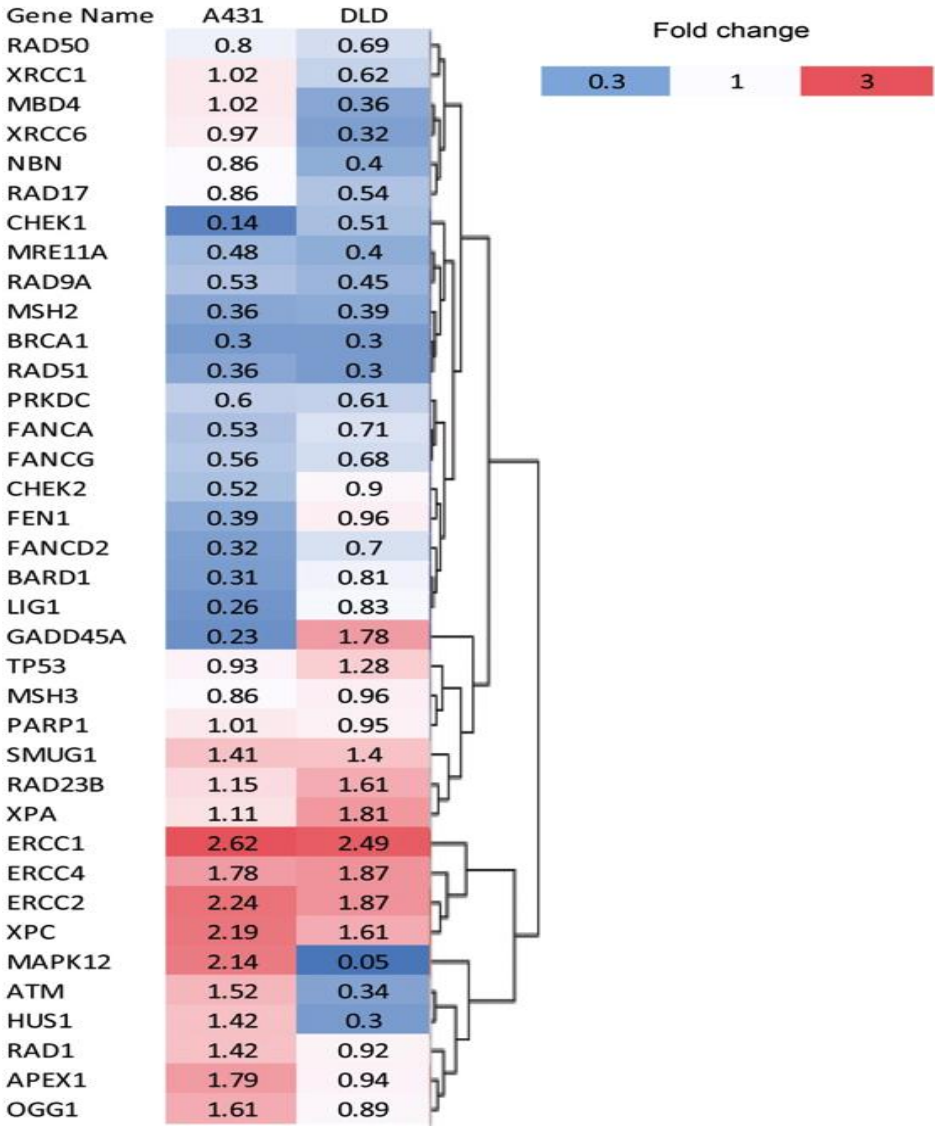

Figure 38: SIP1/ZEB2 expression up-regulates expression of multiple genes involved in the nucleotide excision repair (NER) pathway. SIP1/ZEB2 inducible A431 and DLD cells were subjected to a qPCR array with the focus on DNA damage response/repair. The genes that show significant increase/decrease ($p<0.05$ as calculated by student *t* test) were presented as heat map. Note multiple genes implicated in NER pathway (ERCC1, ERCC4, ERCC2, XPA and XPC) were clustered (indicating a similar trend in regulation) and up regulated in both cell lines upon SIP1/ZEB2 induction.

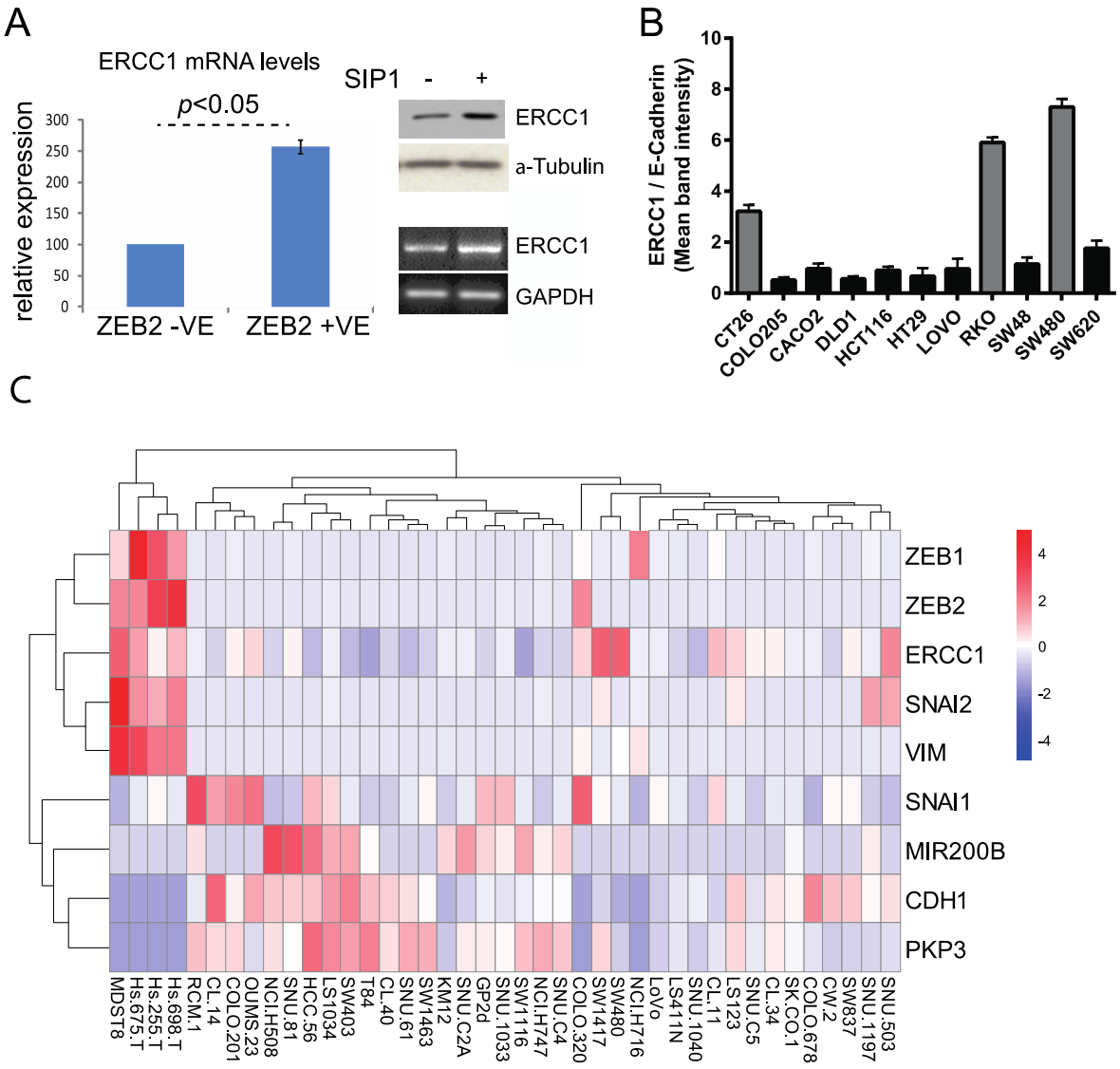

Figure 39: SIP1/ZEB2 regulates ERCC1 expression. (A) SIP1/ZEB2 induction increased ERCC1 expression as assessed by qPCR, RT-PCR (ERCC1-202 form, full length ERCC1) and western blotting (37kDa, full length form). **(B)** ERCC1 expression is associated with EMT status of CRC cell lines. The ratio of ERCC1-202/CDH1 expression was plotted according to quantification of bands from 3 independent RT-PCR experiments. Mesenchymal CRC cell lines CT26, RKO and SW480 displayed the highest ERCC1 and lowest CDH1 expression. (C)The CRC cell lines in the CCLE cohort of Geneatlas database were probed for epithelial (MIR200B, E-Cadherin (*CDH1*), Plakophilin 3 (*PKP3*) and mesenchymal (Vimentin (*VIM*), *ZEB1*, SIP1/*ZEB2*, *SNAI1*, *SNAI2*) genes to observe correlation with *ERCC1* expression. ERCC1 is abundantly expressed when *CDH1* or *PKP3* were low and when *VIM*, *ZEB1*, SIP1/*ZEB2* or *SNAIL2* were high. Four out of 6 High ERCC1 expressing CRC cell lines were also positive for SIP1/ZEB2 or SNAIL2. These results suggest ERCC1 expression is induced when CRC cells undergo EMT.

5.4 SIP1/ZEB2 directly binds to E-boxes in the promoter region of the ERCC1 gene to induce gene expression

Due to the positive correlation observed between SIP1/ZEB2 and ERCC1 expression we hypothesised SIP1/ZEB2 directly controls ERCC1 transcription. An earlier study had reported the presence of several E-Boxes, the DNA motif that SIP1/ZEB2 binds, in *ERCC1* promoter (321). Our extended *in silico* analysis identified eight E-box elements in the 2kb regulatory region encompassing the promoter and the first exon of *ERCC1* gene **(Figure 40A)**. We, therefore, cloned *ERCC1* promoter into PGL3 vector as two segments (ERCC1-lucA and ERCC1-lucB, **Figure 40B**). A significant increase in luciferase signal was detected after SIP1/ZEB2 expression in DLD-ZEB2 cells transfected with segments A or B containing E-Boxes 4-8 **(Figure 40C)**. Luciferase activity reduced as the number of E-boxes in the cloned segment decreased suggesting interaction of SIP1/ZEB2 with E-boxes in the promoter contributes to increased gene expression. Due to possible complications in analysing reporter activity in transcribed regions of ERCC1, we performed chromatin immunoprecipitation (ChIP) to analyse SIP1/ZEB2 binding to E-Boxes 1-3. We found interaction of SIP1/ZEB2 with both *ERCC1* and *CDH1* (Positive control) transcriptional regulatory regions and the functional effect of this binding has been demonstrated by alterations of RNA pol II presence on these promoters **(Figure 40C)**. These results demonstrate that SIP1/ZEB2 directly binds to *ERCC1* promoter and up regulates its expression.

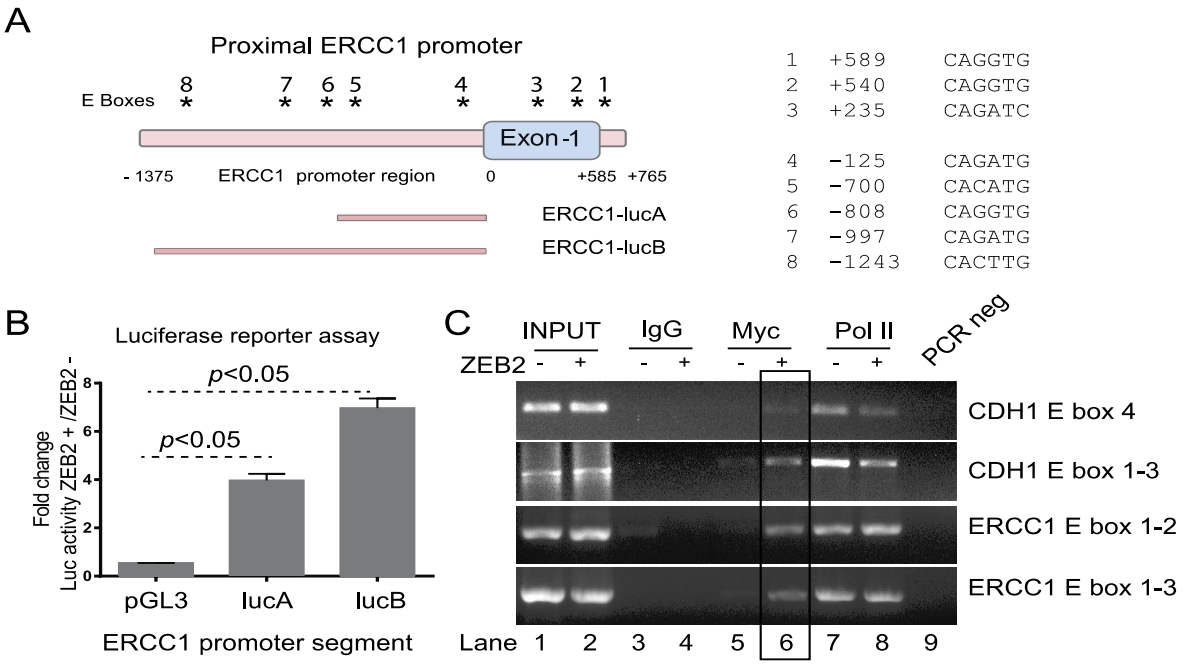

Figure 40: SIP1/ZEB2 directly binds to E-boxes in the promoter of ERCC1. **(A)** Scheme of potential SIP1/ZEB2 binding sites (E-boxes, CANNTG) on the left and sequence presented on the right in relation to ERCC1 transcription start site marked as "0". **(B)** Luciferase reporter assay of segments A and B of ERCC1 promoter as measured in un-induced and induced DLD-SIP1 cells. **(C)** SIP1/ZEB2 binds to regulatory regions of ERCC1. Exogenous SIP1/ZEB2 was immuno-precipitated by tag (myc) antibody; negative control IgG and RNA Pol II were used as controls. SIP1/ZEB2 enrichment was detected at both ERCC1 and CDH1 (SIP1/ZEB2 binding positive control) regulatory regions (lane 6 highlighted by a box as compared to lane 5). SIP1/ZEB2 repression of *CDH1* was evident as Pol II binding to *CDH1* promoter decreased (lane 8).

5.5 ERCC1 overexpressing CRC cells register less DNA damage, attenuated DNA damage response, reduced apoptosis signalling and enhanced resistance to oxaliplatin.

We next aimed to study if ERCC1 is the main effector of oxaliplatin resistance in SIP1/ZEB2 expressing CRC cells. Wild type (epithelial) DLD-1 cells were transfected with mCherry-ERCC1 or mCherry alone (control) to create stable cell lines. Two clones expressing differing levels of ERCC1 were selected to dissect the contribution of ERCC1 overexpression to oxaliplatin resistance. Both control (DLD-C1 and DLD-C2) and ERCC1 overexpressing clones (DLD-E1 and E2) were E-Cadherin-positive and retained epithelial features of parental DLD-1 cells **(Figure 41A)**. Despite the epithelial phenotype, DLD-E1 and E2 exhibited up to 10 fold increased resistance to oxaliplatin treatment as determined by viability assays **(Figure 41B)**. DLD-E1 and E2 also exhibited resistance to apoptosis (reduced PARP cleavage) and attenuated γH2AX phosphorylation (marker of DNA damage) after treatment with increasing concentrations of oxaliplatin, when compared to

controls **(Figure 41C)**. To investigate if mesenchymal CRC cell lines become sensitive to oxaliplatin via high ERCC1 expression we knocked down ERCC1 in RKO and SW480 cells which showed the highest ERCC1/CDH1 ratio **(Figure 39B)**. Decreased ERCC1 expression sensitised both cell lines to oxaliplatin-induced apoptosis **(Figure 42A)**. A possible explanation of these observations is ERCC1 overexpressing cells possess enhanced DNA repair capacity to oxaliplatin induced DNA damage. Improved repair capacity may in turn result in reduced DNA damage signalling and apoptosis. To investigate if ERCC1 facilitates resistance to other chemotherapeutic agents that cause alternative types of DNA damage, ERCC1 over-expressing and control cells were treated with doxorubicin and 5-FU. Extent of apoptosis assessed by PARP cleavage revealed no difference in the magnitude of cell death when compared to controls **(Figure 42B)** suggesting ERCC1 plays a key role in regulating oxaliplatin induced DNA repair.

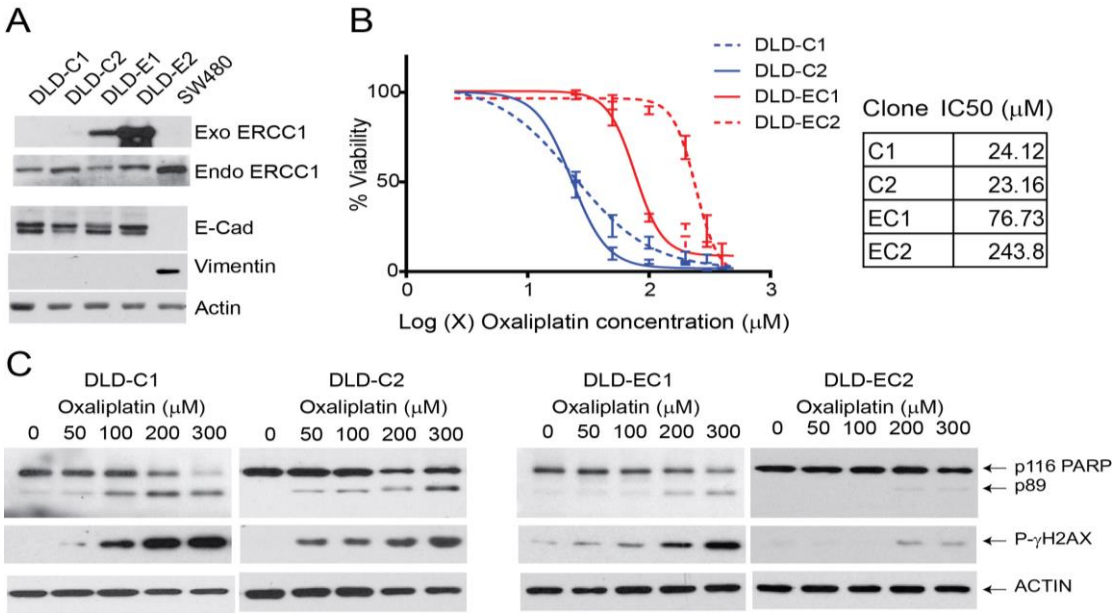

Figure 41: ERCC1 induces oxaliplatin resistance. (A) ERCC1 expression in relation to EMT status (E-cadherin and vimentin expression) is shown. Both control (DLD-C1 and C2) and ERCC1 expressing clones (DLD-EC1 and EC2) retained epithelial identity. SW480 cells were used as a positive control for mesenchymal features (Reduced/no E-cadherin, increased vimentin and high ERCC1). Exogenous (mCherry tagged, 67kDa) and endogenous (37kDa) ERCC1 are presented separately because of size difference. **(B)** Viability assay for control and ERCC1 clones showed increased IC50 values and stratification for chemoresistance according to ERCC1 protein abundance. **(C)** ERCC1 clones were treated with increasing concentrations of oxaliplatin. PARP cleavage (presence of p89 PARP) and increased γH2AX phosphorylation were assessed to determine apoptosis and DNA damage response pathway activation. DLD-EC1 and EC2 showed reduced pro-apoptotic signaling as compared to DLD-C1 and C2

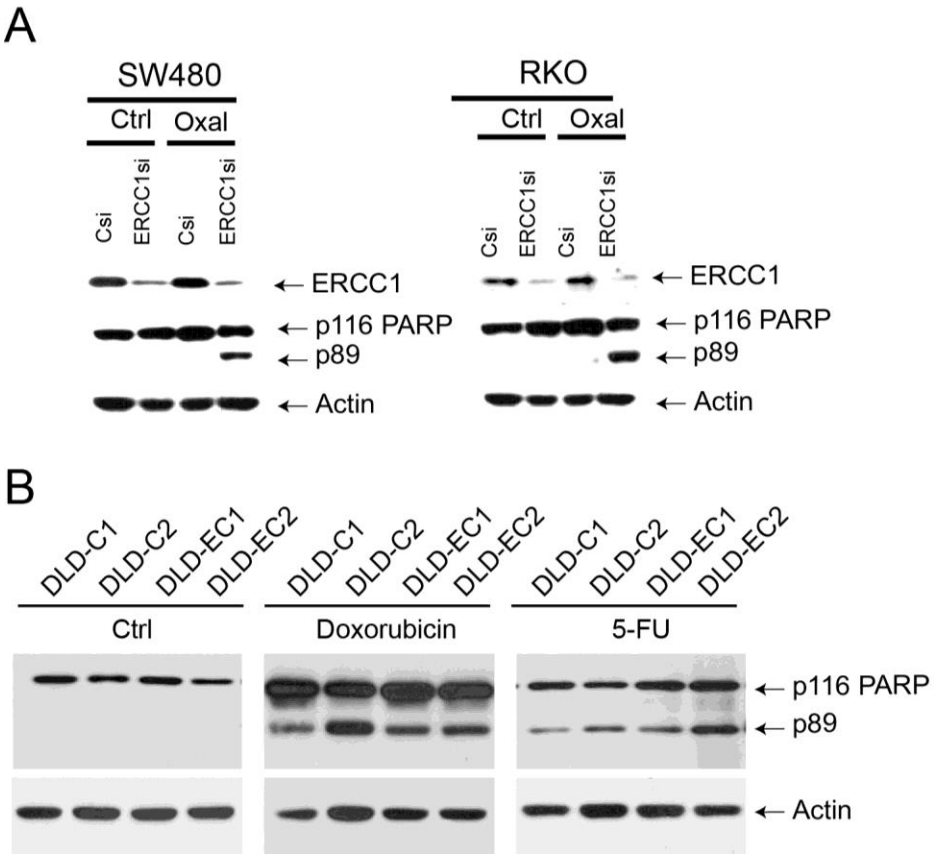

Figure 42: ERCC1 knockdown sensitises mesenchymal CRC cells to Oxaliplatin. (A) ERCC1 was knocked down in mesenchymal CRC cell lines SW480 and RKO and these cells were treated with 100mM oxaliplatin for 24h. Control siRNA transfected cells no apoptotic response however ERCC1 down regulation (ERCC1si) induced significant cell death, as assessed by PARP cleavage (p89 PARP). (B) Control (C1 and C2) and ERCC1 overexpressing (EC1, EC2) DLD cells were incubated with chemotherapeutic agents (doxorubicin or 5-FU). All clones, overexpressing, ERCC1 or controls mCherry transfected ERCC1 cell, died at a similar magnitude as shown by PARP cleavage (p89 PARP).

5.6 Efficient repair of oxaliplatin induced DNA crosslinks is due to ERCC1 overexpression.

Next we investigated if ERCC1 enhances apoptosis resistance due to enhanced NER capacity. The platinum adduct antibody (ICR4) was used to detect DNA damage and quantify repair after oxaliplatin treatment. ERCC1 overexpressing cells registered lower DNA damage at all doses tested as compared to controls **(Figure 43A)**. Further, DLD-EC1 and EC2 cells exhibited enhanced repair kinetics. A one hour oxaliplatin treatment and twelve hours recovery revealed the kinetics of DNA repair correlated with ERCC1 protein abundance, with the highest ERCC1 expresser's exhibiting the fastest repair capacity **(Figure 43B)**. The same pattern of enhanced DNA repair was also observed in SIP1/ZEB2 induced DLD-SIP1 cells as compared to uninduced counterpart **(Figure 43C)**.

The above evidence suggests SIP1/ZEB2-induced ERCC1 enhances DNA repair capacity of CRC cells and consequently may promote an apoptosis-resistance phenotype in CRC patients treated with oxaliplatin containing combination chemotherapy.

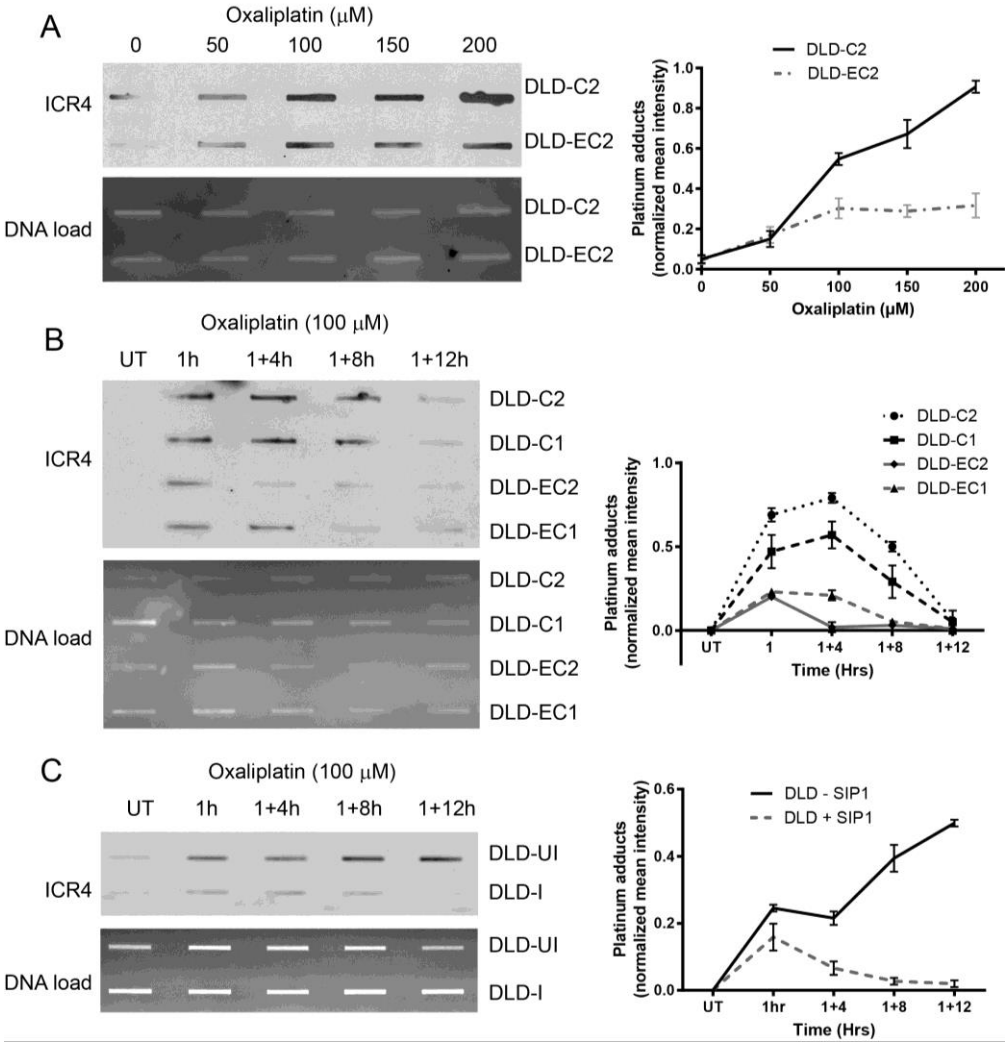

Figure 43: ERCC1 overexpression augments clearance of platinum-DNA crosslinks. All experiments in this figure has been repeated at least 3 times and a representative figure (left) and quantification (right) are presented. **(A)** DLD-C2 and DLD-EC2 cells were treated with increasing concentrations of oxaliplatin for 4 hours. Genomic DNA was isolated and equal amount (1μg) from each sample was transferred to nitrocellulose membrane. Platinum-DNA adduct antibody (ICR4) was used to assess the abundance of oxaliplatin induced DNA damage (upper panel). DLD-EC2 cells registered to have less oxaliplatin damage as normalized to total DNA load (bottom). **(B)** Control and ERCC1 overexpressing DLD1 clones were treated with 100μM oxaliplatin, washed and assessed for DNA repair capacity for 12 hours as mentioned in Fig. 5A. DLD-EC1 and EC2 cleared oxaliplatin induced DNA crosslinks quicker than controls indicating faster DNA repair. **(C)** SIP1/ZEB2 inducible DLD cells (un-induced or induced foe 3 days) were incubated with 100μM oxaliplatin, washed and assessed for platinum adduct clearance. Induced cells registered less damage and quicker recovery

5.7 ERCC1 expression levels predict response to oxaliplatin *in vivo*.

We next evaluated the effects of ERCC1 over expressing (DLD-EC2) and control (DLD-C2) cells in an orthotopic immuno-compromised murine model by direct intra-caecal implantation of tumour cells. Mice were allowed to recover from surgery and control (PBS) or oxaliplatin was administered intra-peritoneally at weekly intervals. Tumour growth was assessed by measuring mCherry fluorescence intensity. Distant metastasis was not detected in lung, liver or spleen by fluorescence imaging or histopathological analysis of the organs confirming the epithelial identity of DLD-C2 and DLD-EC2 cells. Tumour formation and ERCC1 expression in tumours were confirmed by histopathological analysis and IHC **(Figure 44A, 44B)**. Primary tumours expressing low/no ERCC1 (DLD-C2) exhibited a significant reduction in fluorescence signal indicating tumour shrinkage upon Oxaliplatin treatment **(Figure 44C)**. ERCC1 overexpressing primary tumours (DLD-EC2), however, exhibited a limited response to oxaliplatin treatment when compared to controls **(Figure 41D)**. This data suggests ERCC1 over-expression contributes to oxaliplatin resistance in CRC and may explain why SIP1/ZEB2 expressing CRC tumours show limited response upon FOLXOX treatment.

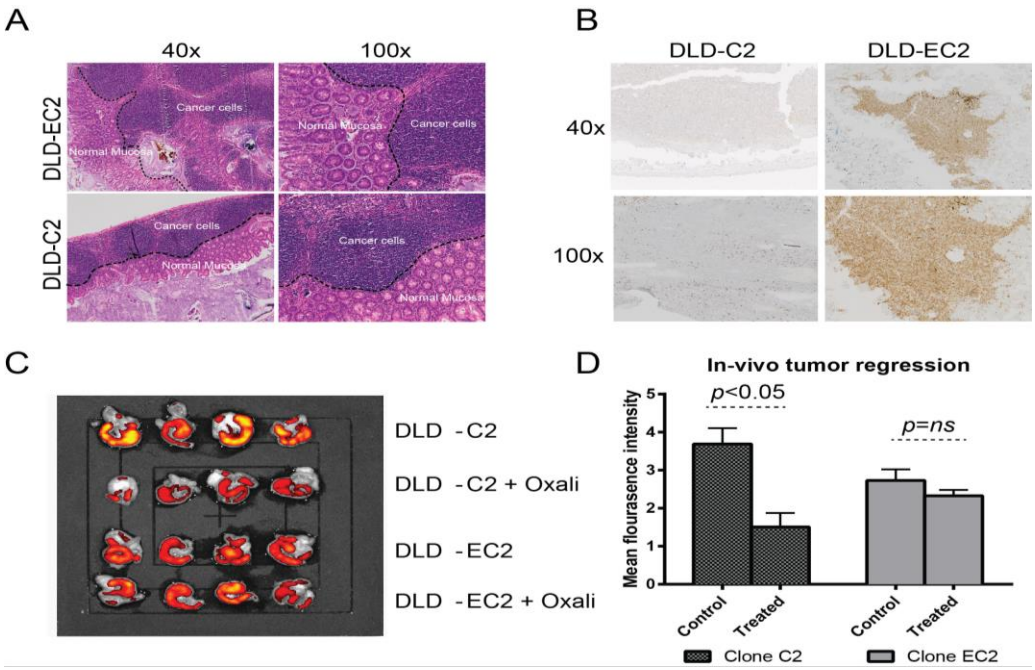

Figure 44: ERCC1 overexpression predicts therapy response in CRC. (A) DLD-EC2 and DLD-C2 clones were injected to the caecum of immuno-compromised mice and allowed to grow for 7 weeks. The tumours were taken out and assessed for histopathological properties. Both cell lines produced similar sized tumours consistent with differentiated primary CRC and **(B)** clone EC2 retained ERCC1 expression as assessed by IHC. **(C)** Imaging primary tumour generated by DLD-C2 and EC2, with or without oxaliplatin treatment, showed a decrease in fluorescence signal in DLD-C2 but not in DLD-EC2 as quantified in **(D)**. The starting fluorescence of DLD-EC2 was less than DLD-C1, possibly because the fusion protein of mCherry-ERCC1 is emitting less light than mCherry alone.

5.8 Results and discussion

Metastasis and therapy resistance are major causes of cancer-associated mortality (1). A growing body of data suggests EMT signature is associated with poor oncological outcomes in CRC (42). In this study, we demonstrate that nuclear SIP1/ZEB2 expression predicts early recurrence and reduced survival in patients that received adjuvant FOLFOX chemotherapy after a surgical resection for primary CRC. SIP1/ZEB2 enhanced resistance of mesenchymal CRC cells to oxaliplatin induced DNA damage, by increasing NER capacity. Enhanced DNA repair capacity resulted in reduced pro-apoptotic signalling and treatment resistance both *in vitro* and *in vivo*.

Chemotherapeutic regimens encompassing use of conventional DNA damaging agents (FOLFOX, FOLFIRI) continue to represent a major treatment option in patients with CRC (355). Although the association between chemo/radio-resistance and EMT has been documented previously, the mechanistic details remain poorly understood and are

likely to be multifactorial (66, 107, 108). Clinical studies suggest CRC patients with tumours belonging to the mesenchymal molecular subtype exhibit poor response to conventional adjuvant chemotherapy (274). We previously reported SIP1/ZEB2 expression promotes resistance to DNA damage induced apoptosis due to attenuated ATM/ATR activation (66). This finding may have different explanations: SIP1/ZEB2 either compromises recognition of the damaged DNA or enhances repair capacity. Our results suggest that faster and more efficient repair of oxaliplatin-induced damage is the main contributing factor to chemoresistance. A central role for SIP1/ZEB1 in promoting resistance to ionising radiation by enhancing homologous recombination (HR) has also been demonstrated recently (356). Hence, SIP1/ZEB-mediated activation of DNA repair pathways emerges as a viable cellular strategy to gain chemo/radio-resistance.

The majority of DNA damage inflicted by platinum-based chemotherapeutic agents are intra-strand G-G dimers, although inter-stand cross-links between two Guanines nucleotides are also observed (357). These DNA adducts distort DNA helix, inhibit replication and transcription to drive cells into apoptosis (351). Of several DNA repair systems in eukaryotic cells, NER is credited with playing a central role in removal of platinum induced DNA adducts (351). The process of intra-strand crosslink removal involves, DNA damage recognition, unwinding, adduct excision by endonucleases, DNA re-synthesis and ligation. The key feature of NER is the introduction of incisions by XPG (at 3') and ERCC1-XPF (at 5') into the damaged DNA strand on either side of the adduct, resulting in the excision and removal of a single strand DNA fragment, containing the DNA adduct (307). In contrast, inter-strand crosslinks are converted into a DSB during DNA replication where the ERCC1-XPF complex plays a key role in removal of non-homologous 3' single stranded flaps, which is subsequently repaired by HR (358).

Among all NER proteins ERCC1 stands out as it is also involved in Fanconi Anaemia pathway and DSB repair (308, 359). Hypersensitivity of ERCC1 mutants to DNA crosslinking agents, when compared to other NER proteins is also well accepted (351). In CRC cell lines, mRNA levels of ERCC1 directly correlated with enhanced repair capacity;

whilst small interfering RNA mediated knockdown increased sensitivity, as shown in this article and by others (360, 361) (362). Ovarian, bladder and lung cancer cell lines that exhibit resistance to platinum derivatives have been shown to possess enhanced NER activity (363-365). The hypersensitivity of testicular cancer to platinum-based chemotherapy is also associated with low abundance of ERCC1 and impaired DNA repair capacity (366). In early clinical trials, high ERCC1 expression has also been associated with cisplatin resistance in ovarian and non-small cell lung cancers (367-369). A single nucleotide polymorphism of the *ERCC1* gene (C118T), is associated with reduced protein translation and improved response to therapy involving platinum compounds in both CRC and NSCLC (370) (371). However, to date, the cellular mechanisms controlling ERCC1 expression and promoting intrinsic platinum resistance in CRC have remained elusive. Here we demonstrate, for the first time, that the activation of EMT by SIP1/ZEB2 is instrumental for ERCC1 overexpression, enhanced NER capacity and oxaliplatin resistance.

Over the years there has been significant attention to the clinical use of ERCC1 as a predictive biomarker of platinum resistance (372-376). IHC, RNA expression and polymorphism genotyping have been trialled with mixed results (353). The FOCUS trial (n=1197) utilised IHC to associate ERCC1 protein expression to predict clinical response to platinum treatment. ERCC1 expression was reported not to be predictive of response to FOLFOX therapy (377). This conclusion, however, needs to be interpreted with caution. Protein quantification of ERCC1 in clinical samples is complicated by the existence of four functionally distinct protein isoforms that differentially impact DNA repair. Of the recognised isoforms, only ERCC1-202 (297aa) was associated with nucleotide excision and inter-strand crosslink repair capacity (359). A meticulous screen of commercially available ERCC1 antibodies demonstrated an inability to differentiate between the four isoforms, consequently, rendering quantification of functionally relevant ERCC1 by IHC impossible (378). Therefore, we did not attempt to stain our CRC cohorts with ERCC1 antibody and associate SIP1/ZEB2 with ERCC1 expression levels in this study. Another important biasing feature of ERCC1 as a biomarker to platinum resistance in clinical

samples is its expression pattern. *ERCC1* is a ubiquitously expressed gene and as shown in this article, its expression is enhanced during EMT. Although ERCC1 up-regulation can have a dramatic impact on oxaliplatin response, it has proven to be difficult to quantify accurately by IHC without a standardised reporting system. Whilst some clinical trials have reported negative results with regards to the predictive capacity of ERCC1, this conclusion needs to be interpreted with caution due to the factors summarised above.

A paucity of data relating to EMT inducing transcription factors and their association with chemoresistance, in particular for SIP1/ZEB2, exists due to the absence of effective antibodies that have been meticulously validated. We overcame this hurdle by generating and validating our own SIP1/ZEB2 antibody and demonstrating specificity in western blotting and IHC (66, 348, 379). Kahlert et al previously reported cytoplasmic expression of SIP1/ZEB2 at the invasive front of primary CRC's prognosticated for poor cancer specific survival (65). Surprisingly, nuclear nature of SIP1/ZEB2 and its prognostics value to differentiate response to chemotherapy were not considered. In this study, we investigated and validated for the first time, the prognostic value of SIP1/ZEB2 expression in a cohort CRC patients, who received adjuvant FOLFOX therapy after surgical resection of the primary tumour. Nuclear SIP1ZEB2 expression was associated with poor oncological outcomes in terms of both OS and DFS. We emphasize the importance of nuclear expression of SIP1/ZEB2 in our scoring system, as SIP1/ZEB2 proteins are transcription factors executing their function in the nucleus.

In this study, we demonstrate that SIP1/ZEB2 directly induces ERCC1 expression, thus enhancing DNA damage repair capacity and apoptosis resistance *in vitro* and *in vivo*. Due to the intrinsic complexity of scoring ERCC1 using IHC, we propose SIP1/ZEB2 is a promising candidate biomarker, predicting FOLFOX resistance in patients with primary CRC. Unlike ERCC1, that is expressed in normal cells, nuclear SIP1/ZEB2 protein is not observed in normal colonic epithelium, but exclusively detected in mesenchymal CRC cells, which simplifies scoring and its application as a clinical tool. Another important feature of SIP1/ZEB2, as shown in this article, is its capacity to induce resistance to both

components of the FOLFOX regimen. The molecular mechanism driving 5-FU resistance in CRC was highlighted as up regulation of thymidylate synthase (380) however the contribution of SIP1/ZEB2 to this phenomenon should be investigated in a separate study.

In conclusion our results show that SIP1/ZEB2 expression is associated with multiple aspects (metastasis and chemoresistance) of tumour progression, making it a valuable biomarker to prognosticate disease trajectory. Further validation and progression to a prospective clinical trial will aid the application of SIP1/ZEB2 immuno-expression as a useful clinical tool in the near future.

Chapter 6: SIP1/ZEB2 induced EMT promotes radio resistance through enhanced double strand break repair.

Radiation therapy is a major tool for cancer treatment, and is widely used in the neo-adjuvant setting in the treatment of rectal adenocarcinoma (32). Ionising radiation (IR) induces apoptosis by producing DNA double strand breaks (DSB's) directly or via the generation of reactive oxygen species (ROS) (226). Over the last three decades multiple clinical trials have investigated the efficacy of IR in the management of rectal cancer. Cumulative analysis of this data has clearly demonstrated that IR improves oncological outcomes in patients with advanced (T3/T4, N1/2) rectal cancer, making neo-adjuvant chemo-radiotherapy the standard of care (381). Despite these advances, it is clear that all patients with rectal cancer do not respond in a ubiquitous manner to IR (32). There is also mounting evidence from in vitro and animal models that suggest certain cancer cells subpopulations acquire resistance to IR induced apoptosis, though currently poorly understood mechanisms (66, 356, 382). Greater capacity to differentiate patients that will acquire benefit from neo-adjuvant treatment from those that will poorly and dissecting cellular mechanism that drive apoptosis resistance to IR will greatly improve treatment outcomes in patients with rectal cancer in future years.

In recent years, there has been growing acknowledgement that mesenchymal cancer cells that express EMT inducing TF's such as SLUG, SNAIL, ZEB1 and ZEB2 acquire apoptosis resistance to IR (66, 382-384). A mechanism that could drive apoptosis resistance to IR is enhanced DNA repair. We previously reported SIP1/ZEB2 expressing bladder cancer cells are protected from cytotoxic injury induced by UV radiation (66). In addition, ZEB1 has also been implicated in stabilising CHK1, in an ATM dependent manner and enhancing homologous recombination (HR) in response to IR (356). Although the above data suggests an association between ZEB proteins and enhanced DNA repair, paucity in detail remains in terms of the contribution of the underlying chromatin structure towards DNA repair. The access-repair-restore model highlights the

initial need to modify histones at the site of injury for successful repair of DSB induced by IR (226) . The impact of chromatin architecture at the site of injury on DNA repair is highlighted by studies that have reported slower rates of DNA repair in heterochromatin rich DNA domains (318). However, the contribution EMT inducing TF's towards chromatin structure and consequently DNA repair is yet to be studied. In this chapter I investigate the contribution SIP1/ZEB2 mediated EMT towards chromatin structure, DNA repair and consequently apoptosis resistance.

6.1 SIP1/ZEB2 expression promotes apoptosis resistance to IR

The association between expression of EMT TF's and apoptosis resistance to radiotherapy has been previously described. In Figure 24 of this thesis, I demonstrated tetracycline treatment of DIP-SIP1 cells in culture induces SIP1/ZEB2 mediated EMT. To evaluate the contribution of SIP1/ZEB2 mediated EMT towards apoptosis resistance in CRC, uninduced (ui) and induced (i) cells were exposed to increasing doses of ionising radiation (IR). Cells were allowed to recover for 48hrs and apoptotic cell populations quantified by detecting PARP cleavage by western blotting. The results revealed, SIP1/ZEB2 expressing mesenchymal cells were resistant to IR induced apoptosis induced. The attenuation in PARP cleavage, which was used a marker of caspase activation, was observed at all doses tested**.** PARP cleavage was not observed in untreated cells and actin was used as an equal loading control **(Figure 45A)**.

γH2AX (Ser139) is a well-recognised marker of DNA damage, in particular double strand breaks. ATM mediated phosphorylation of H2AX at serine 139 in response to DNA damage results in the activation of DNA damage recognition and repair (226). To evaluate if the observed apoptosis resistance is secondary to enhanced DNA repair, γH2AX was quantified in uninduced and induced DLD-SIP1 cells after exposure to increasing doses of IR. A dramatic reduction in γH2AX levels was noted in SIP1/ZEB2 expressing cells when compared to uninduced counterparts, at all doses tested; suggesting SIP1/ZEB2 expressing mesenchymal cells possess the capacity for enhanced DNA repair, γH2AX clearance and consequently apoptosis resistance. Total H2AX levels

in uninduced and induced cells were quantified and demonstrated to be equal to ensure, the observed results are not biased by baseline changes in total H2AX expression after SIP1/ZEB2 induced EMT **(Figure 45A)**.

To evaluate weather the apoptosis resistance observed *in vitro* translates to improved cell viability, DLD-SIP1 cells were exposed to increasing doses of IR after SIP1/ZEB2 induced EMT. Cells were allowed to recover for 1 week and number of colonies quantified using imageJ software. A statistically significant improvement in cell viability was observed in mesenchymal (induced) DLD-SIP1 cells when compared to uninduced cells **(Figure 45B)**. These results demonstrate SIP1/ZEB2 induced EMT results in enhanced DNA repair and consequently apoptosis and resistance after exposure to IR.

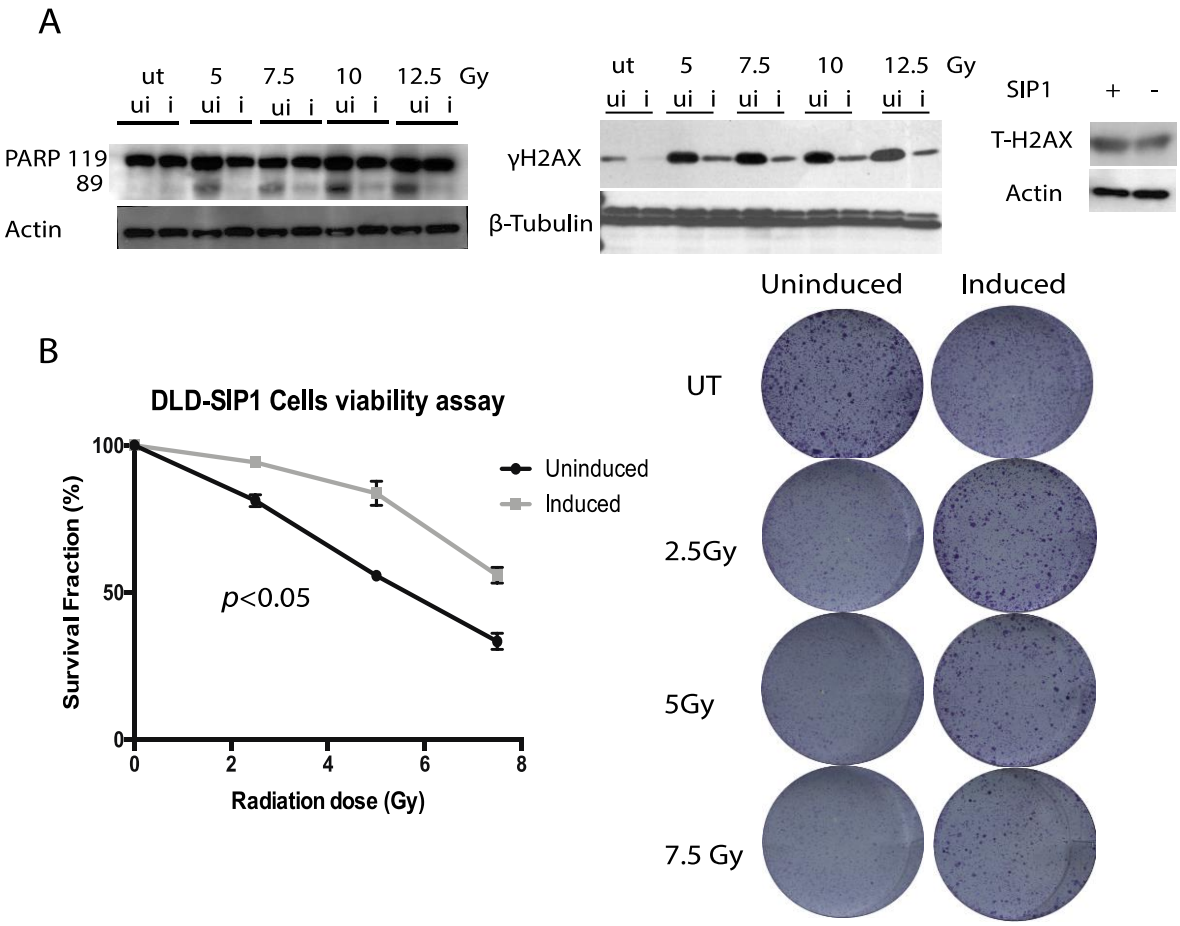

Figure 45:SIP1/ZEB2 expression promotes resistance to ionizing radiation (IR) in CRC. (A) Uninduced and induced DLD-SIP1 cells were exposed to increasing doses of IR. Cells were collected after 48 hours and WB analysis for features of DNA damage (γH2AX) and apoptosis (PARP cleavage) performed. The results revealed SIP1/ZEB2 expressing cells exhibited a dramatic reduction in H2AX phosphorylation and PARP cleavage when compared to uninduced counterparts. Untreated cells did not reveal any evidence of DNA damage or apoptosis and were used as negative controls, whilst β-Tubulin and actin were equal loading controls. Total H2AX levels were quantified before and after induction of SIP1/ZEB2 to ensure observed differences in H2AX phosphorylation are not secondary to baseline changes H2AX expression after EMT. **(B)** Uninduced and induced DLD-SIP1 cells were exposed to increasing doses of IR. Cells were allowed to recover for 1 week and viability assessed by colony formation assay. Colonies were stained using crystal violet and numbers counted using imageJ software. At all doses tested, induced cells exhibited greater capacity to survive DNA damage and form colonies when compared to uninduced cells. Mean differences in colony formation (experiment conducted in triplicate) capacity between uninduced and induced cells were compared and statistical significance calculated using a student T-test. Significance was set to <0.05. Gy-Gray, UI-uniniduce, i-induced, γH2AX- Histone H2AX phosphorylated at serine 139.

6.2 SIP1/ZEB2 expression associates with faster DSB repair

Next I wanted to investigate whether the observed differences in apoptosis and DNA damage, which was observed in SIP1/ZEB2 expressing cells is secondary to faster DNA repair. To achieve this aim, DLD-SIP1 cells were exposed to 2.5Gy of IR before and after SIP1/ZEB2 induced EMT. A pulse-chase experiment was performed and cells fixed using

paraformaldehyde at varying time points over an 8-hours window. IF for γH2AX was performed and foci detected using fluorescence microscopy. γH2AX foci generation and clearance was used as a surrogate marker for DNA double strand breaks and their subsequent repair. Results are presented as a 100-cell mean, which was obtained by manually counting γH2AX foci in DLD-SIP1 cells.

The results revealed SIP1/ZEB2 expressing cells exhibit an enhanced capacity to recognise DNA damage and subsequently repair the DSB. At earlier time points (30min-2 hrs.) induced cells expressed twice the number of γH2AX foci when compared to uninduced cells ($p<0.05$). By contrast at 8 hours induced cells had cleared the majority of γH2AX foci and exhibited half the number of foci when compared to uninduced cells ($p<0.05$). This data suggests, SIP1/ZEB2 expression associates with enhanced capacity to detect and repair DSB's that occur as a consequence of exposure to IR **(Figure 46A)**. The enhanced ability to repair DSB's will contribute to the apoptosis resistance and increased viability observed previously. From a clinical perspective, patients that express SIP1/ZEB2 in rectal adenocarcinoma may exhibit apoptosis resistance to radiation therapy and consequently experience limited tumour regression. Delaying surgical intervention in this subgroup may consequently be ill advised as these patients may acquire minimal benefit from neo-adjuvant radiation therapy, whilst enduring the associated side effects. The current evidence for the above suggestions is however limited and clinical translation will require greater evidence from *in vitro* studies and clinical trials.

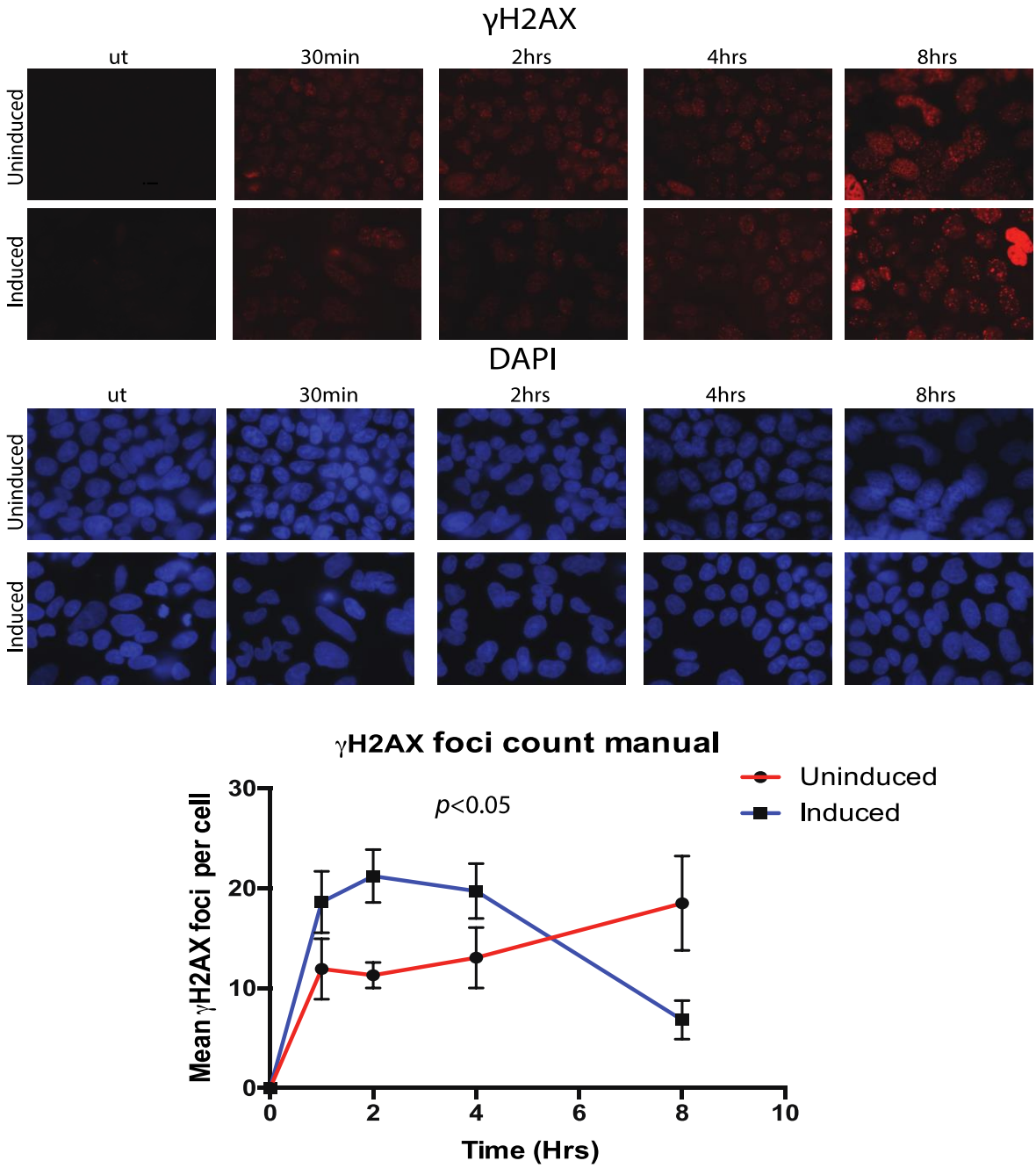

Figure 46: SIP/ZEB2 expression enhances of the kinetics of DNA damage repair after exposure to IR. DLD-SIP1 cells were exposed to 2.5Gy of IR before and after SIP1/ZEB2 induced EMT. A pulse-chase experiment was performed and cells fixed using paraformaldehyde at varying time points over an 8-hours window. IF for γH2AX was performed and foci detected using fluorescence microscopy. γH2AX foci generation and clearance was used as a surrogate marker for DNA double strand breaks and their subsequent repair. Results are presented as a 100-cell mean, which was obtained by manually counting γH2AX foci in individual DLD-SIP1 cells. SIP1/ZEB2 cells expressed twice and many foci (p<0.05) at the earlier time points (30min-2 hours), however repaired the DSB's and consequently cleared the majority of foci by 8hrs (p<0.05). These findings suggest SIP1/ZEB2 mediated EMT associates with mesenchymal cells that possess enhanced capacity to recognise DNA damage, repair DSB and consequently exhibit apoptosis resistance to radiation therapy. Statistical significance was calculated using student t-test. Hrs-hours, γH2AX- histone H2AX phosphorylated at ser-139.

6.3 SIP1/ZEB2 results in genome wide loss of heterochromatin mark H3K27me3

The above data suggests SIP1/ZEB2 expressing cells intrinsically possess enhanced capacity to recognised DNA damage and repair DSB's more rapidly when compared to uninduced cells. To repair DSB's efficiently, the repair machinery needs to be able to access the DNA, repair the damage and restore chromatin conformation. The critical influence of chromatin organisation in modulating DNA repair is underscored by studies that have highlighted slower rates of DNA repair and higher levels of mutations in compact heterochromatin (318, 385). These findings imply that chromatin content at the site of damage can influence the detection and repair of DSB's and consequently apoptosis signalling. In simple terms, the ability of the DNA repair machinery to access the DSB's can have a significant influence on repair kinetics and genomic stability.

Consequently, I wanted to investigate whether SIP1/ZEB2 induced EMT, resulted in genome scale modification in heterochromatin marks and dissect the impact of observed changes to chromatin organisation to DNA damage recognition and repair. Previous, studies using a TGFβ and Twist inducible EMT model have suggested EMT results in a net loss of heterochromatin histone H3 modifications and transition to a more open chromatin structure (225). Loss of heterochromatin marks and adoption of a more open chromatin structure could in-turn promote easier access, enhanced recognition and faster repair of DNA damage. In general, H3K9me3 and H3K27me3 are considered heterochromatin marks, whilst H3K4me3 associates with euchromatin. To investigate the impact of ZEB1 protein expression on genome wide heterochromatin content, I undertook WB analysis on three SIP1/ZEB2 inducible cell lines (MCF-7-SIP1, A431-SIP1, and DLD-SIP1) and one ZEB1 inducible cell line (MCF7-ZEB1) for heterochromatin histone modifications after EMT. The results exhibited consistency with previous studies and revealed a striking reduction in heterochromatin expression (H3K9me3 / H3K27me3) after mesenchymal transition **(Figure 47A)**. Due to lack of sensitivity of WB as a

technique to detect genome scale changes in methylation marks, I also performed ChIP-Seq on DLD-SIP1 cells before and after mesenchymal transformation. Peak calling was performed by a bio-information and results presented as density plots for heterochromatin mark H3K27me3. The ChIP-Seq results exhibited consistency with the findings from the WB and highlighted a dramatic loss of heterochromatin mark H3K27me3 after SIP1/ZEB2 induced EMT **(Figure 47B)**. These findings suggest mesenchymal transition secondary to expression of SIP1/ZEB2 protein results in genome wide loss of heterochromatin mark and adoption of a more open chromatin formation, which could in turn facilitate more efficient DNA damage recognition and repair.

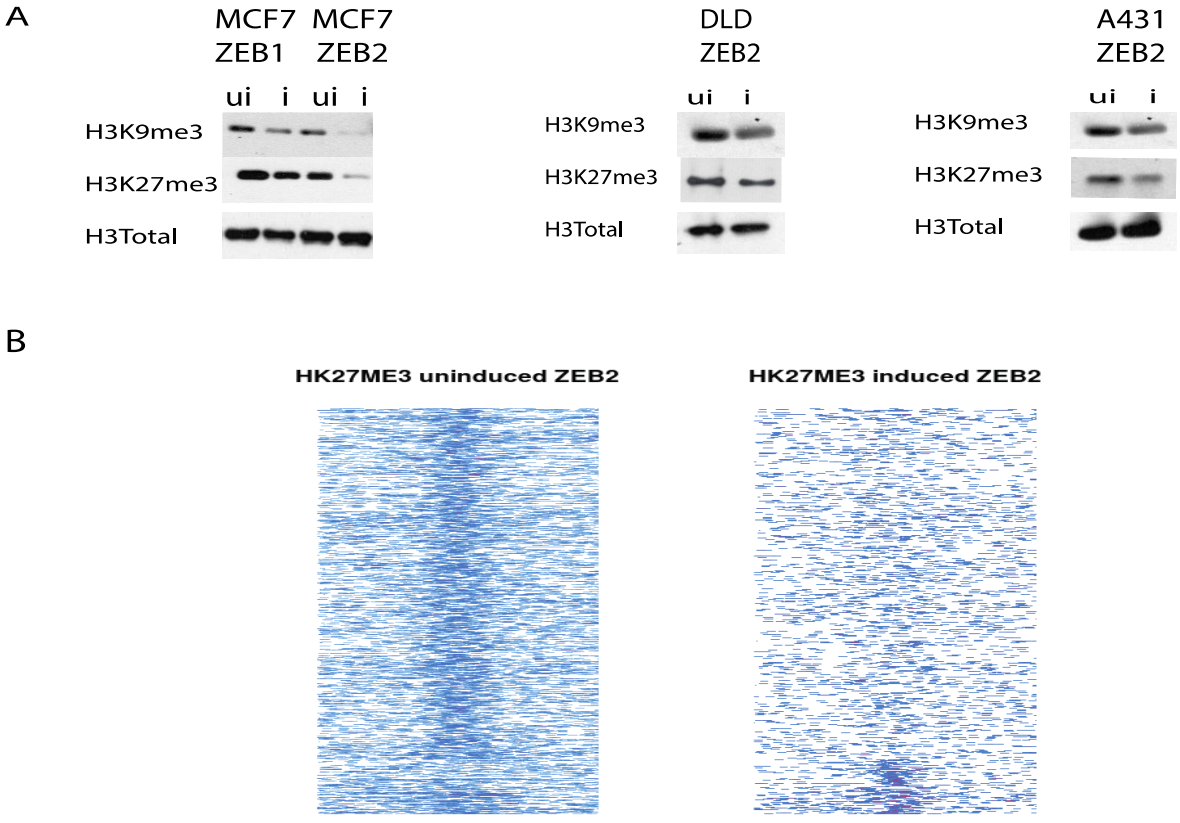

Figure 47: SIP1/ZEB2 expression in multiple inducible models associated with a reduction in total genomic heterochromatin. **(A)** WB performed on three SIP1/ZEB2 inducible cell lines (MCF7-SIP1/ZEB2, A431-SIP1/ZEB2, DLD-SIP1/ZEB2) and one (MCF7-ZEB1) inducible cell line for heterochromatin mark H3K27me3 and H3K9me3 revealed mesenchymal transition resulted in genome wide loss of heterochromatin marks. Total histone H3 was used as an equal loading control and to ensure EMT dose not result in baseline expression changes in histone H3 protein. **(B)** ChIP-Seq performed after immuno-precipitating using H3K27me3 antibody on uninduced and induced DLD-SIP1 cells reveled a dramatic paucity in H3K27me3 read density in induced SIP1/ZEB2 expressing cells when compared to uninduced counterparts.

6.4 H3K27me3 loss occurs secondary to SIP1/ZEB2 mediated transcriptional repression of enhancer of zeste homolog 2 (EZH2)

Next I investigated the mechanism which regulates SIP1/ZEB2 mediated H3K27me3 hypo-methylation. Methylation of histone H3 at lysine-27 is catalysed by the enzyme enhancer of zeste homolog 2 (EZH2) a histone lysine N-methyltransferase. EZH2 is a subunit of the polycomb repressive complex (PRC2), which is primarily implicated in epigenetic regulation of gene expression by catalysing the formation of transcriptionally repressive heterochromatin (H3K27me3) structures at the promoter of target genes. The genome scale hypomethylation observed in SIP1/ZEB2 expressing mesenchymal cells may be secondary to the reduced catalytic activity of histone methyltransferases (EZH2) or enhanced activity of histone demethylases. To evaluate whether SIP1/ZEB2 regulates EZH2 protein expression, WB was performed on two SIP1/ZEB2 inducible cell lines, before and after induction of EMT. SIP1/ZEB2 expression resulted in a striking reduction in EZH2 protein expression after mesenchymal transformation in both cell lines, suggesting direct or indirect regulation of EZH2 by SIP1/ZEB2 **(Figure 48A)**. Repression of EZH2 protein expression could in-turn result in reduced methyltransferases activity of the PRC2 complex and mediate the hypomethylation of H3K27me3 observed in SIP1/ZEB2 expressing mesenchymal cells. To ensure the observed association is not confined to the cell lines studied, a mutual exclusivity analysis was performed on a TCGA dataset using the CBioPortal software. High mRNA expression levels of SIP/ZEB2 was detected in 29% of colorectal adenocarcinoma tumour samples analysed in the nature cohort of the TCGA data set, which exhibited a statistically significant association with low or absent EZH2 mRNA expression. This data suggests EZH2 expression and consequently chromatin conformation is regulated by SIP1/ZEB2 transcription factor by modulating transcription of the *EZH2* gene **(Figure 48A)**. To evaluate, whether SIP1/ZEB2 regulates EZH2 protein expression by direct interaction with E-boxes in the promoter region of the *EZH2* gene, in-silico analysis was performed on Ensemble to identify E-box (CANNTG) motifs in the EZH2 promoter (1Kb from 1st intron). ChIP was performed on DLD-SIP1 cells before and after induction of EMT for SIP1/ZEB2 and RNA

polymerase II. qPCR was undertaken using two sets of primers, designed to in cooperate regions of the promoter that contained clusters E-boxes that could represent putative binding sites. The results revealed a 4-fold (p<0.05) increase signal from the first cluster of E-box elements and a 1.5 fold (p<0.05) increase from the second in induced SIP1/ZEB2 expressing DLD-SIP1 cells **(Figure 48B/C)**. This data suggests SIP1/ZEB2 directly binds to the promoter segment of the *EZH2* gene to mediate transcriptional repression. To further validate the suggestion of transcriptional repression, qPCR was also performed after chromatin immuno-precipitation with RNA polymerase II antibody. The RNA Pol II qPCR exhibited a significant (p<0.05) reduction in signal after SIP1/ZEB2 expression, validating the suggestion that binding of SIP1/ZEB2 to E-boxes in the promoter of EZH2 enforces transcriptional repression.

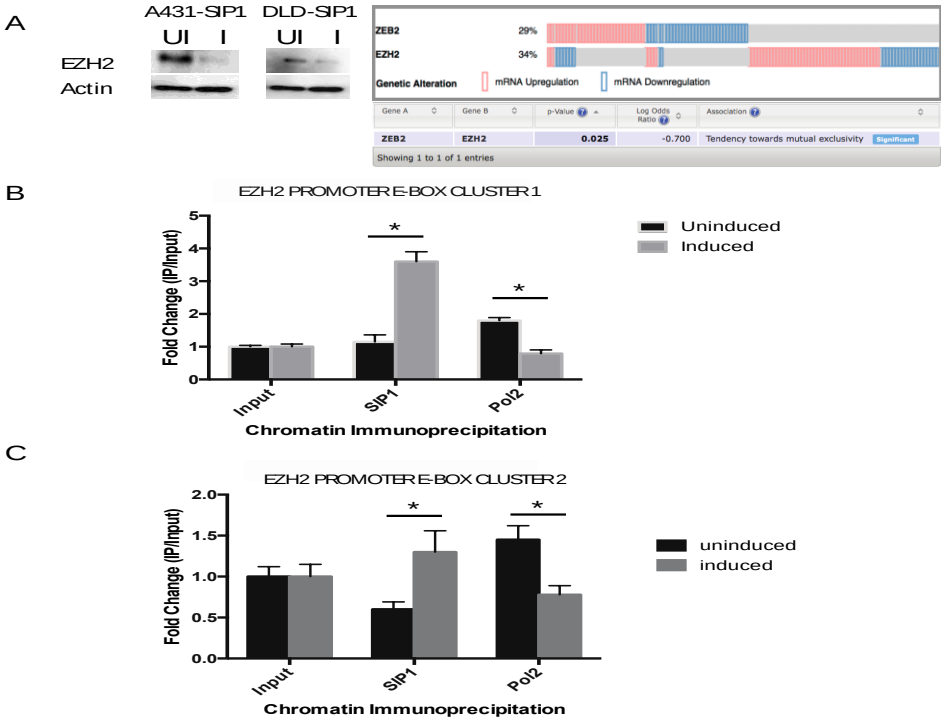

Figure 48:SIP1/ZEB2 expression represses EZH2 expression. (A) WB was performed on DLD-SIP1 and A431-SIP1 cells before and after induction of EMT for EZH2. The EZH2 band intensity dramatically reduced in both cell lines after SIP1/ZEB2 expression. This association was further validated by mutual exclusivity analysis performed on the nature TCGA colorectal adenocarcinoma cohort using the CBioPortal software. The analysis revealed an inverse association between SIP1/ZEB2 high expression levels and EZH2 mRNA levels (p<0.025). (B/C) qPCR was performed after ChIP using SIP/ZEB2 and RNA Pol II antibody on uninduced and induced DLD-SIP1 cells. The results demonstrated a statically significant increase in SIP1/ZEB2 signal (p<0.05) and reduction in RNA Pol II signal (p<0.05) suggesting, SIP1/ZEB2 directly binds E-box elements in the promoter of the EZH2 gene inducing transcriptional repression. Statistical significance was calculated using a t-test for results presented in B/C.

6.5 EZH2 inhibition by GSK126 promotes radio-resistance in uninduced DLD-SIP1 cells.

My data suggests SIP1/ZEB2 mediated repression of EZH2 promotes loss of heterochromatin mark (H3K27me3), which may in turn enhance DNA damage recognition, DSB repair and apoptosis resistance. To evaluate the contribution of loss of heterochromatin (H3K27me3) towards promoting apoptosis resistance to radiation therapy, I treated DLD-SIP1 cells with increasing concentrations of a highly selective EZH2 inhibitor GSK126. To evaluate the impact of GSK126 mediated inhibition of EZH2 on chromatin conformation, I pre-treated uninduced and induced DLD-SIP1 cells for 12 hours with increasing concentrations of EZH2 and undertook WB analysis to detect changes in euchromatin (H3K4me3) and heterochromatin (H3K27me3, H3K27me3). The WB revealed GSK126 pre-treatment lead to a highly specific depletion of H3K27 tri-methylation secondary to selective inhibition of EZH2. No change in WB band intensity was observed with respect to euchromatin mark (H3K4me3) or heterochromatin mark (H3K9me3) highlighting the selectivity of GSK126 as an EZH2 inhibitor. It is important to note that the complete depletion of H3K27 tri-methylation occurred at much lower doses (2.5μM) in induced cells when compared to uninduced (10μM) counterparts. This observation is likely to be secondary to SIP1/ZEB2 mediated transcriptional repression of EZH2 resulting in the reduction in the dose of the inhibitor required for complete inhibition of catalytic activity.

To evaluate the association between loss of H3K27me3 and apoptosis resistance to radiation therapy I pre-treated uninduced DLD-SIP1 cells with 5μM and 10μM of GSK126. My previous WB **(Figure 49A)** had demonstrated 10μM pre-treatment with GSK126 of uninduced DLD-SIP1 cells for 12 hours results in complete depletion of H3K27me3 marks and adoption of a more open chromatin structure akin to induced cells that express SIP1/ZEB2. Therefore, I postulated pre-treatment of uninduced DLD-SIP1 cells with GSK126 will result in an open chromatin conformation which will promote the acquisition of apoptosis resistance observed in mesenchymal cells that express SIP1/ZEB2. To investigate my hypothesis I pre-treated uninduced DLD-SIP1 cells with 5μM and 10μM of

GSK126 and subsequently exposed them to 7.5Gy of IR. Cells were collected after 24 hours and apoptosis detected by WB for PARP cleavage. The results demonstrated that uninduced cells treated with 7.5Gy of IR exhibited PARP cleavage, however pre-treatment of uninduced cells with 5/10μM of GSK126 before exposure to IR resulted in acquisition of apoptosis resistance detected by absence of the cleaved PARP band on the WB **(Figure 49B)**. Untreated cells, Sham (DMSO) and uninduced cells pre-treated with GSK126 but not exposed to IR were used as negative controls. Actin was used as a marker of equal protein loading. I also performed a colony formation assay to investigate if GSK126 pre-treatment of uninduced DLD-SIP1 cells improves cell viability after treatment with IR. Pre-treatment of un-induced cells with GSK126 before exposure to IR also lead to a statistically significant improvement ($p<0.05$) in cell viability detected by ability to form colonies after exposure to radiation therapy **(Figure 49C)**. The above results suggests hypomethylation and depletion of genomic heterochromatin may improve the ability SIP1/ZEB2 expressing mesenchymal CRC cells to detect and repair DNA DSB's and consequently avoid activation of apoptosis pathways in response to radiation therapy. The application of SIP1/ZEB2 as a marker of resistance to radiation therapy however requires further validation in human tissue specimens and clinical trials before translational potential as a biomarker can be fully assessed.

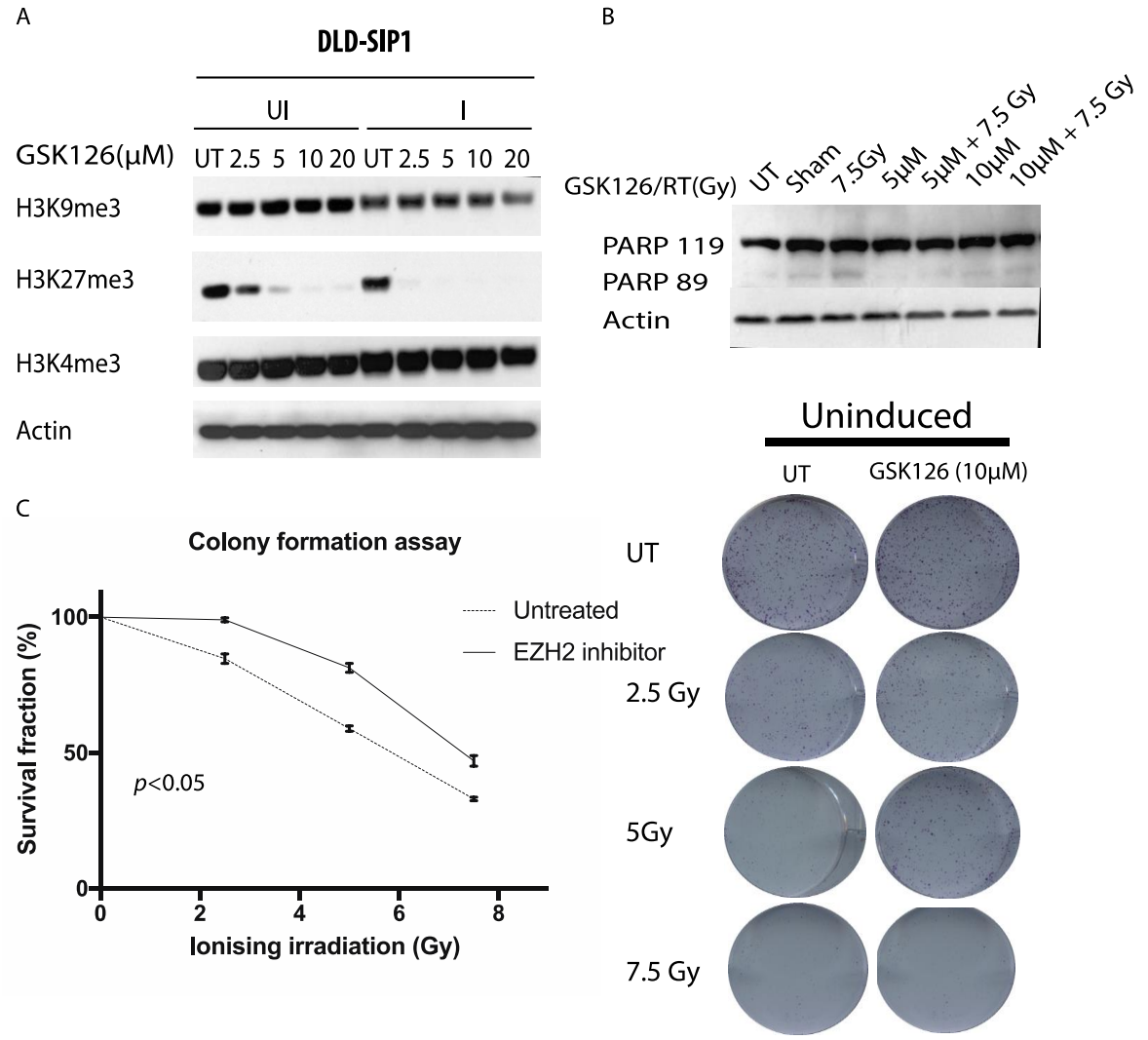

Figure 49: Loss of heterochromatin mark H3K27me3 in uninduced DLD-SIP1 cells by treatment with GSK126 promotes acquisition radioresistance properties. (A) WB performed on DLD-UI and DLD-I cells after 12-hour pre-treatment with EZH2 inhibitor GSK-126. The WB demonstrates specific loss of H3K27me3 in UI and I cells. Loss of other tri-methylation marks is not observed highlighting the specificity of GSK126 as a competitive inhibitor of the catalytic activity of EZH2. Actin was used as a marker of equal loading control. (B) DLD-UI cells pre-treated with GSK126 were exposed to 7.5Gy of IR. The pretreated cells exhibited apoptosis resistance to IR when compared DLD-UI cells that retained H3K27me3 marks. This suggests loss of heterochromatin mark H3K27me3 associates with radio-resistance independent of SIP1/ZEB2 mediated EMT. (C) Cell viability assessed by colony formation assay also highlighted a statistically significant improvement in cell viability in DLD-SIP1 cells pre-treated with GSK126. The colony formation assay was performed in triplicate and statistical significance calculated using a T-test.

6.6 Results summary and discussion

The findings presented here provide the first evidence to comprehensively demonstrate an important association between SIP1/ZEB2 mediated EMT and apoptosis resistance to radiation therapy in CRC. SIP1/ZEB2 mediated EMT resulted in the formation of mesenchymal cells with enhanced ability to recognise DNA damage, repair DSB's faster and consequently exhibit apoptosis resistance to IR. Previous studies have

highlighted the association between heterochromatin marks and delayed DNA repair kinetics (318). In this study, we demonstrate for the first time, that SIP/ZEB2 mediated EMT results in genome scale loss of heterochromatin mark H3K27me3. EZH2 the catalytic subunit of the PRC2 complex, which is primarily responsible for tri-methylation of histone H3 at lysine 27 is repressed by the interaction of SIP1/ZEB2 with E-Boxes in the promoter segment of the EZH2 gene. Repression of EZH2 protein expression leads to a more open chromatin conformation and associated with enhanced apoptosis resistance. Uninduced DLD-SIP1 cells pre-treated with GSK126, lost their H3K27me3 chromatin modifications and acquire apoptosis resistance to radiation therapy. This study for the first time highlights a potentially important interaction between EMT, loss of genome scale heterochromatin, enhanced DNA repair and apoptosis resistance to radiation therapy.

Radiation therapy is a common strategy that continues to be used in the management of rectal cancer (32). The association between epithelial mesenchymal transition and chemoresistance has been reported by many studies in multiple tissue types (65, 66, 115). However, the evidence linking SIP1/ZEB2 mediated EMT and radiation therapy resistance remains sparse. Sayan and colleagues previous highlighted attenuation in ATM activation and reduced γH2AX phosphorylation after exposure to UV-irradiation in SIP1/ZEB2 expressing mesenchymal cells (66). SIP1/ZEB2 expressing cells were found to protected from DNA damage induced cell death and highlighted to have independent prognostic value as a biomarker in bladder cancer (66). More recently ZEB1 protein phosphorylation by ATM in response to radiation therapy was found to enhance DNA damage repair and resistance (356). Despite Radiation therapy being a commonly used modality of treatment in locally advanced rectal cancer, mechanism that mediate resistance to radiotherapy remains poorly elucidated. In this study we present in vitro evidence, which strongly suggests SIP1/ZEB2 mediated EMT, promotes apoptosis resistance to IR, secondary to improved recognition of DNA damage and faster kinetics of DNA repair. Enhanced apoptosis resistance is demonstrated by a reduction in caspase mediated PARP cleavage and improved cell viability in response to IR. The increased

capacity to recognise DNA damage and repair DSB's was identified by the following the kinetics of γH2AX generation and clearance.

For decades, models of DNA damage repair have recognised the critical importance of a permissive chromatin architecture to access and efficiently repair DNA damage (226). Sequencing of multiple cancer genomes has revealed mutations accrue at a higher rate in compact heterochromatin when compared to euchromatin, providing evidence for the notion that DNA repair is less efficient when the damage is encountered in heterochromatin rich domains (385). Slower rates of DNA repair and increased requirement for ATM mediated DNA damage signalling has also been reported in heterochromatin regions (318). However, the impact of genome scale epigenetic alterations to chromatin architecture, DNA damage repair and EMT is yet to be studied. Recently, 2 studies have suggested, TGFβ and TWIST mediated EMT results in genome scale loss of heterochromatin (H3K27me3, H3K9me3) and gain of euchromatin histone modifications (224, 225). Therefore, it is logical to postulate that the depletion of heterochromatin rich histone modifications will contribute towards enhanced DNA damage recognition, repair and apoptosis resistance observed in mesenchymal cancer cells.

In this study we demonstrate by Western Blotting and ChIP-Seq analysis that SIP1/ZEB2 mediated mesenchymal transition associates with a dramatic depletion in heterochromatin histone modification H3K27me3. These findings exhibit consistency with previously reported studies, even though the mechanism by which EMT was induced varied in each case (TGFβ, Twist, SIP1/ZEB2). Further, the loss of histone modification H3K27me3 was found to be secondary to transcriptional repression of the methyltransferases EZH2 by direct interaction of SIP1/ZEB2 TF with E-boxes in the promoter of the *EZH2* gene. Malouf and colleagues previously suggested the loss of H3K27me3 peaks observed after Twist mediated EMT is due to phosphorylation of EZH2 at Ser21, resulting in loss of catalytic function (225). However, we demonstrate using two SIP1/ZEB2 inducible cell lines clear down regulation in expression of EZH2 protein after mesenchymal transformation. Further; mutual exclusivity analysis on the TCGA CRC

dataset further affirms this suggestion. The biological reason for this observed difference in regulation of EZH2 activity remains unclear, however differences in TF, cell line and tissue studied may be contribute towards the observed differences. ChIP and qPCR of DLD-SIP1 cells before and after induction of EMT also clearly demonstrated SIP1/ZEB2 directly binds the promoter regions of the EZH2 gene to mediate transcriptional repression of the gene, in a RNA POL II dependent manner. This suggests binding of SIP1/ZEB2 likely results in dissociation or reduced affinity of the transcriptional machinery to the promoter of the gene. The epigenetic modifications that ensue after SIP1/ZEB2 binds to the promoter resulting in transcriptional repression needs careful dissection in future studies.

Radiation therapy remains a major modality of treatment in the management of locally advanced rectal cancer. Currently, there are no known biomarkers that could predict response neo-adjuvant therapy and mechanism that mediate resistance remain poorly elucidated. Through the above work, we present compelling *in vitro* evidence for a novel mechanism by which SIP1/ZEB2 expressing mesenchymal cancer cells accrue apoptosis resistance to IR. SIP1/ZEB2 mediated EMT has also been previously associated with chemoresistance and increased risk of metastasis (65, 66). Further translational efforts are urgently needed to aid the clinical application of SIP1/ZEB2 as a predictive biomarker with the ability to differentiate patients that will acquire maximal benefit from neo-adjuvant chemo-radiotherapy therapy from non-responders.

Chapter 7: Final Discussion

In this thesis I believe I provide compelling evidence that SIP1/ZEB2 induced EMT results in acquisition of all the cardinal features of mesenchymal transition. SIP1/ZEB2 expressing cells down regulated E-cadherin, transformed to acquire a more metastatic phenotype and acquired resistance to of chemo-radio therapeutic strategies routinely used in the clinical setting. Although the association between EMT, metastasis and chemoresistance is not new, translational efforts to utilise EMT inducing TF's in the clinical setting are yet succeed. In particular, a scarcity in knowledge exists with regard to assessing the contribution of SIP1/ZEB2 in promoting metastasis and chemo-radio resistance in CRC. Through my work, I highlight the exciting translational potential of SIP1/ZEB2 as a biomarker with the ability to identify patients that are at high risk of distant recurrence after curative surgery.

Many studies in multiple cancers have previously reported a strong association between activation EMT pathways, increased metastatic capacity and poor survival (65, 66, 188). A large-scale consortium of leading scientist within the colorectal field have recently highlighted the importance of identifying tumours expressing a mesenchymal phenotype(33). Cumulative analysis of six independent cohorts by genomic subtyping studies reported that patients with tumours expressing a mesenchymal gene profile were repeatedly found to have a worse prognosis and increased risk of distant recurrence (42, 272, 273, 275, 276, 342). Further, Kahlert and colleagues previously associated cytoplasmic expression of SIP1/ZEB2 at the invasive front of primary CRC's as an independent prognostic marker of poor oncological outcomes (65).

However a number of limitations to study design, scoring and data analysis have hampered progression towards clinical trials. For example the IHC data presented in this thesis is he first emphasis the importance of nuclear expression in the scoring system as SIP/ZEB2 mediates transcriptional regulation by interacting with specific DNA motifs in the nucleus. Other limitations include failure to validate findings in an independent patients

cohort, not differentiating distant from local recurrence and not assessing the added value of cooperating SIP1/ZEB2 expression score to the currently used TNM staging system. The data presented in Chapter 4 highlights the clinical utility of SIP1/ZEB2 as a biomarker to aid in identifying patients at high risk of recurrence independent of stage. The clinical utility of analysing SIP/ZEB2 expression in CRC, in concordance with other recently identified biomarkers such as KRAS mutation or microsatellite instability through clinical trials will aid in the successful application of these biomarkers in the clinical setting, improving the precision with high risk patients are identified and treated.

Next, I investigated the mechanism, which mediated apoptosis resistance in SIP1/ZEB2 expressing cells to routinely used chemotherapeutic agent in the management of CRC. Nuclear expression of SIP1/ZEB2 in a cohort of (n=99) patients that received adjuvant FOLFOX chemotherapy after curative surgical resection highlighted SIP1/ZEB2 positivity as an independent prognostic marker of poor survival outcomes after adjuvant FOLFOX therapy. This finding mirrors the apoptosis resistance observed in SIP1/ZEB2 expressing cells *in vitro* and strongly supports the notion that SIP1/ZEB2 expressing cells promote chemoresistance in CRC. Several studies have demonstrated EMT promotes resistance to DNA damaging chemotherapeutic agents (66, 115). However, the mechanism promoting metastasis is as yet poorly understood.

To dissect cellular mechanism promoting chemoresistance, a qPCR array with a focus on DNA damage repair was undertaken. The results highlighted up regulation of several components of the NER pathway. In particular a 2.5 fold up regulation of ERCC1 a critical component of the NER pathway was observed after SIP1/ZEB2 expression in both DLD and A431-SIP1 inducible models. To validate this observation real time PCR and WB analysis was undertaken in DLD-SIP1 cells. The generality of this observation was investigated by RT-PCR of 11 CRC cell lines, which demonstrated a perfect correlation between mesenchymal status and *ERCC1* overexpression.

Excision repair cross complementation group 1 (*ERCC1*) is a gene known to play a critical a role in nucleotide excision repair (NER) and double strand break repair pathway (293, 300). ERCC1 forms a heterodimer with XPF and functions as a 5'->3' structure specific endonuclease (386). It is essential for repair of inter and intra strand cross links created by UV radiation, platinum based chemotherapeutic agents and DSB created by ionising radiation (387). Within the *ERCC1-XPF* heterodimer, *ERCC1* is catalytically inactive and regulates DNA and protein-protein interactions whilst XPF possesses the capacity to undertake endonuclease activity(388). During NER, *ERCC1-XPF* makes an incision at the 5' end, and is essential for excision of a single strand of DNA which contains the adduct (351, 388). A review of NER and the sensitivity of mammalian NER mutants to ICL agents found that while all XP mutants were sensitised to platinum based chemotherapeutic agents, ERCC1 mutants were hyper sensitive. A potential explanation for this evidence is the suggestion that endonuclease action of *ERCC1-XPF* may be the rate limiting reaction during NER (307). The importance of *ERCC1-XPF* in DSB repair was shown in budding yeast, where mutations in RAD10 or RAD1, orthologous of ERCC1 and XPF disrupts HR and NHEJ. The key activity of *ERCC1-XPF* in both types of DNA repair (HR/NHEJ) is its ability to remove 3' single stranded flaps at broken ends before they are ligated(307).

Over the years there has been significant attention on the potential use of *ERCC1* as a predictive biomarker of response to platinum based chemotherapeutic agents (372-376). *In-vitro* analysis in colon, ovarian and testicular cancer cells have demonstrated that low ERCC1 and mRNA protein levels correlate with sensitivity to cisplatin in various cell lines (353). Arnould et al demonstrated low ERCC1 expression was associated with sensitivity to Oxaliplatin in CRC cell lines (360). Youn et al demonstrated transient knockdown of *ERCC1* with siRNA resulted in sensitisation to cisplatin in fibroblasts (389). Boyer et al demonstrated higher levels *ERCC1* mRNA levels in CRC cells when compared to parental cells(390). Recently, SNAIL1 an EMT inducing TF was reported as a direct regulator of ERCC1 expression in head and neck tumours, thus promoting resistance to Oxaliplatin (321).

Several clinical trials have also investigated the potential use of *ERCC1* as a predictive or prognostic biomarker (376, 391, 392). Three techniques, IHC, RT-PCR and genotyping for single nucleotide polymorphisms have been used. The most common polymorphism studied is a synonymous C>T SNP situated at codon 118. The T variant has been shown to associate with lower mRNA and protein levels thus altering DNA repair capacity. Unfortunately these studies reported mixed results(353, 393). Several studies have reported the association between mRNA levels of *ERCC1* and response to Oxaliplatin by RT-PCR. Shirota and colleagues in a cohort of 50 CRC patients reported *ERCC1* correlated with poor response to FOLFOX chemotherapy when *ERCC1* expression levels are high (393). More recently a Phase 1 clinical trial demonstrated high *ERCC1* levels was associated with shorter time to treatment failure, highlighting *ERCC1* as a potential predictive marker of response to chemotherapy with platinum based agents (394). Several large trials have also used IHC as a tool to measure protein levels of *ERCC1* and use expression levels to predict clinical response. Braun et al in the FOCUS trial evaluated ERCC1 expression levels in 1197 patients with CRC (377). Disappointingly *ERCC1* expression was not linked to outcome. This data, however, has to be interpreted with caution. IHC as a technique has many pitfalls, the primary being the dependence of antibody specificity for antigen detection. Previously conducted studies have not used identical protocols in terms of antigen retrieval, antibody clone used and scoring system, making the results prone to bias.

Friboulet et al dissected the specificity of commercially available *ERCC1* anti-bodies in IHC and reported non-specificity of the available antibodies to differentiate between 4 isoforms of the ERCC1 protein. The authors postulated whilst some large clinical trials have reported negative results with regards to predictive capacity to platinum based chemotherapy, this observation might be biased by the inability of available antibodies to specifically recognise the epitope of the active isoform (378). In this study, we demonstrate SIP1/ZEB2 directly binds E-box elements in the promoter of the *ERCC1*

gene and consequently directly regulates transcription and protein expression. Consequently, due to the innate complexity introduced by the existence of active and inactive isoforms of *ERCC1* and inability of existing commercially available antibodies to identify the active isoform of *ERCC1*, SIP1/ZEB2 could instead be used as a predictive biomarker to identify patients that will respond poor to adjuvant chemotherapeutic strategies that encompass oxaliplatin.

The final chapter of my thesis highlights the novel association between SIP1/ZEB2 expression and apoptosis resistance to IR. In recent years there has been growing acknowledgement of the significant impact chromatin architecture has on DNA repair. Models of DSB repair have been constructed within the principles that successful DNA repair fist requires histone modifications that facilitate access to damaged DNA within a complex chromatin architecture (226). Previous studies have reported, mutations accrue at a much higher rate and DNA repair kinetics is attenuated if DNA damage is encountered within compact heterochromatin (318). These findings suggest the chromatin architecture imposes significant influence on DNA damage recognition and repair.

Mesenchymal transformation requires genome scale re-programming of the cells epigenetic architecture (64). Recent studies report, TGFβ and Twist induced EMT results in genome scale loss of histone H3 heterochromatin modification (H3K9me2, H3K27me3) (224, 225). Therefore it was logical to hypothesise, SIP1/ZEB2 induced EMT, will lead to genome scale loss of heterochromatin rich histone modifications, resulting in enhanced capacity to recognise DNA damage and successfully repair the insult. The enhanced capacity to repair DNA more proficiently may in-turn attenuate apoptotic signalling and promote acquisition of resistance to radiation therapy. WB and ChIP-Seq analysis of SIP1/ZEB2 inducible cell lines demonstrated a dramatic reduction in heterochromatin mark H3K27me3. The transcriptional repression of the methyltransferase EZH2 by SIP1/ZEB2 was identified as the mechanism responsible for the genome scale switch in the chromatin landscape and inhibition of EZH2 by small molecule inhibitor GSK126

resulted in acquisition of apoptosis resistance to DNA damage independent of EMT. This suggests an SIP1/ZEB2 mediated EMT, promotes genome scale loss of heterochromatin mark H3K27me3, which in turn associates with enhanced apoptosis resistance to IR.

Radiation therapy continue to represent a major modality of treatment of patients locally advanced CRC. Subgroups of these patients however, respond poorly and exhibit minimal tumour regression, whilst enduring the significant side effects associated with IR. The data above provides a novel mechanism by which CRC cells may acquire resistance to cytotoxic stress. More detailed dissection of cellular mechanism that may drive this resistance mechanism will aid in the development and translational application of agents, which may sensitise resistant tumour to IR or as a minimum provide a diagnostic tool, whereby SIP1/ZEB2 expression may be utilised as a predictive biomarker of resistance to neo-adjuvant chemo-radio therapeutic strategies. Successful development and clinical application of SIP1/ZEB2 will improve the precision with which treatment strategies are tailored and administered to patients with rectal cancer in future years.

Appendix

Figure 46: Formula used for preparation of SDS gels for Western blotting

TABLE 18.3 Solutions for Preparing Resolving Gels for Tris-glycine SDS-Polyacrylamide Gel Electrophoresis

Solution components	Component volumes (ml) per gel mold volume of 5 ml	10 ml	15 ml	20 ml	25 ml	30 ml	40 ml	50 ml
6%								
H_2O	2.6	5.3	7.9	10.6	13.2	15.9	21.2	26.5
30% acrylamide mix	1.0	2.0	3.0	4.0	5.0	6.0	8.0	10.0
1.5 M Tris (pH 8.8)	1.3	2.5	3.8	5.0	6.3	7.5	10.0	12.5
10% SDS	0.05	0.1	0.15	0.2	0.25	0.3	0.4	0.5
10% ammonium persulfate	0.05	0.1	0.15	0.2	0.25	0.3	0.4	0.5
TEMED	0.004	0.008	0.012	0.016	0.02	0.024	0.032	0.04
8%								
H_2O	2.3	4.6	6.9	9.3	11.5	13.9	18.5	23.2
30% acrylamide mix	1.3	2.7	4.0	5.3	6.7	8.0	10.7	13.3
1.5 M Tris (pH 8.8)	1.3	2.5	3.8	5.0	6.3	7.5	10.0	12.5
10% SDS	0.05	0.1	0.15	0.2	0.25	0.3	0.4	0.5
10% ammonium persulfate	0.05	0.1	0.15	0.2	0.25	0.3	0.4	0.5
TEMED	0.003	0.006	0.009	0.012	0.015	0.018	0.024	0.03
10%								
H_2O	1.9	4.0	5.9	7.9	9.9	11.9	15.9	19.8
30% acrylamide mix	1.7	3.3	5.0	6.7	8.3	10.0	13.3	16.7
1.5 M Tris (pH 8.8)	1.3	2.5	3.8	5.0	6.3	7.5	10.0	12.5
10% SDS	0.05	0.1	0.15	0.2	0.25	0.3	0.4	0.5
10% ammonium persulfate	0.05	0.1	0.15	0.2	0.25	0.3	0.4	0.5
TEMED	0.002	0.004	0.006	0.008	0.01	0.012	0.016	0.02
12%								
H_2O	1.6	3.3	4.9	6.6	8.2	9.9	13.2	16.5
30% acrylamide mix	2.0	4.0	6.0	8.0	10.0	12.0	16.0	20.0
1.5 M Tris (pH 8.8)	1.3	2.5	3.8	5.0	6.3	7.5	10.0	12.5
10% SDS	0.05	0.1	0.15	0.2	0.25	0.3	0.4	0.5
10% ammonium persulfate	0.05	0.1	0.15	0.2	0.25	0.3	0.4	0.5
TEMED	0.002	0.004	0.006	0.008	0.01	0.012	0.016	0.02
15%								
H_2O	1.1	2.3	3.4	4.6	5.7	6.9	9.2	11.5
30% acrylamide mix	2.5	5.0	7.5	10.0	12.5	15.0	20.0	25.0
1.5 M Tris (pH 8.8)	1.3	2.5	3.8	5.0	6.3	7.5	10.0	12.5
10% SDS	0.05	0.1	0.15	0.2	0.25	0.3	0.4	0.5
10% ammonium persulfate	0.05	0.1	0.15	0.2	0.25	0.3	0.4	0.5
TEMED	0.002	0.004	0.006	0.008	0.01	0.012	0.016	0.02

TABLE 18.4 Solutions for Preparing 5% Stacking Gels for Tris-glycine SDS-Polyacrylamide Gel Electrophoresis

Solution components	Component volumes (ml) per gel mold volume of 1 ml	2 ml	3 ml	4 ml	5 ml	6 ml	8 ml	10 ml
H_2O	0.68	1.4	2.1	2.7	3.4	4.1	5.5	6.8
30% acrylamide mix	0.17	0.33	0.5	0.67	0.83	1.0	1.3	1.7
1.0 M Tris (pH 6.8)	0.13	0.25	0.38	0.5	0.63	0.75	1.0	1.25
10% SDS	0.01	0.02	0.03	0.04	0.05	0.06	0.08	0.1
10% ammonium persulfate	0.01	0.02	0.03	0.04	0.05	0.06	0.08	0.1
TEMED	0.001	0.002	0.003	0.004	0.005	0.006	0.008	0.01

Tables 18.3 and 18.4 are modified from Harlow and Lane (1988).

Table 18: List of primary and secondary antibodies used in the thesis.

Primary antibody	Used as	Molecular Weight	Animal host	Supplier
Human Vimentin	Mesenchymal marker	57	C5741 / Rabbit monoclonal	Cell Signalling
Human ERCC1	NER component	37	Rabbit monoclonal D6G6	Cell signalling
Human SIP1	Mesenchymal marker	220	Rabbit monoclonal	In House antibody (Sayan, Griffiths et al., 2009)
Human E-Cadherin	Epithelial marker	140	Rabbit monoclonal 24E01	BD Transduction Laboratories™
Human PARP	Mesenchymal marker	119-89	Rabbit monoclonal 46d11	Cell signalling
Human Actin	Equal loading marker	45	Goat Monoclonal SC-1615	Santa Cruz
Myc-Tag	Tag	30	Mouse monoclonal 9B11	Cell signalling
α-Tubulin	Equal Loading control	52	Rabbit Monoclonal 11H10	Cell signalling
RNA Pol II	Positive control	217	Mouse Monoclonal	Active Motif ChIP-IT Cat no. 53010
Bridging antibody	Increase IP efficiency	N/A	Mouse Monoclonal	Active Motif ChIP-IT Cat no. 53010
Human anti-mouse IgG	Negative control	N/A	Mouse Monoclonal	Active Motif ChIP-IT Cat no. 53010
γH2AX	DNA damage marker	15	Rabbit Monolclonal	Cell signalling
H3K27me3	Heterochromatin	15	Rabbit monoclonal	Cell signalling
H3K9me3	Heterochromatin	15	Rabbit Monoclonal	Cell signalling
H3K4me3	Euchromatin	15	Rabbit monoclonal	Cell signalling
Total H2AX	H2AX histone	15	Rabbit monoclonal	Cell signalling

Table 19: Formula used for preparation of reagents and buffers

Buffer Name	Buffer Components	Supplier
30% (w/v) 37.5:1 Acrylamide: Bis-acrylamide solution	37.5 g Acrylamide (Fisher) 1 g Bis-Acrylamide (Fisher) Dissolved in dH_2O to a final concentration of 30%	Geneflow
30% (w/v) 29:1 Acrylamide : Bis-acrylamide solution	29.0 g Acrylamide (Fisher) 1 g Bis-Acrylamide (Fisher) Dissolved in dH_2O to a final concentration of 30%	Geneflow
1.5M Tris buffer (pH 8.0 and pH 8.8)	182.25g Tris (Fisher). dH_2O Adjust pH to 8.0, adjust volume to 1L Adjust pH to 8.8, adjust volume to 1L	In house
1M Tris buffer (pH 6.8)	121.1g Tris-base (Fisher) dH_2O Adjust pH to 6.8, adjust volume to 1 L	In house
10% APS	1 g APS (Fisher) Adjust volume to 10 ml with dH_2O Store at 4ºC for several weeks	In house
10% SDS	1 g SDS (Fisher) Adjust volume to 10 ml with dH_2O Store at RT	In house
5 X SDS-PAGE buffer	dH_20 0.5 M Tris (pH 6.8) ----------12.5% Glycerol (Sigma)----------10% 10% SDS (w/v) ----------20%	In house
5 X SDS-PAGE Gel Loading buffer	dH_20 0.5 M Tris (pH 6.8) ----------12.5% glycerol----------10% 10% SDS (w/v)----------20% 2β- Me----------5% 0.05%(w/v) BPB----------5%	In house
10 X Tris-Glycine-SDS (TGS)	0.25M Tris 1.92M Glycine 1% SDS dH_2O	Geneflow/In house
10 X Tris-Glycine-Methanol (TGM)	0.25M Tris 1.92M Glycine 20% Menthol (Fisher) dH_2O	Geneflow/ In house
10 X TBS	100 mM Tris (pH 8.0) 1.5 M NaCl dH_2O	In house

1 X TBS-T (1 litre)	100ml 10X TBS (Geneflow) 900ml dH_2O 0.1% Tween®20 (Sigma)	In house
4% Dried skimmed milk in TBS-T	2g dried skimmed milk (Marvel) 50 ml 1X TBS-T	In house
2.5% BSA in TBS-T	1.25g BSA (Fisher) 50 ml 1X TBS-T	In house
PBS	125mM NaCl (Fisher) 16mM $Na_2HPO_4.7H_20$ 10mM KH_2PO_4 HCL to Adjust pH 7.3-7.6	In house
PBS -T	1 x PBS buffer 0.1%-1.0% Tween-20	In house
0.05 M EDTA (Di sodium Ethylenediaminetetraacetic acid)	8.61 g EDTA (Sigma) 80 ml dH_2O Adjust pH to 8.0, Adjust volume to 100 ml	In house
TAE Electrophoresis buffer (50X stock solution)	242 g Tris-base 57.1 ml glacial acetic acid 100 ml 0.5 M EDTA (pH 8.0) Adjust volume to 1 litre	In house
1% agarose	1g agarose (Fisher) 100ml TAE buffer	In house
4% paraformaldehyde (v/v)	4ml paraformaldehyde (Fisher) 96 ml dH_2O	In house
0.2% Triton in PBS	98.8 ml 1 x PBS 200µl Triton	In house
Specific cell lysate for human chemokine and cytokine arrays	1% Igepal CA-630, 20 mM Tris-HCl (pH 8.0), 137 mM NaCl, 10% glycerol, 2 mM EDTA and tablet contains 10 µg/mL Aprotinin, 10 µg/mL Leupeptin, and 10 µg/mL Pepstatin.	In house
Luria Bertani (LB)	10g/L Tryptone, 5 g/L Yeast extract and 10 g/L NaCl	In house

Table 20: List of primers used during the thesis

Name	Sequence (5'-3')	Product Size	Purpose	Supplier
GAPDH-F	CAAGGTCATCCATGACAACTTTG	496 bp	Expression analysis	Sigma
GAPDH-R	GTCCACCACCCTGTTGCTGTAG			
CDH1-F	CACTCGGGCTGAGCTGGACAGGG	619 bp	Expression analysis	Sigma
CDH1-R	CCGGGTGTCATCCTCTGGG			
ZEB2-F	AAGATAGGTGGCGCGTGTTT	752 bp	Expression analysis	Sigma
ZEB2-R	CTGGCCCCATAGTGTCATAGTC			
Pol II-F	Not disclosed by supplier	180 bp	ChIP	Active Motif
Pol II-R	Not disclosed by supplier			
ERCC1-F	ATGGACCCTGGGAAGGAC	822 bp	Expression analysis /PCR	Sigma
ERCC1-R	TCAGGGTACTTTCAAGAAGGG			
ERCC1-P-Forward 1	TAGGAGCTCTTGGTCAACTTGAGACA ATTGG	1554 bp	Promoter/ Cloning	Sigma
ERCC1 Reverse	TGTAAGCTTACATTGACTTGGCTTCAG TTTCCTC			
ERCC1-P-Forward 2	TAGGAGCTCTCAGAACGGAACGGGAT TGATAAATAG	667 bp	Promoter / Cloning	Sigma
ERCC1- F1 EBOX 1-3	ACCAAGTTGGATCTCCTGCG	435 bp	PCR/ ChIP	Sigma
ERCC1-F2 EBOX 1-2	GTACAGAGATCGCCCTGCTC	267 bp	PCR/ChIP	Sigma
ERCC1-PR1	TCCATCTCTCAGACTCGGCA		PCR/ChIP	Sigma
CDH1-F E-box 4	ACCCTAGCAACTCCAGGCTA	224 bp	PCR/ChIP	Sigma
CDH1-R E- E-box 4	CAAGCTCACAGGTGCTTTGC		PCR/ChIP	Sigma
CDH1-F E-box 1-3	GTAATCCAACACTTCAGGAG	524	PCR/ChIP	Sigma
CDH1-R E-box 1-3	GCC TCT CTA GTA GCT GGG AG		PCR/ChIP	Sigma
EZH2-F1	AGATCGAGACCATCCTGGCT	300	qPCR	Sigma
EZH2-R1	TGGTCTCGAACTCCCGACTT			
EZH2-F2	CCACAGCTGAGCCGACC	264	qPCR	Sigma
EZH2-R2	GAGGATAGGTGGCGGGAACC			

Appendix

Table 21: Methodological detail of the FOLFOX resistance biomarker study reported in accordance with REMARK guidelines.

REMARK guidelines for biomarker reporting	
Biomarker examined	SIP1/ZEB2
Disease studied	Colorectal adenocarcinoma
Database	Prospective
Time period	2005-2013
Hypothesis	SIP1 expression prognosticates poor patient survival after adjuvant FOLFOX chemotherapy
Inclusion criteria	Primary colorectal adenocarcinoma + Surgical resection
Exclusion criteria	Synchronous metastasis at presentation
Treatment	Surgical resection + FOLFOX chemotherapy
Biological material	Paraffin embedded human tissue
Biomarker detection	Automated Immunohistochemistry / Leica XL Autostainer
Antibody	In-house/Rabbit/Polyclonal/1:750 dilution
Quality control	Antibody optimisation on uterine myometrium Positive Control – Fibroblasts / Uterine tissue / Tonsil Negative control – Normal colon
Scoring	2 independent blinded pathologists / Nuclear SIP1 staining / >10% of cancer cells / Positive or Negative
Median follow up	
Pilot study	36 months
Validation study	42 months
Clinical end points	Overall survival – time to death (Clinical records) from date of surgery Disease free survival – Radiological detection of recurrence from date of surgery. Distant recurrence – Radiological detection of metastasis outside the colon/rectum after surgery Local recurrence – Radiological evidence of recurrence in the colon or rectum after surgery
Cox regression model	Age, T stage, Node positivity, Differentiation, SIP1/ZEB2,

Table 22: Methodological detail of the SIP1/ZEB2 biomarker study reported in accordance with REMARK guidelines.

REMARK guidelines for biomarker reporting	
Biomarker examined	SIP1/ZEB2
Disease studied	Colorectal adenocarcinoma
Database	Prospective
Time period	2005-2013
Hypothesis	SIP1 expression prognosticates poor patient survival after adjuvant FOLFOX chemotherapy
Inclusion criteria	Primary colorectal adenocarcinoma + Surgical resection
Exclusion criteria	Synchronous metastasis at presentation
Treatment	Surgical resection + FOLFOX chemotherapy
Biological material	Paraffin embedded human tissue
Biomarker detection	Automated Immunohistochemistry / Leica XL Autostainer
Antibody	In-house/Rabbit/Polyclonal/1:750 dilution
Quality control	Antibody optimisation on uterine myometrium Positive Control – Fibroblasts / Uterine tissue / Tonsil Negative control – Normal colon
Scoring	2 independent blinded pathologists / Nuclear SIP1 staining / >10% of cancer cells / Positive or Negative
Median follow up	
Pilot study	36 months
Validation study	42 months
Clinical end points	Overall survival – time to death (Clinical records) from date of surgery Disease free survival – Radiological detection of recurrence from date of surgery. Distant recurrence – Radiological detection of metastasis outside the colon/rectum after surgery Local recurrence – Radiological evidence of recurrence in the colon or rectum after surgery
Cox regression model	Age, T stage, Node positivity, Differentiation, SIP1/ZEB2,

Table 23: List of cell lines used during PhD with source, morphology and depositor

Cell line	Organism	Source	Morphology	oncogene	Depositor	Supplier
CT26	*Mus musculus*	Undifferentiated colon carcinoma (BALB/c mouse)	Fibroblast/ adherent	Not known	(395)	ATCC® CCL2638™
Caco-2	*Homo sapiens*	Colorectal adenocarcinoma (Dukes' type ND^{o})	Epithelial /adherent	c-myc+; ras+; myb+; fos+; sis+; p53+abl- ; ros-; src-	(396, 397)	ATCC® HTB -37™
COLO205	*Homo sapiens*	Colorectal adenocarcinoma (Dukes' type D)	Epithelial mixed, adherent and suspension	c-myc+; ras+; myb+; fos+; sis+; p53+abl- ; ros-; src-	(397, 398)	ATCC® CCL 222™
DLD-1	*Homo sapiens*	Colorectal adenocarcinoma (Dukes' type C).	Epithelial/ adherent	c-myc+; ras+; myb+;fos+;sis+; p53+abl- ; ros-; src-	(397, 399, 400)	ATCC® CCL 221™
HCT116	*Homo sapiens*	Colorectal carcinoma	Epithelial with very few scattered mesenchymal cells/adherent	c-myc+; ras+; myb+; fos+; sis+; p53+abl- ; ros-; src- TGFβ1 and TGFβ2 Positive	(401)	ATCC® CCL -247™
HT29	*Homo sapiens*	Colorectal adenocarcinoma (Dukes' stage ND)	Epithelial / adherent	c-myc+; ras+; myb+; fos+; sis+; p53+abl- ; ros-; src-	(396, 397)1	ATCC® CCL -38™
LoVo	*Homo sapiens*	Colorectal adenocarcinoma Derived from a metastatic site (left supraclavicular region- Dukes' type ND)	Epithelial with many scattered mesenchymal cells/adherent	c-myc+; ras+; myb+; fos+; sis+; p53+abl- ; ros-; src-	(402)	ATCC® CCL229™
RKO	*Homo sapiens*	Poorly differentiated primary Colon carcinoma	Mesenchymal phenotype/ adherent	p53+	(403)	Packham Laboratory, University of Southampton- ATCC® CCL2577™
SW48	*Homo sapiens*	Colorectal adenocarcinoma (Dukes' typeC, grade IV)	Epithelial / adherent	c-myc+; ras+; myb+; fos+; sis+; p53+abl- ; ros-; src	(396, 397, 404)	ATCC® CCL 231™
SW480	*Homo sapiens*	Colorectal adenocarcinoma (Dukes' type B).	Mesenchymal	c-myc+; ras+; myb+; fos+; sis+;p53+abl- ros-; src	(396, 397) (405)	Not known
SW620	*Homo sapiens*	Colorectal adenocarcinoma Derived from a metastatic site (lymph node). The line was derived from the same tissue as SW480 (Dukes' type ND)	Epithelial with some scattered mesenchymal cells /adherent	c-myc+; ras+; myb+;fos+; sis+;p53+abl- ; ros-; src-	(396) (397, 405)	ATCC® CCL227™

Bibliography

1. Ferlay J, Parkin DM, Steliarova-Foucher E. Estimates of cancer incidence and mortality in Europe in 2008. European journal of cancer (Oxford, England : 1990). 2010;46(4):765-81.

2. Manfredi S, Bouvier AM, Lepage C, Hatem C, Dancourt V, Faivre J. Incidence and patterns of recurrence after resection for cure of colonic cancer in a well defined population. The British journal of surgery. 2006;93(9):1115-22.

3. Andre N, Schmiegel W. Chemoradiotherapy for colorectal cancer. Gut. 2005;54(8):1194-202.

4. Simmonds PC. Palliative chemotherapy for advanced colorectal cancer: systematic review and meta-analysis. Colorectal Cancer Collaborative Group. BMJ. 2000;321(7260):531-5.

5. Grothey A, Sargent D, Goldberg RM, Schmoll HJ. Survival of patients with advanced colorectal cancer improves with the availability of fluorouracil-leucovorin, irinotecan, and oxaliplatin in the course of treatment. Journal of clinical oncology : official journal of the American Society of Clinical Oncology. 2004;22(7):1209-14.

6. Cunningham D, Humblet Y, Siena S, Khayat D, Bleiberg H, Santoro A, et al. Cetuximab monotherapy and cetuximab plus irinotecan in irinotecan-refractory metastatic colorectal cancer. N Engl J Med. 2004;351(4):337-45.

7. Hsu HC, Thiam TK, Lu YJ, Yeh CY, Tsai WS, You JF, et al. Mutations of KRAS/NRAS/BRAF predict cetuximab resistance in metastatic colorectal cancer patients. Oncotarget. 2016;7(16):22257-70.

8. Wells K, Wise PE. Hereditary Colorectal Cancer Syndromes. The Surgical clinics of North America. 2017;97(3):605-25.

9. Kinzler KW, Vogelstein B. Lessons from hereditary colorectal cancer. Cell. 1996;87(2):159-70.

10. Markowitz SD, Bertagnolli MM. Molecular origins of cancer: Molecular basis of colorectal cancer. N Engl J Med. 2009;361(25):2449-60.

11. Vogelstein B, Fearon ER, Hamilton SR, Kern SE, Preisinger AC, Leppert M, et al. Genetic alterations during colorectal-tumor development. N Engl J Med. 1988;319(9):525-32.

12. Guillem JG, Puig-La Calle J, Jr., Cellini C, Murray M, Ng J, Fazzari M, et al. Varying features of early age-of-onset "sporadic" and hereditary nonpolyposis colorectal cancer patients. Diseases of the colon and rectum. 1999;42(1):36-42.

13. Vazquez A, Bond EE, Levine AJ, Bond GL. The genetics of the p53 pathway, apoptosis and cancer therapy. Nature reviews Drug discovery. 2008;7(12):979-87.

14. Sjoblom T, Jones S, Wood LD, Parsons DW, Lin J, Barber TD, et al. The consensus coding sequences of human breast and colorectal cancers. Science (New York, NY). 2006;314(5797):268-74.

15. Haq AI, Schneeweiss J, Kalsi V, Arya M. The Dukes staging system: a cornerstone in the clinical management of colorectal cancer. Lancet Oncol. 2009;10(11):1128.

16. Edge SB, Compton CC. The American Joint Committee on Cancer: the 7th edition of the AJCC cancer staging manual and the future of TNM. Ann Surg Oncol. 2010;17(6):1471-4.

17. Ueno H, Mochizuki H, Akagi Y, Kusumi T, Yamada K, Ikegami M, et al. Optimal colorectal cancer staging criteria in TNM classification. Journal of clinical oncology : official journal of the American Society of Clinical Oncology. 2012;30(13):1519-26.

18. Cunningham D, Atkin W, Lenz HJ, Lynch HT, Minsky B, Nordlinger B, et al. Colorectal cancer. Lancet (London, England). 2010;375(9719):1030-47.

19. Sargent D, Sobrero A, Grothey A, O'Connell MJ, Buyse M, Andre T, et al. Evidence for cure by adjuvant therapy in colon cancer: observations based on individual patient data from 20,898 patients on 18 randomized trials. Journal of clinical oncology : official journal of the American Society of Clinical Oncology. 2009;27(6):872-7.

20. Andre T, Boni C, Mounedji-Boudiaf L, Navarro M, Tabernero J, Hickish T, et al. Oxaliplatin, fluorouracil, and leucovorin as adjuvant treatment for colon cancer. N Engl J Med. 2004;350(23):2343-51.

21. Tsuji Y, Sugihara K. Adjuvant chemotherapy for colon cancer: the difference between Japanese and western strategies. Expert opinion on pharmacotherapy. 2016;17(6):783-90.

22. Brandi G, De Lorenzo S, Nannini M, Curti S, Ottone M, Dall'Olio FG, et al. Adjuvant chemotherapy for resected colorectal cancer metastases: Literature review and meta-analysis. World journal of gastroenterology. 2016;22(2):519-33.

23. Andre T, Boni C, Navarro M, Tabernero J, Hickish T, Topham C, et al. Improved overall survival with oxaliplatin, fluorouracil, and leucovorin as adjuvant treatment in stage II or III colon cancer in the MOSAIC trial. Journal of clinical oncology : official journal of the American Society of Clinical Oncology. 2009;27(19):3109-16.

24. de Gramont A, Tournigand C, Andre T, Larsen AK, Louvet C. Targeted agents for adjuvant therapy of colon cancer. Seminars in oncology. 2006;33(6 Suppl 11):S42-5.

25. de Gramont A, Van Cutsem E, Schmoll HJ, Tabernero J, Clarke S, Moore MJ, et al. Bevacizumab plus oxaliplatin-based chemotherapy as adjuvant treatment for colon cancer (AVANT): a phase 3 randomised controlled trial. Lancet Oncol. 2012;13(12):1225-33.

26. Van Cutsem E, Labianca R, Bodoky G, Barone C, Aranda E, Nordlinger B, et al. Randomized phase III trial comparing biweekly infusional fluorouracil/leucovorin alone or with irinotecan in the adjuvant treatment of stage III colon cancer: PETACC-3. Journal of clinical oncology : official journal of the American Society of Clinical Oncology. 2009;27(19):3117-25.

27. McCall JL, Cox MR, Wattchow DA. Analysis of local recurrence rates after surgery alone for rectal cancer. International journal of colorectal disease. 1995;10(3):126-32.

28. Adjuvant radiotherapy for rectal cancer: a systematic overview of 8,507 patients from 22 randomised trials. Lancet (London, England). 2001;358(9290):1291-304.

29. Thomas PR, Lindblad AS. Adjuvant postoperative radiotherapy and chemotherapy in rectal carcinoma: a review of the Gastrointestinal Tumor Study Group experience. Radiotherapy and oncology : journal of the European Society for Therapeutic Radiology and Oncology. 1988;13(4):245-52.

30. Bosset JF, Calais G, Mineur L, Maingon P, Stojanovic-Rundic S, Bensadoun RJ, et al. Fluorouracil-based adjuvant chemotherapy after preoperative chemoradiotherapy in rectal cancer: long-term results of the EORTC 22921 randomised study. Lancet Oncol. 2014;15(2):184-90.

31. Gerard JP, Conroy T, Bonnetain F, Bouche O, Chapet O, Closon-Dejardin MT, et al. Preoperative radiotherapy with or without concurrent fluorouracil and leucovorin in T3-4

rectal cancers: results of FFCD 9203. Journal of clinical oncology : official journal of the American Society of Clinical Oncology. 2006;24(28):4620-5.

32. Smith CA, Kachnic LA. Evolving Role of Radiotherapy in the Management of Rectal Carcinoma. Surgical oncology clinics of North America. 2017;26(3):455-66.

33. Guinney J, Dienstmann R, Wang X, de Reynies A, Schlicker A, Soneson C, et al. The consensus molecular subtypes of colorectal cancer. Nature medicine. 2015;21(11):1350-6.

34. Roth AD, Delorenzi M, Tejpar S, Yan P, Klingbiel D, Fiocca R, et al. Integrated analysis of molecular and clinical prognostic factors in stage II/III colon cancer. Journal of the National Cancer Institute. 2012;104(21):1635-46.

35. Liebig C, Ayala G, Wilks J, Verstovsek G, Liu H, Agarwal N, et al. Perineural invasion is an independent predictor of outcome in colorectal cancer. Journal of clinical oncology : official journal of the American Society of Clinical Oncology. 2009;27(31):5131-7.

36. Dienstmann R, Mason MJ, Sinicrope FA, Phipps AI, Tejpar S, Nesbakken A, et al. Prediction of overall survival in stage II and III colon cancer beyond TNM system: a retrospective, pooled biomarker study. Annals of oncology : official journal of the European Society for Medical Oncology. 2017;28(5):1023-31.

37. Vilar E, Tabernero J. Molecular dissection of microsatellite instable colorectal cancer. Cancer discovery. 2013;3(5):502-11.

38. Dienstmann R, Salazar R, Tabernero J. Personalizing colon cancer adjuvant therapy: selecting optimal treatments for individual patients. Journal of clinical oncology : official journal of the American Society of Clinical Oncology. 2015;33(16):1787-96.

39. Bokemeyer C, Van Cutsem E, Rougier P, Ciardiello F, Heeger S, Schlichting M, et al. Addition of cetuximab to chemotherapy as first-line treatment for KRAS wild-type metastatic colorectal cancer: pooled analysis of the CRYSTAL and OPUS randomised clinical trials. European journal of cancer (Oxford, England : 1990). 2012;48(10):1466-75.

40. Sievers CK, Kratz JD, Zurbriggen LD, LoConte NK, Lubner SJ, Uboha N, et al. The Multidisciplinary Management of Colorectal Cancer: Present and Future Paradigms. Clinics in colon and rectal surgery. 2016;29(3):232-8.

41. Bokemeyer C, Bondarenko I, Hartmann JT, de Braud F, Schuch G, Zubel A, et al. Efficacy according to biomarker status of cetuximab plus FOLFOX-4 as first-line treatment

for metastatic colorectal cancer: the OPUS study. Annals of oncology : official journal of the European Society for Medical Oncology. 2011;22(7):1535-46.

42. Roepman P, Schlicker A, Tabernero J, Majewski I, Tian S, Moreno V, et al. Colorectal cancer intrinsic subtypes predict chemotherapy benefit, deficient mismatch repair and epithelial-to-mesenchymal transition. International journal of cancer. 2014;134(3):552-62.

43. Kroepil F, Fluegen G, Vallbohmer D, Baldus SE, Dizdar L, Raffel AM, et al. Snail1 expression in colorectal cancer and its correlation with clinical and pathological parameters. BMC cancer. 2013;13:145.

44. Kalluri R, Weinberg RA. The basics of epithelial-mesenchymal transition. The Journal of clinical investigation. 2009;119(6):1420-8.

45. Coghlin C, Murray GI. Current and emerging concepts in tumour metastasis. The Journal of pathology. 2010;222(1):1-15.

46. Klein CA. Cancer. The metastasis cascade. Science (New York, NY). 2008;321(5897):1785-7.

47. Podsypanina K, Du YC, Jechlinger M, Beverly LJ, Hambardzumyan D, Varmus H. Seeding and propagation of untransformed mouse mammary cells in the lung. Science (New York, NY). 2008;321(5897):1841-4.

48. Friedl P, Wolf K. Tumour-cell invasion and migration: diversity and escape mechanisms. Nature reviews Cancer. 2003;3(5):362-74.

49. Ye X, Weinberg RA. Epithelial-Mesenchymal Plasticity: A Central Regulator of Cancer Progression. Trends in cell biology. 2015;25(11):675-86.

50. Yang J, Mani SA, Donaher JL, Ramaswamy S, Itzykson RA, Come C, et al. Twist, a master regulator of morphogenesis, plays an essential role in tumor metastasis. Cell. 2004;117(7):927-39.

51. Cavallaro U, Christofori G. Cell adhesion in tumor invasion and metastasis: loss of the glue is not enough. Biochimica et biophysica acta. 2001;1552(1):39-45.

52. Yang J, Weinberg RA. Epithelial-mesenchymal transition: at the crossroads of development and tumor metastasis. Developmental cell. 2008;14(6):818-29.

53. Nieto MA, Huang RY, Jackson RA, Thiery JP. EMT: 2016. Cell. 2016;166(1):21-45.

54. Sun D, Baur S, Hay ED. Epithelial-mesenchymal transformation is the mechanism for fusion of the craniofacial primordia involved in morphogenesis of the chicken lip. Developmental biology. 2000;228(2):337-49.

55. Thiery JP, Sleeman JP. Complex networks orchestrate epithelial-mesenchymal transitions. Nature reviews Molecular cell biology. 2006;7(2):131-42.

56. Thiery JP, Lim CT. Tumor dissemination: an EMT affair. Cancer cell. 2013;23(3):272-3.

57. Lamouille S, Xu J, Derynck R. Molecular mechanisms of epithelial-mesenchymal transition. Nature reviews Molecular cell biology. 2014;15(3):178-96.

58. Thiery JP. Epithelial-mesenchymal transitions in tumour progression. Nature reviews Cancer. 2002;2(6):442-54.

59. Yu Y, Elble RC. Homeostatic Signaling by Cell-Cell Junctions and Its Dysregulation during Cancer Progression. Journal of clinical medicine. 2016;5(2).

60. Perez-Moreno M, Jamora C, Fuchs E. Sticky business: orchestrating cellular signals at adherens junctions. Cell. 2003;112(4):535-48.

61. Shih W, Yamada S. N-cadherin-mediated cell-cell adhesion promotes cell migration in a three-dimensional matrix. Journal of cell science. 2012;125(Pt 15):3661-70.

62. Kotb AM, Hierholzer A, Kemler R. Replacement of E-cadherin by N-cadherin in the mammary gland leads to fibrocystic changes and tumor formation. Breast cancer research : BCR. 2011;13(5):R104.

63. Zhang J, Tian XJ, Xing J. Signal Transduction Pathways of EMT Induced by TGF-beta, SHH, and WNT and Their Crosstalks. Journal of clinical medicine. 2016;5(4).

64. Tam WL, Weinberg RA. The epigenetics of epithelial-mesenchymal plasticity in cancer. Nature medicine. 2013;19(11):1438-49.

65. Kahlert C, Lahes S, Radhakrishnan P, Dutta S, Mogler C, Herpel E, et al. Overexpression of ZEB2 at the invasion front of colorectal cancer is an independent prognostic marker and regulates tumor invasion in vitro. Clinical cancer research : an official journal of the American Association for Cancer Research. 2011;17(24):7654-63.

66. Sayan AE, Griffiths TR, Pal R, Browne GJ, Ruddick A, Yagci T, et al. SIP1 protein protects cells from DNA damage-induced apoptosis and has independent prognostic

value in bladder cancer. Proceedings of the National Academy of Sciences of the United States of America. 2009;106(35):14884-9.

67. Lamouille S, Subramanyam D, Blelloch R, Derynck R. Regulation of epithelial-mesenchymal and mesenchymal-epithelial transitions by microRNAs. Current opinion in cell biology. 2013;25(2):200-7.

68. Ikenouchi J, Matsuda M, Furuse M, Tsukita S. Regulation of tight junctions during the epithelium-mesenchyme transition: direct repression of the gene expression of claudins/occludin by Snail. Journal of cell science. 2003;116(Pt 10):1959-67.

69. Dhawan P, Singh AB, Deane NG, No Y, Shiou SR, Schmidt C, et al. Claudin-1 regulates cellular transformation and metastatic behavior in colon cancer. The Journal of clinical investigation. 2005;115(7):1765-76.

70. Osanai M, Murata M, Chiba H, Kojima T, Sawada N. Epigenetic silencing of claudin-6 promotes anchorage-independent growth of breast carcinoma cells. Cancer science. 2007;98(10):1557-62.

71. Hewitt KJ, Agarwal R, Morin PJ. The claudin gene family: expression in normal and neoplastic tissues. BMC cancer. 2006;6:186.

72. Beeman NE, Baumgartner HK, Webb PG, Schaack JB, Neville MC. Disruption of occludin function in polarized epithelial cells activates the extrinsic pathway of apoptosis leading to cell extrusion without loss of transepithelial resistance. BMC cell biology. 2009;10:85.

73. Mamuya FA, Duncan MK. aV integrins and TGF-beta-induced EMT: a circle of regulation. Journal of cellular and molecular medicine. 2012;16(3):445-55.

74. Cochard P, Paulin D. Initial expression of neurofilaments and vimentin in the central and peripheral nervous system of the mouse embryo in vivo. The Journal of neuroscience : the official journal of the Society for Neuroscience. 1984;4(8):2080-94.

75. Dellagi K, Vainchenker W, Vinci G, Paulin D, Brouet JC. Alteration of vimentin intermediate filament expression during differentiation of human hemopoietic cells. The EMBO journal. 1983;2(9):1509-14.

76. Hu L, Lau SH, Tzang CH, Wen JM, Wang W, Xie D, et al. Association of Vimentin overexpression and hepatocellular carcinoma metastasis. Oncogene. 2004;23(1):298-302.

77. Raymond WA, Leong AS. Vimentin--a new prognostic parameter in breast carcinoma? The Journal of pathology. 1989;158(2):107-14.

78. Satelli A, Li S. Vimentin in cancer and its potential as a molecular target for cancer therapy. Cellular and molecular life sciences : CMLS. 2011;68(18):3033-46.

79. Huang L, Xu AM, Liu S, Liu W, Li TJ. Cancer-associated fibroblasts in digestive tumors. World journal of gastroenterology. 2014;20(47):17804-18.

80. Pan B, Liao Q, Niu Z, Zhou L, Zhao Y. Cancer-associated fibroblasts in pancreatic adenocarcinoma. Future oncology (London, England). 2015;11(18):2603-10.

81. Le Bras GF, Taubenslag KJ, Andl CD. The regulation of cell-cell adhesion during epithelial-mesenchymal transition, motility and tumor progression. Cell adhesion & migration. 2012;6(4):365-73.

82. Polette M, Mestdagt M, Bindels S, Nawrocki-Raby B, Hunziker W, Foidart JM, et al. Beta-catenin and ZO-1: shuttle molecules involved in tumor invasion-associated epithelial-mesenchymal transition processes. Cells, tissues, organs. 2007;185(1-3):61-5.

83. Homberg M, Magin TM. Beyond expectations: novel insights into epidermal keratin function and regulation. International review of cell and molecular biology. 2014;311:265-306.

84. Toivola DM, Boor P, Alam C, Strnad P. Keratins in health and disease. Current opinion in cell biology. 2015;32:73-81.

85. Gurzu S, Jung I. Aberrant pattern of the cytokeratin 7/cytokeratin 20 immunophenotype in colorectal adenocarcinomas with BRAF mutations. Pathology, research and practice. 2012;208(3):163-6.

86. Khan FM, Komarla AR, Mendoza PG, Bodenheimer HC, Jr., Theise ND. Keratin 19 demonstration of canal of Hering loss in primary biliary cirrhosis: "minimal change PBC"? Hepatology (Baltimore, Md). 2013;57(2):700-7.

87. Fortier AM, Asselin E, Cadrin M. Keratin 8 and 18 loss in epithelial cancer cells increases collective cell migration and cisplatin sensitivity through claudin1 up-regulation. The Journal of biological chemistry. 2013;288(16):11555-71.

88. Kim HJ, Choi WJ, Lee CH. Phosphorylation and Reorganization of Keratin Networks: Implications for Carcinogenesis and Epithelial Mesenchymal Transition. Biomolecules & therapeutics. 2015;23(4):301-12.

89. Haws HJ, McNeil MA, Hansen MD. Control of cell mechanics by RhoA and calcium fluxes during epithelial scattering. Tissue barriers. 2016;4(3):e1187326.

90. Diepenbruck M, Christofori G. Epithelial-mesenchymal transition (EMT) and metastasis: yes, no, maybe? Current opinion in cell biology. 2016;43:7-13.

91. Husemann Y, Geigl JB, Schubert F, Musiani P, Meyer M, Burghart E, et al. Systemic spread is an early step in breast cancer. Cancer cell. 2008;13(1):58-68.

92. Perl AK, Wilgenbus P, Dahl U, Semb H, Christofori G. A causal role for E-cadherin in the transition from adenoma to carcinoma. Nature. 1998;392(6672):190-3.

93. Derksen PW, Liu X, Saridin F, van der Gulden H, Zevenhoven J, Evers B, et al. Somatic inactivation of E-cadherin and p53 in mice leads to metastatic lobular mammary carcinoma through induction of anoikis resistance and angiogenesis. Cancer cell. 2006;10(5):437-49.

94. Ota I, Li XY, Hu Y, Weiss SJ. Induction of a MT1-MMP and MT2-MMP-dependent basement membrane transmigration program in cancer cells by Snail1. Proceedings of the National Academy of Sciences of the United States of America. 2009;106(48):20318-23.

95. Murphy DA, Courtneidge SA. The 'ins' and 'outs' of podosomes and invadopodia: characteristics, formation and function. Nature reviews Molecular cell biology. 2011;12(7):413-26.

96. Drake JM, Strohbehn G, Bair TB, Moreland JG, Henry MD. ZEB1 enhances transendothelial migration and represses the epithelial phenotype of prostate cancer cells. Molecular biology of the cell. 2009;20(8):2207-17.

97. Rhim AD, Mirek ET, Aiello NM, Maitra A, Bailey JM, McAllister F, et al. EMT and dissemination precede pancreatic tumor formation. Cell. 2012;148(1-2):349-61.

98. Tsai JH, Donaher JL, Murphy DA, Chau S, Yang J. Spatiotemporal regulation of epithelial-mesenchymal transition is essential for squamous cell carcinoma metastasis. Cancer cell. 2012;22(6):725-36.

99. Tsai JH, Yang J. Epithelial-mesenchymal plasticity in carcinoma metastasis. Genes & development. 2013;27(20):2192-206.

100. Stoletov K, Kato H, Zardouzian E, Kelber J, Yang J, Shattil S, et al. Visualizing extravasation dynamics of metastatic tumor cells. Journal of cell science. 2010;123(Pt 13):2332-41.

101. Mejlvang J, Kriajevska M, Vandewalle C, Chernova T, Sayan AE, Berx G, et al. Direct repression of cyclin D1 by SIP1 attenuates cell cycle progression in cells undergoing an epithelial mesenchymal transition. Molecular biology of the cell. 2007;18(11):4615-24.

102. Ocana OH, Corcoles R, Fabra A, Moreno-Bueno G, Acloque H, Vega S, et al. Metastatic colonization requires the repression of the epithelial-mesenchymal transition inducer Prrx1. Cancer cell. 2012;22(6):709-24.

103. Yamada S, Okumura N, Wei L, Fuchs BC, Fujii T, Sugimoto H, et al. Epithelial to mesenchymal transition is associated with shorter disease-free survival in hepatocellular carcinoma. Ann Surg Oncol. 2014;21(12):3882-90.

104. Busch EL, McGraw KA, Sandler RS. The potential for markers of epithelial-mesenchymal transition to improve colorectal cancer outcomes: a systematic review. Cancer epidemiology, biomarkers & prevention : a publication of the American Association for Cancer Research, cosponsored by the American Society of Preventive Oncology. 2014;23(7):1164-75.

105. Tan TZ, Miow QH, Miki Y, Noda T, Mori S, Huang RY, et al. Epithelial-mesenchymal transition spectrum quantification and its efficacy in deciphering survival and drug responses of cancer patients. EMBO molecular medicine. 2014;6(10):1279-93.

106. Grosse-Wilde A, Fouquier d'Herouel A, McIntosh E, Ertaylan G, Skupin A, Kuestner RE, et al. Stemness of the hybrid Epithelial/Mesenchymal State in Breast Cancer and Its Association with Poor Survival. PloS one. 2015;10(5):e0126522.

107. Zheng X, Carstens JL, Kim J, Scheible M, Kaye J, Sugimoto H, et al. Epithelial-to-mesenchymal transition is dispensable for metastasis but induces chemoresistance in pancreatic cancer. Nature. 2015;527(7579):525-30.

108. Fischer KR, Durrans A, Lee S, Sheng J, Li F, Wong ST, et al. Epithelial-to-mesenchymal transition is not required for lung metastasis but contributes to chemoresistance. Nature. 2015;527(7579):472-6.

109. Findlay VJ, Wang C, Watson DK, Camp ER. Epithelial-to-mesenchymal transition and the cancer stem cell phenotype: insights from cancer biology with therapeutic implications for colorectal cancer. Cancer gene therapy. 2014;21(5):181-7.

110. Mani SA, Guo W, Liao MJ, Eaton EN, Ayyanan A, Zhou AY, et al. The epithelial-mesenchymal transition generates cells with properties of stem cells. Cell. 2008;133(4):704-15.

111. Beerling E, Seinstra D, de Wit E, Kester L, van der Velden D, Maynard C, et al. Plasticity between Epithelial and Mesenchymal States Unlinks EMT from Metastasis-Enhancing Stem Cell Capacity. Cell reports. 2016;14(10):2281-8.

112. Krebs AM, Mitschke J, Lasierra Losada M, Schmalhofer O, Boerries M, Busch H, et al. The EMT-activator Zeb1 is a key factor for cell plasticity and promotes metastasis in pancreatic cancer. Nature cell biology. 2017;19(5):518-29.

113. Sommers CL, Heckford SE, Skerker JM, Worland P, Torri JA, Thompson EW, et al. Loss of epithelial markers and acquisition of vimentin expression in adriamycin- and vinblastine-resistant human breast cancer cell lines. Cancer research. 1992;52(19):5190-7.

114. Deng J, Wang L, Chen H, Hao J, Ni J, Chang L, et al. Targeting epithelial-mesenchymal transition and cancer stem cells for chemoresistant ovarian cancer. Oncotarget. 2016.

115. Gupta PB, Onder TT, Jiang G, Tao K, Kuperwasser C, Weinberg RA, et al. Identification of selective inhibitors of cancer stem cells by high-throughput screening. Cell. 2009;138(4):645-59.

116. Wang Y, Ngo VN, Marani M, Yang Y, Wright G, Staudt LM, et al. Critical role for transcriptional repressor Snail2 in transformation by oncogenic RAS in colorectal carcinoma cells. Oncogene. 2010;29(33):4658-70.

117. Yang AD, Fan F, Camp ER, van Buren G, Liu W, Somcio R, et al. Chronic oxaliplatin resistance induces epithelial-to-mesenchymal transition in colorectal cancer cell lines. Clinical cancer research : an official journal of the American Association for Cancer Research. 2006;12(14 Pt 1):4147-53.

118. Singh A, Settleman J. EMT, cancer stem cells and drug resistance: an emerging axis of evil in the war on cancer. Oncogene. 2010;29(34):4741-51.

119. Cao H, Xu E, Liu H, Wan L, Lai M. Epithelial-mesenchymal transition in colorectal cancer metastasis: A system review. Pathology, research and practice. 2015;211(8):557-69.

120. Zhang P, Sun Y, Ma L. ZEB1: at the crossroads of epithelial-mesenchymal transition, metastasis and therapy resistance. Cell cycle (Georgetown, Tex). 2015;14(4):481-7.

121. Lee HJ, Li CF, Ruan D, Powers S, Thompson PA, Frohman MA, et al. The DNA Damage Transducer RNF8 Facilitates Cancer Chemoresistance and Progression through Twist Activation. Molecular cell. 2016;63(6):1021-33.

122. Kajiyama H, Shibata K, Terauchi M, Yamashita M, Ino K, Nawa A, et al. Chemoresistance to paclitaxel induces epithelial-mesenchymal transition and enhances metastatic potential for epithelial ovarian carcinoma cells. International journal of oncology. 2007;31(2):277-83.

123. Teicher BA, Holden SA, Ara G, Chen G. Transforming growth factor-beta in in vivo resistance. Cancer chemotherapy and pharmacology. 1996;37(6):601-9.

124. Wu Y, Ginther C, Kim J, Mosher N, Chung S, Slamon D, et al. Expression of Wnt3 activates Wnt/beta-catenin pathway and promotes EMT-like phenotype in trastuzumab-resistant HER2-overexpressing breast cancer cells. Molecular cancer research : MCR. 2012;10(12):1597-606.

125. Galluzzi L, Vitale I, Michels J, Brenner C, Szabadkai G, Harel-Bellan A, et al. Systems biology of cisplatin resistance: past, present and future. Cell death & disease. 2014;5:e1257.

126. Tsou SH, Hou MH, Hsu LC, Chen TM, Chen YH. Gain-of-function p53 mutant with 21-bp deletion confers susceptibility to multidrug resistance in MCF-7 cells. International journal of molecular medicine. 2016;37(1):233-42.

127. Saxena M, Stephens MA, Pathak H, Rangarajan A. Transcription factors that mediate epithelial-mesenchymal transition lead to multidrug resistance by upregulating ABC transporters. Cell death & disease. 2011;2:e179.

128. Chung YH, Kim D. Enhanced TLR4 Expression on Colon Cancer Cells After Chemotherapy Promotes Cell Survival and Epithelial-Mesenchymal Transition Through Phosphorylation of GSK3beta. Anticancer research. 2016;36(7):3383-94.

129. Huang L, Fu L. Mechanisms of resistance to EGFR tyrosine kinase inhibitors. Acta pharmaceutica Sinica B. 2015;5(5):390-401.

130. Hou J, Zhou Z, Chen X, Zhao R, Yang Z, Wei N, et al. HER2 reduces breast cancer radiosensitivity by activating focal adhesion kinase in vitro and in vivo. Oncotarget. 2016.

131. Huang RY, Wong MK, Tan TZ, Kuay KT, Ng AH, Chung VY, et al. An EMT spectrum defines an anoikis-resistant and spheroidogenic intermediate mesenchymal state that is sensitive to e-cadherin restoration by a src-kinase inhibitor, saracatinib (AZD0530). Cell death & disease. 2013;4:e915.

132. Halbleib JM, Nelson WJ. Cadherins in development: cell adhesion, sorting, and tissue morphogenesis. Genes & development. 2006;20(23):3199-214.

133. Chu YS, Eder O, Thomas WA, Simcha I, Pincet F, Ben-Ze'ev A, et al. Prototypical type I E-cadherin and type II cadherin-7 mediate very distinct adhesiveness through their extracellular domains. The Journal of biological chemistry. 2006;281(5):2901-10.

134. Grande MT, Sanchez-Laorden B, Lopez-Blau C, De Frutos CA, Boutet A, Arevalo M, et al. Snail1-induced partial epithelial-to-mesenchymal transition drives renal fibrosis in mice and can be targeted to reverse established disease. Nature medicine. 2015;21(9):989-97.

135. Chang JT, Mani SA. Sheep, wolf, or werewolf: cancer stem cells and the epithelial-to-mesenchymal transition. Cancer letters. 2013;341(1):16-23.

136. Reya T, Morrison SJ, Clarke MF, Weissman IL. Stem cells, cancer, and cancer stem cells. Nature. 2001;414(6859):105-11.

137. Ginestier C, Hur MH, Charafe-Jauffret E, Monville F, Dutcher J, Brown M, et al. ALDH1 is a marker of normal and malignant human mammary stem cells and a predictor of poor clinical outcome. Cell stem cell. 2007;1(5):555-67.

138. Wellner U, Schubert J, Burk UC, Schmalhofer O, Zhu F, Sonntag A, et al. The EMT-activator ZEB1 promotes tumorigenicity by repressing stemness-inhibiting microRNAs. Nature cell biology. 2009;11(12):1487-95.

139. Hwang WL, Jiang JK, Yang SH, Huang TS, Lan HY, Teng HW, et al. MicroRNA-146a directs the symmetric division of Snail-dominant colorectal cancer stem cells. Nature cell biology. 2014;16(3):268-80.

140. Calon A, Lonardo E, Berenguer-Llergo A, Espinet E, Hernando-Momblona X, Iglesias M, et al. Stromal gene expression defines poor-prognosis subtypes in colorectal cancer. Nature genetics. 2015;47(4):320-9.

141. Lau EY, Lo J, Cheng BY, Ma MK, Lee JM, Ng JK, et al. Cancer-Associated Fibroblasts Regulate Tumor-Initiating Cell Plasticity in Hepatocellular Carcinoma through c-Met/FRA1/HEY1 Signaling. Cell reports. 2016;15(6):1175-89.

142. Li R, Liang J, Ni S, Zhou T, Qing X, Li H, et al. A mesenchymal-to-epithelial transition initiates and is required for the nuclear reprogramming of mouse fibroblasts. Cell stem cell. 2010;7(1):51-63.

143. Huang RY, Guilford P, Thiery JP. Early events in cell adhesion and polarity during epithelial-mesenchymal transition. Journal of cell science. 2012;125(Pt 19):4417-22.

144. Diaz-Lopez A, Moreno-Bueno G, Cano A. Role of microRNA in epithelial to mesenchymal transition and metastasis and clinical perspectives. Cancer management and research. 2014;6:205-16.

145. Puisieux A, Brabletz T, Caramel J. Oncogenic roles of EMT-inducing transcription factors. Nature cell biology. 2014;16(6):488-94.

146. Kim NH, Kim HS, Li XY, Lee I, Choi HS, Kang SE, et al. A p53/miRNA-34 axis regulates Snail1-dependent cancer cell epithelial-mesenchymal transition. The Journal of cell biology. 2011;195(3):417-33.

147. Warzecha CC, Carstens RP. Complex changes in alternative pre-mRNA splicing play a central role in the epithelial-to-mesenchymal transition (EMT). Seminars in cancer biology. 2012;22(5-6):417-27.

148. Bonomi S, di Matteo A, Buratti E, Cabianca DS, Baralle FE, Ghigna C, et al. HnRNP A1 controls a splicing regulatory circuit promoting mesenchymal-to-epithelial transition. Nucleic acids research. 2013;41(18):8665-79.

149. Braeutigam C, Rago L, Rolke A, Waldmeier L, Christofori G, Winter J. The RNA-binding protein Rbfox2: an essential regulator of EMT-driven alternative splicing and a mediator of cellular invasion. Oncogene. 2014;33(9):1082-92.

150. Conn SJ, Pillman KA, Toubia J, Conn VM, Salmanidis M, Phillips CA, et al. The RNA binding protein quaking regulates formation of circRNAs. Cell. 2015;160(6):1125-34.

151. Herranz N, Pasini D, Diaz VM, Franci C, Gutierrez A, Dave N, et al. Polycomb complex 2 is required for E-cadherin repression by the Snail1 transcription factor. Molecular and cellular biology. 2008;28(15):4772-81.

152. Lin T, Ponn A, Hu X, Law BK, Lu J. Requirement of the histone demethylase LSD1 in Snai1-mediated transcriptional repression during epithelial-mesenchymal transition. Oncogene. 2010;29(35):4896-904.

153. Millanes-Romero A, Herranz N, Perrera V, Iturbide A, Loubat-Casanovas J, Gil J, et al. Regulation of heterochromatin transcription by Snail1/LOXL2 during epithelial-to-mesenchymal transition. Molecular cell. 2013;52(5):746-57.

154. Peinado H, Ballestar E, Esteller M, Cano A. Snail mediates E-cadherin repression by the recruitment of the Sin3A/histone deacetylase 1 (HDAC1)/HDAC2 complex. Molecular and cellular biology. 2004;24(1):306-19.

155. Spaderna S, Schmalhofer O, Wahlbuhl M, Dimmler A, Bauer K, Sultan A, et al. The transcriptional repressor ZEB1 promotes metastasis and loss of cell polarity in cancer. Cancer research. 2008;68(2):537-44.

156. Chaffer CL, Marjanovic ND, Lee T, Bell G, Kleer CG, Reinhardt F, et al. Poised chromatin at the ZEB1 promoter enables breast cancer cell plasticity and enhances tumorigenicity. Cell. 2013;154(1):61-74.

157. Hong J, Zhou J, Fu J, He T, Qin J, Wang L, et al. Phosphorylation of serine 68 of Twist1 by MAPKs stabilizes Twist1 protein and promotes breast cancer cell invasiveness. Cancer research. 2011;71(11):3980-90.

158. Zhou BP, Deng J, Xia W, Xu J, Li YM, Gunduz M, et al. Dual regulation of Snail by GSK-3beta-mediated phosphorylation in control of epithelial-mesenchymal transition. Nature cell biology. 2004;6(10):931-40.

159. Barrallo-Gimeno A, Nieto MA. The Snail genes as inducers of cell movement and survival: implications in development and cancer. Development (Cambridge, England). 2005;132(14):3151-61.

160. Peinado H, Olmeda D, Cano A. Snail, Zeb and bHLH factors in tumour progression: an alliance against the epithelial phenotype? Nature reviews Cancer. 2007;7(6):415-28.

161. Tong ZT, Cai MY, Wang XG, Kong LL, Mai SJ, Liu YH, et al. EZH2 supports nasopharyngeal carcinoma cell aggressiveness by forming a co-repressor complex with HDAC1/HDAC2 and Snail to inhibit E-cadherin. Oncogene. 2012;31(5):583-94.

162. Dong C, Wu Y, Wang Y, Wang C, Kang T, Rychahou PG, et al. Interaction with Suv39H1 is critical for Snail-mediated E-cadherin repression in breast cancer. Oncogene. 2013;32(11):1351-62.

163. Bernstein BE, Mikkelsen TS, Xie X, Kamal M, Huebert DJ, Cuff J, et al. A bivalent chromatin structure marks key developmental genes in embryonic stem cells. Cell. 2006;125(2):315-26.

164. Wu Y, Evers BM, Zhou BP. Small C-terminal domain phosphatase enhances snail activity through dephosphorylation. The Journal of biological chemistry. 2009;284(1):640-8.

165. Jorda M, Olmeda D, Vinyals A, Valero E, Cubillo E, Llorens A, et al. Upregulation of MMP-9 in MDCK epithelial cell line in response to expression of the Snail transcription factor. Journal of cell science. 2005;118(Pt 15):3371-85.

166. Vincent T, Neve EP, Johnson JR, Kukalev A, Rojo F, Albanell J, et al. A SNAIL1-SMAD3/4 transcriptional repressor complex promotes TGF-beta mediated epithelial-mesenchymal transition. Nature cell biology. 2009;11(8):943-50.

167. De Craene B, Berx G. Regulatory networks defining EMT during cancer initiation and progression. Nature reviews Cancer. 2013;13(2):97-110.

168. Yang F, Sun L, Li Q, Han X, Lei L, Zhang H, et al. SET8 promotes epithelial-mesenchymal transition and confers TWIST dual transcriptional activities. The EMBO journal. 2012;31(1):110-23.

169. Yang MH, Hsu DS, Wang HW, Wang HJ, Lan HY, Yang WH, et al. Bmi1 is essential in Twist1-induced epithelial-mesenchymal transition. Nature cell biology. 2010;12(10):982-92.

170. Yang MH, Wu MZ, Chiou SH, Chen PM, Chang SY, Liu CJ, et al. Direct regulation of TWIST by HIF-1alpha promotes metastasis. Nature cell biology. 2008;10(3):295-305.

171. Farge E. Mechanical induction of Twist in the Drosophila foregut/stomodeal primordium. Current biology : CB. 2003;13(16):1365-77.

172. Kang Y, Chen CR, Massague J. A self-enabling TGFbeta response coupled to stress signaling: Smad engages stress response factor ATF3 for Id1 repression in epithelial cells. Molecular cell. 2003;11(4):915-26.

173. Xu J, Lamouille S, Derynck R. TGF-beta-induced epithelial to mesenchymal transition. Cell research. 2009;19(2):156-72.

174. Dave N, Guaita-Esteruelas S, Gutarra S, Frias A, Beltran M, Peiro S, et al. Functional cooperation between Snail1 and twist in the regulation of ZEB1 expression during epithelial to mesenchymal transition. The Journal of biological chemistry. 2011;286(14):12024-32.

175. Sanchez-Tillo E, Lazaro A, Torrent R, Cuatrecasas M, Vaquero EC, Castells A, et al. ZEB1 represses E-cadherin and induces an EMT by recruiting the SWI/SNF chromatin-remodeling protein BRG1. Oncogene. 2010;29(24):3490-500.

176. Postigo AA, Depp JL, Taylor JJ, Kroll KL. Regulation of Smad signaling through a differential recruitment of coactivators and corepressors by ZEB proteins. The EMBO journal. 2003;22(10):2453-62.

177. Liu Y, Sanchez-Tillo E, Lu X, Huang L, Clem B, Telang S, et al. The ZEB1 transcription factor acts in a negative feedback loop with miR200 downstream of Ras and Rb1 to regulate Bmi1 expression. The Journal of biological chemistry. 2014;289(7):4116-25.

178. Hill L, Browne G, Tulchinsky E. ZEB/miR-200 feedback loop: at the crossroads of signal transduction in cancer. International journal of cancer. 2013;132(4):745-54.

179. Long J, Zuo D, Park M. Pc2-mediated sumoylation of Smad-interacting protein 1 attenuates transcriptional repression of E-cadherin. The Journal of biological chemistry. 2005;280(42):35477-89.

180. Eijkelenboom A, Burgering BM. FOXOs: signalling integrators for homeostasis maintenance. Nature reviews Molecular cell biology. 2013;14(2):83-97.

181. Bresnick EH, Lee HY, Fujiwara T, Johnson KD, Keles S. GATA switches as developmental drivers. The Journal of biological chemistry. 2010;285(41):31087-93.

182. Kondoh H, Kamachi Y. SOX-partner code for cell specification: Regulatory target selection and underlying molecular mechanisms. The international journal of biochemistry & cell biology. 2010;42(3):391-9.

183. Mercado-Pimentel ME, Runyan RB. Multiple transforming growth factor-beta isoforms and receptors function during epithelial-mesenchymal cell transformation in the embryonic heart. Cells, tissues, organs. 2007;185(1-3):146-56.

184. Gressner AM, Weiskirchen R, Breitkopf K, Dooley S. Roles of TGF-beta in hepatic fibrosis. Frontiers in bioscience : a journal and virtual library. 2002;7:d793-807.

185. Willis BC, Borok Z. TGF-beta-induced EMT: mechanisms and implications for fibrotic lung disease. American journal of physiology Lung cellular and molecular physiology. 2007;293(3):L525-34.

186. Cantelli G, Crosas-Molist E, Georgouli M, Sanz-Moreno V. TGFBeta-induced transcription in cancer. Seminars in cancer biology. 2016.

187. Chen W, Zhou S, Mao L, Zhang H, Sun D, Zhang J, et al. Crosstalk between TGF-beta signaling and miRNAs in breast cancer metastasis. Tumour biology : the journal of the International Society for Oncodevelopmental Biology and Medicine. 2016;37(8):10011-9.

188. Giannelli G, Koudelkova P, Dituri F, Mikulits W. Role of epithelial to mesenchymal transition in hepatocellular carcinoma. Journal of hepatology. 2016;65(4):798-808.

189. Ikushima H, Miyazono K. Biology of transforming growth factor-beta signaling. Current pharmaceutical biotechnology. 2011;12(12):2099-107.

190. Massague J. TGFbeta signalling in context. Nature reviews Molecular cell biology. 2012;13(10):616-30.

191. Feng XH, Derynck R. Specificity and versatility in tgf-beta signaling through Smads. Annual review of cell and developmental biology. 2005;21:659-93.

192. Valcourt U, Kowanetz M, Niimi H, Heldin CH, Moustakas A. TGF-beta and the Smad signaling pathway support transcriptomic reprogramming during epithelial-mesenchymal cell transition. Molecular biology of the cell. 2005;16(4):1987-2002.

193. Lamouille S, Derynck R. Cell size and invasion in TGF-beta-induced epithelial to mesenchymal transition is regulated by activation of the mTOR pathway. The Journal of cell biology. 2007;178(3):437-51.

194. Katsuno Y, Lamouille S, Derynck R. TGF-beta signaling and epithelial-mesenchymal transition in cancer progression. Current opinion in oncology. 2013;25(1):76-84.

195. Lamouille S, Derynck R. Emergence of the phosphoinositide 3-kinase-Akt-mammalian target of rapamycin axis in transforming growth factor-beta-induced epithelial-mesenchymal transition. Cells, tissues, organs. 2011;193(1-2):8-22.

196. Lamouille S, Connolly E, Smyth JW, Akhurst RJ, Derynck R. TGF-beta-induced activation of mTOR complex 2 drives epithelial-mesenchymal transition and cell invasion. Journal of cell science. 2012;125(Pt 5):1259-73.

197. Ridley AJ. Life at the leading edge. Cell. 2011;145(7):1012-22.

198. Tavares AL, Mercado-Pimentel ME, Runyan RB, Kitten GT. TGF beta-mediated RhoA expression is necessary for epithelial-mesenchymal transition in the embryonic chick heart. Developmental dynamics : an official publication of the American Association of Anatomists. 2006;235(6):1589-98.

199. Bhowmick NA, Ghiassi M, Bakin A, Aakre M, Lundquist CA, Engel ME, et al. Transforming growth factor-beta1 mediates epithelial to mesenchymal transdifferentiation through a RhoA-dependent mechanism. Molecular biology of the cell. 2001;12(1):27-36.

200. Bakin AV, Tomlinson AK, Bhowmick NA, Moses HL, Arteaga CL. Phosphatidylinositol 3-kinase function is required for transforming growth factor beta-mediated epithelial to mesenchymal transition and cell migration. The Journal of biological chemistry. 2000;275(47):36803-10.

201. Lee MK, Pardoux C, Hall MC, Lee PS, Warburton D, Qing J, et al. TGF-beta activates Erk MAP kinase signalling through direct phosphorylation of ShcA. The EMBO journal. 2007;26(17):3957-67.

202. Xie L, Law BK, Chytil AM, Brown KA, Aakre ME, Moses HL. Activation of the Erk pathway is required for TGF-beta1-induced EMT in vitro. Neoplasia (New York, NY). 2004;6(5):603-10.

203. Grande M, Franzen A, Karlsson JO, Ericson LE, Heldin NE, Nilsson M. Transforming growth factor-beta and epidermal growth factor synergistically stimulate epithelial to mesenchymal transition (EMT) through a MEK-dependent mechanism in primary cultured pig thyrocytes. Journal of cell science. 2002;115(Pt 22):4227-36.

204. Uttamsingh S, Bao X, Nguyen KT, Bhanot M, Gong J, Chan JL, et al. Synergistic effect between EGF and TGF-beta1 in inducing oncogenic properties of intestinal epithelial cells. Oncogene. 2008;27(18):2626-34.

205. Makrodouli E, Oikonomou E, Koc M, Andera L, Sasazuki T, Shirasawa S, et al. BRAF and RAS oncogenes regulate Rho GTPase pathways to mediate migration and invasion properties in human colon cancer cells: a comparative study. Molecular cancer. 2011;10:118.

206. Savagner P, Yamada KM, Thiery JP. The zinc-finger protein slug causes desmosome dissociation, an initial and necessary step for growth factor-induced epithelial-mesenchymal transition. The Journal of cell biology. 1997;137(6):1403-19.

207. Graham TR, Zhau HE, Odero-Marah VA, Osunkoya AO, Kimbro KS, Tighiouart M, et al. Insulin-like growth factor-I-dependent up-regulation of ZEB1 drives epithelial-to-mesenchymal transition in human prostate cancer cells. Cancer research. 2008;68(7):2479-88.

208. Grotegut S, von Schweinitz D, Christofori G, Lehembre F. Hepatocyte growth factor induces cell scattering through MAPK/Egr-1-mediated upregulation of Snail. The EMBO journal. 2006;25(15):3534-45.

209. Lu Z, Ghosh S, Wang Z, Hunter T. Downregulation of caveolin-1 function by EGF leads to the loss of E-cadherin, increased transcriptional activity of beta-catenin, and enhanced tumor cell invasion. Cancer cell. 2003;4(6):499-515.

210. Lo HW, Hsu SC, Xia W, Cao X, Shih JY, Wei Y, et al. Epidermal growth factor receptor cooperates with signal transducer and activator of transcription 3 to induce epithelial-mesenchymal transition in cancer cells via up-regulation of TWIST gene expression. Cancer research. 2007;67(19):9066-76.

211. Moody SE, Perez D, Pan TC, Sarkisian CJ, Portocarrero CP, Sterner CJ, et al. The transcriptional repressor Snail promotes mammary tumor recurrence. Cancer cell. 2005;8(3):197-209.

212. Knutson KL, Lu H, Stone B, Reiman JM, Behrens MD, Prosperi CM, et al. Immunoediting of cancers may lead to epithelial to mesenchymal transition. Journal of immunology (Baltimore, Md : 1950). 2006;177(3):1526-33.

213. Niehrs C. The complex world of WNT receptor signalling. Nature reviews Molecular cell biology. 2012;13(12):767-79.

214. Briscoe J, Therond PP. The mechanisms of Hedgehog signalling and its roles in development and disease. Nature reviews Molecular cell biology. 2013;14(7):416-29.

215. Timmerman LA, Grego-Bessa J, Raya A, Bertran E, Perez-Pomares JM, Diez J, et al. Notch promotes epithelial-mesenchymal transition during cardiac development and oncogenic transformation. Genes & development. 2004;18(1):99-115.

216. Sullivan NJ, Sasser AK, Axel AE, Vesuna F, Raman V, Ramirez N, et al. Interleukin-6 induces an epithelial-mesenchymal transition phenotype in human breast cancer cells. Oncogene. 2009;28(33):2940-7.

217. Jing Y, Han Z, Zhang S, Liu Y, Wei L. Epithelial-Mesenchymal Transition in tumor microenvironment. Cell & bioscience. 2011;1:29.

218. Wendt MK, Smith JA, Schiemann WP. Transforming growth factor-beta-induced epithelial-mesenchymal transition facilitates epidermal growth factor-dependent breast cancer progression. Oncogene. 2010;29(49):6485-98.

219. Zavadil J, Bottinger EP. TGF-beta and epithelial-to-mesenchymal transitions. Oncogene. 2005;24(37):5764-74.

220. Yang J, Dai C, Liu Y. A novel mechanism by which hepatocyte growth factor blocks tubular epithelial to mesenchymal transition. Journal of the American Society of Nephrology : JASN. 2005;16(1):68-78.

221. Agger K, Christensen J, Cloos PA, Helin K. The emerging functions of histone demethylases. Current opinion in genetics & development. 2008;18(2):159-68.

222. Pasini D, Bracken AP, Agger K, Christensen J, Hansen K, Cloos PA, et al. Regulation of stem cell differentiation by histone methyltransferases and demethylases. Cold Spring Harbor symposia on quantitative biology. 2008;73:253-63.

223. Ezponda T, Popovic R, Shah MY, Martinez-Garcia E, Zheng Y, Min DJ, et al. The histone methyltransferase MMSET/WHSC1 activates TWIST1 to promote an epithelial-mesenchymal transition and invasive properties of prostate cancer. Oncogene. 2013;32(23):2882-90.

224. McDonald OG, Wu H, Timp W, Doi A, Feinberg AP. Genome-scale epigenetic reprogramming during epithelial-to-mesenchymal transition. Nature structural & molecular biology. 2011;18(8):867-74.

225. Malouf GG, Taube JH, Lu Y, Roysarkar T, Panjarian S, Estecio MR, et al. Architecture of epigenetic reprogramming following Twist1-mediated epithelial-mesenchymal transition. Genome biology. 2013;14(12):R144.

226. Price BD, D'Andrea AD. Chromatin remodeling at DNA double-strand breaks. Cell. 2013;152(6):1344-54.

227. Clapier CR, Cairns BR. The biology of chromatin remodeling complexes. Annual review of biochemistry. 2009;78:273-304.

228. Fujita N, Jaye DL, Kajita M, Geigerman C, Moreno CS, Wade PA. MTA3, a Mi-2/NuRD complex subunit, regulates an invasive growth pathway in breast cancer. Cell. 2003;113(2):207-19.

229. Jordan NV, Prat A, Abell AN, Zawistowski JS, Sciaky N, Karginova OA, et al. SWI/SNF chromatin-remodeling factor Smarcd3/Baf60c controls epithelial-mesenchymal transition by inducing Wnt5a signaling. Molecular and cellular biology. 2013;33(15):3011-25.

230. Sun L, Fang J. Epigenetic regulation of epithelial-mesenchymal transition. Cellular and molecular life sciences : CMLS. 2016;73(23):4493-515.

231. Carmona FJ, Davalos V, Vidal E, Gomez A, Heyn H, Hashimoto Y, et al. A comprehensive DNA methylation profile of epithelial-to-mesenchymal transition. Cancer research. 2014;74(19):5608-19.

232. Lombaerts M, van Wezel T, Philippo K, Dierssen JW, Zimmerman RM, Oosting J, et al. E-cadherin transcriptional downregulation by promoter methylation but not mutation is related to epithelial-to-mesenchymal transition in breast cancer cell lines. British journal of cancer. 2006;94(5):661-71.

233. Reinhold WC, Reimers MA, Maunakea AK, Kim S, Lababidi S, Scherf U, et al. Detailed DNA methylation profiles of the E-cadherin promoter in the NCI-60 cancer cells. Molecular cancer therapeutics. 2007;6(2):391-403.

234. Dong C, Wu Y, Yao J, Wang Y, Yu Y, Rychahou PG, et al. G9a interacts with Snail and is critical for Snail-mediated E-cadherin repression in human breast cancer. The Journal of clinical investigation. 2012;122(4):1469-86.

235. Papageorgis P, Lambert AW, Ozturk S, Gao F, Pan H, Manne U, et al. Smad signaling is required to maintain epigenetic silencing during breast cancer progression. Cancer research. 2010;70(3):968-78.

236. Lee KK, Workman JL. Histone acetyltransferase complexes: one size doesn't fit all. Nature reviews Molecular cell biology. 2007;8(4):284-95.

237. Hao S, He W, Li Y, Ding H, Hou Y, Nie J, et al. Targeted inhibition of beta-catenin/CBP signaling ameliorates renal interstitial fibrosis. Journal of the American Society of Nephrology : JASN. 2011;22(9):1642-53.

238. Zhou B, Liu Y, Kahn M, Ann DK, Han A, Wang H, et al. Interactions between beta-catenin and transforming growth factor-beta signaling pathways mediate epithelial-mesenchymal transition and are dependent on the transcriptional co-activator cAMP-response element-binding protein (CREB)-binding protein (CBP). The Journal of biological chemistry. 2012;287(10):7026-38.

239. Kapoor-Vazirani P, Kagey JD, Powell DR, Vertino PM. Role of hMOF-dependent histone H4 lysine 16 acetylation in the maintenance of TMS1/ASC gene activity. Cancer research. 2008;68(16):6810-21.

240. Liu YN, Lee WW, Wang CY, Chao TH, Chen Y, Chen JH. Regulatory mechanisms controlling human E-cadherin gene expression. Oncogene. 2005;24(56):8277-90.

241. Aghdassi A, Sendler M, Guenther A, Mayerle J, Behn CO, Heidecke CD, et al. Recruitment of histone deacetylases HDAC1 and HDAC2 by the transcriptional repressor ZEB1 downregulates E-cadherin expression in pancreatic cancer. Gut. 2012;61(3):439-48.

242. Tripathi MK, Misra S, Khedkar SV, Hamilton N, Irvin-Wilson C, Sharan C, et al. Regulation of BRCA2 gene expression by the SLUG repressor protein in human breast cells. The Journal of biological chemistry. 2005;280(17):17163-71.

243. Zhang L, Deng L, Chen F, Yao Y, Wu B, Wei L, et al. Inhibition of histone H3K79 methylation selectively inhibits proliferation, self-renewal and metastatic potential of breast cancer. Oncotarget. 2014;5(21):10665-77.

244. Cho MH, Park JH, Choi HJ, Park MK, Won HY, Park YJ, et al. DOT1L cooperates with the c-Myc-p300 complex to epigenetically derepress CDH1 transcription factors in breast cancer progression. Nature communications. 2015;6:7821.

245. Gao Y, Zhao Y, Zhang J, Lu Y, Liu X, Geng P, et al. The dual function of PRMT1 in modulating epithelial-mesenchymal transition and cellular senescence in breast cancer cells through regulation of ZEB1. Scientific reports. 2016;6:19874.

246. Hojfeldt JW, Agger K, Helin K. Histone lysine demethylases as targets for anticancer therapy. Nature reviews Drug discovery. 2013;12(12):917-30.

247. Lee MG, Wynder C, Cooch N, Shiekhattar R. An essential role for CoREST in nucleosomal histone 3 lysine 4 demethylation. Nature. 2005;437(7057):432-5.

248. Lin Y, Wu Y, Li J, Dong C, Ye X, Chi YI, et al. The SNAG domain of Snail1 functions as a molecular hook for recruiting lysine-specific demethylase 1. The EMBO journal. 2010;29(11):1803-16.

249. Shi YJ, Matson C, Lan F, Iwase S, Baba T, Shi Y. Regulation of LSD1 histone demethylase activity by its associated factors. Molecular cell. 2005;19(6):857-64.

250. Shi Y, Sawada J, Sui G, Affar el B, Whetstine JR, Lan F, et al. Coordinated histone modifications mediated by a CtBP co-repressor complex. Nature. 2003;422(6933):735-8.

251. Metzger E, Wissmann M, Yin N, Muller JM, Schneider R, Peters AH, et al. LSD1 demethylates repressive histone marks to promote androgen-receptor-dependent transcription. Nature. 2005;437(7057):436-9.

252. Wang Y, Zhang H, Chen Y, Sun Y, Yang F, Yu W, et al. LSD1 is a subunit of the NuRD complex and targets the metastasis programs in breast cancer. Cell. 2009;138(4):660-72.

253. Zhang H, Cai K, Wang J, Wang X, Cheng K, Shi F, et al. MiR-7, inhibited indirectly by lincRNA HOTAIR, directly inhibits SETDB1 and reverses the EMT of breast cancer stem cells by downregulating the STAT3 pathway. Stem cells (Dayton, Ohio). 2014;32(11):2858-68.

254. Di Croce L, Helin K. Transcriptional regulation by Polycomb group proteins. Nature structural & molecular biology. 2013;20(10):1147-55.

255. Margueron R, Reinberg D. The Polycomb complex PRC2 and its mark in life. Nature. 2011;469(7330):343-9.

256. Mills AA. Throwing the cancer switch: reciprocal roles of polycomb and trithorax proteins. Nature reviews Cancer. 2010;10(10):669-82.

257. Molofsky AV, Pardal R, Iwashita T, Park IK, Clarke MF, Morrison SJ. Bmi-1 dependence distinguishes neural stem cell self-renewal from progenitor proliferation. Nature. 2003;425(6961):962-7.

258. Iwama A, Oguro H, Negishi M, Kato Y, Morita Y, Tsukui H, et al. Enhanced self-renewal of hematopoietic stem cells mediated by the polycomb gene product Bmi-1. Immunity. 2004;21(6):843-51.

259. Sangiorgi E, Capecchi MR. Bmi1 is expressed in vivo in intestinal stem cells. Nature genetics. 2008;40(7):915-20.

260. Italiano A. Role of the EZH2 histone methyltransferase as a therapeutic target in cancer. Pharmacology & therapeutics. 2016;165:26-31.

261. Kim KH, Roberts CW. Targeting EZH2 in cancer. Nature medicine. 2016;22(2):128-34.

262. Kouso H, Yano T, Maruyama R, Shikada Y, Okamoto T, Haro A, et al. Differences in the expression of epithelial-mesenchymal transition related molecules between primary tumors and pulmonary metastatic tumors in colorectal cancer. Surgery today. 2013;43(1):73-80.

263. Fan XJ, Wan XB, Huang Y, Cai HM, Fu XH, Yang ZL, et al. Epithelial-mesenchymal transition biomarkers and support vector machine guided model in preoperatively predicting regional lymph node metastasis for rectal cancer. British journal of cancer. 2012;106(11):1735-41.

264. Kevans D, Wang LM, Sheahan K, Hyland J, O'Donoghue D, Mulcahy H, et al. Epithelial-mesenchymal transition (EMT) protein expression in a cohort of stage II colorectal cancer patients with characterized tumor budding and mismatch repair protein status. International journal of surgical pathology. 2011;19(6):751-60.

265. Mesker WE, Liefers GJ, Junggeburt JM, van Pelt GW, Alberici P, Kuppen PJ, et al. Presence of a high amount of stroma and downregulation of SMAD4 predict for worse survival for stage I-II colon cancer patients. Cellular oncology : the official journal of the International Society for Cellular Oncology. 2009;31(3):169-78.

266. Bellovin DI, Bates RC, Muzikansky A, Rimm DL, Mercurio AM. Altered localization of p120 catenin during epithelial to mesenchymal transition of colon carcinoma is prognostic for aggressive disease. Cancer research. 2005;65(23):10938-45.

267. Fujikawa H, Tanaka K, Toiyama Y, Saigusa S, Inoue Y, Uchida K, et al. High TrkB expression levels are associated with poor prognosis and EMT induction in colorectal cancer cells. Journal of gastroenterology. 2012;47(7):775-84.

268. Shioiri M, Shida T, Koda K, Oda K, Seike K, Nishimura M, et al. Slug expression is an independent prognostic parameter for poor survival in colorectal carcinoma patients. British journal of cancer. 2006;94(12):1816-22.

269. Franci C, Gallen M, Alameda F, Baro T, Iglesias M, Virtanen I, et al. Snail1 protein in the stroma as a new putative prognosis marker for colon tumours. PloS one. 2009;4(5):e5595.

270. Gomez I, Pena C, Herrera M, Munoz C, Larriba MJ, Garcia V, et al. TWIST1 is expressed in colorectal carcinomas and predicts patient survival. PloS one. 2011;6(3):e18023.

271. Liu Z, Sun B, Qi L, Li H, Gao J, Leng X. Zinc finger E-box binding homeobox 1 promotes vasculogenic mimicry in colorectal cancer through induction of epithelial-to-mesenchymal transition. Cancer science. 2012;103(4):813-20.

272. Marisa L, de Reynies A, Duval A, Selves J, Gaub MP, Vescovo L, et al. Gene expression classification of colon cancer into molecular subtypes: characterization, validation, and prognostic value. PLoS medicine. 2013;10(5):e1001453.

273. De Sousa EMF, Wang X, Jansen M, Fessler E, Trinh A, de Rooij LP, et al. Poor-prognosis colon cancer is defined by a molecularly distinct subtype and develops from serrated precursor lesions. Nature medicine. 2013;19(5):614-8.

274. Del Rio M, Mollevi C, Bibeau F, Vie N, Selves J, Emile JF, et al. Molecular subtypes of metastatic colorectal cancer are associated with patient response to irinotecan-based therapies. European journal of cancer (Oxford, England : 1990). 2017;76:68-75.

275. Sadanandam A, Lyssiotis CA, Homicsko K, Collisson EA, Gibb WJ, Wullschleger S, et al. A colorectal cancer classification system that associates cellular phenotype and responses to therapy. Nature medicine. 2013;19(5):619-25.

276. Budinska E, Popovici V, Tejpar S, D'Ario G, Lapique N, Sikora KO, et al. Gene expression patterns unveil a new level of molecular heterogeneity in colorectal cancer. The Journal of pathology. 2013;231(1):63-76.

277. Dunne PD, Alderdice M, O'Reilly PG, Roddy AC, McCorry AMB, Richman S, et al. Cancer-cell intrinsic gene expression signatures overcome intratumoural heterogeneity bias in colorectal cancer patient classification. Nature communications. 2017;8:15657.

278. Isella C, Brundu F, Bellomo SE, Galimi F, Zanella E, Porporato R, et al. Selective analysis of cancer-cell intrinsic transcriptional traits defines novel clinically relevant subtypes of colorectal cancer. Nature communications. 2017;8:15107.

279. Giannelli G, Villa E, Lahn M. Transforming growth factor-beta as a therapeutic target in hepatocellular carcinoma. Cancer research. 2014;74(7):1890-4.

280. Rodon J, Carducci M, Sepulveda-Sanchez JM, Azaro A, Calvo E, Seoane J, et al. Pharmacokinetic, pharmacodynamic and biomarker evaluation of transforming growth

factor-beta receptor I kinase inhibitor, galunisertib, in phase 1 study in patients with advanced cancer. Investigational new drugs. 2015;33(2):357-70.

281. Infante JR, Camidge DR, Mileshkin LR, Chen EX, Hicks RJ, Rischin D, et al. Safety, pharmacokinetic, and pharmacodynamic phase I dose-escalation trial of PF-00562271, an inhibitor of focal adhesion kinase, in advanced solid tumors. Journal of clinical oncology : official journal of the American Society of Clinical Oncology. 2012;30(13):1527-33.

282. Puls LN, Eadens M, Messersmith W. Current status of SRC inhibitors in solid tumor malignancies. The oncologist. 2011;16(5):566-78.

283. Byers LA, Diao L, Wang J, Saintigny P, Girard L, Peyton M, et al. An epithelial-mesenchymal transition gene signature predicts resistance to EGFR and PI3K inhibitors and identifies Axl as a therapeutic target for overcoming EGFR inhibitor resistance. Clinical cancer research : an official journal of the American Association for Cancer Research. 2013;19(1):279-90.

284. Sheridan C. First Axl inhibitor enters clinical trials. Nature biotechnology. 2013;31(9):775-6.

285. Ceppi P, Mudduluru G, Kumarswamy R, Rapa I, Scagliotti GV, Papotti M, et al. Loss of miR-200c expression induces an aggressive, invasive, and chemoresistant phenotype in non-small cell lung cancer. Molecular cancer research : MCR. 2010;8(9):1207-16.

286. Vrba L, Jensen TJ, Garbe JC, Heimark RL, Cress AE, Dickinson S, et al. Role for DNA methylation in the regulation of miR-200c and miR-141 expression in normal and cancer cells. PloS one. 2010;5(1):e8697.

287. Tryndyak VP, Beland FA, Pogribny IP. E-cadherin transcriptional down-regulation by epigenetic and microRNA-200 family alterations is related to mesenchymal and drug-resistant phenotypes in human breast cancer cells. International journal of cancer. 2010;126(11):2575-83.

288. Strasser A, O'Connor L, Dixit VM. Apoptosis signaling. Annual review of biochemistry. 2000;69:217-45.

289. Rufini A, Melino G. Cell death pathology: the war against cancer. Biochemical and biophysical research communications. 2011;414(3):445-50.

290. Giglia-Mari G, Zotter A, Vermeulen W. DNA damage response. Cold Spring Harbor perspectives in biology. 2011;3(1):a000745.

291. Fulda S, Debatin KM. Extrinsic versus intrinsic apoptosis pathways in anticancer chemotherapy. Oncogene. 2006;25(34):4798-811.

292. Jackson SP, Bartek J. The DNA-damage response in human biology and disease. Nature. 2009;461(7267):1071-8.

293. Errol C. Freiberg RDW, editor. Chapter 8 : DNA Excision Repair Pathway Cold Spring Harbor Laboratory Press 1996.

294. Lou Z, Minter-Dykhouse K, Franco S, Gostissa M, Rivera MA, Celeste A, et al. MDC1 maintains genomic stability by participating in the amplification of ATM-dependent DNA damage signals. Molecular cell. 2006;21(2):187-200.

295. Melander F, Bekker-Jensen S, Falck J, Bartek J, Mailand N, Lukas J. Phosphorylation of SDT repeats in the MDC1 N terminus triggers retention of NBS1 at the DNA damage-modified chromatin. The Journal of cell biology. 2008;181(2):213-26.

296. Kolas NK, Chapman JR, Nakada S, Ylanko J, Chahwan R, Sweeney FD, et al. Orchestration of the DNA-damage response by the RNF8 ubiquitin ligase. Science (New York, NY). 2007;318(5856):1637-40.

297. Xu Y, Sun Y, Jiang X, Ayrapetov MK, Moskwa P, Yang S, et al. The p400 ATPase regulates nucleosome stability and chromatin ubiquitination during DNA repair. The Journal of cell biology. 2010;191(1):31-43.

298. Falck J, Coates J, Jackson SP. Conserved modes of recruitment of ATM, ATR and DNA-PKcs to sites of DNA damage. Nature. 2005;434(7033):605-11.

299. Ashwell S, Zabludoff S. DNA damage detection and repair pathways--recent advances with inhibitors of checkpoint kinases in cancer therapy. Clinical cancer research : an official journal of the American Association for Cancer Research. 2008;14(13):4032-7.

300. Lindahl T, Karran P, Wood RD. DNA excision repair pathways. Current opinion in genetics & development. 1997;7(2):158-69.

301. Wood RD. DNA repair in eukaryotes. Annual review of biochemistry. 1996;65:135-67.

302. Sancar GB. DNA photolyases: physical properties, action mechanism, and roles in dark repair. Mutation research. 1990;236(2-3):147-60.

303. Sancar A. Structure and function of DNA photolyase. Biochemistry. 1994;33(1):2-9.

304. Zamble DB, Mu D, Reardon JT, Sancar A, Lippard SJ. Repair of cisplatin--DNA adducts by the mammalian excision nuclease. Biochemistry. 1996;35(31):10004-13.

305. Mitra S, Kaina B. Regulation of repair of alkylation damage in mammalian genomes. Progress in nucleic acid research and molecular biology. 1993;44:109-42.

306. Lindahl T, Sedgwick B, Sekiguchi M, Nakabeppu Y. Regulation and expression of the adaptive response to alkylating agents. Annual review of biochemistry. 1988;57:133-57.

307. Sancar A. DNA excision repair. Annual review of biochemistry. 1996;65:43-81.

308. Wood RD. Nucleotide excision repair in mammalian cells. The Journal of biological chemistry. 1997;272(38):23465-8.

309. Reardon JT, Sancar A. Nucleotide excision repair. Progress in nucleic acid research and molecular biology. 2005;79:183-235.

310. Sancar A. Mechanisms of DNA Repair by Photolyase and Excision Nuclease (Nobel Lecture). Angewandte Chemie (International ed in English). 2016;55(30):8502-27.

311. Chapman JR, Taylor MR, Boulton SJ. Playing the end game: DNA double-strand break repair pathway choice. Molecular cell. 2012;47(4):497-510.

312. Iyama T, Wilson DM, 3rd. DNA repair mechanisms in dividing and non-dividing cells. DNA repair. 2013;12(8):620-36.

313. Ceccaldi R, Rondinelli B, D'Andrea AD. Repair Pathway Choices and Consequences at the Double-Strand Break. Trends in cell biology. 2016;26(1):52-64.

314. Lieber MR. The mechanism of double-strand DNA break repair by the nonhomologous DNA end-joining pathway. Annual review of biochemistry. 2010;79:181-211.

315. Frit P, Barboule N, Yuan Y, Gomez D, Calsou P. Alternative end-joining pathway(s): bricolage at DNA breaks. DNA repair. 2014;17:81-97.

316. Mello JA, Sillje HH, Roche DM, Kirschner DB, Nigg EA, Almouzni G. Human Asf1 and CAF-1 interact and synergize in a repair-coupled nucleosome assembly pathway. EMBO reports. 2002;3(4):329-34.

317. Waters R, Teng Y, Yu Y, Yu S, Reed SH. Tilting at windmills? The nucleotide excision repair of chromosomal DNA. DNA repair. 2009;8(2):146-52.

318. Goodarzi AA, Noon AT, Deckbar D, Ziv Y, Shiloh Y, Lobrich M, et al. ATM signaling facilitates repair of DNA double-strand breaks associated with heterochromatin. Molecular cell. 2008;31(2):167-77.

319. Tsai RY. Balancing self-renewal against genome preservation in stem cells: How do they manage to have the cake and eat it too? Cellular and molecular life sciences : CMLS. 2016;73(9):1803-23.

320. Momcilovic O, Knobloch L, Fornsaglio J, Varum S, Easley C, Schatten G. DNA damage responses in human induced pluripotent stem cells and embryonic stem cells. PloS one. 2010;5(10):e13410.

321. Hsu DS, Lan HY, Huang CH, Tai SK, Chang SY, Tsai TL, et al. Regulation of excision repair cross-complementation group 1 by Snail contributes to cisplatin resistance in head and neck cancer. Clinical cancer research : an official journal of the American Association for Cancer Research. 2010;16(18):4561-71.

322. Nouspikel T, Hanawalt PC. Impaired nucleotide excision repair upon macrophage differentiation is corrected by E1 ubiquitin-activating enzyme. Proceedings of the National Academy of Sciences of the United States of America. 2006;103(44):16188-93.

323. Nouspikel T, Hanawalt PC. Terminally differentiated human neurons repair transcribed genes but display attenuated global DNA repair and modulation of repair gene expression. Molecular and cellular biology. 2000;20(5):1562-70.

324. Vandewalle C, Comijn J, De Craene B, Vermassen P, Bruyneel E, Andersen H, et al. SIP1/ZEB2 induces EMT by repressing genes of different epithelial cell-cell junctions. Nucleic acids research. 2005;33(20):6566-78.

325. Cellura D, Pickard K, Quaratino S, Parker H, Strefford JC, Thomas GJ, et al. miR-19-Mediated Inhibition of Transglutaminase-2 Leads to Enhanced Invasion and Metastasis in Colorectal Cancer. Molecular cancer research : MCR. 2015;13(7):1095-105.

326. Bullock MD, Pickard K, Mitter R, Sayan AE, Primrose JN, Ivan C, et al. Stratifying risk of recurrence in stage II colorectal cancer using deregulated stromal and epithelial microRNAs. Oncotarget. 2015;6(9):7262-79.

327. Ling H, Pickard K, Ivan C, Isella C, Ikuo M, Mitter R, et al. The clinical and biological significance of MIR-224 expression in colorectal cancer metastasis. Gut. 2016;65(6):977-89.

328. Zhang L, Pickard K, Jenei V, Bullock MD, Bruce A, Mitter R, et al. miR-153 supports colorectal cancer progression via pleiotropic effects that enhance invasion and chemotherapeutic resistance. Cancer research. 2013;73(21):6435-47.

329. Association of Coloproctology of Great B, Ireland. Guidelines for the management of colorectal cancer (2007). London: ACPGBI; 2007.

330. Kattan MW, Hess KR, Amin MB, Lu Y, Moons KG, Gershenwald JE, et al. American Joint Committee on Cancer acceptance criteria for inclusion of risk models for individualized prognosis in the practice of precision medicine. CA: a cancer journal for clinicians. 2016;66(5):370-4.

331. Pathmanathan N, Balleine RL. Ki67 and proliferation in breast cancer. Journal of clinical pathology. 2013;66(6):512-6.

332. Webster MT, Rozycka M, Sara E, Davis E, Smalley M, Young N, et al. Sequence variants of the axin gene in breast, colon, and other cancers: an analysis of mutations that interfere with GSK3 binding. Genes, chromosomes & cancer. 2000;28(4):443-53.

333. Nicolay NH, Lopez Perez R, Saffrich R, Huber PE. Radio-resistant mesenchymal stem cells: mechanisms of resistance and potential implications for the clinic. Oncotarget. 2015;6(23):19366-80.

334. Lugo TG, Braun S, Cote RJ, Pantel K, Rusch V. Detection and measurement of occult disease for the prognosis of solid tumors. Journal of clinical oncology : official journal of the American Society of Clinical Oncology. 2003;21(13):2609-15.

335. Gray R, Barnwell J, McConkey C, Hills RK, Williams NS, Kerr DJ. Adjuvant chemotherapy versus observation in patients with colorectal cancer: a randomised study. Lancet (London, England). 2007;370(9604):2020-9.

336. Caramel J, Papadogeorgakis E, Hill L, Browne GJ, Richard G, Wierinckx A, et al. A switch in the expression of embryonic EMT-inducers drives the development of malignant melanoma. Cancer cell. 2013;24(4):466-80.

337. Consensus statement on the multidisciplinary management of patients with recurrent and primary rectal cancer beyond total mesorectal excision planes. The British journal of surgery. 2013;100(8):1009-14.

338. Kelley RK, Venook AP. Prognostic and predictive markers in stage II colon cancer: is there a role for gene expression profiling? Clinical colorectal cancer. 2011;10(2):73-80.

339. Amado RG, Wolf M, Peeters M, Van Cutsem E, Siena S, Freeman DJ, et al. Wild-type KRAS is required for panitumumab efficacy in patients with metastatic colorectal cancer. Journal of clinical oncology : official journal of the American Society of Clinical Oncology. 2008;26(10):1626-34.

340. Van Cutsem E, Kohne CH, Lang I, Folprecht G, Nowacki MP, Cascinu S, et al. Cetuximab plus irinotecan, fluorouracil, and leucovorin as first-line treatment for metastatic colorectal cancer: updated analysis of overall survival according to tumor KRAS and BRAF mutation status. Journal of clinical oncology : official journal of the American Society of Clinical Oncology. 2011;29(15):2011-9.

341. Spaderna S, Schmalhofer O, Hlubek F, Berx G, Eger A, Merkel S, et al. A transient, EMT-linked loss of basement membranes indicates metastasis and poor survival in colorectal cancer. Gastroenterology. 2006;131(3):830-40.

342. Schlicker A, Beran G, Chresta CM, McWalter G, Pritchard A, Weston S, et al. Subtypes of primary colorectal tumors correlate with response to targeted treatment in colorectal cell lines. BMC medical genomics. 2012;5:66.

343. Cheang MC, Chia SK, Voduc D, Gao D, Leung S, Snider J, et al. Ki67 index, HER2 status, and prognosis of patients with luminal B breast cancer. Journal of the National Cancer Institute. 2009;101(10):736-50.

344. Cheang MC, Voduc D, Bajdik C, Leung S, McKinney S, Chia SK, et al. Basal-like breast cancer defined by five biomarkers has superior prognostic value than triple-negative phenotype. Clinical cancer research : an official journal of the American Association for Cancer Research. 2008;14(5):1368-76.

345. Fakih MG. Metastatic colorectal cancer: current state and future directions. J Clin Oncol. 2015;33(16):1809-24.

346. Bowden NA. Nucleotide excision repair: why is it not used to predict response to platinum-based chemotherapy? Cancer letters. 2014;346(2):163-71.

347. Singh A, Settleman J. EMT, cancer stem cells and drug resistance: an emerging axis of evil in the war on cancer. Oncogene. 2010;29:4741-51.

348. Caramel J, Papadogeorgakis E, Hill L, Browne GJ, Richard G, Wierinckx A, et al. A Switch in the Expression of Embryonic EMT-Inducers Drives the Development of Malignant Melanoma. Cancer Cell. 2013.

349. Altman DG, McShane LM, Sauerbrei W, Taube SE. Reporting Recommendations for Tumor Marker Prognostic Studies (REMARK): explanation and elaboration. PLoS medicine. 2012;9(5):e1001216.

350. Brabletz T. To differentiate or not--routes towards metastasis. Nat Rev Cancer. 2012;12(6):425-36.

351. Wood RD. Mammalian nucleotide excision repair proteins and interstrand crosslink repair. Environmental and molecular mutagenesis. 2010;51(6):520-6.

352. Wood RD, Araujo SJ, Ariza RR, Batty DP, Biggerstaff M, Evans E, et al. DNA damage recognition and nucleotide excision repair in mammalian cells. Cold Spring Harbor symposia on quantitative biology. 2000;65:173-82.

353. Bohanes P, Labonte MJ, Lenz HJ. A review of excision repair cross-complementation group 1 in colorectal cancer. Clinical colorectal cancer. 2011;10(3):157-64.

354. Petryszak R, Keays M, Tang YA, Fonseca NA, Barrera E, Burdett T, et al. Expression Atlas update--an integrated database of gene and protein expression in humans, animals and plants. Nucleic Acids Res. 2016;44(D1):D746-52.

355. Kelly H, Goldberg RM. Systemic therapy for metastatic colorectal cancer: current options, current evidence. Journal of clinical oncology : official journal of the American Society of Clinical Oncology. 2005;23(20):4553-60.

356. Zhang P, Wei Y, Wang L, Debeb BG, Yuan Y, Zhang J, et al. ATM-mediated stabilization of ZEB1 promotes DNA damage response and radioresistance through CHK1. Nature cell biology. 2014;16(9):864-75.

357. Eastman A. The formation, isolation and characterization of DNA adducts produced by anticancer platinum complexes. Pharmacol Ther. 1987;34(2):155-66.

358. McNeil EM, Melton DW. DNA repair endonuclease ERCC1-XPF as a novel therapeutic target to overcome chemoresistance in cancer therapy. Nucleic acids research. 2012;40(20):9990-10004.

359. Friboulet L, Postel-Vinay S, Sourisseau T, Adam J, Stoclin A, Ponsonnailles F, et al. ERCC1 function in nuclear excision and interstrand crosslink repair pathways is mediated exclusively by the ERCC1-202 isoform. Cell cycle (Georgetown, Tex). 2013;12(20):3298-306.

360. Arnould S, Hennebelle I, Canal P, Bugat R, Guichard S. Cellular determinants of oxaliplatin sensitivity in colon cancer cell lines. European journal of cancer (Oxford, England : 1990). 2003;39(1):112-9.

361. Chang IY, Kim MH, Kim HB, Lee DY, Kim SH, Kim HY, et al. Small interfering RNA-induced suppression of ERCC1 enhances sensitivity of human cancer cells to cisplatin. Biochemical and biophysical research communications. 2005;327(1):225-33.

362. Damia G, Imperatori L, Stefanini M, D'Incalci M. Sensitivity of CHO mutant cell lines with specific defects in nucleotide excision repair to different anti-cancer agents. International journal of cancer. 1996;66(6):779-83.

363. Johnson SW, Perez RP, Godwin AK, Yeung AT, Handel LM, Ozols RF, et al. Role of platinum-DNA adduct formation and removal in cisplatin resistance in human ovarian cancer cell lines. Biochemical pharmacology. 1994;47(4):689-97.

364. Bedford P, Fichtinger-Schepman AM, Shellard SA, Walker MC, Masters JR, Hill BT. Differential repair of platinum-DNA adducts in human bladder and testicular tumor continuous cell lines. Cancer research. 1988;48(11):3019-24.

365. Zeng-Rong N, Paterson J, Alpert L, Tsao MS, Viallet J, Alaoui-Jamali MA. Elevated DNA repair capacity is associated with intrinsic resistance of lung cancer to chemotherapy. Cancer research. 1995;55(21):4760-4.

366. Welsh C, Day R, McGurk C, Masters JR, Wood RD, Koberle B. Reduced levels of XPA, ERCC1 and XPF DNA repair proteins in testis tumor cell lines. International journal of cancer. 2004;110(3):352-61.

367. Lord RV, Brabender J, Gandara D, Alberola V, Camps C, Domine M, et al. Low ERCC1 expression correlates with prolonged survival after cisplatin plus gemcitabine chemotherapy in non-small cell lung cancer. Clinical cancer research : an official journal of the American Association for Cancer Research. 2002;8(7):2286-91.

368. Azuma K, Komohara Y, Sasada T, Terazaki Y, Ikeda J, Hoshino T, et al. Excision repair cross-complementation group 1 predicts progression-free and overall survival in non-small cell lung cancer patients treated with platinum-based chemotherapy. Cancer science. 2007;98(9):1336-43.

369. Dabholkar M, Vionnet J, Bostick-Bruton F, Yu JJ, Reed E. Messenger RNA levels of XPAC and ERCC1 in ovarian cancer tissue correlate with response to platinum-based chemotherapy. The Journal of clinical investigation. 1994;94(2):703-8.

370. Li F, Sun X, Sun N, Qin S, Cheng H, Feng J, et al. Association between polymorphisms of ERCC1 and XPD and clinical response to platinum-based chemotherapy in advanced non-small cell lung cancer. American journal of clinical oncology. 2010;33(5):489-94.

371. Viguier J, Boige V, Miquel C, Pocard M, Giraudeau B, Sabourin JC, et al. ERCC1 codon 118 polymorphism is a predictive factor for the tumor response to oxaliplatin/5-fluorouracil combination chemotherapy in patients with advanced colorectal cancer. Clinical cancer research : an official journal of the American Association for Cancer Research. 2005;11(17):6212-7.

372. Hirakawa M, Sato Y, Ohnuma H, Takayama T, Sagawa T, Nobuoka T, et al. A phase II study of neoadjuvant combination chemotherapy with docetaxel, cisplatin, and S-1 for locally advanced resectable gastric cancer: nucleotide excision repair (NER) as potential chemoresistance marker. Cancer chemotherapy and pharmacology. 2013;71(3):789-97.

373. Huang J, Zhou Y, Zhang H, Qu T, Mao Y, Zhu H, et al. A phase II study of biweekly paclitaxel and cisplatin chemotherapy for recurrent or metastatic esophageal squamous cell carcinoma: ERCC1 expression predicts response to chemotherapy. Medical oncology (Northwood, London, England). 2013;30(1):343.

374. Milovic-Kovacevic M, Srdic-Rajic T, Radulovic S, Bjelogrlic S, Gavrilovic D. Expression of ERCC1 protein in biopsy specimen predicts survival in advanced ovarian cancer patients treated with platinum-based chemotherapy. Journal of BUON : official journal of the Balkan Union of Oncology. 2011;16(4):708-14.

375. Tiseo M, Bordi P, Bortesi B, Boni L, Boni C, Baldini E, et al. ERCC1/BRCA1 expression and gene polymorphisms as prognostic and predictive factors in advanced NSCLC treated with or without cisplatin. British journal of cancer. 2013;108(8):1695-703.

376. Yamada Y, Boku N, Nishina T, Yamaguchi K, Denda T, Tsuji A, et al. Impact of excision repair cross-complementing gene 1 (ERCC1) on the outcomes of patients with advanced gastric cancer: correlative study in Japan Clinical Oncology Group Trial JCOG9912. Annals of oncology : official journal of the European Society for Medical Oncology. 2013;24(10):2560-5.

377. Braun MS, Richman SD, Quirke P, Daly C, Adlard JW, Elliott F, et al. Predictive biomarkers of chemotherapy efficacy in colorectal cancer: results from the UK MRC FOCUS trial. Journal of clinical oncology : official journal of the American Society of Clinical Oncology. 2008;26(16):2690-8.

378. Friboulet L, Olaussen KA, Pignon JP, Shepherd FA, Tsao MS, Graziano S, et al. ERCC1 isoform expression and DNA repair in non-small-cell lung cancer. N Engl J Med. 2013;368(12):1101-10.

379. Oztas E, Avci ME, Ozcan A, Sayan AE, Tulchinsky E, Yagci T. Novel monoclonal antibodies detect Smad-interacting protein 1 (SIP1) in the cytoplasm of human cells from multiple tumor tissue arrays. Experimental and molecular pathology. 2010;89(2):182-9.

380. Ahn JY, Lee JS, Min HY, Lee HY. Acquired resistance to 5-fluorouracil via HSP90/Src-mediated increase in thymidylate synthase expression in colon cancer. Oncotarget. 2015;6(32):32622-33.

381. Bosset JF, Collette L, Calais G, Mineur L, Maingon P, Radosevic-Jelic L, et al. Chemotherapy with preoperative radiotherapy in rectal cancer. N Engl J Med. 2006;355(11):1114-23.

382. Bouquet F, Pal A, Pilones KA, Demaria S, Hann B, Akhurst RJ, et al. TGFbeta1 inhibition increases the radiosensitivity of breast cancer cells in vitro and promotes tumor control by radiation in vivo. Clinical cancer research : an official journal of the American Association for Cancer Research. 2011;17(21):6754-65.

383. Jin C, Yan B, Lu Q, Lin Y, Ma L. The role of MALAT1/miR-1/slug axis on radioresistance in nasopharyngeal carcinoma. Tumour biology : the journal of the International Society for Oncodevelopmental Biology and Medicine. 2016;37(3):4025-33.

384. Escriva M, Peiro S, Herranz N, Villagrasa P, Dave N, Montserrat-Sentis B, et al. Repression of PTEN phosphatase by Snail1 transcriptional factor during gamma radiation-induced apoptosis. Molecular and cellular biology. 2008;28(5):1528-40.

385. Schuster-Bockler B, Lehner B. Chromatin organization is a major influence on regional mutation rates in human cancer cells. Nature. 2012;488(7412):504-7.

386. Rahn JJ, Adair GM, Nairn RS. Multiple roles of ERCC1-XPF in mammalian interstrand crosslink repair. Environmental and molecular mutagenesis. 2010;51(6):567-81.

387. Chaney SG, Sancar A. DNA repair: enzymatic mechanisms and relevance to drug response. Journal of the National Cancer Institute. 1996;88(19):1346-60.

388. EC WRF. DNA EXCISION REPAIR DNA replication in eukaryotic cells cold spring harbour laboratory press 1996.

389. Youn CK, Kim MH, Cho HJ, Kim HB, Chang IY, Chung MH, et al. Oncogenic H-Ras up-regulates expression of ERCC1 to protect cells from platinum-based anticancer agents. Cancer research. 2004;64(14):4849-57.

390. Boyer J, McLean EG, Aroori S, Wilson P, McCulla A, Carey PD, et al. Characterization of p53 wild-type and null isogenic colorectal cancer cell lines resistant to 5-fluorouracil, oxaliplatin, and irinotecan. Clinical cancer research : an official journal of the American Association for Cancer Research. 2004;10(6):2158-67.

391. Bauman JE, Austin MC, Schmidt R, Kurland BF, Vaezi A, Hayes DN, et al. ERCC1 is a prognostic biomarker in locally advanced head and neck cancer: results from a randomised, phase II trial. British journal of cancer. 2013;109(8):2096-105.

392. He YW, Zhao ML, Yang XY, Zeng J, Deng QH, He JX. Prognostic value of ERCC1, RRM1, and TS proteins in patients with resected non-small cell lung cancer. Cancer chemotherapy and pharmacology. 2015;75(4):861-7.

393. Shirota Y, Stoehlmacher J, Brabender J, Xiong YP, Uetake H, Danenberg KD, et al. ERCC1 and thymidylate synthase mRNA levels predict survival for colorectal cancer patients receiving combination oxaliplatin and fluorouracil chemotherapy. Journal of clinical oncology : official journal of the American Society of Clinical Oncology. 2001;19(23):4298-304.

394. Uchida K, Hayashi K, Kuramochi H, Kudo K, Miyakura S, Fujita I, et al. ERCC1 expression as a predictor for chemosensitivity in recurrent colorectal cancer patients receiving cisplatinum (CDDP) plus S-1 chemotherapy. Journal of clinical oncology : official journal of the American Society of Clinical Oncology. 2006;24(18_suppl):13065.

395. Wang M, Bronte V, Chen PW, Gritz L, Panicali D, Rosenberg SA, et al. Active immunotherapy of cancer with a nonreplicating recombinant fowlpox virus encoding a model tumor-associated antigen. Journal of immunology. 1995;154(9):4685-92.

396. Fogh J, Fogh JM, Orfeo T. One hundred and twenty-seven cultured human tumor cell lines producing tumors in nude mice. Journal of the National Cancer Institute. 1977;59(1):221-6.

397. Trainer DL, Kline T, McCabe FL, Faucette LF, Feild J, Chaikin M, et al. Biological characterization and oncogene expression in human colorectal carcinoma cell lines. International journal of cancer Journal international du cancer. 1988;41(2):287-96.

398. Semple TU, Quinn LA, Woods LK, Moore GE. Tumor and lymphoid cell lines from a patient with carcinoma of the colon for a cytotoxicity model. Cancer Res. 1978;38(5):1345-55.

399. Tibbetts LM, Chu MY, Hager JC, Dexter DL, Calabresi P. Chemotherapy of cell-line-derived human colon carcinomas in mice immunosuppressed with antithymocyte serum. Cancer. 1977;40(5 Suppl):2651-9.

400. Dexter DL, Barbosa JA, Calabresi P. N,N-dimethylformamide-induced alteration of cell culture characteristics and loss of tumorigenicity in cultured human colon carcinoma cells. Cancer Res. 1979;39(3):1020-5.

401. Brattain MG, Fine WD, Khaled FM, Thompson J, Brattain DE. Heterogeneity of malignant cells from a human colonic carcinoma. Cancer Res. 1981;41(5):1751-6.

402. Drewinko B, Romsdahl MM, Yang LY, Ahearn MJ, Trujillo JM. Establishment of a human carcinoembryonic antigen-producing colon adenocarcinoma cell line. Cancer Res. 1976;36(2 Pt 1):467-75.

403. Boyd D, Florent G, Chakrabarty S, Brattain D, Brattain MG. Alterations of the biological characteristics of a colon carcinoma cell line by colon-derived substrata material. Cancer Res. 1988;48(10):2825-31.

404. Leibovitz A, Stinson JC, McCombs WB, 3rd, McCoy CE, Mazur KC, Mabry ND. Classification of human colorectal adenocarcinoma cell lines. Cancer Res. 1976;36(12):4562-9.

405. Lelbovitz A, Wright WC, Pathak S, Siciliano MJ, Daniels WP. Detection and analysis of a glucose 6-phosphate dehydrogenase phenotype B cell line contamination. Journal of the National Cancer Institute. 1979;63(3):635-45.